Hay Man Hilde Tsui

Synthetic strategies towards 4,6-disubstituted pyrrolo[2,3-*d*]pyrimidines as potential CSF-1R inhibitors

Master's thesis in Chemical Engineering and Biotechnology
Supervisor: Professor Bård Helge Hoff
Co-supervisor: PhD Candidate Thomas Ihle Aarhus
June 2019

Master's thesis

NTNU
Norwegian University of Science and Technology
Faculty of Natural Sciences
Department of Chemistry

NTNU
Norwegian University of
Science and Technology

Hay Man Hilde Tsui

Synthetic strategies towards 4,6-disubstituted pyrrolo[2,3-*d*]pyrimidines as potential CSF-1R inhibitors

Master's thesis in Chemical Engineering and Biotechnology
Supervisor: Professor Bård Helge Hoff
Co-supervisor: PhD Candidate Thomas Ihle Aarhus
June 2019

Norwegian University of Science and Technology
Faculty of Natural Sciences
Department of Chemistry

NTNU
Norwegian University of
Science and Technology

I hereby declare that this master's thesis is an independent work according to the exam regulations of the Norwegian University of Science and Technology.

Trondheim, June 2019

Hilde Hay Man Tsui

Acknowledgements

The work presented in this master's thesis has been carried out at the Department of Chemistry at NTNU, Trondheim, during the spring of 2019. The work has been performed under supervision of Professor Bård Helge Hoff and PhD candidate Thomas Ihle Aarhus.

First, I would like to thank Bård and Thomas for welcoming me into the Hoff/-Sundby research group. Their excitement towards this project have increased my motivation, especially on the longer days at the laboratory this spring. Thanks to Bård for his help during the writing process and at the laboratory, and thanks to Thomas for his patience for my many, many questions, and for showing me his tips and tricks. I would also like to thank the rest of the Hoff/Sundby group for a good and uplifting atmosphere.

A special thanks to Roger Aarvik for providing chemicals and equipment when needed, and to Susana Villa Gonzales and Julie Asmussen for running my MS samples. A big thanks to Torun Melø as well, for help while conducting NMR temperature experiments.

A big thanks to my mother and brother for supporting me through 18 years of schooling, and also to my father, 非常感谢我的父亲。

Lastly, a special thanks to Fredrik Buvarp for his invaluable patience, support and help the past few years.

Abstract

The aim of this master's thesis was to synthesize new 4,6-disubstituted pyrrolo[2,3-*d*]pyrimidines as inhibitors of colony stimulating factor 1 receptor (CSF-1R) tyrosine kinase. A new synthetic strategy was examined as well. Overstimulating CSF-1R has been associated with several pathological conditions such as inflammatory diseases, bone diseases and cancers. Thus, inhibition of CSF-1R has become an important target in attempt to treat these conditions. The research group has developed highly potent inhibitors of pyrrolo[2,3-*d*]pyrimidines with carbonaromatic substituents in position 4 and 6. A new group of structures with non-aromatic substituents are to be explored, hence the target molecules in this project.

The synthetic routes towards the target molecules **HHMT-070**, **HHMT-170**, and **HHMT-178**, are presented in Scheme 1. The yields of these routes varied from poor to excellent.
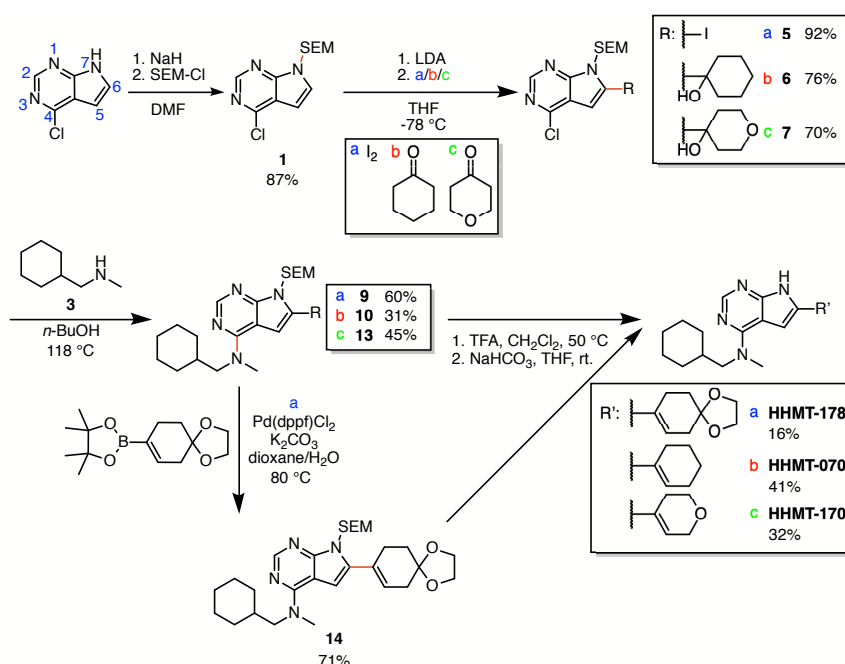
Scheme 1: Synthetic route I towards target molecule **HHMT-178** (*a*), and route II towards **HHMT-070** (*b*) and **HHMT-170** (*c*).

The first step towards the target molecules was protection of 4-chloro-7*H*-pyrrolo-[2,3-*d*]pyrimidine with a 2-(trimethylsilyl)ethoxymethyl (SEM) group in position 7, resulting in compound **1**. Iodination of compound **1** in position 6 through

ortho-lithiation gave compound **5**. The new synthetic strategy involved *ortho*-lithiation and nucleophilic attack on cyclic ketones, which resulted in compound **6** and **7**. Thermal amination of compound **5**, **6**, and **7**, yielded compound **9**, **10**, and **13**, respectively. The iodinated compound **9** proceeded to a Suzuki cross-coupling reaction, which gave compound **14**. Finally, removal of the SEM protection group resulted in compound **HHMT-178**, **HHMT-070**, and **HHMT-170**.

HHMT-070 has previously been synthesized following route I. Comparing the two routes for synthesizing compound **HHMT-070**, the new route (II) should result in a higher yield than route I if alterations are considered. Furthermore, enzymatic screening of **HHMT-170** showed promising results for inhibition of CSF-1R.

Sammendrag

Målet med denne masteroppgaven var å syntetisere nye 4,6-disubstituerte pyrrolo-[2,3-*d*]pyrimidiner som hemmere for CSF-1R ("colony stimulating factor 1 receptor") tyrosinkinase. En ny strategi for syntese av disse er også undersøkt. Overaktivitet av CSF-1R har vært knyttet til flere patologiske sykdommer som betennelsessykdommer, beinsykdommer og kreft. Hemming av CSF-1R har derfor blitt et viktig angrepspunkt for behandling av disse. Forskningsgruppa har utviklet hemmere av pyrrolo[2,3-*d*]pyrimidiner med høyt potensial. Disse forbindelsene har inneholdt aromatiske substituenter i posisjon 4 og 6. Videre skal en ny gruppe strukturer med ikke-aromatiske substituenter undersøkes.

Synteserutene til målmolekylene **HHMT-070**, **HHMT-170** og **HHMT-178**, er presentert i Skjema 2.
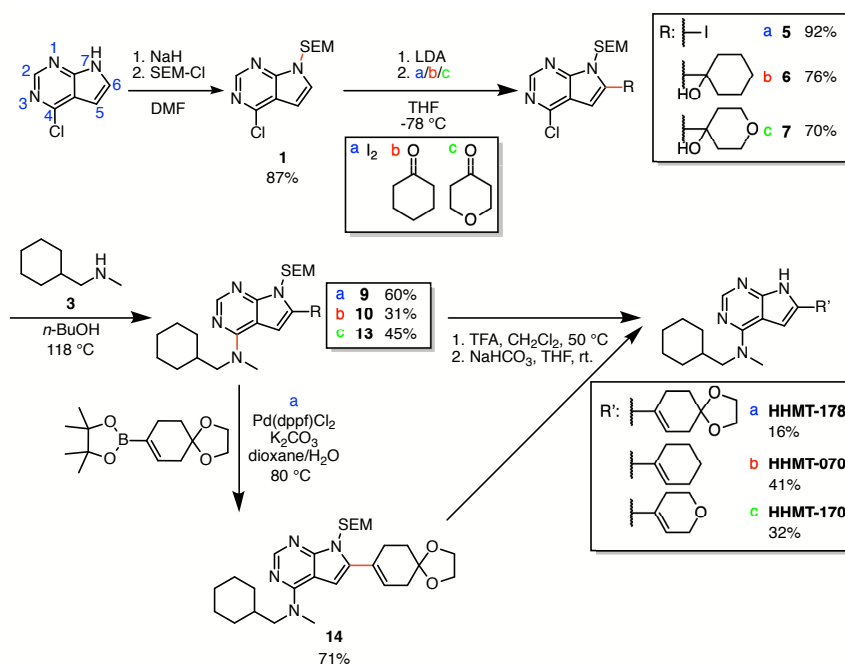
Skjema 2: Synteserute I for målmolekyl **HHMT-178** (*a*), og rute II for **HHMT-070** (*b*) og **HHMT-170** (*c*).

Det første steget var beskyttelse av 4-klor-7*H*-pyrrolo[2,3-*d*]pyrimidin med 2-(trimetylsilyl)etoksymetyl (SEM) i posisjon 7, for syntese av forbindelse **1**. Jodering av forbindelse **1** i posisjon 6 *via orto*-litiering ga forbindelse **5**. En ny syntesestrategi involverte *orto*-litiering og reaksjon med sykliske ketoner, hvilket ga forbindelsene **6** og **7**. Termisk aminering av forbindelse **5**, **6** og **7**, resulterte

henholdsvis i forbindelse **9**, **10** og **13**. Videre, ble forbindelse **14** dannet i en Suzuki kryss-koblingsreaksjon med forbindelse **9**. Til slutt ble målmolekylene **HHMT-178**, **HHMT-070** og **HHMT-170** dannet ved avbeskyttelse.

HHMT-070 har tidligere blitt syntetisert *via* rute I. Ved sammenligning av strategiene for syntese av forbindelse **HHMT-070**, så det ut til at den nye ruta (II) vil resultere i høyere utbytte enn rute I dersom endringer tas i betraktning. Videre viste **HHMT-170** lovende resultater ved inhibering av CSF-1R.

Contents

Symbols and Abbreviations

δ	Chemical shift in ppm
ν	Frequency in cm^{-1}
^{13}C-NMR	Carbon nuclear magnetic resonance
^{1}H-NMR	Proton nuclear magnetic resonance
J	Coupling constant in Hz
m/z	Mass per charge ratio
ATP	Adenosine triphosphate
BuOH	Butanol
br	Broad
c-FMS	Cellular FMS
COSY	Correlation spectroscopy
CSF-1	Colony stimulation factor 1
CSF-1R	Colony stimulating factor 1 receptor
d	Doublet
dd	Doublet of doublets
DMF	Dimethylformamide
DMSO	Dimethyl sulfoxide
DMSO-d_6	Deuterated dimethylsulfoxide
E1	Unimolecular elimination reaction
EGFR	Epidermal growth factor receptor
EtOAc	Ethyl acetate
FMS	Oncogene for Feline McDonough Sarcoma
HMBC	Heteronuclear multiple bond correlation
HRMS	High resolution mass spectrometry
HSQC	Heteronuclear single quantum coherence
IL-34	Interleukin 34
IR	Infrared
LDA	Lithium diisopropylamide
Lit.	Literature value
LTMP	Lithium tetramethylpiperidide
m	Multiplet
mp	Melting point
MS	Mass spectrometry
NRTK	Non-receptor protein tyrosine kinase

Pd(dppf)Cl$_2$	[1,1'-Bis(diphenylphosphino)ferrocene]dichloropalladium(II)
PDGFR	Platelet-derived growth factor receptor
ppm	Parts per million
R$_f$	Retention factor
RTK	Receptor tyrosine kinase
s	Singlet
SEM	2-(Trimethylsilyl)ethoxymethyl
SEM-Cl	2-(Trimethylsilyl)ethoxymethyl chloride
sept	Septet
S$_N$1	Unimolecular nucleophilic substitution reaction
S$_N$Ar	Nucleophilic aromatic substitution
t	Triplet
td	Triplet of doublets
TFA	Trifloroacetic acid
TLC	Thin-layer chromatography
THF	Tetrahydrofuran
TMS	Tetramethylsilane

Compound Numbering

1

2

3

4

5

6

7

8

9

10

11

12

13

14

15

HHMT-070

HHMT-170

HHMT-178
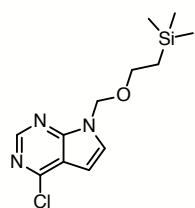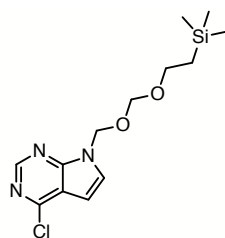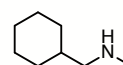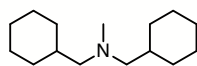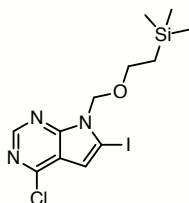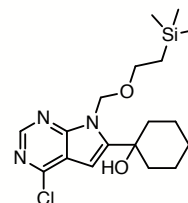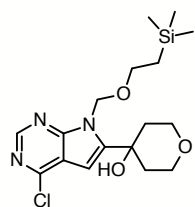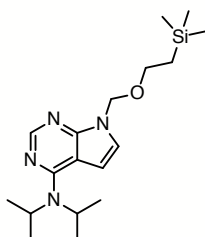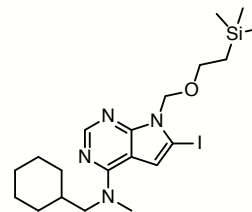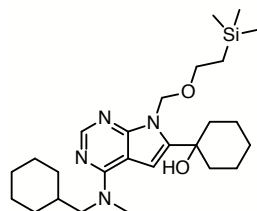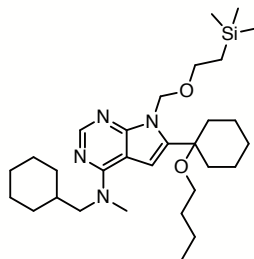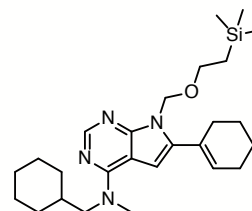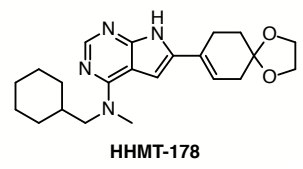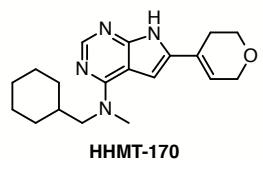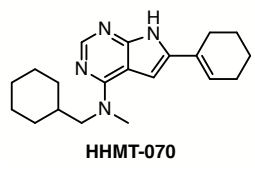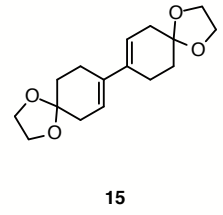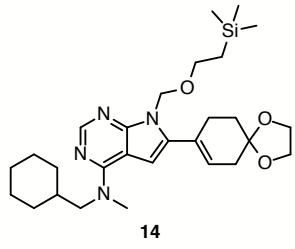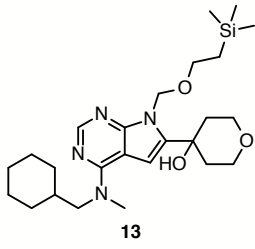
Chapter 1

Introduction and Theory

Design of small molecules as drugs has become an important field of medicinal chemistry. Mutations in receptor tyrosine kinases and abnormalities of their intracellular signaling cascade have been linked to cancers, diabetes, inflammation, severe bone disorders and arteriosclerosis.[1–4] Inhibition of specific receptor tyrosine kinases has allowed treatment of some of these diseases with small-molecule inhibitors.[5–7] Fused pyrimidines have attracted considerable attention because of their wide spectrum of biological activities.[8–10] The aim of this project was to synthesize 4,6-disubstituted pyrrolo[2,3-*d*]pyrimidines based on previous work by the research group as possible CSF-1R inhibitors, see Scheme 1.1. **HHMT-070** has previously been synthesized and showed poor water solubility, which is an essential property for drug development. The similar derivatives, **HHMT-170** and **HHMT-178**, were therefore targeted as they were thought to have higher water solubilities. Examination of a new strategy for synthesizing compound **HHMT-070** and **HHMT-170** was desired as well. The bioactivity of compound **HHMT-170** was tested.

HHMT-070   **HHMT-170**   **HHMT-178**
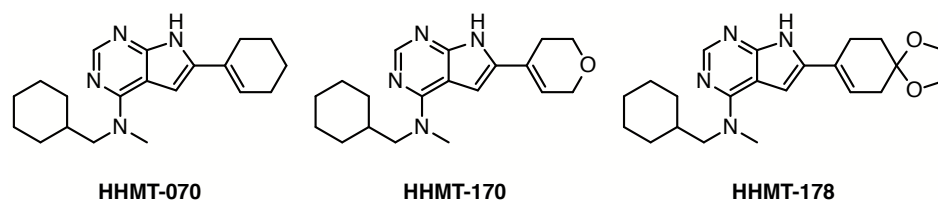
Scheme 1.1: Target molecules prepared as potential CSF-1R inhibitors.

The new synthetic strategy for compound **HHMT-070** and **HHMT-170** (route II), involved *ortho*-lithiation and a nucleophilic attack on ketones, see Scheme 1.2. The synthesis route for compound **HHMT-178** (route I) included a Suzuki cross-coupling reaction, which has been the usual approach within the research group.[11,12]
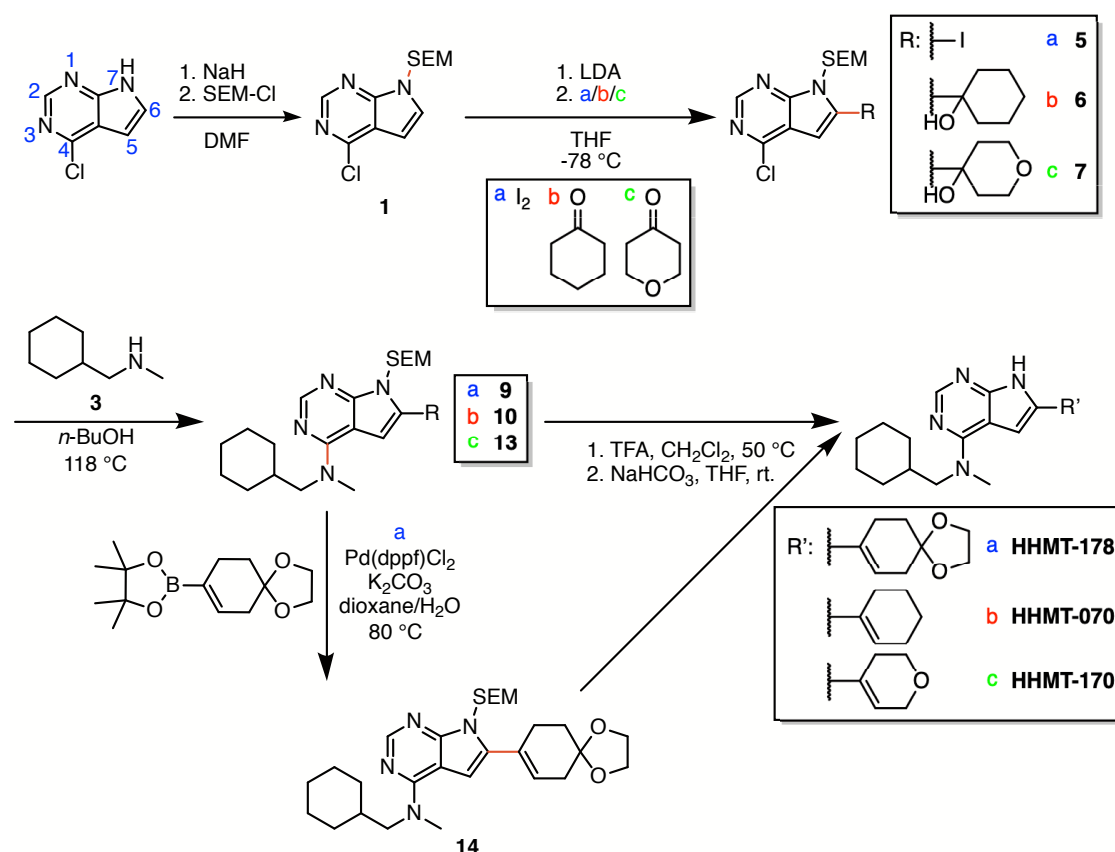
Scheme 1.2: Synthetic route I towards target molecule **HHMT-178** (*a*), and route II towards **HHMT-070** (*b*) and **HHMT-170** (*c*).

1.1 Tyrosine Kinase

Tyrosine phosphorylation is one of the key covalent modifications in multicellular organisms and modulates enzymatic activity, thus creating binding sites for the recruitment of downstream signaling proteins. The phosphorylation of tyrosine is carried out by enzymes called protein tyrosine kinases (PTKs). PTKs transfer the γ-phosphate of adenosine triphosphate (ATP) to the hydroxy group on tyrosine residues in protein substrates, as shown in Scheme 1.3.[13]
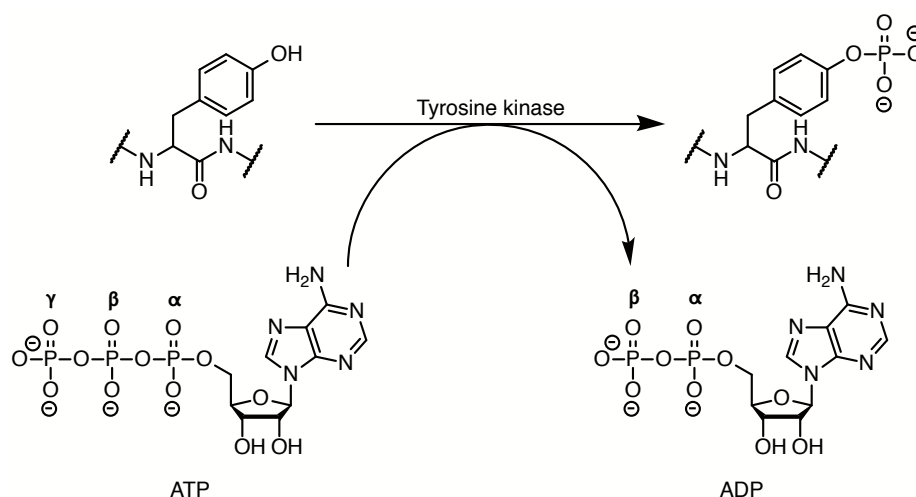
Scheme 1.3: Phosphorylation of tyrosine residue with tyrosine kinase.

The protein tyrosine kinases are critical components of cellular signaling pathways and can be divided into two classes: the transmembrane receptor protein tyrosine kinases (RTKs) and the non-receptor protein tyrosine kinases (NRTKs). RTKs transduce extracellular signals to the cytoplasm through autophosphorylation of tyrosine residues and on downstream signaling proteins.[13] Activation of RTKs are critical for regulation of cellular processes, such as proliferation, differentiation, survival, metabolism, migration and metabolic changes (cell-cycle control).[1,2,14–16]

As RTKs are key components of the intracellular signaling pathways, numerous diseases result from genetic changes or abnormalities that alter the activity, abundance, cellular distribution or regulations of RTKs. This has been causally linked to cancers, diabetes, inflammation, severe bone disorders and arteriosclerosis.[1,15,17–20] Development of new drugs that can block or attenuate RTK acitivity is therefore highly needed.

1.1.1 Colony Stimulating Factor 1 Receptor (CSF-1R)

Colony stimulating factor 1 receptor (CSF-1R) is a type III receptor tyrosine kinase, meaning that it is in the platelet-derived growth factor receptor (PDGFR) family.[21] CSF-1R is transcribed and translated from the proto-oncogene c-FMS (cellular FMS), which is named after the viral homologue oncogene responsible for Feline McDonough Sarcoma.[21,22] Activation of the receptor results in survival, proliferation and differentiation of monocyte or macrophage lineage.[1,2,14,15] The

macrophage or monocyte colony stimulation factor (CSF-1 or M-CSF) is involved in local regulation of target cells and interacts with the cells through its specific transmembrane receptor CSF-1R, and is an important growth factor for bone progenitor cells, osteoclasts and dendritic cells. Overexpression of CSF-1 and/or CSF-1R is associated with the growth of several tumor types, initiation and growth of metastasis of certain types of cancer, and many inflammatory disorders.[1,19,21]

CSF-1R is activated by CSF-1 and an additional ligand called Interleukin-34 (IL-34). Computational modeling suggests that CSF-1 and IL-34 binds to different sites of the extracellular part of CSF-1R.[23,24] There are two main inhibiting strategies to block the signaling cascade, see Figure 1.1. The first strategy is using antibodies on the cytokins, CSF-1 or IL-34, or their corresponding receptors to inhibit binding. It is uncertain if antibodies can block binding of CSF-1 or IL-34 or both. The second strategy is using small molecules as a competitive inhibitor for the intracellular binding site for ATP.[18,25]
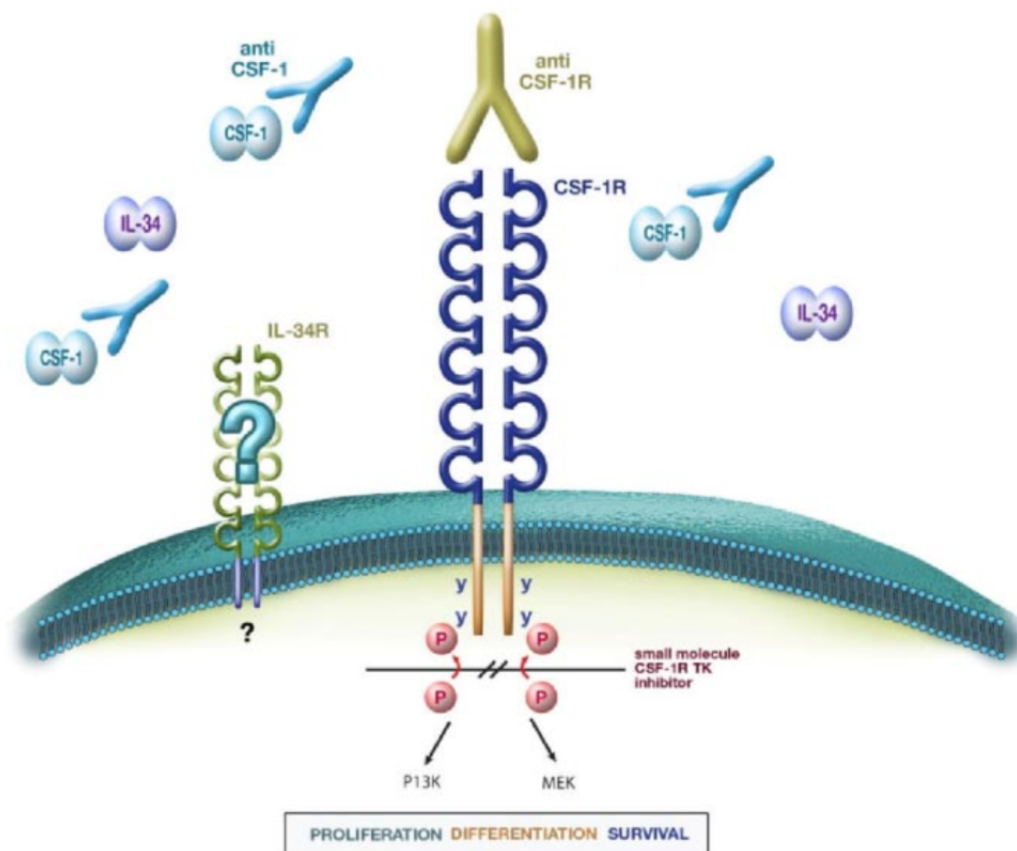
Figure 1.1: Illustration of colony stimulating factor 1 receptor tyrosine kinase blockage strategies using anti-bodies or inhibitors.[18]

There are several ATP competitive CSF-1R inhibitors with *in vivo* anti-inflammatory effects reported in the literature.[18] *In vivo* studies have shown that oral administration of Ki20227 can inhibit CSF-1R and suppress osteoclast-like cell accumulation and bone resorption induced by metastatic tumor cells in rats.[26] Ki20227 has also prevented inflammatory cell infiltration and bone destruction, as well as suppressed disease progression.[27] GW2580 is another orally bioavailable inhibitor with CSF-1R inhibitory activity.[28] It has the ability to inhibit bone degradation *in vitro* and tumor growth *in vivo*. *In vitro*, human CSF-1R was completely inhibited at 60 nM and it was inactive against 26 other kinases. Its selective inhibition of monocyte growth and bone degradation is also useful in determining the role of CSF-1 in normal and abnormal processes as it inhibits CSF-1 signaling cascade through CSF-1R.[28] Another inhibitor that has shown to be highly potent is PLX3397 by Plexxikon Inc., which is currently under clinical investigation for multiple types of cancers.[29,30] The structures of Ki20227, GW2580, and PLX3397, are shown in Scheme 1.4.
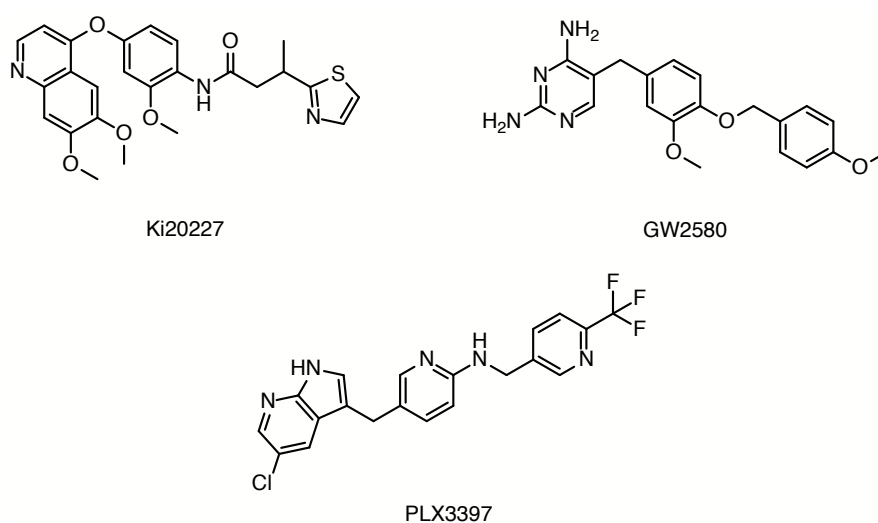
Scheme 1.4: The structures of Ki20227, GW2580 and PLX3397.[26,28]

1.2 Previous Work by the Research Group

Previous work by the research group has been focused around inhibitors for epidermal growth factor receptor (EGFR).[11,12] Pyrrolo-, thieno- and furopyrimidines have previously been used as core structures, see Figure 1.2. In the past few years, the focus has shifted towards CSF-1R, as some of the previously synthesized molecules have shown promising inhibition of CSF-1R.

X = NH, S, O
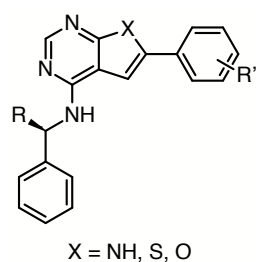
Figure 1.2: The core structure of previous synthesized molecules in the research group.

Some pyrrolopyrimidines that have showed high degree of CSF-1R inhibition are shown in Scheme 1.5, and have been the lead structures towards synthesis of new potential CSF-1R inhibitors.

JH06-118-02

92%

JH06-142

92%

KUL02-056

95%

KUL01-123

96%
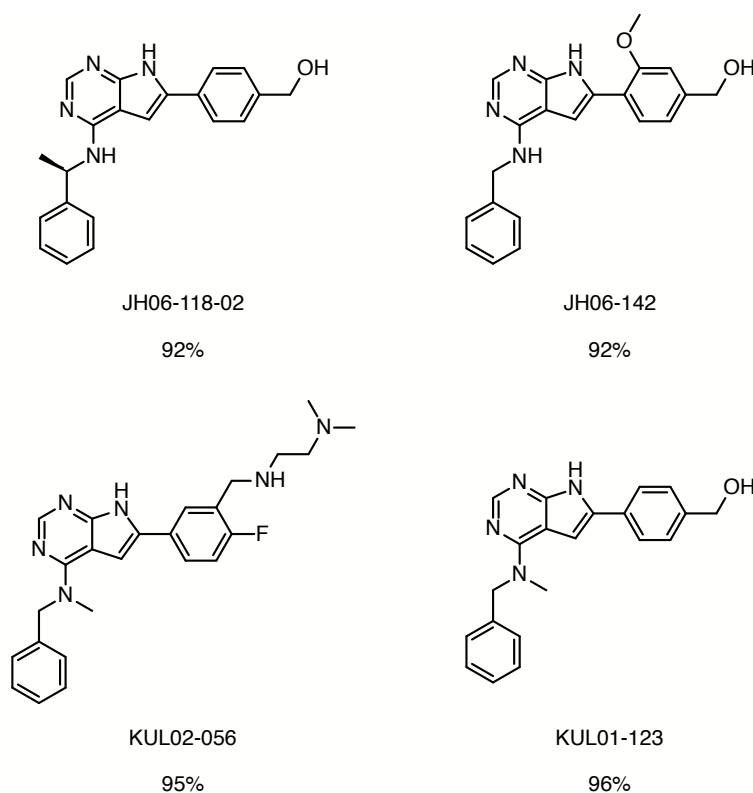
Scheme 1.5: Pyrrolo[2,3-*d*]pyrimidine lead structures previously synthesized by the research group. The activities are measured as percent inhibition of CSF-1R kinase at 500 nM concentration of inhibitor.[12,31]

According to Ritchie *et al.*,[32] increased ring counts in drug design have negative, slightly unfavourable effects on the drugs developability. Especially carboaromatic rings have a detrimental effect on human bioavailability parameters.[32] The aim of this master's thesis was therefore to synthesize substituted pyrrolo[2,3-*d*]pyrimidine (see Scheme 1.1) without aromatic substituents.

Compound **HHMT-070** has previously been synthesized through Suzuki cross-coupling reaction, which has been the usual approach within the group for the past few years.[11,12] For comparison with the new approach presented in this thesis (route II, Scheme 1.2), the previous route is given in Scheme 1.6.
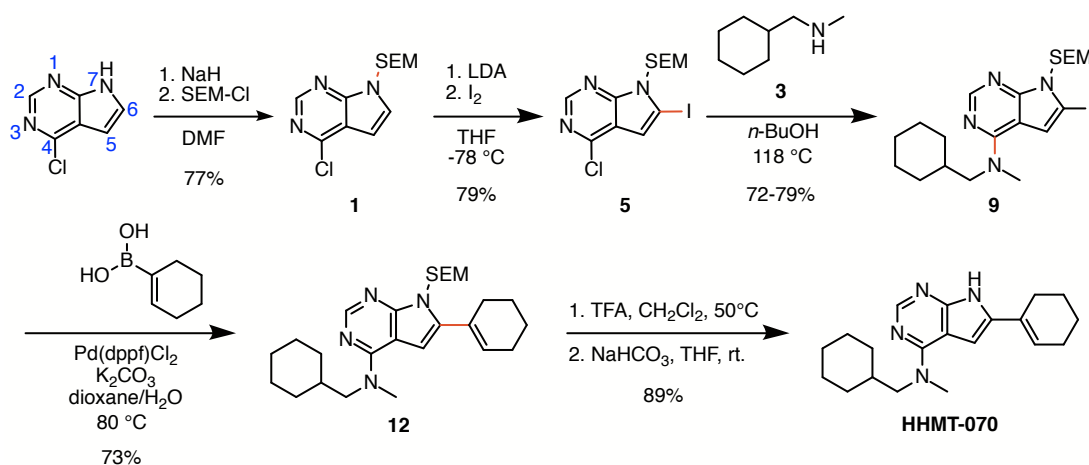
Scheme 1.6: Synthesis of compound **HHMT-070** from previously reported synthetic route.[33]

1.3 Chemical Reactions

The chemical reactions used to achieve the target molecules are presented in this section.

1.3.1 Protective Group for Pyrroles

Pyrroles can undergo electrophilic aromatic substitutions as it is fairly electron rich.[34] Alkaline conditions may lead to deprotonation of the pyrrolo nitrogen and unwanted reactions may occur. Thus, protection might sometimes be needed. Protection of pyrrolo[2,3-*d*]pyrimidines with 2-(trimethylsilyl)ethyoxymethyl (SEM) has been reported to result in smoother amination and cross-coupling reactions, in addition to more facile purification by silica-gel column chromatography.[35] The SEM group is frequently used for protection of alcohols and amines, see Scheme 1.7. The group is robust against harsh conditions, such as bromination, basic hydrolysis and oxidation.[36] In addition to protection, the group is useful for directing aromatic substitution through *ortho*-lithiation.[34]
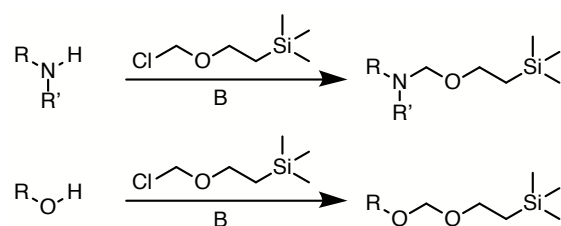
Scheme 1.7: SEM protection of amines and alcohols with a base B.

SEM deprotection can be problematic due to the robustness of the group. However, it can be removed using hydrochloric acid or tetrabutylammonium fluoride.[36,37] Other fluoride sources has also been successfully employed, such as sodium fluoride and trifluoroacetic acid (TFA).[11,37–39] The mechanism for deprotection is proposed to be conducted through an one-step or a two-step approach with fluoride ion, see Scheme 1.8.[37,39,40]
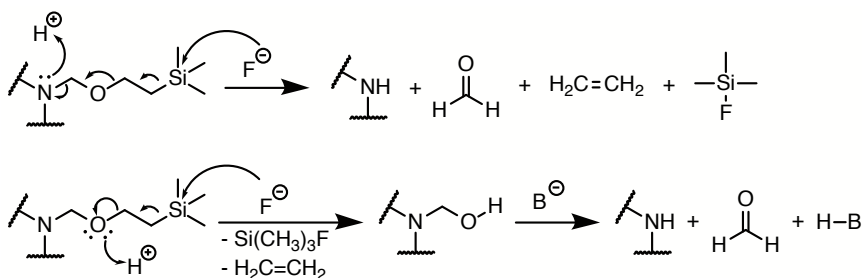
Scheme 1.8: Proposed one-step and two-step mechanism with a base B for SEM deprotection of an amine.[37,39,40]

In addition, formation of another derivative is proposed by Kan *et al.*[37] The mechanism is presented in Scheme 1.9.
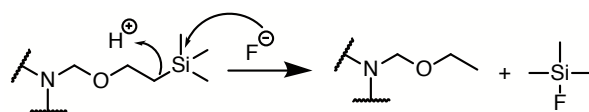
Scheme 1.9: Possible derivative during SEM deprotection.[37]

As can be seen, several derivatives can be formed. This complicates the monitoring of the reaction.

1.3.2 *Ortho*-lithiation

A method for directing aromatic substitution is through organometallic reagents where a hydrogen-metal exchange (or metalation) takes place. Hydrogen exchange with lithium is known as lithiation. The site of proton removal is dictated by the relative acidity of available hydrogens and the directing effects of substituent groups. Substituents that have electron lone pairs, such as alkoxy, amido, sulfoxide, and sulfonyl, have a powerful influence on both the regioselectivity and the rate of lithiation. The electron lone pair can coordinate with lithium, and the polarity can stabilize the anionic character, so that the base deprotonates the adjacent (*ortho*) proton despite it being in the most hindered position. Amide bases, such as lithium diisopropylamide (LDA) and lithium tetramethylpiperidide (LTMP), gives higher selectivity than alkyllithium reagents. A general mechanism is shown in Scheme 1.10. Deprotonation of a sp^2 hybridized carbon atom is preferred as it is more acidic than a sp^3 hybridized carbon atom. This results in an aryllithium intermediate where the anion and the substituent coordinates with lithium and forms a complex.[34,41]
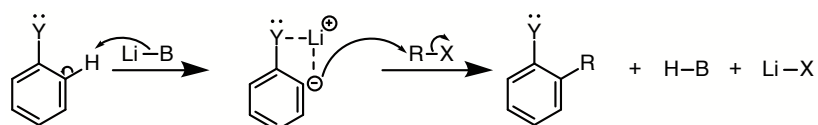
Scheme 1.10: General mechanism of *ortho*-lithiation followed by a substitution reaction.[34]

The mechanism for a more specific example of *ortho*-lithiation followed by a nucleophilic attack on a ketone is assumed to be as presented in Scheme 1.11.
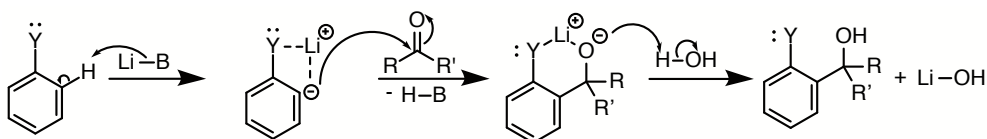
Scheme 1.11: Presumed mechanism for *ortho*-lithiation and reaction with a carbonyl group.

Several examples of *ortho*-lithiation on derivatives of benzene, pyrroles, and pyrrolo[2,3-*d*]pyrimidines, followed by a nucleophilic attack on a carbonyl group are reported in the literature.[42–44]

1.3.3 Reductive Amination

A useful way of synthesizing secondary amines from primary amines and carbonyl compounds is through reductive amination. Both aldehydes and ketones may be applied, making these types of reactions extremely versatile.[34,45] The mechanism proceeds over two steps. In the first step the primary amine and the carbonyl compound are in equilibrium with the imine (or iminium ion) and water. In the second step the imine is reduced with a hydride, which results in a secondary amine, see Scheme 1.12.[34]

Iminium ion
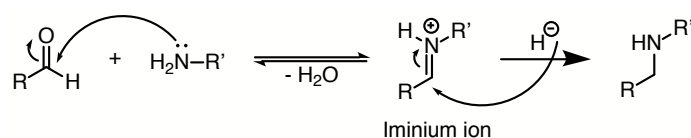
Scheme 1.12: General mechanism for reductive amination.[34]

As presented by Abdel-Magid *et al.*,[46] the reduction of imines from aldehydes gives high yields and have short reaction time when carried out in methanol and is reduced *in situ* with sodium borohydride ($NaBH_4$). This procedure was designed to reduce the amount of unwanted dialkylated products formed. Reductive amination with aldehydes and ketones containing *n*-membered rings in α-position are reported in the literature.[47,48]

1.3.4 Nucleophilic Aromatic Substitution

Nucleophilic aromatic substitution (S_NAr) can be performed under specific conditions. A typical S_NAr has an oxygen, nitrogen, or cyanide nucleophile, and a halide for a leaving group.[34,41] Thermal amination is a S_NAr reaction where an aromatic substrate undergoes a nucleophilic attack by an amine at an elevated temperature.[49] A heteroatom, or an electron-withdrawing group, *ortho* or *para* to the leaving group is necessary in order to stabilize the anion intermediate. The mechanism is an addition-elimination mechanism involving two steps: addition of the nucleophile at the carbon with the leaving group and elimination of the leaving group, see Scheme 1.13.[34,41]
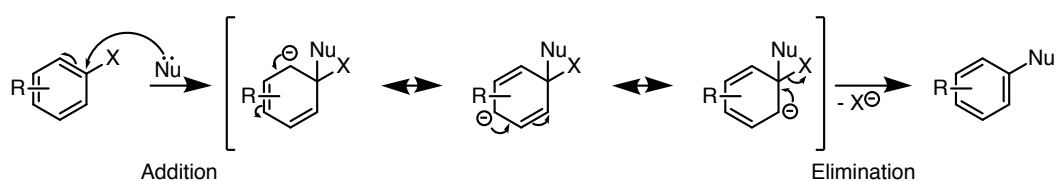
Scheme 1.13: A mechanism for general nucleophile aromatic substitution.[34]

The first step is rate limiting as it disrupts the aromaticity, while the second step is faster as it restores the aromaticity. Thus, the rate of which the leaving group is eliminated has usually no effect on the overall rate of the reaction. The effect of the leaving group is only visible on the first step, where highly electronegative halides favours this step. Other leaving groups are alkoxy, cyano, nitro, and sulfonyl groups. The rate of the addition step is highly dependent on the positioning of the heteroatom or the substituents on the substrate, and whether they are electron-withdrawing or electron-donating. The type of solvent is also a factor for the rate of the reaction, especially for charged reagents. The polarity of the solvent is positively correlated with the stability of charged compounds. Polar aprotic solvents enables a high reactivity of anionic reagents as the cationic counterparts are stabilized by high coordination with the solvent. This coordination can not be formed with the anion. Polar aprotic solvents with low polarity (as long as the nucleophile can be dissolved) is therefore favorable.[34,41]

1.3.5 Suzuki Cross-Coupling Reaction

Suzuki cross-coupling reaction is a palladium-catalyzed reaction with organoboron compounds for formation of sp^2-sp^2 carbon-carbon bonds.[50] The Suzuki reaction is probably one of the most important methods for synthesizing biaryl derivatives, which are present in natural products and pharmaceuticals. The reaction has several advantages such as low toxicity, stability towards air and moisture, as well as toleration of many functional groups.[51] Another advantage of this reaction is the retention of absolute configurations.[41]

The reaction involves coupling between two reagents that consists of two parts each, where one consists of an aryl or vinyl, and a halide, triflate or diazo group. The other species consists of an aryl, vinyl, or alkyl part, and a boronic acid, ester or borane. This results in the desired product of the coupled hydrocarbon parts of each reagent.[34,41]

The mechanism is proposed as a cycle of three steps as the palladium catalyst is regenerated in the last step, see Scheme 1.14.[34]
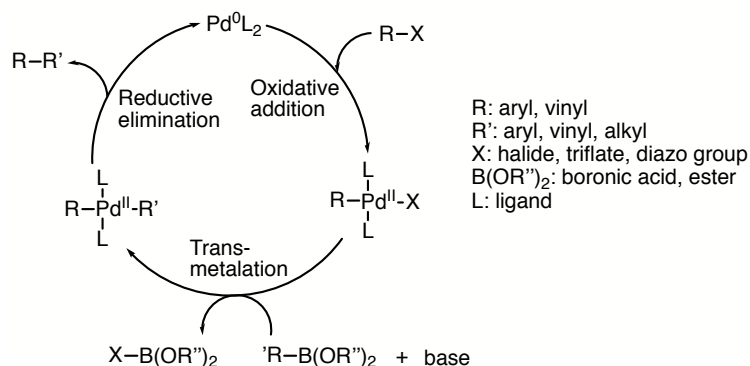
Scheme 1.14: A proposed mechanism for general Suzuki cross-coupling reaction.[34]

Oxidative addition of aromatic or vinylic halides (or triflates or diazo groups) to palladium(0) results in a palladium(II) intermediate that further undergoes transmetallation with an organoboron compound.[34,41]

An additional base is necessary as it accelerates the transmetallation step, which is rate determining, by enabling a nucleophilic attack of the organoboron compound to the palladium(II) intermediate. The boron atom in the organoboron compound is electron poor so that the electrons in the bond to the aryl, vinyl or alkyl group are shifted towards the boron atom. The base forms a complex with the organoboron compound, which results in increased electron density throughout the organoboron compound and therefore increased nucleophilicity of the aryl, vinyl or alkyl towards the palladium(II) intermediate.[41,52] For the same reason, when planning a synthesis with a Suzuki cross-coupling reaction, the substituent on the boronic acid, ester, or boronate, should have more of a nucleophilic character (more electron rich) than the one with the leaving group.[41]

Reductive elimination results in the product and the regenerated palladium(0) complex.[34,41] The cycle stops when all the starting material is consumed and the oxidative addition is no longer possible. Palladium(0) is known to aggregate as dimers or trimers forming palladium black, which deactivates the process.[53,54]

Common side reactions of the Suzuki cross-coupling reaction are protodeboronation, oxidation, and palladium catalyzed homocoupling of the boronic acids.[55] Formation of homocoupled dimer from the organoboron reagents are due to the presence of solvent-dissolved oxygen, which can stem from incomplete degassing

of solvents, or entry of oxygen through joints in the equipment.[55,56] As presented by Adamo *et al.*[57] the mechanism for formation of the homocoupled dimer involves a peroxo complex generated from the PdL_2 (or palladium(0)) complex and dioxygen. Removal of oxygen prior to the experiment should prevent formation of homocoupled dimers from the organoboron reagents.

Chapter 2

Results and Discussion

The aim of this master's thesis was to synthesize the 4,6-disubstituted pyrrolo[2,3-
d]pyrimidine compounds, **HHMT-070**, **HHMT-170**, and **HHMT-178**, see
Scheme 2.1. In addition, a new synthetic method for compound **HHMT-070**
and **HHMT-170** was investigated. The bioactivity of compound **HHMT-170**
was tested as well.

The first step towards the target molecules involved SEM protection of 4-chloro-
7*H*-pyrrolo[2,3-*d*]pyrimidine in position 7, resulting in compound **1**. Compound
5 was obtained through *ortho*-lithiation of the protected analogue **1** and nucle-
ophilic attack on molecular iodine, and compound **6** and **7** were obtained through
ortho-lithiation and reaction with cyclic ketones. The oxygen in the protection
group allowed selective lithiations in all three cases. Thermal amination of the io-
dinated derivative **5**, and the hydroxy derivatives **6** and **7** in position 4 resulted in
compound **9**, **10** and **13**, respectively. Iodination enabled Suzuki cross-coupling
of compound **9** in position 6 to achieve compound **14**. Lastly, SEM deprotection
of compounds **10**, **13** and **14**, resulted in the target molecules **HHMT-070**,
HHMT-170 and **HHMT-178**, respectively.
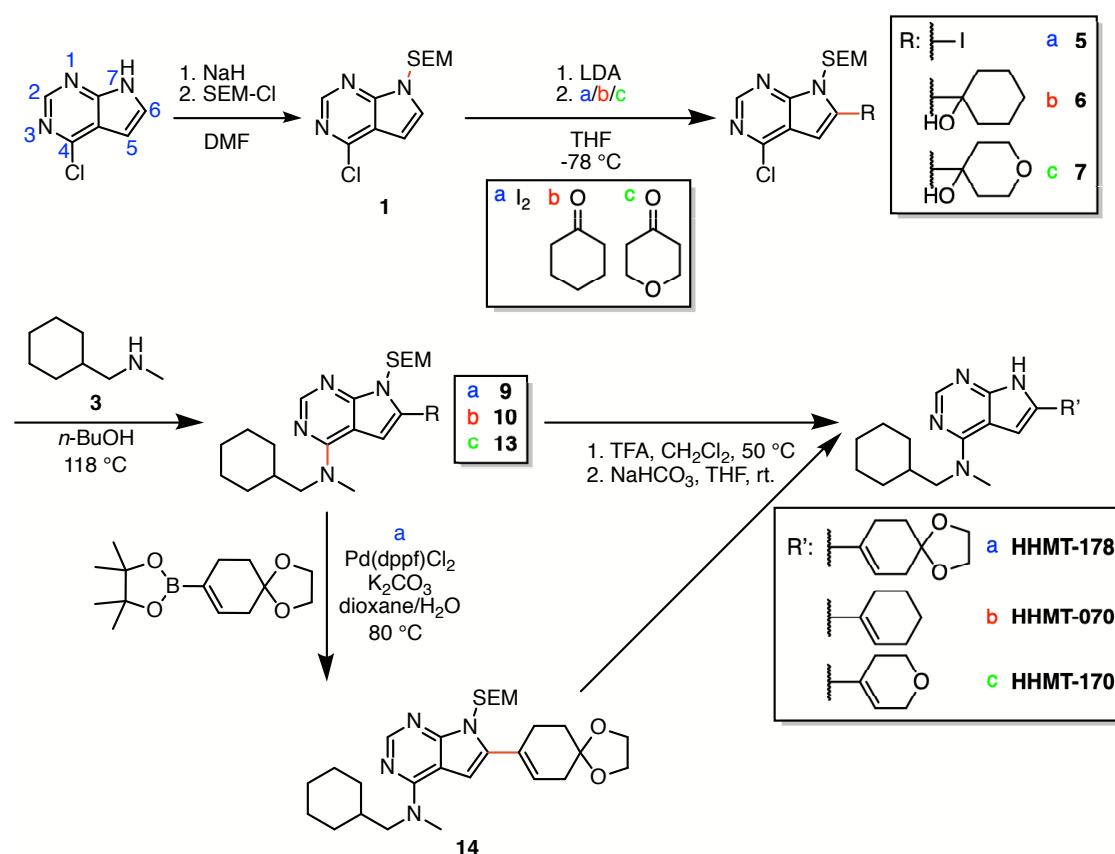
Scheme 2.1: Synthetic route I towards target molecule **HHMT-178** (*a*), and route II towards **HHMT-070** (*b*) and **HHMT-170** (*c*).

Compound **HHMT-070** has previously been synthesized through route I with iodination followed by a Suzuki cross-coupling, see Scheme 2.2.[33] The previous route will be compared to route II, which is presented in this master's thesis.
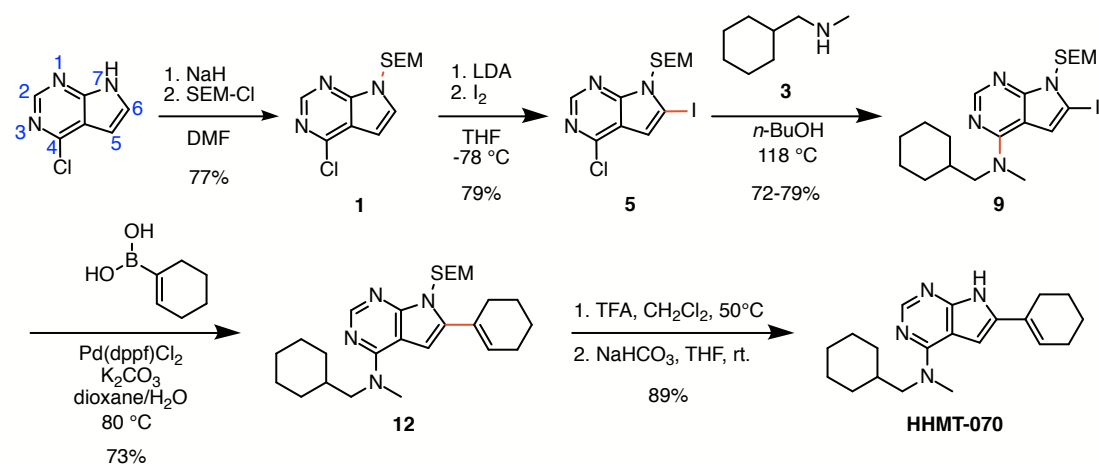
Scheme 2.2: Synthesis of compound **HHMT-070** from previously reported synthetic route.[33]

In the following sections, each step of the synthetic routes towards the target molecules will be discussed in more detail. Structure elucidations of the compounds will be presented at the end of this chapter.

2.1 SEM Protection – Synthesis of compound 1

The first step towards the target molecules was protection of the nitrogen in position 7 of 4-chloro-7H-pyrrolo[2,3-d]pyrimidine. The procedure was modified from the ones described in the pre-master's project by K. U. Larsen and the article by Lin *et al.*, see Scheme 2.3.[31,58]
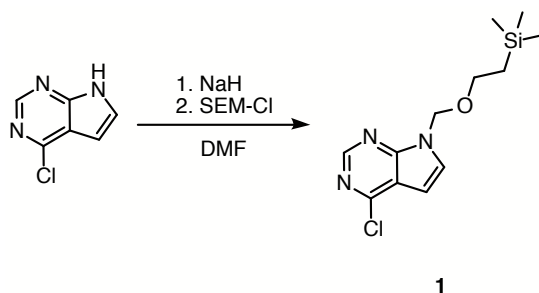
Scheme 2.3: Protection of 4-chloro-7H-pyrrolo[2,3-d]pyrimidine with SEM group to achieve compound **1**.

4-Chloro-7H-pyrrolo[2,3-d]pyrimidine and sodium hydride (NaH) were dissolved in dry dimethylformamide (DMF) under an inert atmosphere. 2-(Trimethylsilyl)-ethoxymethyl chloride (SEM−Cl) was added dropwise after the mixture was cooled to 0 °C. The mixture was then stirred at room temperature.

This reaction was performed in 2 g scale. Full conversion was obtained after stirring at room temperature for 1 hour. Extraction and purification by silica-gel column chromatography resulted in 87% yield of a colourless oil that was pure as observed by ^{1}H-NMR spectroscopy. Addition of a seed crystal gave white crystals with the short melting point interval of 33 - 34 °C, which indicated a high level of purity. The spectroscopic data for compound **1** are presented in Appendix A.

Byproduct **2**, see Figure 2.1, was also isolated in 1% yield as a colourless oil in semi-pure form after purification. This byproduct has previously been identified

by Kristin U. Larsen.[31] The spectroscopic data for byproduct **2** are presented in in Appendix B.
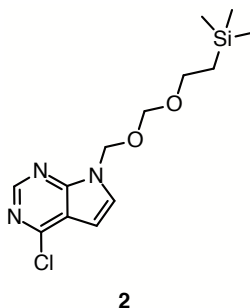
Figure 2.1: Structure of observed byproduct **2**.

2.2   Reductive Amination – Synthesis of compound 3

Compound **3** was synthesized from cyclohexanecarbaldehyde and methylamine *via* reductive amination. The procedure for synthesizing compound **3** was modified from the one described by Ehrhardt *et al.*,[59] see Scheme 2.4.
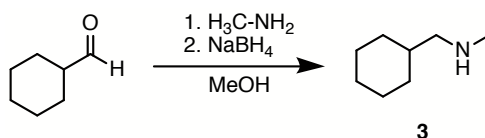
Scheme 2.4: Reductive amination of cyclohexanecarbaldehyde to achieve compound **3**.

Cyclohexanecarbaldehyde and methylamine were stirred in methanol at room temperature. Complete formation of the imine was observed by ^{1}H-NMR spectroscopy before sodium borohydride ($NaBH_4$) was added at 0 °C.

The first trial was performed in 3 g scale, and resulted in 4% yield with a purity of 39% determined by ^{1}H-NMR spectroscopy. The impurity has previously been identified in the pre-master's project, see Figure 2.2.[33]
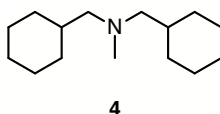
Figure 2.2: Structure of observed byproduct **4**.

The loss of product may be due to difficulties during the acid-base extraction. The pH was 13 during the basic extraction. Adjusting the pH of the water phase to 11 after the first acid-base extraction did not yield any more of compound **3** when extracting with CH_2Cl_2. Compound **3** is likely to be partly soluble in water, which could lead to further loss of product. The product may also have evaporated upon concentration *in vacuo* as it is a volatile compound with a low boiling point (Lit.[60] 144 °C at 760 torr).

The second trial was performed in 700 mg scale, and resulted in 45% yield with a purity of 77% as determined by ^{1}H-NMR spectroscopy. The impurity was byproduct **4**. The purpose of the acid-base extraction was to remove cyclohexylmethanol, which is a possible byproduct when the starting material is reduced with $NaBH_4$. This may have been the byproduct that was observed by ^{1}H-NMR spectroscopy of the reaction mixture prior to the extraction. This time the acidic extraction was performed with Et_2O, rather than CH_2Cl_2, as Et_2O is better for extracting oxygen-containing compounds and is less likely to dissolve the protonated product.[61] The reaction has previously been performed in 2 g scale and resulted in 63% yield with a purity of 95% determined by ^{1}H-NMR spectroscopy.[33] The main difference was the scale of the reaction, where a smaller scale is more water sensitive as the equilibrium position is dependent on the amount of water present (see Scheme 1.12).

A third trial of the reaction was conducted where a fraction of the reaction mixture underwent a slightly different work-up. After addition of $NaBH_4$ and stirring at room temperature for 3 hours, the mixture was divided into two parts of 20 mL and approximately 80 mL portions. The larger part underwent the same procedure as before, whereas the smaller part was stirred at pH 0 for 1 hour before proceeding to the regular work-up routine. The purpose of stirring at pH 0 was to split up the suspected formation of amine-boron complex, causing difficulties during extraction. Assuming a homogeneous mixture prior to the separation of the mixture, the procedures resulted in 42% yield with a purity of 92% for the larger part, and a yield of 22% with a purity of 86% for the smaller part. The purities were determined by ^{1}H-NMR spectroscopy, and the impurity was byproduct **4** in both cases. Hence, the standard work-up procedure resulted in approximately twice the amount of compound **3** and half the amount of **4** compared to the new procedure.

In an attempt to prevent the formation of byproduct **4**, a one-pot reaction was performed after studying the proposed mechanism presented in Scheme 2.5.
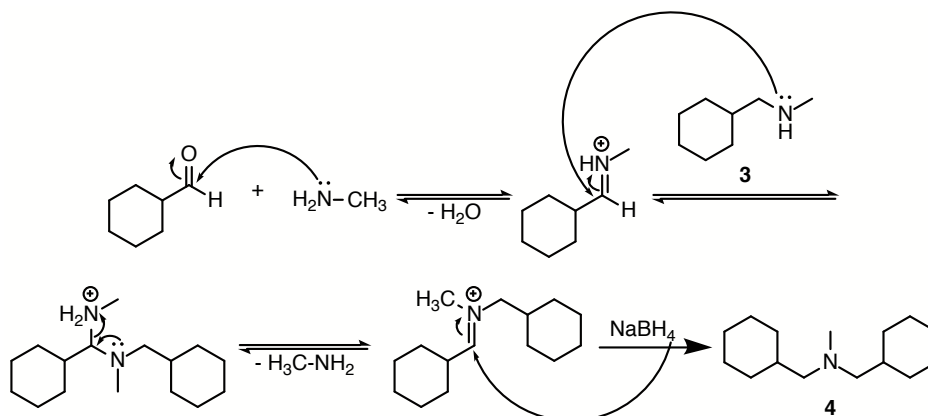
Scheme 2.5: Proposed mechanism for formation of byproduct **4**.

The one-pot reaction was performed with a weaker reducing reagent to prevent reduction of the starting material. Thus, $NaBH_4$ was replaced with sodium triacetoxyborohydride ($NaBH(OAc)_3$), see Scheme 2.6.
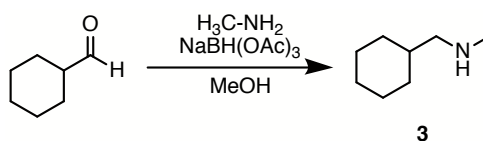
Scheme 2.6: Reductive amination of cyclohexanecarbaldehyde with sodium triacetoxyborohydride to achieve compound **3**.

The reaction was performed in 700 mg scale, and the mixture was stirred at room temperature for 3 days. No conversion was observed by ^{1}H-NMR spectroscopy. The reaction mixture was heated to 70 °C and stirred at this temperature for another 3 days. Finally, $NaBH_4$ was added due to low conversion, which resulted in 41% yield with a purity of 64% as determined by ^{1}H-NMR spectroscopy. This procedure did not prevent or reduce the formation of byproduct **4**. To prevent the formation of the byproduct another method for synthesizing compound **3** may be necessary. A suggestion is the substitution reaction with (bromomethyl)cyclohexane and methylamine in MeOH and water as reported by Daun *et al.*[62] The suggested procedure removes the water sensitivity problem with the imine as well. The spectroscopic data for compound **3** and byproduct **4** are presented in Appendix C. Purification of amine **3** by silica-gel column chro-

matography or by distillation was not performed before proceeding to thermal amination of compounds **5**, **6** and **7**.

2.3   *Ortho*-lithiation – Synthesis of compound 5-7

The procedure for iodination of compound **1** was modified from the ones described by Frank *et al.*[63] and by Kaspersen *et al.*,[64] see Scheme 2.7.
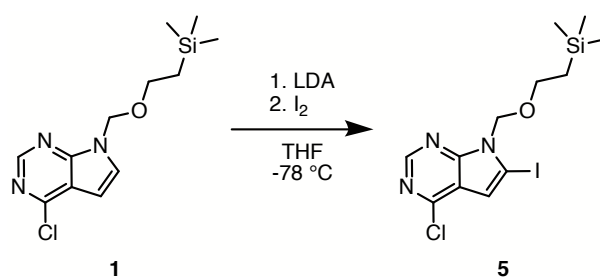
Scheme 2.7: Iodination of compound **1** to achieve compound **5**.

Compound **1** was dissolved in dry THF under an inert atmosphere. The reaction mixture was cooled to -78 °C with dry ice and acetone. LDA was added and stirred for 2 hours before addition of molecular iodine. Ammonium chloride was used to quench the reaction and the mixture was washed with sodium thiosulphate to remove excess iodine. The reaction was performed in 1 g scale. Full conversion was obtained and compound **5** was isolated in 92% yield. It was pure as observed by ^{1}H-NMR spectroscopy. The short melting point interval of 101 - 104 °C (Lit.[31,33] 101 - 103 °C) indicated a high level of purity as well. The spectroscopic data for compound **5** are presented in Appendix E.

Synthesis of compound **6** and **7** were performed following the same procedure as for the iodination with small alterations. Molecular iodine was replaced with cyclohexanone and tetrahydro-4*H*-pyran-4-one to achieve compound **6** and **7**, respectively. Sodium thiosulphate was not used during work-up. Compound **6** was synthesized from compound **1** through *ortho*-lithiation and reaction with cyclohexanone, see Scheme 2.8.
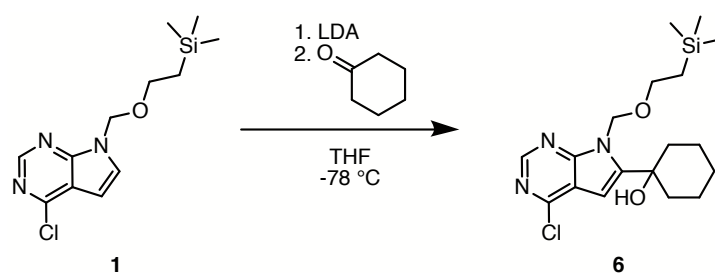
Scheme 2.8: *Ortho*-lithiation of compound **1** to achieve compound **6**.

The reaction for synthesis of compound **6** was performed twice at 200 mg scale. The first trial resulted in 93% conversion by ^{1}H-NMR spectroscopy, and a yield of 36%. During the reaction, the conversion was followed by TLC and a weak shadow of starting material may have been present on the TLC plate. The low yield was mainly due to mechanical loss during evaporation of the solvent. In addition, some product was discarded during purification by silica-gel column chromatography as the product overlapped with the starting material. The product was pure as observed by ^{1}H-NMR spectroscopy, and the short melting point interval of 72 - 74 °C indicated a high level of purity as well.

The second trial resulted in 87% conversion, and a yield of 76% with a purity of 98% determined by ^{1}H-NMR spectroscopy. Traces of methanol, observed in the ^{1}H-NMR spectrum, probably caused the larger melting point interval of 73 - 79 °C. The conversion was examined by TLC twice, 12 hours apart, and both TLC plates showed a shadow of the starting material. As there was no obvious change in conversion within 12 hours, the reaction was quenched. The low conversion may be due to previous water contamination in the LDA reagent bottle, resulting in addition of some equivalents of hydroxide, which is a weaker base, and fewer equivalents of LDA to the reaction mixture. In addition, the reaction contained more solvent in the second trial than the first trial, which allowed for more dissolved water. This also resulted in an significantly extended reaction time from 2.5 hours to 18 hours, which enabled more uptake of water from the surroundings through joints in the experimental setup. Once again, some product was discarded during purification by silica-gel column chromatography as the product overlapped with the starting material even with a new eluent system.

The main challenges with synthesis of compound **6**, was the overlap between the starting material and the product during purification by silica-gel column chromatography. However, if full conversion is achieved, problems during purifi-

cation could be avoided. The spectroscopic data for compound **6** are presented in Appendix F.

Compound **7** was synthesized from compound **1** through *ortho*-lithiation followed by reaction with tetrahydro-4*H*-pyran-4-one, see Scheme 2.9.
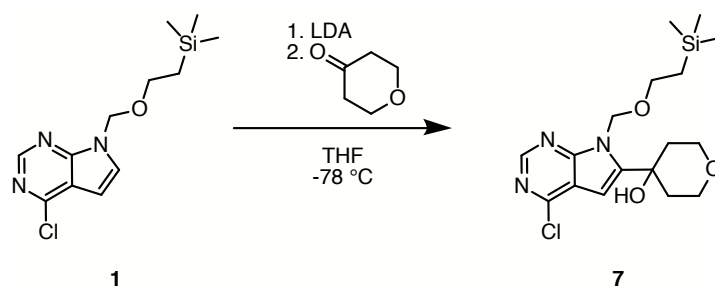
Scheme 2.9: *Ortho*-lithiation of compound **1** to achieve compound **7**.

The reaction was performed in 400 mg scale. This resulted in 79% conversion, and a yield of 70%. The conversion was examined by TLC, and the reaction was quenched when formation of a byproduct was observed. The byproduct was isolated during purification by silica-gel column chromatography, and identified as compound **8**, see Figure 2.3.
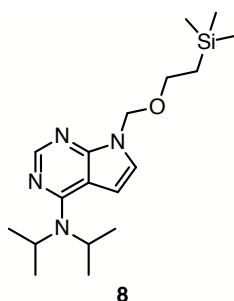
Figure 2.3: Structure of observed byproduct **8**.

Formation of byproduct **8** is likely due to nucleophilic aromatic substitution with LDA on compound **1** (see Section 1.3.4). There was overlap between compound **1** and **8** during purification by silica-gel column chromatography. However, compound **7** was easily separated from the two. Formation of byproduct **8** may be avoided by reducing the amount of LDA. The spectroscopic data for compound **7** and byproduct **8** are presented in Appendix G and H, respectively.

The main challenges with synthesis of compound **6** and **7** were believed to be formation of byproducts from aldol reactions with deprotonation of α-protons

from the cyclic ketones. However, these types of byproducts were not observed. The main obstacle was rather the LDA added to the substrates. Full conversion is hard to achieve with low amount of LDA. On the other hand, a high amount of LDA is likely to increase the formation of byproduct **8**.

Compared to the previous synthesis route for the target molecule **HHMT-070**, this reaction may replace the iodination and the Suzuki cross-coupling steps (see Scheme 2.2). However, the synthesis route is only shortened by one step if full dehydration will occur at a later stage as formation of a hydroxy group occurs at this step.

2.4   Thermal Amination – Synthesis of compound 9, 10 and 13

The procedure for amination of compound **5** was based on the ones described in the pre-master's project by K. U. Larsen and the article by Han *et al.*, see Scheme 2.10.[31,35]
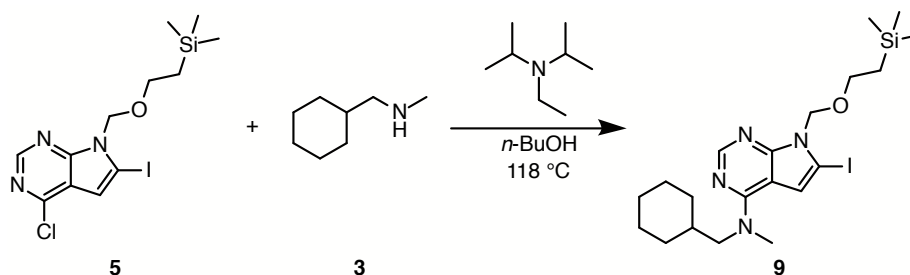
Scheme 2.10: Thermal amination of compound **5** to achieve compound **9**.

The reaction was performed in 1 g scale. Compound **5** was dissolved in *n*-butanol. Amine **3** and *N*-ethyl-*N*-isopropylpropan-2-amine (Hünigs base) were added under an inert atmosphere. The reaction mixture was heated to 118 °C and stirred at that temperature for 5.5 hours. This resulted in 93% conversion, and a yield of 60% with a purity of 98% as determined by ^{1}H-NMR spectroscopy. The mediocre yield was mainly due to mechanical loss when the mixture was heated. During addition of reagents, it was discovered that there was not enough of amine **3** for addition of 3 equivalents. Thus, addition of a co-base was required. It was then intended to run the reaction with 1.5 equivalents of both amine **3** and Hünigs base. However, due to miscalculations of the last minute decision only

0.26 equivalents of Hünigs base was added. The spectroscopic data for compound **9** are presented in Appendix I.

Synthesis of compound **10** and **13** was performed following the same procedure as for the amination of compound **9**. However, synthesis of **10** was done without Hünigs base, see Scheme 2.11.

Scheme 2.11: Thermal amination of compound **6** to achieve compound **10**.

The reaction was performed in 150 mg scale. This resulted in full conversion, a yield of 31% and a purity of 90% as determined by ^{1}H-NMR spectroscopy. The impurity was byproduct **4**, see Figure 2.2, from the synthesis of compound **3**.

The mediocre yield was due to formation of byproduct **11** (6% yield) and **12** (19% yield) during the reaction (see Scheme 2.12). Product loss was partly due to purification by silica-gel column chromatography, which was performed twice. The first purification isolated the product from the byproducts, and the second purification was in attempt to remove all traces of byproduct **4**. The material was proceeded without further purification as this was an intermediate and not the final target molecule. The spectroscopic data for compound **10** are presented in Appendix J.

A protonated hydroxy group is a good leaving group which enable substitution and elimination reactions. Byproduct **11** is proposed to be a product of an S_N1 reaction with n-BuOH, and byproduct **12** from the competing E1 reaction, see Scheme 2.12.
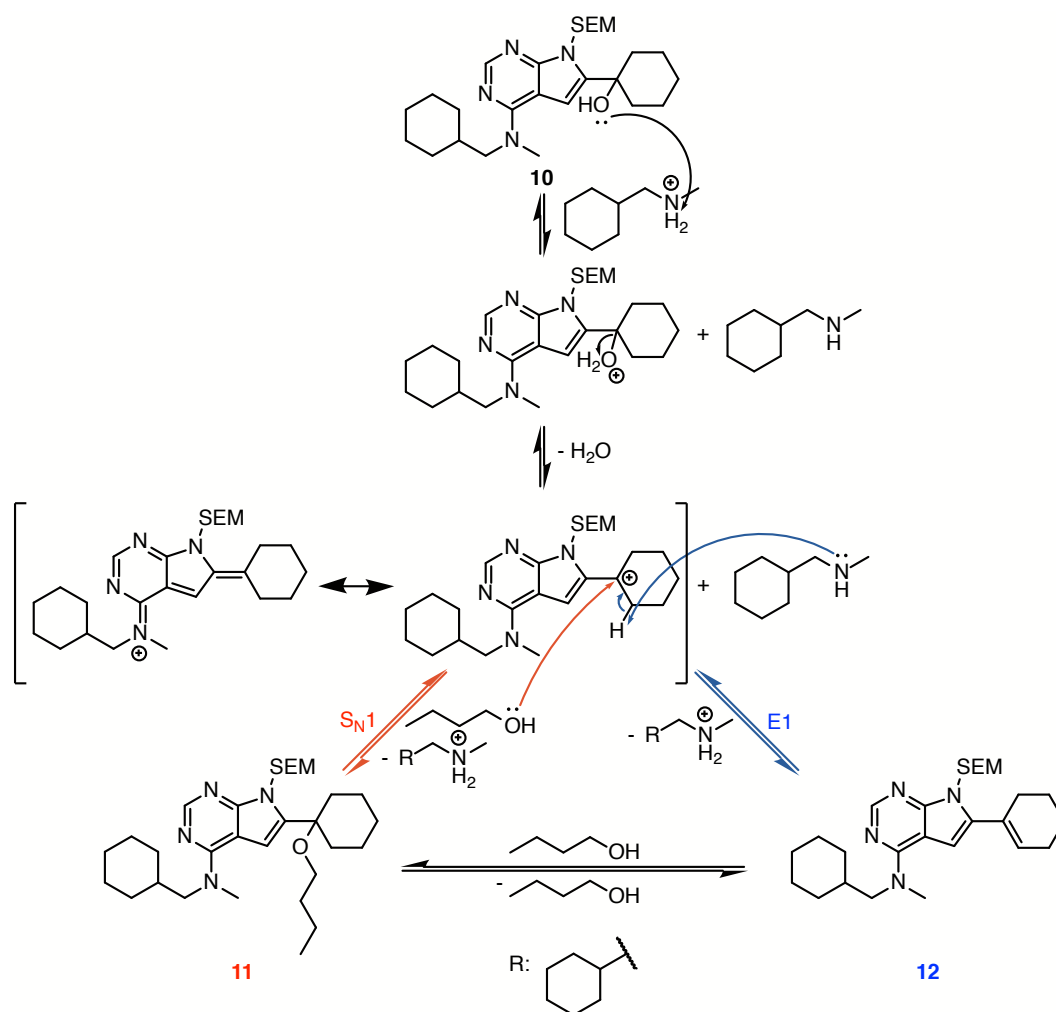
Scheme 2.12: Suggested mechanisms for formation of byproduct **11** and **12**, through S_N1 (red) and E1 (blue), respectively.

To favour E1 and avoid formation of byproduct **11**, *n*-BuOH should be replaced with a polar aprotic solvent. Increased reaction temperature favours E1 as well.[45]

Compound **10**, **11** and **12** could all be used as intermediates towards the synthesis of compound **HHMT-070**. Byproduct **11** could also undergo an elimination reaction to form compound **12** (or **HHMT-070** if this occurs during SEM deprotection where a strong acid is present). Compound **12** is an intermediate in the previous synthetic route (see Scheme 2.2). Thus, contamination by byproduct **4** remains the main challenge of this step. The spectroscopic data for byproduct **11** and **12** are presented in Appendix K and L, respectively.

Synthesis of compound **13** was performed through thermal amination of compound **7**, see Scheme 2.13.
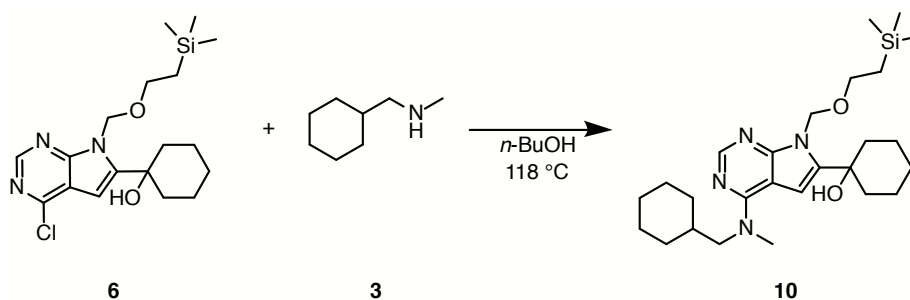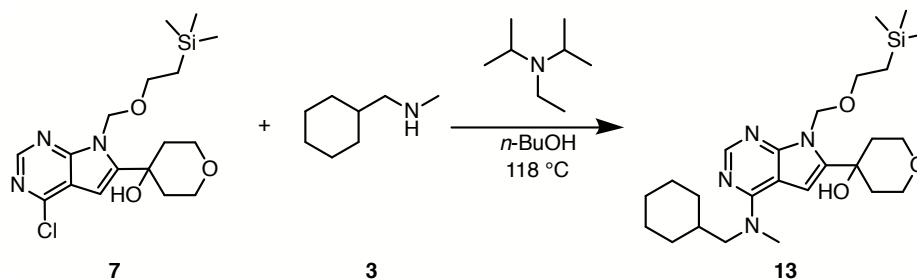

Scheme 2.13: Thermal amination of compound **7** to achieve compound **13**.

The reaction was performed in 370 mg scale. This resulted in full conversion. The crude product was first purified by silica-gel column chromatography, which resulted in a yield of 73% and a purity of 96% as determined by ^{1}H-NMR spectroscopy. The impurity was the amine byproduct **4**. Further purification by recrystallization reduced the yield to 45%. Additional recrystallizations of the mother liquor could probably have increased the yield. The product was pure as observed by ^{1}H-NMR spectroscopy, and the short melting point interval of 160 - 163 °C indicated a high level of purity as well. Purification by recrystallization seemed to be more facile when removing byproduct **4**. However, this method also resulted in a loss of 28% points of yield. On the other hand, multiple purifications by silica-gel column chromatography would also have resulted in significant product loss, in addition to a more demanding work load and the use of more solvents. On the contrary to the thermal amination of compound **6**, no formation of byproducts were observed. The spectroscopic data for compound **13** are presented in Appendix M.

2.5 Suzuki Cross-Coupling Reaction – Synthesis of compound 14

The procedure for synthesis of compound **14** *via* Suzuki cross-coupling reaction was based on the one described by Han *et al.*,[35] see Scheme 2.14.
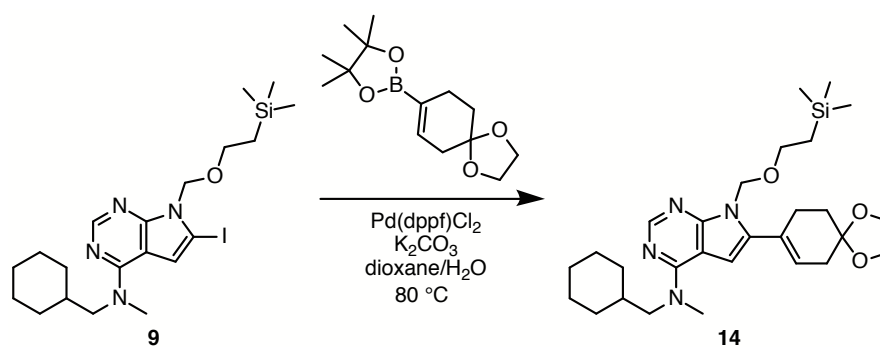
Scheme 2.14: Suzuki cross-coupling of compound **9** to achieve **14**.

Compound **9**, 4,4,5,5-tetramethyl-2-(1,4-dioxaspiro[4.5]dec-7-en-8-yl)-1,3,2-dioxaborolane, K_2CO_3 and Pd(dppf)Cl$_2$ were dissolved in 1,4-dioxane and water (2:1) and mixed at 80 °C under an inert atmosphere for 2 hours. The reaction was performed in 200 mg scale. This resulted in full conversion, and a yield of 71%. An excessive amount of base was added due to a miscalculation. The spectroscopic data for compound **14** are presented in Appendix N. A byproduct was isolated together with the excessive pinacol boronate ester during purification by silica-gel column chromatography. The byproduct is suspected to be the homocoupled dimer, **15**, see Figure 2.4.
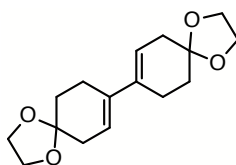
Figure 2.4: Structure of suspected byproduct **15**.

Formation of byproduct **15** is likely due to insufficient degassing of the solvents prior to the experiment (see Section 1.3.5). As presented by Miller *et al.*,[65] in addition to more sufficient degassing, introduction of potassium formate to the reaction may prevent formation of the homocoupled dimer. The spectroscopic data for byproduct **15** are presented in Appendix O.

2.6 SEM Deprotection – Synthesis of compound HHMT-070, HHMT-170 and HHMT-178

The last step towards the target molecules was the SEM-deprotections. The procedure for deprotection of compounds **10**, **13**, and **14**, was modified from the one described by Han *et al.*[35] Deprotection of compound **10** resulted in **HHMT-070**, see Scheme 2.15.
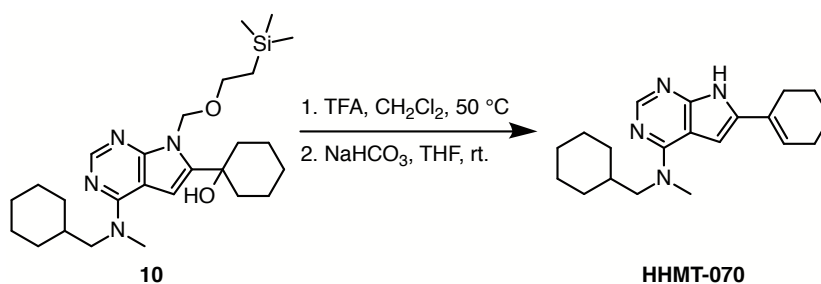
Scheme 2.15: Deprotection of compound **10** to achieve compound **HHMT-070**.

Compound **10** was dissolved in dry CH_2Cl_2 and TFA was added. The reaction mixture was heated and stirred at 50 °C until the $-Si(CH_3)_3$ peak could no longer be observed by ^{1}H-NMR spectroscopy. The reaction mixture was then concentrated *in vacuo*. The residue was dissolved in THF and saturated $NaHCO_3$ was added. The mixture was stirred at room temperature until complete.

The reaction was performed in 60 mg scale. This resulted in full conversion, and a yield of 41%. The crude product had a purity of 83% as determined by ^{1}H-NMR spectroscopy, where the main impurity was byproduct **4**. From synthesis of compound **13** it was discovered that purification by recrystallization was much more efficient than by silica-gel column chromatography for removal of byproduct **4**. After purification, there was some product loss due to its static electricity upon transferring between glass equipments. Additional recrystallizations of the mother liquor could probably have increased the yield, but were not performed. After purification the product was pure as observed by ^{1}H-NMR spectroscopy. The short melting point interval of 234 - 237 °C (Lit.[33] 216 - 234 °C) indicated a high level of purity as well. The spectroscopic data for compound **HHMT-070** are presented in Appendix P.

Compound **10** was completely dehydrated, meaning that an extra dehydration step in the synthetic route to obtain **HHMT-070** was not necessary. Compared to the previous synthetic route for compound **HHMT-070**, this synthetic strategy was one step shorter with an overall yield of 8%, whereas the previous route had an overall yield of 31%.

Similarly, deprotection of **13** resulted in compound **HHMT-170**, see Scheme 2.16.
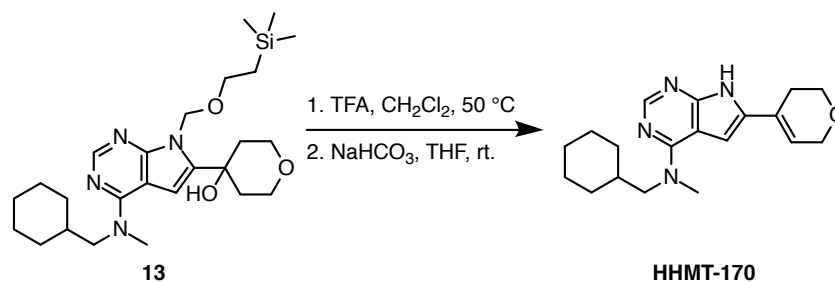
Scheme 2.16: Deprotection of compound **13** to achieve compound **HHMT-170**.

The reaction was performed in 180 mg scale. This resulted in full conversion, and a yield of 32%. A purity of 97% was determined by ^{1}H-NMR spectroscopy, even though the melting point interval of 202 - 207 °C was fairly short. The low yield was due to the many steps during purification. The crude product was first purified by silica-gel column chromatography. However, as the eluent system consisted of stabilized THF and CH_2Cl_2, the purified product contained 2,6-di-*tert*-butyl-4-methylphenol (or butylated hydroxytoluene, BHT), which is used to stabilize THF. After further purification by filtration through a plug of silica-gel, more impurities in low amounts were observed by ^{1}H-NMR spectroscopy, although BHT was removed. In preparation for a new filtration through a silica-gel plug, THF (not stabilized) was added to the previous filtrate in order to dissolve the product. The previously yellow solids became white as the liquid turned yellow. Isolation of the white solids was then done by vacuum filtration. Two additional recrystallizations of the new filtrate were performed. The spectroscopic data for compound **HHMT-170** are presented in Appendix Q.

If the purification had been performed by silica-gel column chromatography with THF that was not stabilized, even with an additional recrystallization if necessary, a higher yield would likely have been achieved.

Compound **HHMT-178** was achieved through deprotection of compound **14**,
see Scheme 2.17.
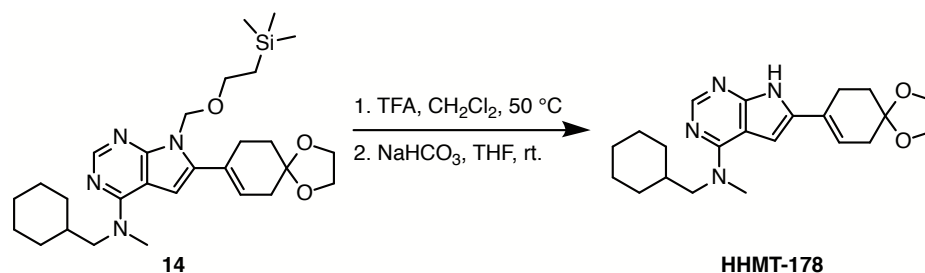
Scheme 2.17: Deprotection of compound **14** to achieve compound **HHMT-178**.

The reaction was performed in 70 mg scale. Compound **14** was dissolved in
CH_2Cl_2. TFA was added under an inert atmosphere and the mixture was stirred
for 2 hours at 50 °C before it was concentrated. At this stage, several pyrimidine
protons were observed by ^{1}H-NMR spectroscopy, as per usual after the first step
of the deprotection. This may be due to the derivatives presented in Section 1.3.1.
After stirring the mixture in $NaHCO_3$ for 21 hours, there were still derivatives of
the product present in the ^{1}H-NMR spectrum. Thus, the mixture was stirred in
another base, NH_3, in order to see if the mixture resolved into a single product.
The derivatives were still present after 47 hours, however. After purification, a
yield of 16% of **HHMT-178** was isolated in semi-pure form.

The ^{1}H-NMR spectrum for compound **HHMT-178** (see Appendix R) contains
two sets of doublets at 7.02 and 6.53 ppm, and 6.02 and 5.44 ppm, similar to the
ones observed for compound **1**. This indicates that there may be two impurities
present similar to compound **1**. Traces of a set of doublets were also observed
after the previous step where compound **14** was synthesized. The lack of SEM
signals in the spectrum indicates that they are deprotected as well. The slightly
increased integrals and small peaks around the amine signals (δ (in ppm): 3.61,
3.36, 1.88-1.82, 1.75-1.72, 1.68-1.66, 1.28-1.15, 1.06-0.98) suggests that one or
both of the impurities are aminated, see Figure 2.5. MS analysis confirmed
a chemical formula of $C_{14}H_{21}N_4$, which matched the suspected impurity (see
Appendix R).
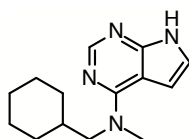
Figure 2.5: Suspected impurity isolated with compound **HHMT-178**.

A possible byproduct is formed by removing the ketal, resulting in a ketone in position 17, see Figure 2.6 (position numbering of compound **HHMT-178** is presented in Scheme 2.21 in Section 2.9.2). Removal of the ketal is usually performed under acidic conditions,[34] and have previously been done with TFA by Seo *et al.*[66] and Jones *et al.*[67] Due to poor separation during purification by silica-gel column chromatography, the byproducts formed were not isolated.
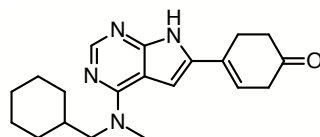
Figure 2.6: Suspected byproduct.

IR spectroscopy (see Appendix R) of the crude product showed absorption bands at 1733 cm^{-1} and 1673 cm^{-1}, which could indicate C=O stretch.[68] If the mixture had been stirred in TFA for more than 2 hours all of compound **HHMT-178** may have been deprotected in position 17, and purification of the crude product could have resulted in an increased yield of this derivative. The bioactivity of the deprotected ketal was also to be tested if the compound was successfully isolated.

Other methods for SEM deprotection could also have been carried out, such as deprotection with hydrochloric acid or tetrabutylammonium fluoride, as suggested by Chandra *et al.*[36]

2.7   Hydrogenation

Saturated derivatives of **HHMT-070**, **HHMT-170**, and **HHMT-178**, were desired as well. Only reduction of **HHMT-070** was tested. The procedure for hydrogenation of compound **HHMT-070** was modified from the ones described by Norman *et al.*[69] and Li *et al.*,[70] for similar structures, see Scheme 2.18. Safety precautions as described by Chandra and Zebrowski were also implemented.[71]
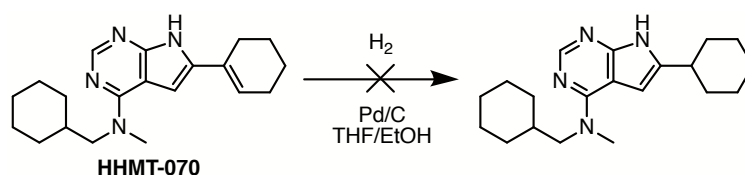
Scheme 2.18: Attempted hydrogenation of compound **HHMT-070** in THF/EtOH.

Compound **HHMT-070** was dissolved in degassed THF and EtOH, and mixed with Pd/C under an inert atmosphere. The mixture was purged with H_2-gas and stirred at room temperature. The first trial resulted in no conversion as observed by ^{1}H-NMR spectroscopy. Due to poor solubility, a lot more solvent was necessary to dissolve the starting material than intended. In addition, less catalyst was added to the mixture than intended as the catalyst was a fine powder that got lost upon addition. The lack of reactivity was believed to be due to too low concentration of the starting material and too small amount of catalyst.

The second trial was performed with more Pd/C and another solvent. As reported by Dyson and Jessop,[72] and Chandra and Zebrowski,[71] polar protic solvents with low flammability are preferable based on safety precautions and the protic solvents ability to promote rapid reactions. Previous experiences with the solubility of compound **HHMT-070**,[33] suggested that $CHCl_3$ may be used as solvent, especially as it fulfills the new criteria of being a polar protic solvent with low flammability. Conversion was still not observed. Eventually, MeOH was added since H_2 has the highest solubility in MeOH as reported by Rajadhyaksha and Karwa.[73] Conversion could still not be observed by ^{1}H-NMR spectroscopy. The reaction was then heated to 65 °C in attempt to activate the catalyst. However, after 3.5 hours there was still no consumption of starting material.

The third trial was partly based on the article by Norman *et al.*,[74] where the hydrogenation was performed at 5 atm of similar structures. This time compound **HHMT-070** was dissolved in $CHCl_3$ and MeOH, and the mixture was stirred at 6 atm H_2 for 25 hours. No conversion was observed. Higher pressure or temperature, or another catalyst, may be necessary to hydrogenate compound **HHMT-070**. The hydrogenation performed by Norman *et al.* was executed with PtO_2.[74]

2.8 *In vitro* CSF-1R inhibitory potency

High throughput screening (HTS) was performed, where an entire compound library was screened in an assay system of CSF-1R (FMS).[75] The compounds were supplied in a 10 mM DMSO solution. Enzymatic CSF-1R (FMS) inhibition potency was determined by Invitrogen (ThermoFisher) using their Z'-LYTE® assay technology, which is based on fluorescence resonance energy transfer.[76,77]

The percent inhibition of the enzyme was measured as the difference in rate of normal activity (a_n) and remaining activity when partly inhibited (a_i), divided by the rate of normal activity, see Equation 2.1.

$$\text{Percent inhibition} = \frac{a_n - a_i}{a_n} \times 100\% \qquad (2.1)$$

The titration curves were based on 20 data points each (2 sets of 10 data points) and the range of concentration was between 0.0495 nM and 1000 nM. Extracted from the data was the IC_{50}-values, which is the measured concentration at half of the maximum inhibition.

Among the compounds tested was **HHMT-170** with an IC_{50}-value of 0.4 nM. For reference, PLX3397 had the IC_{50}-value of 10.2 nM. The titration curves are illustrated in Figure 2.7 (the data points are given in Appendix S).
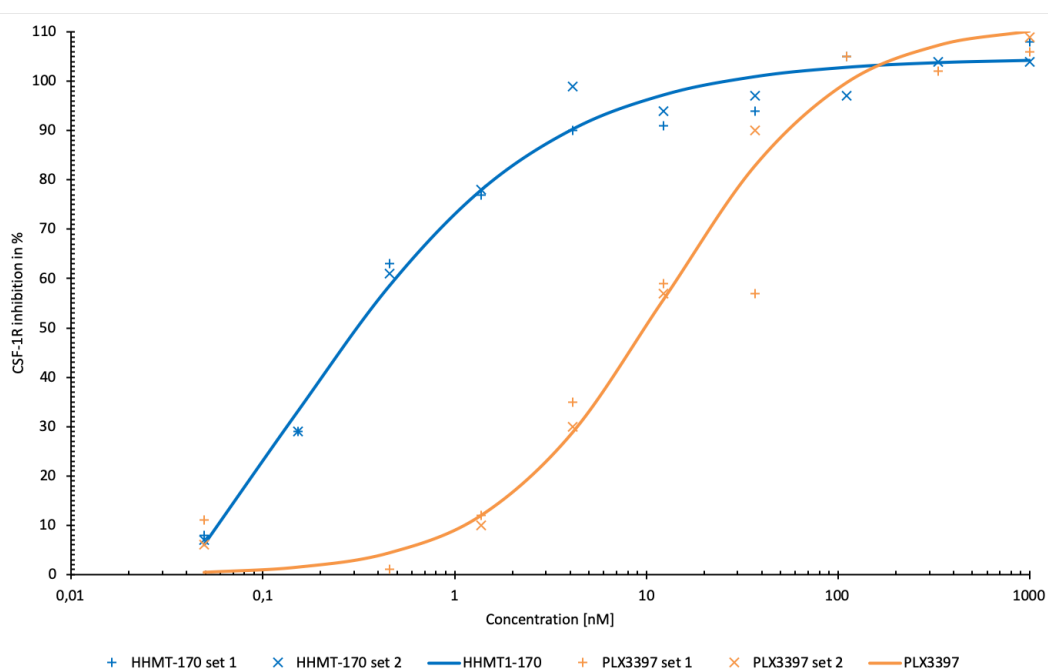
Figure 2.7: CSF-1R IC_{50} measurements of compound **HHMT-170** (IC_{50}: 0.4 nM) and PLX3397 (IC_{50}: 10.2 nM). They are based on 20 data points each.

The IC_{50}-value for compound **HHMT-170** was lower than the value for PLX3397, which is an inhibitor currently under clinical testing. However, due to the low concentration, the uncertainty is large and several additional tests should be conducted.

2.9 Structure Elucidation

Structure characterizations of the compounds were performed. Protons were assigned based on their chemical shifts, multiplicities and integrals from the ^{1}H-NMR spectrum. Couplings observed in the [1]H-^{1}H correlated spectroscopy (COSY) between neighbouring protons were used as well. Their respective carbons were identified by [1]H-^{13}C heteronuclear single quantum coherence spectroscopy (HSQC). The [1]H-^{13}C heteronuclear multiple bond correlation (HMBC) spectra were used to assign the quaternary carbons and neighbourless protons. High resolution mass spectroscopy (HRMS) and infrared spectroscopy (IR) were used to confirm the structures. All spectra can be found in their corresponding appendices A-R. A step by step structure elucidation of compound **13** is given in Section 2.9.1, followed by the position numbering of compound **1**, **6**, **7**, **8**, **10**, **11**, **13**, **14**, **HHMT-070**, **HHMT-170**, and **HHMT-178**, in Scheme 2.19 to Scheme 2.22 in Section 2.9.2. Their respective chemical shifts are presented in Table 2.4 to Table 2.7, followed by the MS and IR analysis.

2.9.1 Structure Elucidation – Step by step

This step by step structure elucidation by NMR is divided into four parts where different groups of the structure are undertaken. The spectra for compound **13** were recorded in $CDCl_3$ at 400 MHz for the proton spectrum and at 100 MHz for the carbon spectrum (see Appendix M). Figure 2.8 illustrates the position numbering of compound **13**. The spectroscopic data retrieved from ^{1}H-NMR and COSY are presented in Table 2.1, and the data retrieved from ^{13}C-NMR, HSQC and HMBC are presented in Table 2.2.
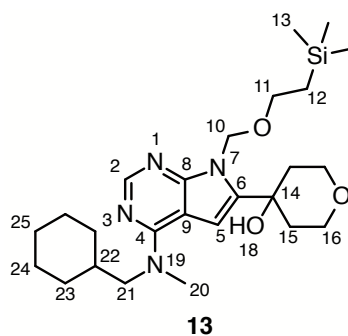
Figure 2.8: Position numbering of compound **13**.

Table 2.1: ^{1}H-NMR (400 MHz) and COSY for compound **13** recorded in CDCl$_3$. All shifts are given in ppm and calibrated with TMS at 0.00 ppm.

	^{1}H-NMR			COSY
Pos.	Chemical shift	Multiplicity	Integral	
2	8.29	s	1H	-
5	6.44	s	1H	-
10	5.90	s	2H	-
11/21	3.61 - 3.55	m	4H	1.86 - 1.81/0.93
12	0.93	dd	2H	3.61 - 3.55
13	-0.06	s	9H	-
15	4.00	td	2H	3.88 - 3.85/2.17/2.06 - 2.03
15	3.88 - 3.85	m	2H	4.00/2.17/2.06 - 2.03
16	2.17	td	2H	4.00/3.88 - 3.85/2.06 - 2.03
16	2.06 - 2.03	m	2H	4.00/3.88 - 3.85/2.17
18	4.13	s	1H	-
20	3.36	s	3H	-
22	1.86 - 1.81	m	1H	3.61 - 3.55/1.06 - 0.97
23	1.06 - 0.97	m	2H	1.75 - 1.68/1.27 - 1.15
23/24/25	1.75 - 1.68	m	5H	1.27 - 1.15/1.06 - 0.97
24/25	1.27 - 1.15	m	3H	1.75 - 1.68/1.06 - 0.97

Table 2.2: ^{13}C-NMR (100 MHz), HSQC and HMBC for compound **13** recorded in CDCl$_3$. All shifts are given in ppm and calibrated with TMS at 0.00 ppm.

Pos.	^{13}C-NMR	HSQC	HMBC
2	151.8	8.29	-
4	157.2	-	8.29/3.61 - 3.55/3.36
5	100.8	6.44	-
6	140.3	-	6.44/5.90/4.13
8	153.5	-	8.29/6.44/5.90
9	101.4	-	6.44
10	71.0	5.90	3.61 - 3.55
11	66.4	3.61 - 3.55	5.90/0.93
12	17.9	0.93	3.61 - 3.55
13	-1.5	-0.06	0.93
14	67.4	-	6.44/4.13/4.00/3.88 - 3.85/2.06 - 2.03
15	63.5	4.00/3.88 - 3.85	4.00/3.88 - 3.85/2.17
16	38.1	2.17/2.06 - 2.03	4.13/4.00
20	39.3	3.36	3.61 - 3.55
21	57.2	3.61 - 3.55	3.36
22	37.3	1.86 - 1.81	3.61 - 3.55
23	30.9	1.75 - 1.68/1.06 - 0.97	3.61 - 3.55
24	25.9	1.75 - 1.68/1.27 - 1.15	-
25	26.5	1.75 - 1.68/1.27 - 1.15	-

The SEM protection group

Starting with one of the most recognizable proton signals from Table 2.1, the singlet at -0.06 ppm with an integral of 9H is assigned to the methyl protons in the SEM group at position 13 (see Figure 2.8). The corresponding carbon is residing at -1.5 ppm as observed by HSQC. Note that the coupling is observed at 199.1 ppm, not -1.5 ppm, along the F1 projection due to spectral aliasing.[78–80] COSY confirms that there are no neighbouring protons to the ones at -0.06 ppm as there are no couplings observed. HMBC shows coupling between the corresponding carbon at -1.5 ppm and the protons at 0.93 ppm. The proton signal at 0.93 ppm is a doublet of doublets with an integral of 2H and is therefore assigned to position 12. The corresponding carbon is residing at 17.9 ppm. COSY is then used to identify the protons in position 11, which are represented as a

multiplet at 3.61 - 3.55 ppm. However, this signal has an integral of 4H, meaning that there are two protons with the same shift in another part of the structure. As a result of this, there are two corresponding carbon shifts to the protons at 3.61 - 3.55 ppm as seen in HSQC. The carbon shift of the carbon at position 11 is recognized by the long-ranged couplings from HMBC, where the carbon at 66.4 ppm is coupled to the protons at 5.90 ppm and 0.93 ppm. The protons at 5.90 ppm can then be assigned to position 10, together with the carbon residing at 71.0 ppm.

The amine group

The singlet residing at 3.36 ppm with an integral of 3H is assigned to position 20 together with the carbon at 39.3 ppm. COSY confirms that there are no neighbouring protons to the ones at 3.36 ppm as there are no couplings observed. However, long-ranged coupling with the protons at 3.61 - 3.55 ppm can be observed, assigning the protons to position 21 together with the carbon at 57.2 ppm. The proton in position 22 is then identified, through COSY, to be at 1.86 - 1.81 ppm. The corresponding carbon resides at 37.2 ppm. The protons in position 23 is identified due to coupling between the proton at 1.86 - 1.81 ppm and the protons at 1.06 - 0.97 ppm in COSY. However, the signal at 1.06 - 0.97 ppm has an integral of 2H only. HSQC shows that the carbons in position 23 at 30.9 ppm, have connected protons that are distributed over two different multiplets. These protons are diastereotopic.[81] Thus, both the protons at 1.06 - 0.97 ppm and two of the protons at 1.75 - 1.68 ppm are assigned to position 23. COSY then shows coupling with a new pair of diastereotopic protons with shifts at 1.75 - 1.68 ppm and 1.27 - 1.15 ppm, which are connected to the carbons at 26.5 ppm and 25.9 ppm. To distinguish between the two carbons, a closer look at the integral at 1.75 - 1.68 ppm is necessary, see Figure 2.9.
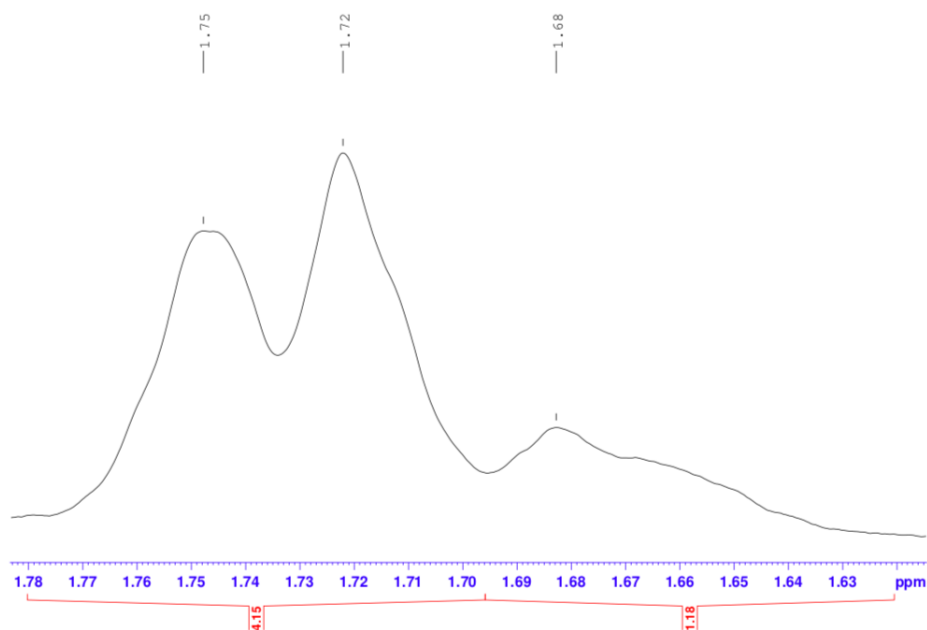
Figure 2.9: Close-up of multiplet at 1.75 - 1.68 ppm in the ^{1}H-NMR spectrum (400 MHz, CDCl$_3$) of compound **13**.

The integral of 5H at 1.75 - 1.68 ppm can roughly be divided into integrals of 4H and 1H if the signal is split into two parts (1.75 - 1.72 ppm and 1.68 ppm). HSQC shows that 1.68 ppm is attached to 26.5 ppm, see Figure 2.10. Due to symmetry of the cyclohexane, these signals are assigned to position 25 as the integral of 1H is an odd number of protons. Lastly, the carbons with shift at 25.9 ppm is assigned to position 24.
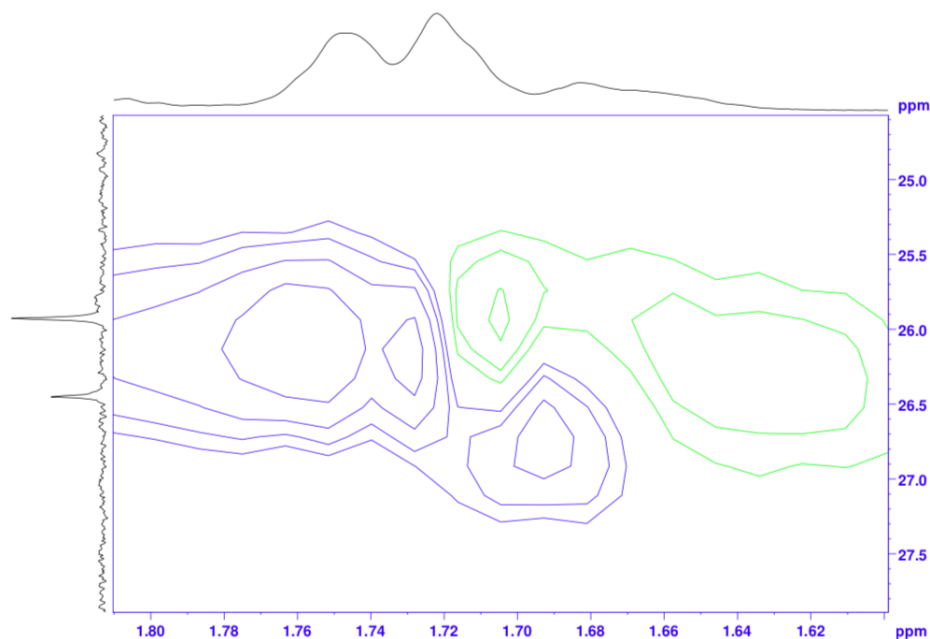
Figure 2.10: Close-up of coupling between the proton signal at 1.75 - 1.68 ppm and the carbon signals at 26.5 ppm and 25.9 ppm in the HSQC spectrum of compound **13** in CDCl$_3$.

The pyrrolo[2,3-*d*]pyrimidine core structure

There are two protons directly attached to the pyrrolo[2,3-*d*]pyrimidine core structure. These protons should have relatively high shifts due to the ring current effect in aromatic heterocycles.[81] Following the structure assignment (Table 2.1) there are three protons shifts left that are not assigned, with an integral of 1H each, the ones at 8.29 ppm, 6.44 ppm, 4.13 ppm. However, coupling between the proton at 4.14 ppm and any carbon is not observed by HSQC, meaning that it is not one of the protons on the pyrrolo[2,3-*d*]pyrimidine core structure. The proton with the highest shift of 8.29 ppm is assigned to position 2 as the proton in this position is deshielded by two nitrogen atoms. Consequently, the proton with the lower shift of 6.44 ppm is assigned to position 5. The carbon shifts at 151.8 ppm and 100.8 ppm is then assigned accordingly by HSQC. The assignment of the tertiary sp^2 carbons are fully based on long-ranged coupling by HMBC. The carbon with shift at 157.2 ppm is coupled with protons at 8.29 ppm, 3.61 - 3.55 ppm and 3.36 ppm (position 2, 21 and 20, respectively), is assigned to position 4. The carbon with shift at 153.5 ppm is coupled with protons at 8.29 ppm, 6.44

ppm and 5.90 ppm (position 2, 5 and 10, respectively), is assigned to position 8. The carbon with shift at 140.3 ppm is coupled with protons at 6.44 ppm and 5.90 ppm (position 5 and 10, respectively), and 4.13 ppm, is assigned to position 6. Lastly, the carbon with shift at 101.4 ppm is coupled with 6.44 ppm (position 5) is assigned to position 9.

The substituted group at position 6

The carbon at 140.3 ppm in position 6 has a long-range coupling to the proton at 4.13 ppm. As mentioned previously, the proton at 4.13 ppm is not coupled with any carbon by HSQC, which indicates that this is the hydroxy group in position 18. The last quaternary carbon with shift at 67.4 ppm was assigned to position 14. This carbon is coupled with the protons at 6.44 ppm, 4.13 ppm, 4.00 ppm, 3.88 - 3.85 ppm and 2.06 - 2.03 ppm. Both 4.00 ppm and 3.88 - 3.85 ppm are diastereotopic protons assigned to carbon at 63.5 ppm in position 15. From COSY, these protons are coupled with the protons at 2.17 ppm and 2.06 - 2.03 ppm, another pair of diastereotopic protons. Together with the carbon at 38.1 ppm, the protons are assigned to position 17.

MS

The results from the MS analysis is used to confirm the structure deduced from the NMR analysis. The MS spectrum given in Appendix M confirmed that compound **13** has the chemical formula $C_{25}H_{42}N_4O_3Si$.

IR

IR spectroscopy is also used to confirm the structure deduced from the NMR analysis. The IR spectrum for compound **13** is given in Appendix M. A strong absorption band at 3388 cm^{-1} indicates the presence of O$-$H stretching vibrations. Strong absorption bands at 2924 cm^{-1} and 2856 cm^{-1} may indicate the presence of sp^3-hybridized C$-$H stretching vibrations. In addition, strong absorption bands at 1575 cm^{-1} and 1508 cm^{-1} are due to C=C or N=C stretching vibrations. C$-$H bending vibrations in cyclohexane are indicated by a medium absorption band at 1449 cm^{-1}. Absorption band at 1386 cm^{-1} indicate the presence of symmetric C$-$H bending from methyl groups. Asymmetric C$-$O$-$C

stretch is observed as a strong absorption band at 1076 cm⁻¹. Lastly, a medium
absorption band at 763 cm⁻¹ is due to C−H out-of-plane bending in aromatics.[68]

2.9.2 Compounds and Assigned Shifts

The compounds are presented in four groups, based on their synthetic steps and
structural similarities. Compound **1**, **6** and **7** are grouped together as compound
6 and **7** are products of *ortho*-lithiation of compound **1**. Amination of **6** and **7**
resulted in compound **10** and **13**, respectively. They are grouped together with
compound **14**, which contains the amine as well. **HHMT-070**, **HHMT-170**
and **HHMT-178** are grouped together as they are all deprotected. Lastly, the
two byproducts **8** and **11** are grouped together. An overview of common solvents
and organics that can be observed in the recorded ¹H-NMR spectra is given in
Table 2.3.

Table 2.3: Common solvents and organics that can be observed in the ¹H-NMR spectra recorded in $CDCl_3$ and DMSO-d_6.[82]

Solvents and organics	In $CDCl_3$	In DMSO-d_6
Acetone	2.17	2.09
Dichloromethane	5.30	5.76
Ethyl acetate	2.05	1.99
	4.12	4.03
	1.26	1.17
Grease	0.84 - 0.87	0.82 - 0.88
	1.25	1.24
Methanol	3.49	3.16
	1.09	4.01
Tetrahydrofuran	3.76	3.60
	1.85	1.76
Water	1.56	3.33

Compound 1, 6 and 7

The position numbering of compound **1**, **6** and **7** are given in Scheme 2.19 and
the assigned chemical shifts in Table 2.4 are extracted from Appendix A, F and
G, respectively.
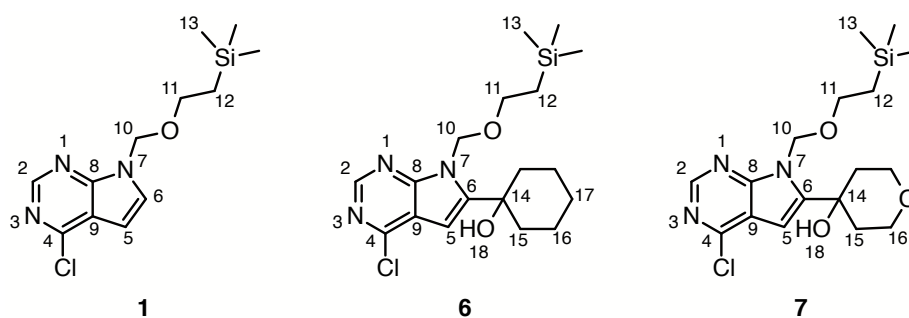
Scheme 2.19: Position numbering of compound **1**, **6** and **7**.

Table 2.4: ^{1}H-NMR and ^{13}C-NMR shifts for compound **1**, **6** and **7**. All shifts are given in ppm. The compounds that are recorded in DMSO-d_6 are calibrated with DMSO at 2.50 ppm in ^{1}H-NMR and 39.52 ppm in ^{13}C-NMR. The compounds that are recorded in CDCl$_3$ are calibrated with TMS at 0.00 in both ^{1}H-NMR and ^{13}C-NMR.[82]

	Compound					
	^{1}H-NMR in ppm				^{13}C-NMR in ppm	
Pos.	**1**	**1**	**6**	**7**	**6**	**7**
	(DMSO-d_6)	(CDCl$_3$)	(DMSO-d_6)	(CDCl$_3$)	(DMSO-d_6)	(CDCl$_3$)
2	8.69	8.67	8.64	8.64	150.5	151.3
4	-	-	-	-	150.0	152.2
5	6.72	6.67	6.54	6.55	96.1	98.4
6	7.88	7.39	-	-	150.7	147.7
8	-	-	-	-	153.2	153.6
9	-	-	-	-	115.8	116.7
10	5.65	5.65	5.99	5.98	71.6	71.8
11	3.52	3.53	3.64	3.59	66.1	67.1
12	0.82	0.91	0.83	0.94	17.4	18.0
13	-0.10	-0.05	-0.09	-0.05	-1.4	-1.4
14	-	-	-	-	69.5	68.2
15	-	-	2.16 - 2.13/	2.24/	36.9	38.1
			1.86 - 1.70	2.09 - 2.05		
16	-	-	1.86 - 1.70/	4.00/	21.3	63.3
			1.53 - 1.50	3.91 - 3.88		
17	-	-	1.63 - 1.60/	-	25.1	-
			1.28 - 1.25			
18	-	-	5.28	3.66	-	-

The proton shifts in the pyrrolo[2,3-*d*]pyrimidine core structure decrease when substituting the proton in position 6 with cyclohexane or tetrahydro-2*H*-pyran (compound **6** and **7**, respectively). This decrease in chemical shifts indicates that the substituents have a shielding, or electron donating, effect on the electron poor aromatic ring. However, the proton shifts in the SEM protection group increases, especially in position 10, indicating a deshielding, or electron withdrawing, effect.

Compound 10, 13 and 14

The position numbering of compound **10**, **13** and **14** are illustrated in Scheme 2.20. The assigned chemical shifts given in Table 2.5 are extracted from Appendix J, M and N, respectively.

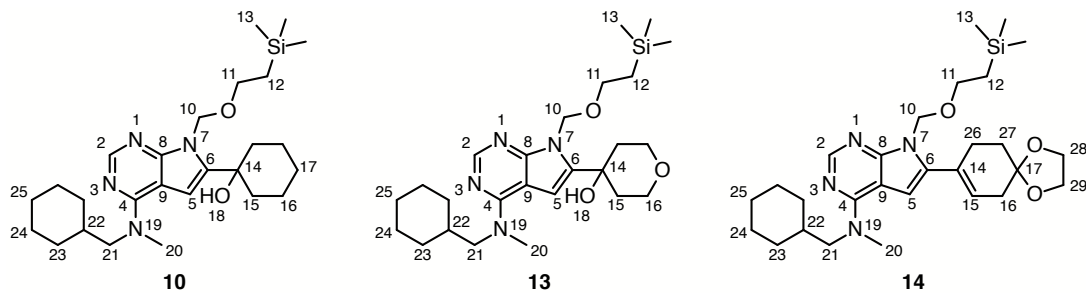**Scheme 2.20:** Position numbering of compound **10**, **13** and **14**.

Table 2.5: ^{1}H-NMR and ^{13}C-NMR shifts for compound **10**, **13** and **14**. All shifts are given in ppm. The compounds are recorded in CDCl$_3$ and calibrated with TMS at 0.00 in both ^{1}H-NMR and ^{13}C-NMR.

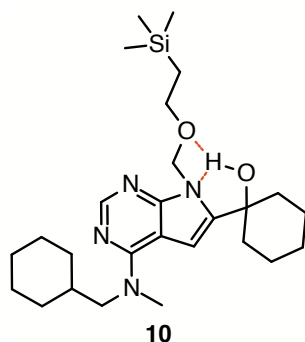|	Compound					
	^{1}H-NMR in ppm			^{13}C-NMR in ppm		
Pos.	**10**	**13**	**14**	**10**	**13**	**14**
2	8.29	8.29	8.29	151.6	151.8	151.4
4	-	-	-	157.2	157.2	156.9
5	6.44	6.44	6.43	100.8	100.8	100.7
6	-	-	-	141.7	140.3	137.2
8	-	-	-	153.5	153.5	153.3
9	-	-	-	101.7	101.4	102.4
10	5.91	5.90	5.57	71.3	71.0	70.8
11	3.61 - 3.57	3.61 - 3.55	3.70	66.4	66.4	66.1
12	0.93	0.93	0.93	18.0	17.9	18.0
13	-0.06	-0.06	-0.04	-1.4	-1.5	-1.4
14	-	-	-	70.2	67.4	128.0
15	2.13 - 2.10/ 1.91 - 1.79	4.00/ 3.88 - 3.85	6.25	38.2	63.5	125.8
16	1.91 - 1.79/ 1.63 - 1.59	2.17/ 2.06 - 2.03	2.52 - 2.51	22.1	38.1	36.2
17	1.75 - 1.68/ 1.25 - 1.18	-	-	25.8	-	107.5
18	3.75	4.13	-	-	-	
20	3.36	3.36	3.35	39.4	39.3	39.1
21	3.61 - 3.57	3.61 - 3.55	3.60	57.3	57.2	57.1
22	1.91 - 1.79	1.86 - 1.81	1.85 - 1.82	37.4	37.3	37.2
23	1.75 - 1.68/ 1.03 - 0.94	1.75 - 1.68/ 1.06 - 0.97	1.74 - 1.68/ 1.05 - 0.97	31.0	30.9	30.8
24	1.75 - 1.68/ 1.25 - 1.18	1.75 - 1.68/ 1.27 - 1.15	1.74 - 1.68/ 1.24 - 1.18	26.1	25.9	25.9
25	1.75 - 1.68/ 1.25 - 1.18	1.75 - 1.68/ 1.27 - 1.15	1.74 - 1.68/ 1.24 - 1.18	26.6	26.5	26.5
26	-	-	1.93	-	-	31.4
27	-	-	2.66	-	-	28.3
28	-	-	4.03	-	-	64.5
29	-	-	4.03	-	-	64.5

The protons in position 28 and 29 in compound **14** are recorded as one singlet with an integral of 4H at 4.03 ppm in the ^{1}H-NMR spectrum. However, the two protons in each position are diastereotopic, and as presented by Friebolin,[81] two diastereotopic protons should have different chemical shifts. The singlet can be explained by the large distance between the protons and the cyclohexene, or by rapid motion over the ketal. ^{1}H-NMR (400 MHz, CDCl$_3$) temperature experiments were conducted at 27 °C, 0 °C, and -10 °C, in attempt to reduce the motion over the ketal. In all three instances, the peak remained a singlet as seen in Figure 2.11.
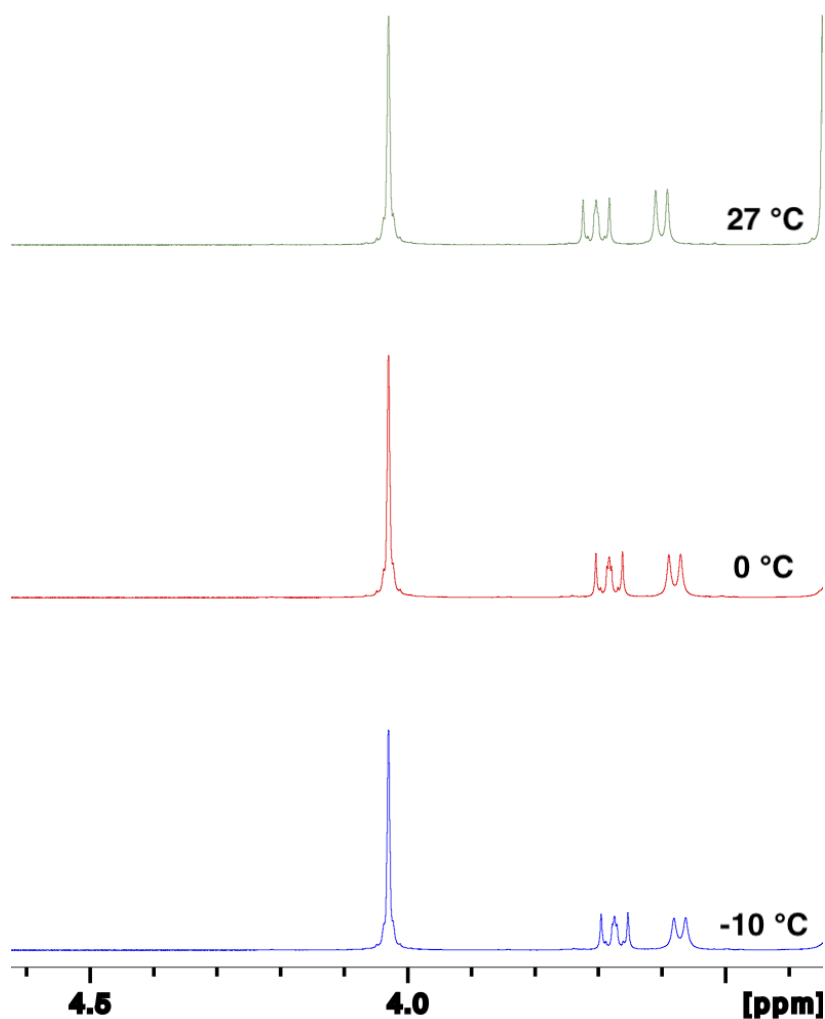
Figure 2.11: Close-up of ^{1}H-NMR spectra (400 MHz, CDCl$_3$) of compound **14** recorded at 27 °C, 0 °C and -10 °C.

As the singlet remained unchanged over almost 40 °C, it was expected that any change in multiplicity would happen at a much lower temperature than −10 °C. Recordings at lower temperatures were not conducted due to instrument restrictions. Further examinations are necessary in order to conclude whether the singlet stems from rapid motion or not.

The chemical shifts of the pyrrolo[2,3-*d*]pyrimidine core structure, the SEM protection group, and the amine group, in compound **10** and **13** are approximately the same. Thus, the oxygen in position 17 in compound **13** has no effect on the rest of the structure. For compound **14** the substituent in position 6 does not seem to affect the chemical shifts on the rest of the structure, except from the decrease in position 10. As mentioned for compound **6** and **7** it seems like a hydroxy group in position 14 increases the chemical shift in position 10. This might be due to hydrogen bonding between the hydroxy proton and the nitrogen in position 7, or the oxygen between position 10 and 11, see Figure 2.12. The hydroxy proton is likely to withdraw electrons with the hydrogen bonding, resulting in deshielding of the protons on the adjacent carbon. Thus, an increase of the chemical shifts may be observed.


Figure 2.12: Suggested intramolecular hydrogen bonding in compound **10**.

Hydrogen bonding with the oxygen between position 10 and 11 forms a seven-membered ring, which is more probable due to more flexibility with the wider angles and shorter distances in between the atoms.[83] However, the chemical shift difference is larger for the protons in position 10, than the ones in position 11. When only considering this effect, it seems like the hydrogen bonding is between the hydroxy proton and the nitrogen in position 7.

Compound HHMT-070, HHMT-170 and HHMT-178

The position numbering of compound **HHMT-070**, **HHMT-170** and **HHMT-178** are illustrated in Scheme 2.21. The assigned chemical shifts given in Table 2.6 are extracted from Appendix P, Q and R, respectively.
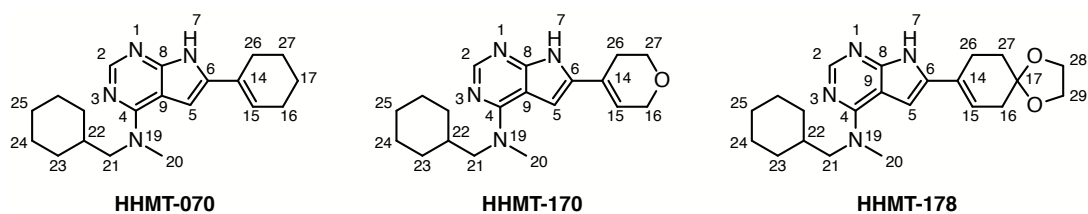
Scheme 2.21: Position numbering of compound **HHMT-070**, **HHMT-170** and **HHMT-178**.
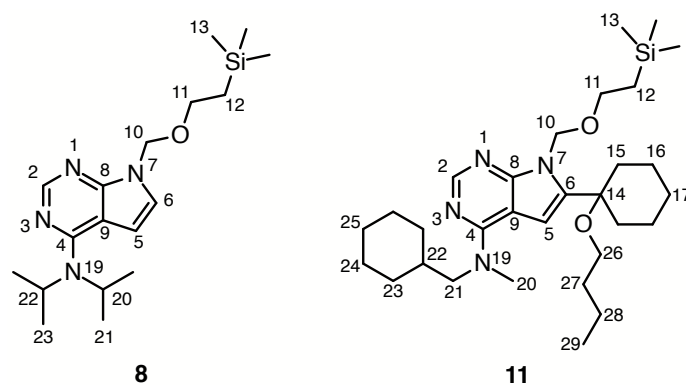
Table 2.6: ^{1}H-NMR and ^{13}C-NMR shifts for compound **HHMT-070**, **HHMT-170** and **HHMT-178**. All shifts are given in ppm. The compounds are recorded in CDCl$_3$ and calibrated with TMS at 0.00 in both ^{1}H-NMR and ^{13}C-NMR.

| | Compound | | | | |
| | ^{1}H-NMR in ppm | | | ^{13}C-NMR in ppm | |
Pos.	HHMT-070	HHMT-170	HHMT-178	HHMT-170	HHMT-178
2	8.23	8.24	8.24	151.5	151.2
4	-	-	-	157.0	156.9
5	6.38	6.43	6.41	98.7	98.6
6	-	-	-	133.4	134.1
7	8.90	10.85	-	-	-
8	-	-	-	152.5	152.2
9	-	-	-	103.3	103.4
14	-	-	-	126.3	128.0
15	6.08	6.17	6.13	120.4	119.7
16	2.26	4.40	2.54	65.6	35.9
17	2.40	-	-	-	107.7
20	3.36	3.38	3.36	39.2	39.2
21	3.61	3.63	3.61	57.1	57.2
22	1.84 - 1.68	1.87 - 1.84	1.88 - 1.82	37.3	37.3
23	1.84 - 1.68/ 1.06 - 0.98	1.74/ 1.06 - 1.00	1.75 - 1.72/ 1.06 - 0.98	30.9	30.9
24	1.84 - 1.68/ 1.27 - 1.16	1.74/ 1.25 - 1.17	1.75 - 1.72/ 1.28 - 1.15	25.9	26.0
25	1.84 - 1.68/ 1.27 - 1.16	1.67/ 1.25 - 1.17	1.68 - 1.66/ 1.28 - 1.15	26.5	26.5
26	1.84 - 1.68	3.96	1.95	64.1	31.1
27	1.84 - 1.68	2.55	2.70	25.8	25.2
28	-	-	4.03	-	64.6
29	-	-	4.03	-	64.6

For compound **HHMT-070**, **HHMT-170**, and **HHMT178**, the chemical shifts of the amine group and the pyrrolo[2,3-*d*]pyrimidine core structure are similar, except for the decrease in position 5 for **HHMT-070**. Comparing the substituents in compound **HHMT-170** and **HHMT-178**, the protons in position 15, 16, 26, and 27, have higher chemical shifts in **HHMT-170**. This indicates that an oxygen in position 17 has a stronger deshielding effect, it is more electron withdrawing, than a ketal in position 17. Comparing the substituents in compound **HHMT-070** and **HHMT-178**, the same protons have higher chemical shifts in compound **HHMT-178** as the ketal in position 17 has a stronger deshielding effect than a methylene group in position 17.

Compound 8 and 11

The position numbering of compound **8** and **11** are illustrated in Scheme 2.22. The assigned chemical shifts given in Table 2.7 are extracted from Appendix H and K, respectively.

Scheme 2.22: Position numbering of compound **8** and **11**.

Table 2.7: ^{1}H-NMR and ^{13}C-NMR shifts for compound **8** and **11**. All shifts are given in ppm. Compound **8** is recorded in $CDCl_3$ and is calibrated with TMS at 0.00 in both ^{1}H-NMR and ^{13}C-NMR. Compound **11** is recorded in DMSO-d_6 and is calibrated with DMSO at 2.50 ppm in ^{1}H-NMR and 39.52 ppm in ^{13}C-NMR.[82]

	Compound			
	^{1}H-NMR in ppm		^{13}C-NMR in ppm	
Pos.	**8**	**11**	**8**	**11**
	($CDCl_3$)	(DMSO-d_6)	($CDCl_3$)	(DMSO-d_6)
2	8.34	8.13	152.1	151.1
4	-	-	119.8	156.2
5	6.22	6.50	109.8	102.2
6	6.43	-	116.3	138.0
8	-	-	150.7	153.1
9	-	-	74.5	100.8
10	5.21	5.73	73.4	70.4
11	3.50	3.66	66.0	65.7
12	0.89	0.84 - 0.79	17.8	17.5
13	-0.03	-0.08	-1.4	-1.4
14	-	-	-	74.2
15	-	2.33/ 1.80 - 1.61	-	34.3
16	-	1.52 - 1.50/ 1.33 - 1.23	-	21.3
17	-	1.80 - 1.61	-	25.3
20	4.65[a]	3.30	46.0[b]	38.6
21	1.27[c]	3.59	29.7[d]	55.9
22	3.63[a]	1.80 - 1.61	47.1[b]	36.5
23	1.33[c]	1.80 - 1.61/ 1.02 - 0.94	23.9[d]	30.2
24	-	1.80 - 1.61/ 1.17 - 1.13	-	25.4
25	-	1.80 - 1.61/ 1.17 - 1.13	-	26.0
26	-	2.93	-	60.7
27	-	1.45 - 1.38	-	31.7
28	-	1.33 - 1.23	-	19.1
29	-	0.84 - 0.79	-	13.8

[a] These ^{1}H-NMR chemical shifts are interchangeable.
[b] These ^{13}C-NMR chemical shifts are interchangeable.
[c] These ^{1}H-NMR chemical shifts are interchangeable.
[d] These ^{13}C-NMR chemical shifts are interchangeable.

The protons in position 20 and 22, as well as the protons in position 21 and 23, in compound **8** are homotopic. However, there are unexpected chemical shift differences in the ^{1}H- and ^{13}C-NMR spectra. This may be due to a partial double bond character, restricting rotation around the chemical bond. Similar effects have previously been presented for dimethylformamide and for purines.[81,84] Tautomerism, due to donation of the lone electron pair in position 19, to the electron poor aromatic pyrrolo[2,3-*d*]pyrimidine ring, results in formation of the imine form. Thus, the rotation around the C−N bond is restricted. The mesomeric canonical forms creates different magnetic environments for the protons and the chemical shifts will be different if the imine form is more preferable than the amine form, see Scheme 2.23.[81]
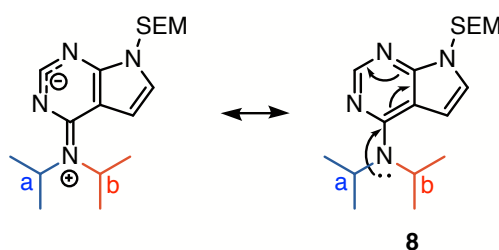
Scheme 2.23: Mesomeric effects can cause different magnetic environments for protons in part a and part b in compound **8**.

This effect may also be present in the other compounds with 1-cyclohexyl-*N*-methylmethanamine. The NMR recordings of these compounds could be of one preferred rotational isomer in every case, which is not unlikely as there are steric effects between cyclohexane and pyrrol. Further examination of this may be possible by conducting ^{1}H-NMR experiments above 27 °C.

2.9.3 MS

MS analysis were performed for the compounds that have not previously been reported in the literature. Compound **6**, **7**, **8**, **10**, **11**, **13**, **14**, **HHMT-170** and **HHMT-178** have been characterized by MS, and their corresponding spectra can be found in Appendix F, G, H, J, K, M, N, Q and R, respectively. Table 2.8 shows the chemical formula as a result of the MS analysis.

Table 2.8: Chemical formula for compound **6**, **7**, **8**, **10**, **11**, **13**, **14**, **HHMT-170** and **HHMT-178** extracted from Appendix F, G, H, J, K, M, N, Q and R, respectively.

Compound	Chemical formula
6	$C_{18}H_{29}N_3O_2SiCl$
7	$C_{17}H_{27}N_3O_3SiCl$
8	$C_{18}H_{33}N_4OSi$
10	$C_{26}H_{45}N_4O_2Si$
11	$C_{30}H_{53}N_4O_2Si$
13	$C_{25}H_{43}N_4O_3Si$
14	$C_{28}H_{45}N_4O_3Si$
HHMT-170	$C_{19}H_{27}N_4O$
HHMT-178	$C_{22}H_{31}N_4O_2$

2.9.4 IR

IR analysis were performed for the compounds that have not previously been reported in the literature. Compound **6**, **7**, **8**, **10**, **11**, **13**, **14**, **HHMT-170** and **HHMT-178** have been characterized by IR, and their corresponding spectra can be found in Appendix F, G, H, J, K, M, N, Q and R, respectively. Since the compounds are of similar structures they have a lot of similarities in their spectra.

Strong absorption bands between 2921 and 2850 cm^{-1} indicates presence of sp^3-hybridized C−H stretch in all compounds. A medium to weak absorption band observed around 760 cm^{-1} in all compounds, are due to C−H "out-of-plane" bending in aromatic compounds. In addition, aromatic ring stretching vibrations are observed between 1600 and 1300 cm^{-1}, or more specifically between 1569 and 1507 cm^{-1}, are due to C=C or N=C stretching vibrations.[68]

Broad absorption bands between 3700 and 3200 cm^{-1} are from O−H stretching vibrations and can be observed in compound **6**, **7**, **10** and **13**. Absorption band around 1452 cm^{-1} in compound **6**, **10**, **11**, **13**, **14**, **HHMT-170**, and **HHMT-178**, may stem from C−H vibrations in cyclohexane.[68]

Furthermore, asymmetric C−O−C stretch is observed as strong absorption bands between 1150 and 1085 cm^{-1} from the SEM protection group in compound **6**, **7**, **8**, **10**, **11**, **13**, **14**. However, in compound **7**, **13**, and **14**, this absorption bands

can also be due to $C-O-C$ stretch vibrations that are from the substituents in position 6 as observed in compound **HHMT-170** and **HHMT-178**.[68]

$N-H$ stretching vibrations are usually observed between 3000 and 2700 cm^{-1}. However, $N-H$ stretching absorption in heteroaromatic rings are observed at higher wavenumbers.[68] In **HHMT-170** and **HHMT-178** they are seen between 3190 and 3092 cm^{-1}.

Chapter 3

Conclusion and Further Work

3.1 Conclusion

The goal of this master's thesis was to synthesize 4,6-disubstituted pyrrolo[2,3-*d*]pyrimidines in order to expand the library of possible candidates for CSF-1R inhibitors. A new synthetic strategy was examined as well. The target molecules **HHMT-070**, **HHMT-170**, and **HHMT-178**, have been synthesized as described in Scheme 3.1. The yields of these routes varied from poor to excellent.
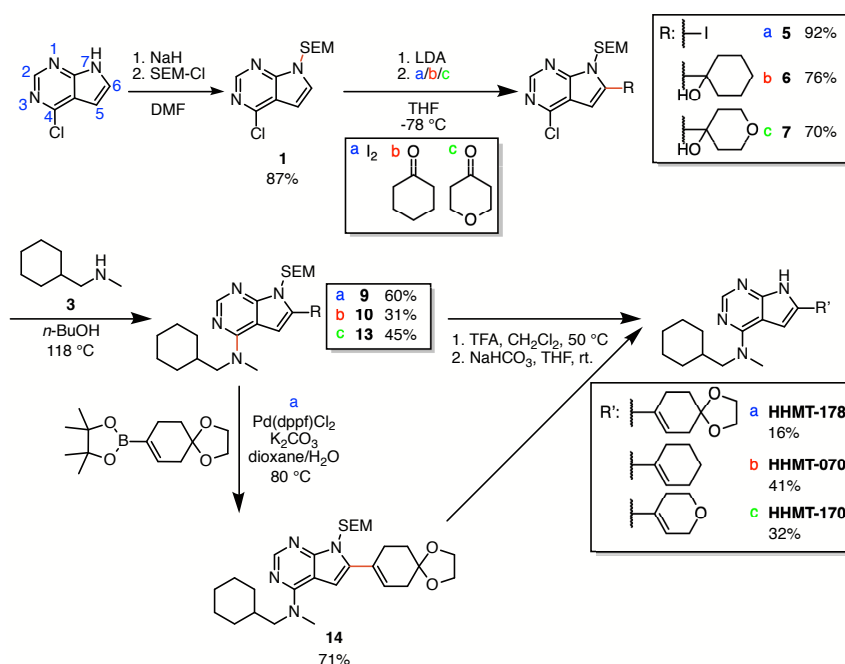
Scheme 3.1: Synthetic route I towards target molecule **HHMT-178** (*a*), and route II towards **HHMT-070** (*b*) and **HHMT-170** (*c*).

The first step was SEM protection of 4-chloro-7*H*-pyrrolo[2,3-*d*]pyrimidine in position 7, which resulted in a yield of 87% of compound **1**. Following route I to achieve **HHMT-178**, compound **1** was iodinated through *ortho*-lithiation and resulted in a yield of 92% of compound **5**. Further amination in position 4 gave compound **9** i 60% yield. Compound **14** was then achieved through Suzuki cross-coupling in a yield of 71%. Finally, compound **HHMT-178** was obtained in a yield of 16% by removing the SEM group. The low yield was likely due to the formation of unknown byproducts.

Compound **HHMT-070** and **HHMT-170** were prepared following route II. *Ortho*-lithiation, followed by nucleophilic attack on carbonyl groups, resulted in a yield of 76% of compound **6** and 70% of compound **7**. Furthermore, thermal amination in position 6 of both compounds gave compound **10** in a yield of 31%, and compound **13** in a yield of 45%. The low yield of compound **10** was due to formation of two byproducts. For both compounds, there were loss due to removal of compound **4** (see Figure 3.1), which was a contamination from synthesis of amine **3** through reductive amination. Lastly, the target molecules were achieved by removing the SEM groups. Compound **HHMT-070** and **HHMT-170** were isolated in yields of 41% and 32%, respectively.
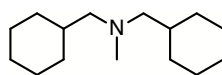
Figure 3.1: Byproduct **4** from synthesis of compound **3** through reductive amination.

In general the mediocre yields were due to experimental mistakes and the presence of amine byproduct **4**, which contributed to challenges during purification. Byproduct **4** should have been removed from compound **3** before proceeding to the thermal aminations.

Compound **HHMT-070** had previously been synthesized following route *a*. The overall yield of the route was 31%, see Scheme 3.2.[33] However, synthesis of compound **1** and **5** have subsequently resulted in higher yields, so that a total yield of 41% should be achievable.
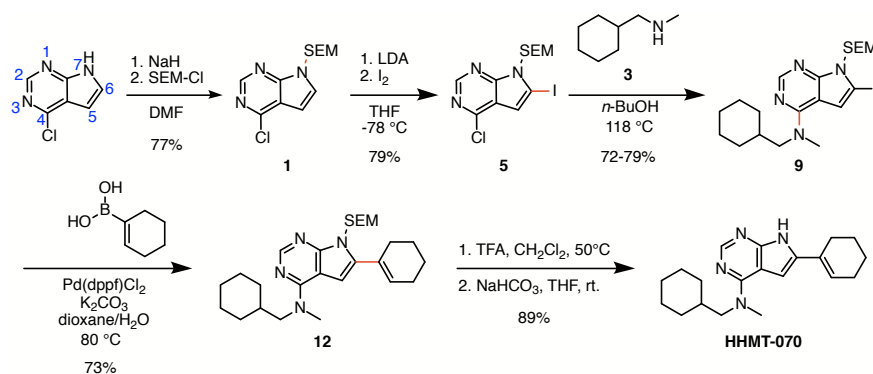
Scheme 3.2: Synthesis of compound **HHMT-070** from previously reported synthetic route.[33]

Compared to the previous synthetic route (I), the alternative strategy (II) had an overall yield of only 8%. However, the overall yield can be drastically increased with small alterations. Full conversion during *ortho*-lithiation of compound **1** to achieve compound **6**, would simplify the purification of the product by silica-gel column chromatography. Further optimization of the eluent system could also be considered. Thermal amination of compound **6** to achieve compound **10**, could easily be improved by using an aprotic solvent. However, both the byproduct from S_N1 reaction with *n*-BuOH, and the dehydrated derivative of compound **10**, could proceed to the SEM deprotection together with compound **10** as they are likely to yield the desired target molecule. Dehydration of compound **10** took place during the SEM deprotection and compound **HHMT-070** was achieved.

If the suggested alterations are implemented, the new route should result in a higher yield than the previous one as it is one step shorter. In addition, the use of iodine was avoided. The organoboron reagents are also more expensive than the ketone derivatives of the three substitutents in position 6. Synthesis of the organoboron compounds extends the previous synthetic route further, and may lead to additional complications. However, the types of products may be more limited compared to the ones from Suzuki cross-coupling reactions. An aryl group directly substituted to position 6 is not achievable following route II.

The IC_{50}-value of **HHMT-170** was analyzed to be 0.4 nM, which showed that the compound was a promising inhibitor of CSF-1R. However, the poor solubilities of all the target molecules are presumably not a desired property of drugs. Hopefully, the results may give an indication of the effects of different substituents that can be used in future projects within the research group.

3.2   Further Work

One aim of this master's thesis was to contribute to the library of analogue structures of potential CSF-1R inhibitors, by substituting different non-aromatic rings in position 6, see Figure 3.2.
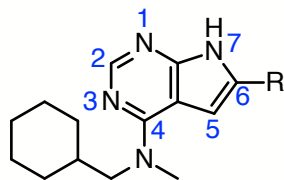
Figure 3.2: The core structure of the pyrrolo[2,3-*d*]pyrimidines that were synthesized in this master's thesis.

If the method of synthesising compounds through *ortho*-lithiation and nucleophilic attack on carbonyl groups is continued, optimizations and further exploration with other cabonyl groups should be carried out. Methods for hydrogenation of substituents in position 6 with different catalysts should be explored as well. Derivatives with saturated substituents will further expand the library of potential inhibitors. A biological screening of **HHMT-070** and **HHMT-178** should be conducted. Further testing of **HHMT-170** should also be done, such as more CSF-1R assays and enzyme selectivity.

Chapter 4

Experimental Data

4.1 General Information

The reagents and solvents used were of analytical grade or higher and commercially available. All reactions were conducted on teflon coated magnetic stirrers, and an oil bath was used for reactions above room temperature, which was 20 - 21 °C. Dry solvents were collected from Braun MB SPS-800 Solvent Purification System, unless stated otherwise, and stored over molecular sieves (4 Å).

4.1.1 Separation Techniques

Thin-layer chromatography (TLC, silica-gel on aluminium plates, F254, Merck) was used for monitoring reactions and for optimizing eluent systems when purifying by silica-gel column chromatography. UV-light (254 nm) was used for visualization of aromatic compounds on TLC-plates, and anisaldehyde stain or phosphomolybdic acid solution (10% in ethanol) were used to develop non-aromatic compounds on the TLC-plates. Column chromatography was performed using silica-gel (40-63 μm) and eluent systems that are specified for each case.

4.1.2 Spectroscopic Analyses

^{1}H- and ^{13}C-NMR spectra were recorded using a Bruker Avance III HD NMR spectrometer from Nanaobay electronics with a Smartprobe 5 mm probehead.

Proton spectra were recorded at 400 MHz or 600 MHz, and carbon spectra were recorded on 100 MHz or 150 MHz, respectively. Samples were mostly analyzed in either DMSO-d_6 or CDCl$_3$, and are specified for each compound. The chemical shifts are reported in δ (ppm) and most spectra are calibrated using the solvent peaks in both solvents. Some are calibrated using the TMS peak in CDCl$_3$. In DMSO-d_6 the solvent peak is at 2.50 ppm in ^{1}H-spectra and at 39.52 ppm in ^{13}C-spectra, and in CDCl$_3$ the solvent peak is at 7.26 ppm in ^{1}H-spectra and at 77.16 ppm in ^{13}C-spectra, relative to TMS. Water traces may be found at 3.33 ppm and 1.56 ppm in DMSO-d_6 and CDCl$_3$, respectively.[82] The signals are described according to their multiplicities: s (singlet), d (doublet), t (triplet), sept (septet), dd (doublet of doublets), td (triplet of doublets), and m (multiplet). Broad signals are denoted by "br". Multiplets are reported as intervals. The coupling constants (J) are reported in hertz (Hz).

For mass spectroscopy (MS), accurate mass determination in positive and negative mode was performed on a "Synapt G2-S" Q-TOF instrument from Water TM. Samples were ionized by the use of ASAP probe (APCI) or ESI probe. No chromatographic separation was used previous to the mass analysis. Calculated exact mass and spectra processing was done by Waters TM Software Masslynx V4.1 SCN871.

Infrared (IR) absorption spectra were recorded with a Bruker Alpha FT-IR Spectrometer and a Platinum ATR single reflection diamond. The IR spectra are normalized and recorded in the range of 4000 - 400 cm^{-1}. The signals are denoted as strong (s), medium (m) or weak (w).

4.1.3   Melting Point

Melting points were determined using an automatic Stuart SMP40 apparatus.

## 4.2 Synthesis of 4-chloro-7-((2-(trimethylsilyl)ethoxy)methyl)-7*H*-pyrrolo[2,3-*d*]pyrimidine (1)[58]

1
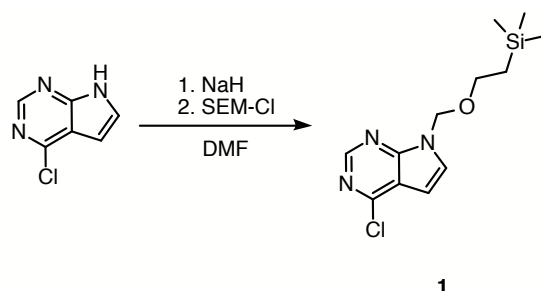
4-Chloro-7*H*-pyrrolo[2,3-*d*]pyrimidine (1.99 g, 13.0 mmol) and NaH (386 mg, 16.1 mmol) were dissolved in dry DMF (50 mL) under an N_2-atmosphere. The solution was cooled to 0 °C and 2-(trimethylsilyl)ethoxymethyl chloride (2.50 mL, 13.8 mmol) was added dropwise over 30 minutes. The reaction was stirred at room temperature for 1 hour. Saturated NH_4Cl-solution (0.5 mL) was slowly added to quench the reaction. The mixture was concentrated *in vacuo* before adding water (60 mL) and EtOAc (40 mL). The layers were separated. The aqueous phase was extracted with more EtOAc (5 × 20 mL) and the combined organic phases were washed with brine (sat., 30 mL), dried over anhydrous Na_2SO_4, filtered and concentrated *in vacuo*. The crude product was purified by silica-gel column chromatography (EtOAc:*n*-pentane, 1:7, R_f = 0.37). Drying gave 3.21 g (11.3 mmol, 87%) of a colourless oil that was pure as observed by ^{1}H-NMR spectroscopy. Addition of seed crystal gave white crystals with mp = 33 - 34 °C.

Spectroscopic data for compound **1** (Appendix A):
^{1}H-NMR (600 MHz, DMSO-d_6) δ: 8.69 (s, 1H), 7.88 (d, 1H, J = 4.2 Hz), 6.72 (d, 1H, J = 3.6 Hz), 5.65 (s, 2H), 3.52 (t, 2H, J = 7.8 Hz), 0.82 (t, 2H, J = 7.8 Hz), -0.10 (s, 9H). This corresponds with previously reported data by K. U. Larsen and Lin *et al.*,[31,58] except that the peak of $-Si(CH_3)_3$ resided at -0.10 ppm instead of 0.24 ppm as reported by Lin *et al*. The triplets at 3.52 ppm and 0.82 ppm have also previously been observed as doublet of doublets.[33] Compound **1** was also recorded in $CDCl_3$ for future reference: ^{1}H-NMR (400 MHz, $CDCl_3$) δ: 8.67 (s, 1H), 7.39 (d, 1H, J = 3.6 Hz), 6.67 (d, 1H, J = 3.6 Hz), 5.65 (s, 2H),

3.53 (dd, 2H, J = 9.2 Hz, 8.4 Hz), 0.91 (dd, 2H, J = 8.4 Hz, 8.4 Hz), -0.05 (s, 9H).

4.3 Isolation of 4-chloro-7-(((2-(trimethylsilyl)ethoxy)methoxy)methyl)-7H-pyrrolo[2,3-d]pyrimidine (2)[31,33]


2
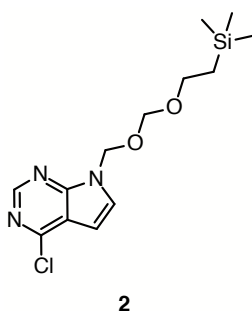
Isolation of semi-pure byproduct **2** following the reaction and purification described in Section 4.2, resulted in 21.9 mg (0.0698 mmol, 1%, R_f = 0.23 with EtOAc:n-pentane, 1:7) of a colourless oil.

Spectroscopic data for byproduct **2** (Appendix B):
^{1}H-NMR (400 MHz, DMSO-d_6) δ: 8.68 (s, 1H), 7.86 (d, 1H, J = 4.0 Hz), 6.71 (d, 1H, J = 3.6 Hz), 5.76 (s, 2H), 4.74 (s, 2H), 3.33 (dd, 2H, J = 9.6 Hz, 8.4 Hz), 0.64 (dd, 2H, J = 9.6 Hz, 7.2 Hz), -0.09 (s, 9H). This corresponds with previously reported data by K. U. Larsen and the data reported in the pre-master's project.[31,33]

4.4 Synthesis of 1-cyclohexyl-N-methylmethanamine (3)[59,85]

3
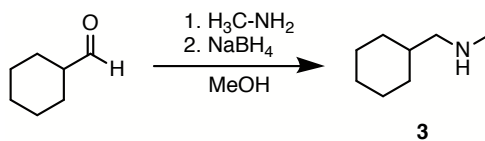
4.4.1 Synthesis in 700 mg scale

Cyclohexanecarbaldehyde (0.76 mL, 6.3 mmol) and methylamine (2 M in MeOH, 3.50 mL, 7.00 mmol) were diluted in dry MeOH (30 mL). The reaction mixture was stirred at room temperature under inert atmosphere for 3 hours. Then, sodium borohydride (253 mg, 6.68 mmol) was added at 0 °C. The mixture was stirred for another 1.5 hours at room temperature. The mixture was then concentrated *in vacuo*. Water (10 mL) was added to the residue. Acid-base extraction was performed with HCl (37%, 1 mL, pH 0) and Et_2O (3 × 7 mL), and NaOH (5 M, 1 mL, pH 11) and CH_2Cl_2 (7 × 7 mL). The combined organic phases of CH_2Cl_2 were washed with brine (sat., 10 mL), dried over Na_2SO_4 and filtered. Drying gave 363 mg (2.85 mmol, 45%) of a colourless oil with white solids. The purity was determined to be 77% by ^{1}H-NMR spectroscopy.

4.4.2 Different procedures during work-up, 3 g scale

Cyclohexanecarbaldehyde (3.50 mL, 28.9 mmol) and methylamine (2 M in MeOH, 15.9 mL, 31.8 mmol) were diluted in dry MeOH (100 mL). The reaction mixture was stirred at room temperature under inert atmosphere for 2.5 hours. Then, sodium borohydride (1.16 g, 30.7 mmol) was added at 0 °C. The mixture was stirred for another 3 hours at room temperature. The reaction mixture was then divided into two parts to undergo different procedures during work-up. HCl (37%, 1 mL, pH 0) was added to the smaller fraction (20 mL) and the mixture was stirred at room temperature for 1 hour. The mixture was then concentrated *in vacuo*. Water (7 mL) was added to the residue. Acid-base extraction was performed with Et_2O (5 × 7 mL), and NaOH (5 M, 4.5 mL, pH 11) and CH_2Cl_2 (7 × 6 mL). The combined organic phases of CH_2Cl_2 were washed with brine (sat., 7 mL), dried over Na_2SO_4 and filtered. Drying gave 159 mg (1.25 mmol, 22%) as a pale yellow oil with white solids. The purity was determined to be 86% by ^{1}H-NMR spectroscopy. The larger fraction (80 mL) was first concentrated *in vacuo*. Water (20 mL) was added to the residue. Acid-base extraction was performed with HCl (37%, 3 mL, pH 0) and Et_2O (5 × 20 mL), and NaOH (5 M, 3 mL, pH 11) and CH_2Cl_2 (7 × 15 mL). The combined organic phases of CH_2Cl_2 were washed with brine (sat., 20 mL), dried over Na_2SO_4 and filtered. Drying gave 1.25 g (9.80 mmol, 42%) of a colourless oil with white solids. The purity was determined to be 92% by ^{1}H-NMR spectroscopy.
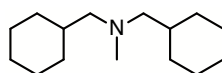
Spectroscopic data for compound **3** (Appendix C):

^{1}H-NMR (400 MHz, DMSO-d_6) δ: 3.31 (br s, 1H), 2.26 (d, 2H, J = 6.8 Hz), 2.24 (s, 3H), 1.72 - 1.60 (m, 5H), 1.41 - 1.30 (m, 1H), 1.23 - 1.09 (m, 3H), 0.88 - 0.80 (m, 2H). The data corresponds with the ^{1}H-NMR recording of compound **3** bought from Sigma-Aldrich (see Appendix D) and the data previously reported in the pre-master's project.[33]

4.4.3   One-pot synthesis using sodium triacetoxyborohydride, 700 mg scale
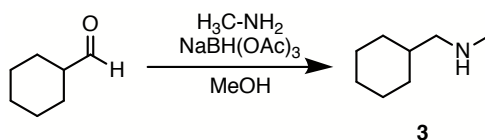
Cyclohexanecarbaldehyde (0.76 mL, 6.3 mmol), methylamine (2 M in MeOH, 3.50 mL, 7.00 mmol) and sodium triacetoxyborohydride (1.49 g, 7.05 mmol) were dissolved in dry MeOH (30 mL). The reaction mixture was stirred at room temperature under inert atmosphere for 3 days. Due to no conversion, the reaction was heated at 70 °C for another 3 days. Sodium borohydride (256 mg, 6.75 mmol) was added at 0 °C. The mixture was stirred for another 2 hours at room temperature before it was concentrated *in vacuo*. Water (10 mL) was added to the residue. Acid-base extraction was performed with HCl (37%, 1 mL, pH 0) and Et$_2$O (4 × 7 mL), and NaOH (5 M, 1 mL, pH 11) and CH$_2$Cl$_2$ (7 × 7 mL). The combined organic phases of CH$_2$Cl$_2$ were washed with brine (sat., 10 mL), dried over Na$_2$SO$_4$ and filtered. Drying gave 328 mg (2.58 mmol, 41%) of a yellow wet-looking solid. The purity was determined to be 64% by ^{1}H-NMR spectroscopy.

4.5 Identification of 1-cyclohexyl-*N*-(cyclohexylmethyl)-*N*-methylmethanamine (4)[33,85]

4

The crude products described in Section 4.4 were contaminated by byproduct **4**.

Spectroscopic data for byproduct **4** (Appendix C):
^{1}H-NMR (400 MHz, DMSO-d_6) δ: 2.06 (s, 3H), 2.00 (d, 4H, J = 7.2 Hz), 1.72 - 1.60 (m, 10H), 1.41 - 1.30 (m, 2H), 1.23 - 1.09 (m, 6H), 0.88 - 0.80 (m, 4H). This corresponds with the previously reported data in the pre-master's project.[33]

4.6 Synthesis of 4-chloro-6-iodo-7-((2-(trimethylsilyl)ethoxy)methyl)-7*H*-pyrrolo[2,3-*d*]pyrimidine (5)[11,63]
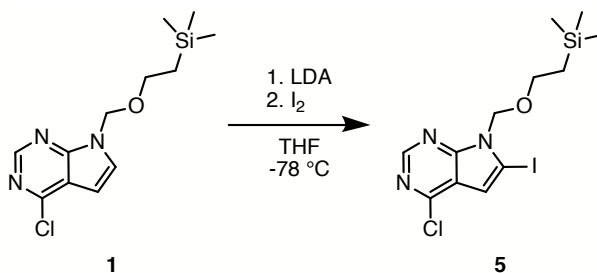
Compound **1** (1.00 g, 3.53 mmol) was dissolved in dry THF (20 mL) under an N_2-atmosphere and cooled to -78 °C. LDA (2 M in THF/heptane/ethylbenzene, 2.64 mL, 5.28 mmol) was added dropwise over 30 minutes using a syringe pump. The reaction mixture was stirred for 2 hours. Molecular iodine (1.11 g, 4.37 mmol) dissolved in dry THF (10 mL) was then added dropwise over 30 minutes using a syringe pump. The reaction mixture was stirred for another 1.5 hours before saturated NH_4Cl-solution (0.5 mL) was added to quench the reaction.

The mixture was then concentrated *in vacuo.* CH$_2$Cl$_2$ (20 mL) was added to the residue and the mixture was washed with sodium thiosulphate solution (10%, 20 mL). The aqueous phase was extracted with CH$_2$Cl$_2$ (7 × 10 mL). The combined organic phases were washed with brine (sat., 20 mL), dried over anhydrous Na$_2$SO$_4$, filtered and concentrated *in vacuo.* The crude product was purified by silica-gel column chromatography (EtOAc:*n*-pentane, gradient from 1:19 to 1:9, R$_f$ = 0.56 at 1:9). Drying gave 1.33 g (3.25 mmol, 92%) of a white solid with mp = 101 - 104 °C (Lit.[31,33] 101 - 103 °C) and was pure as observed by ^{1}H-NMR spectroscopy.

Spectroscopic data for compound **5** (Appendix E):
^{1}H-NMR (400 MHz, DMSO-d_6) δ: 8.64 (s, 1H), 7.13 (s, 1H), 5.62 (s, 2H), 3.54 (t, 2H, *J* = 8.0 Hz), 0.83 (t, 2H, *J* = 8.0 Hz), -0.10 (s, 9H). This corresponds with previously reported data by Frank *et al.*[63] and Han *et al.*[11]

4.7 Synthesis of 1-(4-chloro-7-((2-(trimethylsilyl)ethoxy)methyl)-7*H*-pyrrolo[2,3-*d*]pyrimidin-6-yl)cyclohexan-1-ol (6)
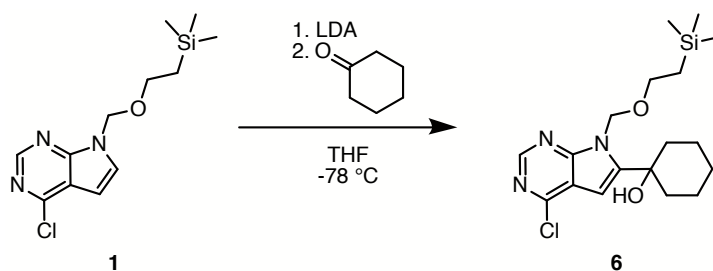
4.7.1 Synthesis in 200 mg scale: first trial

Compound **1** (200 mg, 0.704 mmol) was dissolved in dry THF (4 mL) under an N$_2$-atmosphere and cooled to -78 °C. LDA (2 M in THF/heptane/ethylbenzene, 0.53 mL, 1.1 mmol) was added dropwise over 30 minutes using a syringe pump. The reaction mixture was stirred for 1 hour. Cyclohexanone (0.09 mL, 0.9 mmol) was then added dropwise over 30 minutes using a syringe pump. The reaction

mixture was stirred for another 2.5 hours before saturated NH_4Cl-solution (0.2 mL) was added to quench the reaction. The mixture was stirred until it reached room temperature and was then concentrated *in vacuo*. Water (5 mL) and CH_2Cl_2 (5 mL) were added to the residue and the layers were separated. The aqueous phase was extracted with more CH_2Cl_2 (5 × 3 mL). The combined organic phases were washed with brine (sat., 5 mL), dried over anhydrous Na_2SO_4, filtered and concentrated *in vacuo*. The crude product was purified twice by silica-gel column chromatography (EtOAc:CH_2Cl_2, 1:9, R_f = 0.17). Drying gave 96.2 mg (0.252 mmol, 36%) of a pale yellow solid with mp = 72 - 74 °C and was pure as observed by ^{1}H-NMR spectroscopy.
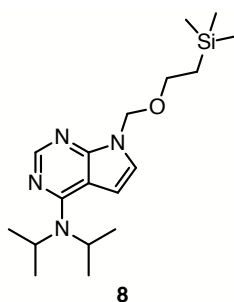
Spectroscopic data for compound **6** (Appendix F):
^{1}H-NMR (400 MHz, DMSO-d_6) δ: 8.64 (s, 1H), 6.54 (s, 1H), 5.99 (s, 2H), 5.28 (s, 1H), 3.64 (t, 2H, J = 8.0 Hz), 2.16 - 2.13 (m, 2H), 1.86 - 1.70 (m, 4H), 1.63 - 1.60 (m, 1H), 1.53 - 1.50 (m, 2H), 1.28 - 1.25 (m, 1H), 0.83 (t, 2H, J = 8.0 Hz), -0.09 (s, 9H); ^{13}C-NMR (100 MHz, DMSO-d_6) δ: 153.2, 150.7, 150.5, 150.0, 115.8, 96.1, 71.6, 69.5, 66.1, 36.9 (2C), 25.1, 21.3 (2C), 17.4, -1.4 (3C); IR (neat, cm^{-1}) ν: 3391 (w), 2934 (s), 2856 (s), 1728 (m), 1585 (s), 1549 (s), 1528 (s), 1448 (s), 1426 (s), 1380 (s), 1353 (s), 1318 (s), 1249 (s), 1205 (s), 1159 (s), 1127 (s), 1079 (s), 969 (s), 935 (s), 911 (s), 861 (s), 836 (s), 774 (s), 752 (s), 729 (s), 713 (m), 693 (m), 664 (m), 638 (w), 613 (m), 594 (m), 555 (m); HRMS (ASAP+, m/z): detected 382.1713, calculated for $C_{18}H_{29}N_3O_2SiCl$ [M+H]$^+$ 382.1718.

4.7.2 Synthesis in 200 mg scale: second trial

This synthesis followed the procedure described in Section 4.7.1. Compound **1** was dissolved in dry THF (10 mL). After addition of LDA the mixture was stirred for 2 hours. Cyhexanone was diluted in dry THF (1.25 mL) prior to addition to the reaction. The mixture was then stirred for 18 hours before saturated NH_4Cl-solution (0.5 mL) was added to quench the reaction. After the mixture was concentrated *in vacuo*, the water residue was extracted with CH_2Cl_2 (5 × 3 mL). The crude product was purified by silica-gel column chromatography (EtOAc:*n*-pentane, 1:7, R_f = 0.21). Drying gave 206 mg (0.539 mmol, 76%) of a pale yellow solid with mp = 73 - 79 °C and purity of 98% as determined by ^{1}H-NMR spectroscopy.

4.8 Synthesis of 4-(4-chloro-7-((2-(trimethylsilyl)ethoxy)methyl)-7*H*-pyrrolo[2,3-*d*]pyrimidin-6-yl)tetrahydro-2*H*-pyran-4-ol (7)
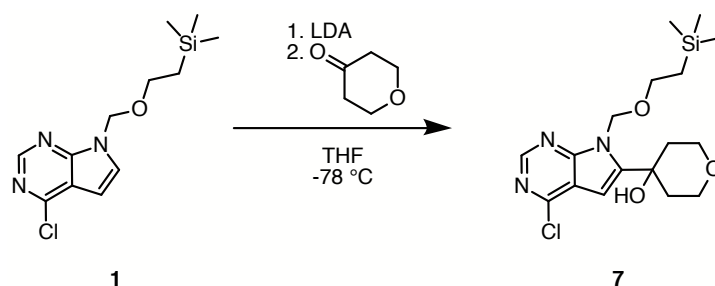
Compound **1** (398 mg, 1.40 mmol) was dissolved in dry THF (10 mL) under an N_2-atmosphere and cooled to -78 °C. LDA (2 M in THF/heptane/ethylbenzene, 1.06 mL, 2.12 mmol) was added dropwise over 30 minutes using a syringe pump. The reaction mixture was stirred for 2 hours. Tetrahydro-4*H*-pyran-4-one (0.16 mL, 1.7 mmol) diluted in dry THF (2 mL) was added dropwise over 30 minutes using a syringe pump. The reaction mixture was stirred for another 25.5 hours before saturated NH_4Cl-solution (0.5 mL) was added to quench the reaction. The mixture was stirred until it reached room temperature and then concentrated *in vacuo*. Water (8 mL) and CH_2Cl_2 (8 mL) were added to the residue and the layers were separated. The aqueous phase was extracted with more CH_2Cl_2 (7 × 6 mL). The combined organic phases were washed with brine (sat., 15 mL), dried over anhydrous Na_2SO_4, filtered and concentrated *in vacuo*. The crude product was purified by silica-gel column chromatography (EtOAc:*n*-pentane, gradient from 1:4 to 1:2, R_f = 0.09 - 0.24). Drying gave 377 mg (0.981 mmol, 70%) of a thick brown oil that was pure as observed by ^{1}H-NMR spectroscopy.

Spectroscopic data for compound **7** (Appendix G):
^{1}H-NMR (400 MHz, CDCl$_3$) δ: 8.64 (s, 1H), 6.55 (s, 1H), 5.98 (s, 2H), 4.00 (td, 2H, J = 11.6 Hz, 2.0 Hz), 3.91 - 3.88 (m, 2H), 3.66 (s, 1H), 3.59 (dd, 2H, J = 8.4 Hz, 8.4 Hz), 2.24 (td, 2H, J = 13.2 Hz, 4.8 Hz), 2.09 - 2.05 (m, 2H), 0.94 (dd, 2H, J = 8.8 Hz, 8.8 Hz), -0.05 (s, 9H); ^{13}C-NMR (100 MHz, CDCl$_3$) δ: 153.6, 152.2, 151.3, 147.7, 116.7, 98.4, 71.8, 68.2, 67.1, 63.3 (2C), 38.1 (2C), 18.0, -1.4 (3C);

IR (neat, cm^{-1}) ν: 3371 (w), 2953 (w), 2868 (w), 1612 (w), 1585 (m), 1550 (m), 1529 (w), 1465 (w), 1450 (w), 1426 (m), 1404 (w), 1383 (w), 1352 (s), 1304 (w), 1248 (s), 1210 (s), 1161 (m), 1151 (m), 1138 (m), 1122 (m), 1074 (s), 1028 (s), 959 (w), 935 (w), 910 (m), 858 (s), 833 (s), 774 (s), 751 (m), 720 (m), 692 (w), 638 (w), 613 (w), 593 (m), 557 (m), 544 (m), 515 (w), 419 (w); HRMS (ASAP+, m/z): detected 384.1505, calculated for $C_{17}H_{27}N_3O_3ClSi$ [M+H]$^+$ 384.1510.

4.9 Isolation of *N,N*-diisopropyl-7-((2-(trimethylsilyl)ethoxy)methyl)-7*H*-pyrrolo[2,3-*d*]pyrimidin-4-amine (8)

Isolation of semi-pure byproduct **8** following the reaction and purification described in Section 4.8, resulted in 13.5 mg (0.0387 mmol, 3%, R_f = 0.74 with EtOAc:*n*-pentane, 1:4) of a brown-orange oil.

Spectroscopic data for byproduct **8** (Appendix H):
^{1}H-NMR (400 MHz, CDCl$_3$) δ: 8.34 (s, 1H), 6.43 (d, 1H, J = 3.2 Hz), 6.22 (d, 1H, J = 3.2 Hz), 5.21 (s, 2H), 4.65 (sept, 1H, J = 7.2 Hz), 3.63 (sept, 1H, J = 6.8 Hz), 3.50 (t, 2H, J = 8.0 Hz), 1.33 (d, 6H, J = 6.8 Hz), 1.27 (d, 6H, J = 6.8 Hz), 0.89 (t, 2H, J = 8.8 Hz), -0.03 (s, 9H); ^{13}C-NMR (100 MHz, CDCl$_3$) δ: 152.1, 150.7, 119.8, 116.3, 109.8, 74.5, 73.4, 66.0, 47.1, 46.0, 29.7 (2C), 23.9 (2C), 17.8, -1.4 (3C); IR (neat, cm^{-1}) ν: 2953 (s), 2925 (s), 2854 (m), 2203 (m), 1614 (s), 1529 (m), 1504 (w), 1479 (m), 1463 (m), 1430 (m), 1396 (w), 1372 (w), 1356 (w), 1302 (m), 1274 (w), 1249 (w), 1202 (m), 1171 (w), 1134 (w), 1093 (m), 1024 (w), 976 (w), 917 (w), 860 (m), 836 (m), 756 (w), 725 (w), 675 (w), 538 (w); HRMS (ASAP+, m/z): detected 349.2418, calculated for $C_{18}H_{33}N_4OSi$ [M+H]$^+$ 349.2424.

4.10   Synthesis of N-(cyclohexylmethyl)-6-iodo-N-methyl-7-((2-(trimethylsilyl)ethoxy)methyl)-7H-pyrrolo[2,3-d]pyrimidin-4-amine (9)[33]
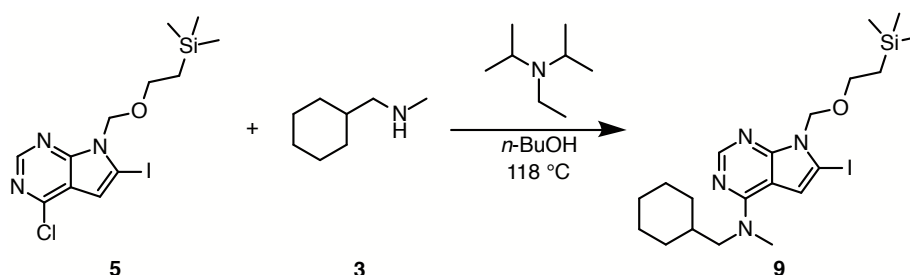
Compound **5** (996 mg, 2.43 mmol) was dissolved in n-BuOH (7 mL), and the secondary amine **3** (0.56 mL, 3.7 mmol) and N-ethyl-N-isopropylpropan-2-amine (Hünigs base, 0.11 mL, 0.63 mmol) were added under an N_2-atmosphere. The oil bath was heated to 118 °C and the reaction was stirred for 5.5 hours. After cooling to room temperature, the mixture was concentrated *in vacuo*. Water (10 mL) was added to the residue and the aqueous phase was extracted with EtOAc (8 × 8 mL). The combined organic phases were washed with brine (sat., 10 mL), dried over anhydrous Na_2SO_4, filtered and concentrated *in vacuo*. The crude product was purified by silica-gel column chromatography (EtOAc:CH_2Cl_2, 1:9, R_f = 0.21). Drying gave 732 mg (1.46 mmol, 60%) of a pale yellow oil with a purity of 98% as determined by ^{1}H-NMR spectroscopy.

Spectroscopic data for compound **9** (Appendix I):
^{1}H-NMR (400 MHz, DMSO-d_6) δ: 8.08 (s, 1H), 6.97 (s, 1H), 5.48 (s, 2H), 3.58 (d, 2H, J = 7.2 Hz), 3.51 (t, 2H, J = 8.0 Hz), 3.29 (s, 3H), 1.79 - 1.73 (m, 1H), 1.66 - 1.59 (m, 5H), 1.19 - 1.12 (m, 3H), 1.00 - 0.94 (m, 2H), 0.80 (t, 2H, J = 8.0 Hz), -0.10 (s, 9H). This corresponds with the previously reported data in the pre-master's project.[33]

4.11 Synthesis of 1-(4-((cyclohexylmethyl)(methyl)amino)-7-((2-(trimethylsilyl)ethoxy)methyl)-7*H*-pyrrolo[2,3-*d*]pyrimidin-6-yl)cyclohexan-1-ol (10)
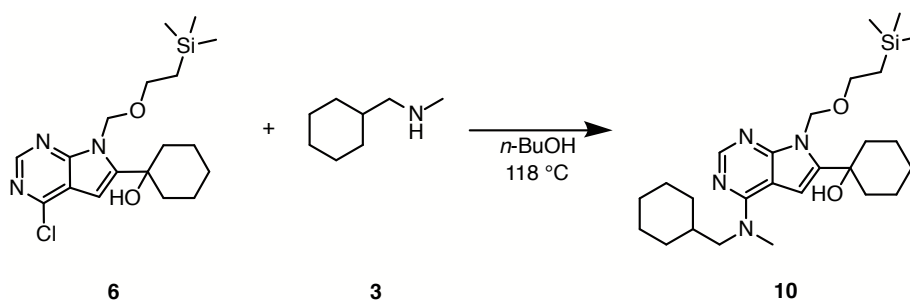
Compound **6** (146 mg, 0.382 mmol) was dissolved in *n*-BuOH (2 mL), and compound **3** (0.18 mL, 1.2 mmol) was added under an N_2-atmosphere. The oil bath was heated to 118 °C and the reaction was stirred for 4 hours. The mixture was concentrated *in vacuo*. Water (5 mL) was added to the residue. The aqueous phase was extracted with EtOAc (6 × 3 mL). The combined organic phases were washed with brine (sat., 5 mL), dried over anhydrous Na_2SO_4, filtered and concentrated *in vacuo*. The crude product was purified twice by silica-gel column chromatography (first time with EtOAc:CH_2Cl_2, 1:7, R_f = 0.07, second time with EtOAc:CH_2Cl_2, 1:5, R_f = 0.32). Drying gave 56.4 mg (0.119 mmol, 31%) of a pale yellow oil with a purity of 90% as determined by ^{1}H-NMR spectroscopy. The impurity was amine **4**.

Spectroscopic data for compound **10** (Appendix J):
^{1}H-NMR (400 MHz, CDCl$_3$) δ: 8.29 (s, 1H), 6.44 (s, 1H), 5.91 (s, 2H), 3.75 (s, 1H), 3.61 - 3.57 (m, 4H), 3.36 (s, 3H), 2.13 - 2.10 (m, 2H), 1.91 - 1.79 (m, 5H), 1.75 - 1.68 (m, 6H), 1.63 - 1.59 (m, 2H), 1.25 - 1.18 (m, 4H), 1.03 - 0.94 (m, 2H), 0.93 (dd, 2H, *J* = 8.4 Hz, 8.4 Hz), -0.06 (s, 9H); ^{13}C-NMR (100 MHz, CDCl$_3$) δ: 157.2, 153.5, 151.6, 141.7, 101.7, 100.8, 71.3, 70.2, 66.4, 57.3, 39.4, 38.2 (2C), 37.4, 31.0 (2C), 26.6, 26.1 (2C), 25.8, 22.1 (2C), 18.0, -1.4 (3C); IR (neat, cm^{-1}) ν: 3379 (w), 2923 (s), 2852 (m), 1572 (s), 1551 (m), 1536 (m), 1508 (m), 1448 (m), 1415 (m), 1365 (m), 1339 (m), 1307 (s), 1285 (m), 1249 (s), 1233 (w), 1210

(w), 1150 (s), 1074 (s), 1038 (m), 966 (w), 937 (w), 910 (w), 897 (w), 858 (s), 835 (s), 762 (m), 695 (w); HRMS (ASAP+, m/z): detected 473.3309, calculated for $C_{26}H_{45}N_4O_2Si$ [M+H]$^+$ 473.3312.

4.12 Isolation of 6-(1-butoxycyclohexyl)-*N*-(cyclohexylmethyl)-*N*-methyl-7-((2-(trimethylsilyl)ethoxy)methyl)-7*H*-pyrrolo[2,3-*d*]pyrimidin-4-amine (11)
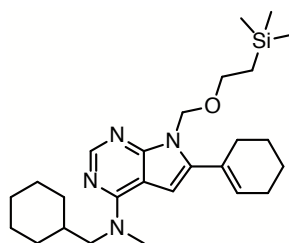

11
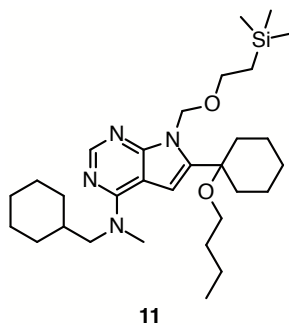
Isolation of byproduct **11** following the reaction and the first purification described in Section 4.11, resulted in 12.6 mg (0.0238 mmol, 6%, R_f = 0.36 with EtOAc:CH$_2$Cl$_2$, 1:7) of a pale yellow oil that was pure as observed by ^{1}H-NMR spectroscopy.

Spectroscopic data for byproduct **11** (Appendix K):
^{1}H-NMR (400 MHz, DMSO-d_6) δ: 8.13 (s, 1H), 6.50 (s, 1H), 5.73 (s, 2H), 3.66 (t, 2H, J = 8.0 Hz), 3.59 (d, 2H, J = 7.6 Hz), 3.30 (s, 3H), 2.93 (br t, 2H, J = 6.4 Hz), 2.33 (br d, 2H, J = 12 Hz), 1.80 - 1.61 (m, 10H), 1.52 - 1.50 (m, 2H), 1.45 - 1.38 (m, 2H), 1.33 - 1.23 (m, 4H), 1.17 - 1.13 (m, 3H), 1.02 - 0.94 (m, 2H), 0.84 - 0.79 (m, 5H), -0.08 (s, 9H); ^{13}C-NMR (100 MHz, DMSO-d_6) δ: 156.2, 153.1, 151.1, 138.0, 102.2, 100.8, 74.2, 70.4, 65.7, 60.7, 55.9, 38.6, 36.5, 34.3 (2C), 31.7, 30.2 (2C), 26.0, 25.4 (2C), 25.3, 21.3 (2C), 19.1, 17.5, 13.8, -1.4 (3C); IR (neat, cm^{-1}) ν: 3393 (s), 2953 (m), 2931 (m), 2893 (m), 2863 (m), 2853 (m), 2257 (w), 2211 (w), 2139 (w), 2126 (w), 2086 (w), 2053 (w), 2017 (w), 1739 (w), 1717 (w), 1673 (w), 1646 (w), 1629 (w), 1573 (s), 1558 (w), 1306 (w), 1051 (s), 1025 (s), 1002 (s), 824 (m), 761 (s), 667 (w), 626 (w), 618 (w), 607 (w), 589 (w), 570 (w),

555 (w), 534 (w), 517 (w), 499 (w), 465 (w), 451 (w); HRMS (ASAP+, m/z): detected 529.3935, calculated for $C_{30}H_{53}N_4O_2Si$ [M+H]$^+$ 529.3938.

4.13 Isolation of 6-(cyclohex-1-en-1-yl)-*N*-(cyclohexylmethyl)-*N*-methyl-7-((2-(trimethylsilyl)ethoxy)methyl)-7*H*-pyrrolo[2,3-*d*]pyrimidin-4-amine (12)

12

Isolation of byproduct **12** following the reaction and the first purification described in Section 4.11, resulted in 33.2 mg (0.0730 mmol, 19%, $R_f = 0.17$ with EtOAc:CH_2Cl_2, 1:7) of a pale yellow oil with a purity of 86% determined by ^{1}H-NMR spectroscopy. The impurity was amine **4**.

Spectroscopic data for byproduct **12** (Appendix L):
^{1}H-NMR (400 MHz, DMSO-d_6) δ: 8.12 (s, 1H), 6.55 (s, 1H), 6.25 (br s, 1H), 5.49 (s, 2H), 3.63 - 3.59 (m, 4H), 3.31 (s, 3H), 2.36 (br s, 2H), 2.20 (br s, 2H), 1.78 - 1.61 (m, 12H), 1.17 - 1.13 (m, 4H), 1.01 - 0.96 (m, 2H), 0.83 (t, 2H, $J = 8.0$ Hz), -0.08 (s, 9H). This corresponds with the previously reported data in the pre-master's project.[33]

4.14   Synthesis of 4-(4-((cyclohexylmethyl)(methyl)amino)-7-((2-(trimethylsilyl)ethoxy)methyl)-7H-pyrrolo[2,3-d]pyrimidin-6-yl)tetrahydro-2H-pyran-4-ol (13)
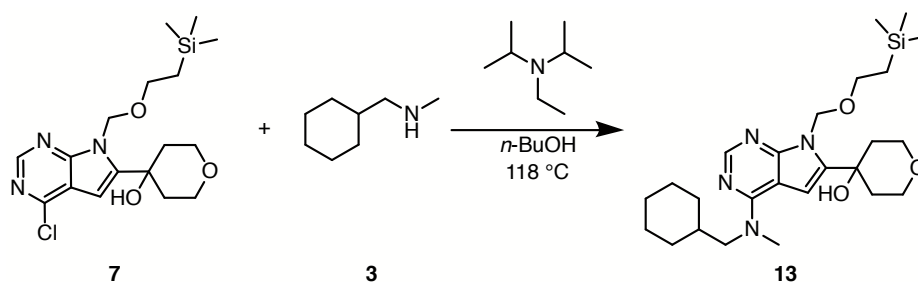
Compound **7** (370 mg, 0.964 mmol) was dissolved in n-BuOH (4 mL). Compound **3** (0.22 mL, 1.4 mmol) and N-ethyl-N-isopropylpropan-2-amine (Hünigs base, 0.25 mL, 1.4 mmol) were added under an N_2-atmosphere. The oil bath was heated to 118 °C and the reaction was stirred for 2 hours. The mixture was concentrated *in vacuo*. Water (7 mL) and CH_2Cl_2 (5 mL) were added to the residue and the layers were separated. The aqueous phase was extracted with CH_2Cl_2 (5 × 3 mL). The combined organic phases were washed with brine (sat., 6 mL), dried over anhydrous Na_2SO_4, filtered and concentrated *in vacuo*. The crude product was first purified by silica-gel column chromatography (EtOAc:CH_2Cl_2, 1:2, R_f = 0.21). Further purification by recrystallization from EtOAc (3 mL) resulted in 207 mg (0.435 mmol, 45%) of a white solid with mp = 160 - 163 °C and was pure as observed by ^{1}H-NMR spectroscopy.

Spectroscopic data for byproduct **13** (Appendix M):
^{1}H-NMR (400 MHz, CDCl$_3$) δ: 8.29 (s, 1H), 6.44 (s, 1H), 5.90 (s, 2H), 4.13 (s, 1H), 4.00 (td, 2H, J = 11.6 Hz, 2.4 Hz), 3.88 - 3.85 (m, 2H), 3.61 - 3.55 (m, 4H), 3.36 (s, 3H), 2.17 (td, 2H, J = 12.0 Hz, 5.6 Hz), 2.06 - 2.03 (m, 2H), 1.86 - 1.81 (m, 1H), 1.75 - 1.68 (m, 5H), 1.27 - 1.15 (m, 3H), 1.06 - 0.97 (m, 2H), 0.93 (dd, 2H, J = 8.4 Hz, 8.4 Hz), -0.06 (s, 9H); ^{13}C-NMR (100 MHz, CDCl$_3$) δ: 157.2, 153.5, 151.8, 140.3, 101.4, 100.8, 71.0, 67.4, 66.4, 63.5 (2C), 57.2, 39.3, 38.1 (2C), 37.3, 30.9 (2C), 26.5, 25.9 (2C), 17.9, -1.5 (3C); IR (neat, cm^{-1}) ν:

3388 (w), 2924 (s), 2856 (m), 2250 (w), 2143 (w), 2111 (w), 2065 (w), 1575 (s), 1551 (m), 1508 (m), 1466 (m), 1449 (m), 1416 (m), 1386 (m), 1364 (m), 1339 (m), 1308 (s), 1285 (m), 1249 (m), 1212 (m), 1151 (m), 1135 (m), 1118 (m), 1076 (s), 1031 (m), 905 (m), 860 (m), 837 (s), 774 (m), 763 (m), 689 (w), 615 (w), 556 (m), 546 (m), 423 (m); HRMS (ASAP+, m/z): detected 475.3097, calculated for $C_{25}H_{43}N_4O_3Si$ $[M+H]^+$ 475.3104.

4.15 Synthesis of *N*-(cyclohexylmethyl)-*N*-methyl-6-(1,4-dioxaspiro[4.5]dec-7-en-8-yl)-7-((2-(trimethylsilyl)ethoxy)methyl)-7*H*-pyrrolo[2,3-*d*]pyrimidin-4-amine (14)
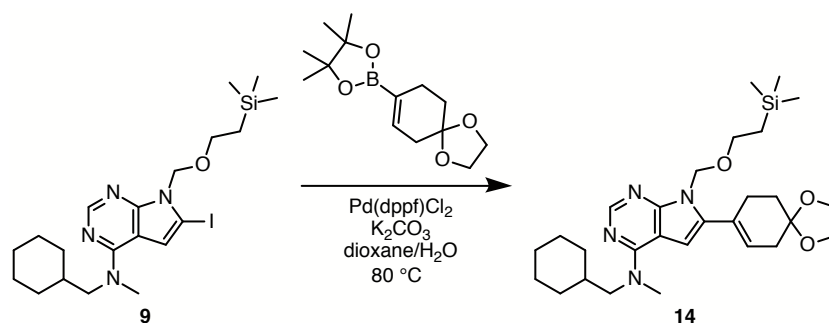
Solvents were degassed using N_2-gas and ultrasonic bath prior to the experiment. Compound **9** (209 mg, 0.417 mmol), 4,4,5,5-tetramethyl-2-(1,4-dioxaspiro[4.5]dec-7-en-8-yl)-1,3,2-dioxaborolane (122 mg, 0.458 mmol), K_2CO_3 (1.20 g, 8.69 mmol) and Pd(dppf)Cl$_2$ (20.6 mg, 0.0282 mmol) were mixed under an N_2-atmosphere. 1,4-Dioxane (4 mL) and water (2 mL) were added. The oil bath was heated to 80 °C and the reaction was stirred for 2 hours. The mixture was concentrated *in vacuo*. Water (5 mL) and CH_2Cl_2 (12 mL) were added and the layers were separated. The aqueous phase was extracted with CH_2Cl_2 (5 × 4 mL). The combined organic phases were washed with brine (sat., 5 mL), dried over anhydrous Na_2SO_4, filtered and concentrated *in vacuo*. The crude product was purified by silica-gel column chromatography (EtOAc:CH_2Cl_2, 1:4, R_f = 0.14). Drying gave 155 mg (0.303 mmol, 73%) of a brown oil that was pure as observed by ^{1}H-NMR spectroscopy.

Spectroscopic data for compound **14** (Appendix N):

^{1}H-NMR (400 MHz, CDCl$_3$) δ: 8.29 (s, 1H), 6.43 (s, 1H), 6.25 (br t, 1H, $J = 4.0$ Hz), 5.57 (s, 2H), 4.03 (s, 4H), 3.70 (dd, 2H, $J = 8.4$ Hz, 8.4 Hz), 3.60 (d, 2H, $J = 7.2$ Hz), 3.35 (s, 3H), 2.66 (br td, 2H, $J = 6.4$ Hz, 1.6 Hz), 2.52 - 2.51 (m, 2H), 1.93 (t, 2H, $J = 6.4$ Hz), 1.85 - 1.82 (m, 1H), 1.74 - 1.68 (m, 5H), 1.24 - 1.18 (m, 3H), 1.05 - 0.97 (m, 2H), 0.93 (dd, 2H, $J = 8.0$ Hz, 8.0 Hz), -0.04 (s, 9H); ^{13}C-NMR (100 MHz, CDCl$_3$) δ: 156.9, 153.3, 151.4, 137.2, 128.0, 125.8, 107.5, 102.4, 100.7, 70.8, 66.1, 64.5 (2C), 57.1, 39.1, 37.2, 36.2, 31.4, 30.8 (2C), 28.3, 26.5, 25.9 (2C), 18.0, -1.4 (3C); IR (neat, cm^{-1}) ν: 3380 (w), 2922 (s), 2851 (m), 1569 (s), 1549 (s), 1509 (m), 1448 (m), 1415 (m), 1365 (m), 1340 (m), 1304 (s), 1286 (m), 1247 (m), 1203 (m), 1147 (m), 1115 (s), 1060 (w), 1025 (s), 990 (w), 968 (w), 943 (m), 908 (m), 896 (w), 858 (s), 834 (s), 799 (w), 765 (s), 721 (w), 692 (m), 653 (w), 628 (w), 586 (w), 552 (w), 467 (w), 426 (w); HRMS (ASAP+, m/z): detected 513.3256, calculated for C$_{28}$H$_{45}$N$_4$O$_3$Si [M+H]$^+$ 513.3261.

4.16 Isolation of 1,1',4,4'-tetraoxa-8,8'-bispiro[4.5]decane-7,7'-diene (15)[86]
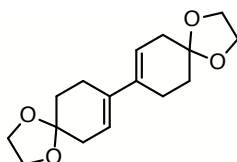
15

Isolation of a mixture of suspected byproduct **15** and 4,4,5,5-tetramethyl-2-(1,4-dioxaspiro[4.5]dec-7-en-8-yl)-1,3,2-dioxaborolane (in ratio 1:8) following the reaction and purification described in Section 4.15, resulted in 12.9 mg of a dark brown oil. The mixture was calculated to contain 1.49 mg (0.00536 mmol, 2%, R$_f$ = 0.76 with EtOAc:CH$_2$Cl$_2$, 1:4) of byproduct **15**.

Spectroscopic data for suspected byproduct **15** (Appendix O):

^{1}H-NMR (400 MHz, DMSO-d_6) δ: 6.01 (m, 2H), 3.92 (s, 8H), 2.56 - 2.54 (m, 4H), 2.37 (br s, 4H), 1.81 (t, 4H, $J = 6.0$ Hz). Spectroscopic data for byproduct **15** has previously been reported in CDCl$_3$ by Zhong *et al.*[86]

4.17   Synthesis of 6-(cyclohex-1-en-1-yl)-*N*-(cyclohexylmethyl)-*N*-methyl-7*H*-pyrrolo[2,3-*d*]pyrimidin-4-amine (HHMT-070)[33]
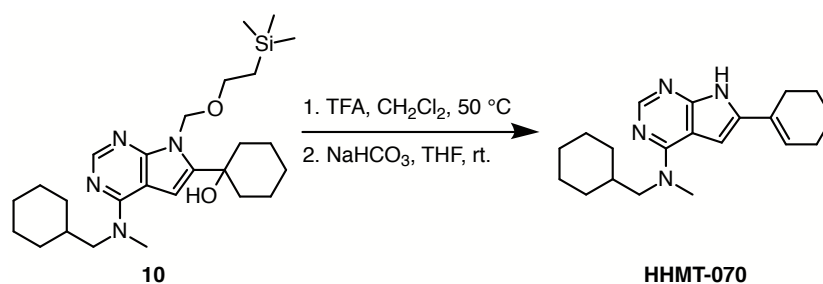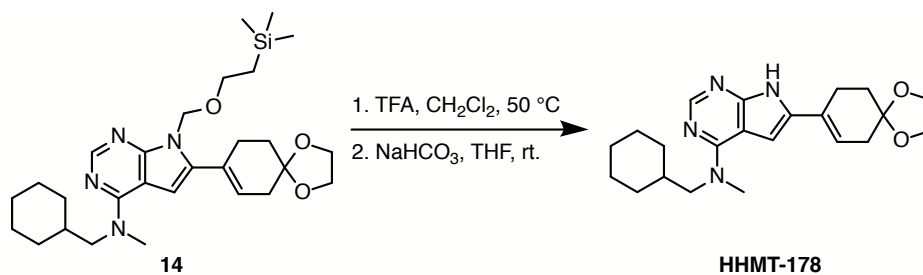

Compound **10** (62.3 mg, 0.132 mmol) was dissolved in CH_2Cl_2 (8 mL) and TFA (0.8 mL) was added under an N_2-atmosphere. The oil bath was heated to 50 °C and the mixture was stirred for 4 hours before it was concentrated *in vacuo*. The residue was dissolved in THF (8 mL) and saturated $NaHCO_3$ (0.8 mL) was added. The mixture was stirred for another 14.5 hours at room temperature before in was concentrated *in vacuo*. Water (15 mL) and CH_2Cl_2 (40 mL) were added to the residue and the layers were separated. The aqueous phase was extracted with CH_2Cl_2 (4 × 10 mL). The combined organic phases were washed with brine (sat., 15 mL), dried over anhydrous Na_2SO_4, filtered and concentrated *in vacuo*. Recrystallization from EtOAc (20 mL) gave 17.5 mg (0.0539 mmol, 41%) of a white solid with mp = 234 - 237 °C (Lit.[33] 216 - 234 °C) and was pure as observed by ^{1}H-NMR spectroscopy.

Spectroscopic data for compound **HHMT-070** (Appendix P):
^{1}H-NMR (600 MHz, CD_3OD:$CDCl_3$, 1:1) δ: 8.08 (s, 1H), 6.39 (s, 1H), 6.27 (br s, 1H), 3.61 (d, 2H, J = 7.8 Hz), 3.35 (s, 3H), 2.42 (br s, 2H), 2.27 (br s, 2H), 1.88 - 1.70 (m, 10H), 1.27 - 1.19 (m, 3H), 1.07 - 1.01 (m, 2H). This corresponds with the previously reported data in the pre-master's project,[33] except that the chemical shifts are about 0.10 ppm higher which may be due to small differences in solvent ratio. Compound **HHMT-070** was also recorded in $CDCl_3$ for future reference: ^{1}H-NMR (400 MHz, $CDCl_3$) δ: 8.90 (br s, 1H), 8.23 (s, 1H), 6.38 (s, 1H), 6.08 (br s, 1H), 3.61 (d, 2H, J = 7.6 Hz), 3.36 (s, 3H), 2.40 (br s, 2H), 2.26

(br s, 2H), 1.84 - 1.68 (m, 10H), 1.27 - 1.16 (m, 3H), 1.06 - 0.98 (m, 2H).

4.18   Synthesis of N-(cyclohexylmethyl)-6-(3,6-dihydro-2H-pyran-4-yl)-N-methyl-7H-pyrrolo[2,3-d]pyrimidin-4-amine (HHMT-170)
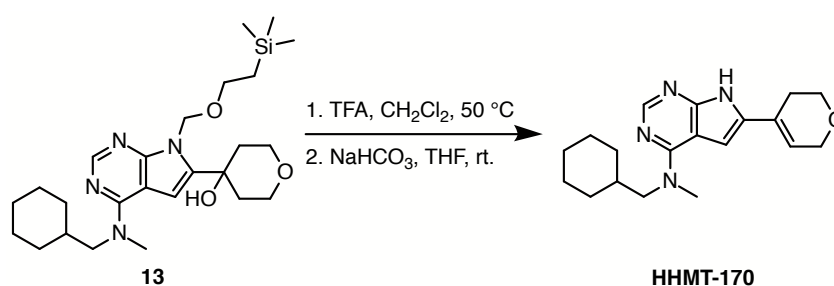
Compound **13** (181 mg, 0.382 mmol) was dissolved in CH_2Cl_2 (18 mL) and TFA (1.8 mL) was added under an N_2-atmosphere. The oil bath was heated to 50 °C and the mixture was stirred for 4 hours before it was concentrated *in vacuo*. The residue was dissolved in THF (18 mL) and saturated $NaHCO_3$ (1.8 mL) was added. The mixture was stirred for another 20.5 hours at room temperature and then concentrated *in vacuo*. Water (50 mL) and CH_2Cl_2 (190 mL) were added to the residue and the layers were separated. The aqueous phase was extracted with CH_2Cl_2 (4 × 20 mL). The combined organic phases were washed with brine (sat., 50 mL), dried over anhydrous Na_2SO_4, filtered and concentrated *in vacuo*. The crude product was first purified by silica-gel column chromatography (gradient from THF:CH_2Cl_2, 1:5, to MeOH:THF, 1:9, R_f = 0.10 - 0.68). Further purification was performed by filtration through a plug of silica-gel (not stabilized THF). The filtrate was then concentrated *in vacuo*. Cold THF (not stabilized, 0.5 mL) was added to the residue and the mixture was filtered. The new filtrate was then recrystallized from THF (not stabilized, 1 mL). The mother liquor was recrystallized from THF (not stabilized, 0.5 mL). The combined fractions of product resulted in 40.8 mg (0.125 mmol, 32%) of a white solid with mp = 202 - 207 °C and purity of 97% as determined by ^{1}H-NMR spectroscopy.

Spectroscopic data for compound **HHMT-170** (Appendix Q):

^{1}H-NMR (600 MHz, CDCl$_3$) δ: 10.85 (br s, 1H), 8.24 (s, 1H), 6.43 (s, 1H), 6.17 (s, 1H), 4.40 (br s, 2H), 3.96 (t, 2H, J = 5.4 Hz), 3.63 (d, 2H, J = 6.0 Hz), 3.38 (s, 3H), 2.55 (br s, 2H), 1.87 - 1.84 (m, 1H), 1.74 (br d, 4H, J = 11.4 Hz), 1.67 (br d, 1H, J = 10.2 Hz), 1.25 - 1.17 (m, 3H), 1.06 - 1.00 (m, 2H); ^{13}C-NMR (150 MHz, CDCl$_3$) δ: 157.0, 152.5, 151.5, 133.4, 126.3, 120.4, 103.3, 98.7, 65.6, 64.1, 57.1, 39.2, 37.3, 30.9 (2C), 26.5, 25.9 (2C), 25.8; IR (neat, cm^{-1}) ν: 3187 (w), 3092 (w), 2922 (s), 2850 (m), 2730 (w), 1569 (s), 1528 (m), 1510 (m), 1448 (w), 1416 (m), 1385 (w), 1363 (w), 1321 (w), 1298 (m), 1285 (w), 1232 (w), 1204 (w), 1171 (w), 1130 (m), 1071 (m), 1030 (w), 970 (w), 937 (w), 926 (w), 910 (w), 896 (w), 873 (w), 850 (w), 818 (w), 781 (w), 762 (w), 733 (w), 476 (w), 466 (w), 456 (w); HRMS (ASAP+, m/z): detected 327.2180, calculated for C$_{19}$H$_{27}$N$_4$O [M+H]$^+$ 327.2185.

4.19 Synthesis of *N*-(cyclohexylmethyl)-*N*-methyl-6-(1,4-dioxaspiro[4.5]dec-7-en-8-yl)-7*H*-pyrrolo[2,3-*d*]pyrimidin-4-amine (HHMT-178)

Compound **14** (65.7 mg, 0.128 mmol) was dissolved in CH$_2$Cl$_2$ (8 mL) and TFA (0.8 mL) was added under an N$_2$-atmosphere. The oil bath was heated to 50 °C and the mixture was stirred for 2 hours before it was concentrated *in vacuo*. The residue was dissolved in THF (8 mL) and saturated NaHCO$_3$ (0.8 mL) was added. The mixture was stirred for another 21 hours at room temperature, filtered and then concentrated *in vacuo*. The residue was dissolved in CH$_2$Cl$_2$ (7 mL) and MeOH (7 mL), and NH$_3$ (25%, 14 mL) was added. The mixture was stirred for 47 hours at room temperature before it was concentrated *in vacuo*. CH$_2$Cl$_2$

(12 mL) was added to the residue and the layers were separated. The aqueous phase was extracted with CH_2Cl_2 (12 × 3 mL). The combined organic phases were washed with brine (sat., 10 mL), dried over anhydrous Na_2SO_4, filtered and concentrated *in vacuo*. A fraction of the crude product (58%) was purified by silica-gel column chromatography (MeOH:CH_2Cl_2, 3:97, R_f = 0.26). Drying gave 4.5 mg (0.012 mmol, 16%) of a brown solid with unknown impurities. Accurate melting point could not be determined due to insufficient amount of product.

Spectroscopic data for compound **HHMT-178** (Appendix R):
^{1}H-NMR (400 MHz, CDCl$_3$) δ: 8.24 (s, 1H), 6.41 (s, 1H), 6.13 (br s, 1H), 4.03 (s, 4H), 3.61 (d, 2H, J = 7.2 Hz), 3.36 (s, 3H), 2.70 (br t, 2H, J = 5.2 Hz), 2.54 (br s, 2H), 1.95 (t, 2H, J = 6.4 Hz), 1.88 - 1.82 (m, 1H), 1.75 - 1.72 (m, 4H), 1.68 - 1.66 (m, 1H), 1.28 - 1.15 (m, 3H), 1.06 - 0.98 (m, 2H); ^{13}C-NMR (100 MHz, CDCl$_3$) δ: 156.9, 152.2, 151.2, 134.1, 128.0, 119.7, 107.7, 103.4, 98.6, 64.6 (2C), 57.2, 39.2, 37.3, 35.9, 31.1, 30.9 (2C), 26.5, 26.0 (2C), 25.2; IR (neat, cm^{-1}) ν: 3190 (w), 3122 (w), 2922 (s), 2850 (m), 2727 (w), 1650 (w), 1567 (s), 1527 (m), 1510 (m), 1448 (m), 1415 (m), 1363 (m), 1318 (m), 1283 (m), 1258 (m), 1210 (w), 1173 (w), 1145 (m), 1117 (m), 1061 (m), 1040 (m), 1007 (w), 983 (w), 970 (w), 938 (w), 926 (w), 894 (w), 867 (m), 781 (w), 731 (m), 688 (w), 657 (w), 645 (w), 628 (w); HRMS (ASAP+, m/z): detected 383.2448, calculated for $C_{22}H_{31}N_4O_2$ [M+H]$^+$ 383.2447.

4.20   Synthesis of 6-cyclohexyl-*N*-(cyclohexylmethyl)-*N*-methyl-7*H*-pyrrolo[2,3-*d*]pyrimidin-4-amine

4.20.1   Attempted hydrogenation in THF/EtOH, 50 mg scale
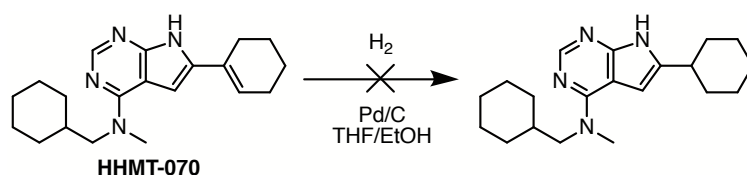
Solvents were degassed using N_2-gas and ultrasonic bath prior to the experiment. Compound **HHMT-070** (49.9 mg, 0.154 mmol) was dissolved in degassed EtOH (3.5 mL) and THF (3.5 mL), and mixed with Pd/C (2.2 mg, 0.021 mmol) under an N_2-atmosphere. The mixture was purged with H_2-gas and then stirred for 24 hours at room temperature before it was concentrated *in vacuo*. The residue was dissolved in THF (3 mL) and filtered through celite. The filtrate was concentrated *in vacuo*. No conversion was observed by ^{1}H-NMR spectroscopy.

4.20.2 Attempted hydrogenation in CHCl$_3$, 50 mg scale
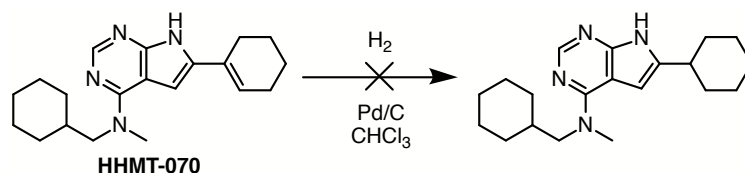
Solvents were degassed using N_2-gas and ultrasonic bath prior to the experiment. Compound **HHMT-070** (49.9 mg, 0.154 mmol) was dissolved in degassed CHCl$_3$ (5 mL) and mixed with Pd/C (3.7 mg, 0.035 mmol) under an N_2-atmosphere. The mixture was purged with H_2 and then stirred for 7.5 hours before it was cooled to 0 °C. The mixture was purged with N_2-gas. Due to no conversion, degassed MeOH (0.5 mL) was added and the mixture was then purged with H_2-gas. The mixture was stirred for another 25.5 hours at room temperature before more CHCl$_3$ (3 mL) and MeOH (1 mL) were added. Due to no conversion, the reaction was heated at 65 °C and stirred under reflux for 3.5 hours. The mixture was then cooled to room temperature and filtered through a syringe filter before it was concentrated *in vacuo*. No conversion was observed by ^{1}H-NMR spectroscopy.

4.20.3 Attempted hydrogenation in CHCl$_3$/MeOH at 6 atm, 20 mg scale
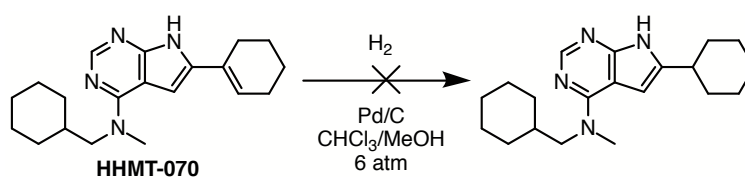
Compound **HHMT-070** (20.2 mg, 0.0623 mmol) was dissolved in MeOH (2.5 mL) and CHCl$_3$ (2.5 mL), and mixed with Pd/C (2.3 mg, 0.022 mmol) at 0°C. The mixture was purged with H$_2$-gas and then stirred for 25 hours at 6 atm at room temperature in a Parr apparatus. The mixture was then filtered through a syringe filter before it was concentrated *in vacuo*. No conversion was observed by ^{1}H-NMR spectroscopy.

Bibliography

1. Lemmon, M. A.; Schlessinger, J. Cell Signaling by Receptor Tyrosine Kinases. *Cell* **2010**, *141*, 1117–1134.

2. Cecchini, M. G.; Dominguez, M. G.; Mocci, S.; Wetterwald, A.; Felix, R.; Fleisch, H.; Chisholm, O.; Hofstetter, W.; Pollard, J. W.; Stanley, E. R. Role of colony stimulating factor-1 in the establishment and regulation of tissue macrophages during postnatal development of the mouse. *Dev.* **1994**, *120*, 1357–1372.

3. Stanley, E. R.; Chen, D.-M.; Lin, H.-S. Induction of macrophage production and proliferation by a purified colony stimulating factor. *Nat.* **1978**, *274*, 168–170.

4. Robinson, D. R.; Wu, Y.-M.; Lin, S.-F. The protein tyrosine kinase family of the human genome. *Oncogene* **2000**, *19*, 5548–5557.

5. Shawver, L. K.; Slamon, D.; Ullrich, A. Smart drugs: Tyrosine kinase inhibitors in cancer therapy. *Cancer cell* **2002**, *1*, 117–123.

6. Ciardiello, F.; Caputo, R.; Bianco, R.; Damiano, V.; Pomatico, G.; Placido, S. D.; Bianco, A. R.; Tortora, G. Antitumor Effect and Potentiation of Cytotoxic Drugs Activity in Human Cancer Cells by ZD-1839 (Iressa), an Epidermal Growth Factor Receptor-selective Tyrosine Kinase Inhibitor. *Clin. Cancer Res.* **2000**, *6*, 2053–2063.

7. Fry, D. W. Inhibition of the epidermal growth factor receptor family of tyrosine kinases as an approach to cancer chemotherapy: progression from reversible to irreversible inhibitors. *Pharmacol. Ther.* **1999**, *82*, 207–218.

8. Dinakaran, V. S.; Bomma, B.; Srinivasan, K. K. Fused pyrimidines: The heterocycle of diverse biological and pharmacological significance. *Der Pharma Chemica* **2012**, *4*, 255–265.

9. Lloyd, R. F.; Skinner, C. G.; Shive, W. 4-(Substituted)pteridines, analogues of kinetin. *Can. J. Chem.* **1967**, *45*, 2213–2216.

10. Litvinov, V. P. *Advances in Heterocyclic Chemistry*, 1st ed.; Academic Press, 2006; Vol. 92; p 83.

11. Han, J.; Henriksen, S.; Nørsett, K. G.; Sundby, E.; Hoff, B. H. Balancing potency, metabolic stability and permeability in pyrrolopyrimidine-based EGFR inhibitors. *Eur. J. Med. Chem.* **2016**, *124*, 583–607.

12. Larsen, K. U. Synthesis of Pyrrolopyrimidines as CSF-1R Kinase Inhibitors. M.Sc. thesis, NTNU, Norway, 2016.

13. Hubbard, S. R.; Till, J. H. Protein Tyrosine Kinase Structure and Function. *Annu. Rev. Biochem.* **2000**, *69*, 373–398.

14. Heldin, C.-H. Dimerization of Cell Surface Receptors in Signal Transduction. *Cell* **1995**, *80*, 213–223.

15. Blume-Jensen, P.; Hunter, T. Oncogenic kinase signalling. *Nat.* **2001**, *411*, 355–365.

16. Ullrich, A.; Schlessinger, J. Signal Transduction by Receptors with Tyrosine Kinase Activity. *Cell* **1990**, *61*, 203–212.

17. Robertson, S. C.; Tynan, J. A.; Donoghue, D. J. RTK mutations and human syndromes. *Trends Genet.* **2000**, *16*, 265–271.

18. Hume, D. A.; MacDonald, P. A. Therapeutic applications of macrophage colony-stimulating factor-1 (CSF-1) and antagonists of CSF-1 receptor (CSF-1R) signaling. *Blood* **2012**, *119*, 1810–1820.

19. Kacinski, B. M. CSF-1 and Its Receptor in Breast Carcinomas and Neoplasms of the Female Reproductive Tract. *Mol. Reprod. Dev.* **1997**, *46*, 71–74.

20. Rajavashisth, T.; Qiao, J.-H.; Tripathi, S.; Tripathi, J.; Mishra, N.; Hua, M.; Wang, X.-P.; Loussararian, A.; Clinton, S.; Libby, P.; Lusis, A. Heterozygous Osteopetrotic (op) Mutation Reduces Atherosclerosis in LDL Receptor-deficient Mice. *J. Clin. Invest.* **1998**, *101*, 2702–2710.

21. El-Gamal, M. I.; Anbar, H. S.; Yoo, K. H.; Oh, C. H. FMS Kinase Inhibitors: Current Status and Future Prospects. *Med. Res. Rev.* **2013**, *33*, 599–636.

22. Hardy, W. D. The Feline Sarcoma Viruses. *J. Am. Anim. Hosp. Assoc.* **1981**, *17*, 981–997.

23. Chen, X.; Liu, H.; Focia, P. J.; Shim, A. H.-R.; He, X. Structure of macrophage colony stimulating factor bound to FMS: Diverse signaling assemblies of class III receptor tyrosine kinases. *PNAS* **2008**, *105*, 18267–18272.

24. Garceau, V.; Smith, J.; Paton, I. R.; Davey, M.; Fares, M. A.; Sester, D. P.; Burt, D. W.; Hume, D. A. Pivotal Advance: Avian colony-stimulating factor 1 (CSF-1), interleukin-34 (IL-34), and CSF-1 receptor genes and gene products. *J. Leukocyte Biol.* **2010**, *87*, 753–764.

25. Yeung, Y.-G.; Wang, Y.; Einstein, D. B.; Lee, P. S. W.; Stanley, E. R. Colony-stimulating Factor-1 Stimulates the Formation of Multimeric Cytosolic Complexes of Signaling Proteins and Cytoskeletal Components in Macrophages. *J. Biol. Chem.* **1998**, *273*, 17128–17137.

26. Ohno, H.; Kubo, K.; Murooka, H.; Kobayashi, Y.; Nishitoba, T.; Shibuya, M.; Yoneda, T.; Isoel, T. A c-fms tyrosine kinase inhibitor, Ki20227, suppresses osteoclast differentiation and osteolytic bone destruction in a bone metastasis model. *Mol. Cancer Ther.* **2006**, *5*, 2634–2643.

27. Ohno, H.; Uemura, Y.; Murooka, H.; Takanashi, H.; Tokieda, T.; Ohzeki, Y.; Kubo, K.; Serizawa, I. The orally-active and selective c-Fms tyrosine kinase inhibitor Ki20227 inhibits disease progression in a collagen-induced arthritis mouse model. *Eur. J. Immunol.* **2008**, *38*, 283–291.

28. Conway, J. G.; McDonald, B.; Parham, J.; Keith, B.; Rusnak, D. W.; Shaw, E.; Jansen, M.; Lin, P.; Payne, A.; Crosby, R. M.; Johnson, J. H.; Frick, L.; Lin, M. J.; Depee, S.; Tadepalli, S.; Votta, B.; James, I.; Fuller, K.; Chambers, T. J.; Kull, F. C.; Chamberlain, S. D.; Hutchins, J. T. Inhibition of colony-stimulating-factor-1 signaling in vivo with the orally bioavailable cFMS kinase inhibitor GW2580. *PNAS* **2005**, *102*, 16078–16083.

29. Xu, J.; Escamilla, J.; Mok, S.; David, J.; Priceman, S.; West, B.; Bollag, G.; McBride, W.; Wu, L. CSF1R Signaling Blockade Stanches Tumor-Infiltrating Myeloid Cells and Improves the Efficacy of Radiotherapy in Prostate Cancer. *Cancer Res.* **2013**, *79*, 2782–2794.

30. DeNardo, D. G.; Brennan, D. J.; Rexhepaj, E.; Ruffell, B.; Shiao, S. L.;

Madden, S. F.; Gallagher, W. M.; Wadhwani, N.; Keil, S. D.; Junaid, S. A.; Rugo, H. S.; Hwang, E. S.; Jirström, K.; West, B. L.; Coussens, L. M. Leukocyte Complexity Predicts Breast Cancer Survival and Functionally Regulates Response to Chemotherapy. *Cancer Discovery* **2011**, *1*, 54–67.

31. Larsen, K. U. Pre-master's project: Synthesis of Pyrrolopyrimidines for Use in SAR Study of CSF-1R Kinase. 2015; NTNU, Norway.

32. Ritchie, T. J.; Macdonald, S. J.; Young, R. J.; Pickett, S. D. The impact of aromatic ring count on compound developability: further insights by examining carbo- and hetero-aromatic and -aliphatic ring types. *Drug Discovery Today* **2011**, *16*, 164–171.

33. Tsui, H. M. H. Pre-master's project: Synthetic strategy towards substituted pyrrolo[2,3-*d*]pyrimidine as potential CSF-1R inhibitor. 2018; NTNU, Norway.

34. Clayden, J.; Greeves, N.; Warren, S. *Organic Chemistry*, 2nd ed.; Oxford University Press, 2012; pp 234–235, 514–518, 549, 563–564, 1085–1087.

35. Han, J.; Henriksen, S.; Nørsett, K. G.; Sundby, E.; Hoff, B. H. Balancing potency, metabolic stability and permeability in pyrrolopyrimidine-based EGFR inhibitors. *Eur. J. Med. Chem.* **2016**, *124*, 583–607.

36. Chandra, T.; Broderick, W. E.; Broderick, J. B. An efficient deprotection of N-trimethylsilylethoxymethyl (SEM) groups from dinucleosides and dinucleotides. *Nucleosides Nucleotides Nucleic Acids* **2010**, *29*, 132–143.

37. Kan, T.; Hashimoto, M.; Yanagiya, M.; Shirahama, H. Effective deprotection of 2-(trimethylsilylethoxy)methylated alcohols (SEM ethers). Synthesis of thyrsiferyl-23 acetate. *Tetrahedron Lett.* **1988**, *29*, 5417–5418.

38. Jolicoeur, B.; Chapman, E. E.; Thompson, A.; Lubell, W. D. Pyrrole protection. *Tetrahedron* **2006**, *62*, 11531–11563.

39. Hatcher, J. M.; Zhang, J.; Choi, H. G.; Ito, G.; Alessi, D. R.; Gray, N. S. Discovery of a Pyrrolopyrimidine (JH-II-127), a Highly Potent, Selective, and Brain Penetrant LRRK2 Inhibitor. *ACS Med. Chem. Lett.* **2015**, *6*, 584–589.

40. Han, J. Investigation of Pyrrolo- and Furopyrimidines as Epidermal Growth Factor Receptor Tyrosine Kinase Inhibitors. Ph.D. thesis, NTNU, Norway, 2016.

41. Carey, F. A.; Sundberg, R. J. *Advanced Organic Chemistry. Part B: Reactions and Synthesis*, 5th ed.; Springer, 2007; pp 627, 739–740, 1035–1037.

42. Zheng, G.-C.; Kakisawa, H. Synthesis of Salvilenone, a Diterpenoid Phenalenone of Salvia miltiorrhiza. *Bull. Chem. Soc. Jpn.* **1989**, *62*, 1117–1122.

43. Brittain, J. M.; Jones, R. A.; Arques, J. S.; Saliente, T. A. Pyrrole Studies XXVII. Utilisation of 1-Methyl-2-pyrrolyl Lithium in the Synthesis of 1-Methyl-2- substituted Pyrroles. *Synth. Commun.* **1982**, *12*, 231–248.

44. Zhao, X.; Huang, W.; Wang, Y.; Xin, M.; Jin, Q.; Cai, J.; Tang, F.; Zhao, Y.; Xiang, H. Discovery of novel Bruton's tyrosine kinase (BTK) inhibitors bearing a pyrrolo[2,3-*d*]pyrimidine scaffold. *Bioorg. Med. Chem.* **2015**, *23*, 891–901.

45. Solomons, G.; Fryhle, C.; Snyder, S. *Organic Chemistry*, 11th ed.; Wiley, 2014; pp 282, 747–749, 911–913.

46. Abdel-Magid, A. F.; Carson, K. G.; Harris, B. D.; Maryanoff, C. A.; Shah, R. D. Reductive Amination of Aldehydes and Ketones with Sodium Triacetoxyborohydride. Studies on Direct and Indirect Reductive Amination Procedures. *J. Org. Chem.* **1996**, *61*, 3849–3862.

47. Pauls, H. W.; Laufer, R.; Liu, Y.; Li, S.-W.; Forrest, B. T.; Lang, Y.; Patel, N. K. B.; Edwards, L. G.; Ng, G.; Sampson, P. B.; Feher, M.; Awrey, D. E. Indazole compounds as kinase inhibitors and method of treating cancer with same. patent WO2013053051A1, 2013.

48. Feng, Y.; Lograsso, P.; Schroeter, T.; Yin, Y. Urea and carbamate compounds and analogs as kinase inhibitors. patent WO2010036316A1, 2010.

49. Luna-Mora, R. A.; Ángeles Torres-Reyes,; González-Cruz, O. A.; Ortega-Jiménez, F.; Ríos-Guerra, H.; González-Carrillo, J. V.; Barrera-Téllez, F.; Perez-Flores, J.; Penieres-Carrillo, J. G. Assessment of amination reactions via nucleophilic aromatic substitution using conventional and eco-friendly energies. *Green Chem. Lett. Rev.* **2018**, *11*, 371–378.

50. Seechurn, C. C. C. J.; Kitching, M. O.; Colacot, T. J.; Snieckus, V. Palladium-Catalyzed Cross-Coupling: A Historical Contextual Perspective to the 2010 Nobel Prize. *Angew. Chem. Int. Ed.* **2012**, *51*, 5062–5085.

51. Wu, X.-F.; Anbarasan, P.; Neumann, H.; Beller, M. From Noble Metal to Nobel Prize: Palladium-Catalyzed Coupling Reactions as Key Methods in Organic Synthesis. *Angew. Chem. Int. Ed.* **2010**, *49*, 9047–9050.

52. Braga, A. A. C.; Morgon, N. H.; Ujaque, G.; Maseras, F. Computational Characterization of the Role of the Base in the Suzuki-Miyaura Cross-Coupling Reaction. *J. Am. Chem. Soc.* **2005**, *127*, 9298–9307.

53. Tromp, M.; Sietsma, J. R. A.; van Bokhoven, J. A.; van Strijdonck, G. P. F.; van Haaren, R. J.; van der Eerden, A. M. J.; van Leeuwenb, P. W. N. M.; Koningsberger, D. C. Deactivation processes of homogeneous Pd catalysts using in situ time resolved spectroscopic techniques. *Chem. Commun.* **2003**, *7*, 128–129.

54. Iwasawa, T.; Tokunaga, M.; Obora, Y.; Tsuji, Y. Homogeneous Palladium Catalyst Suppressing Pd Black Formation in Air Oxidation of Alcohols. *J. Am. Chem. Soc.* **2004**, *126*, 6554–6555.

55. Lennox, A. J. J.; Lloyd-Jones, G. C. Selection of boron reagents for Suzuki–Miyaura coupling. *Chem. Soc. Rev.* **2014**, *43*, 412–443.

56. Kurti, L.; Czako, B. *Strategic Applications of Named Reactions in Organic Synthesis*, 1st ed.; Academic Press, 2005; p 448.

57. Adamo, C.; Amatore, C.; Ciofini, I.; Jutand, A.; Lakmini, H. Mechanism of the Palladium-Catalyzed Homocoupling of Arylboronic Acids: Key Involvement of a Palladium Peroxo Complex. *J. Am. Chem. Soc.* **2006**, *128*, 6829–6836.

58. Lin, Q.; Meloni, D.; Pan, Y.; Xia, M.; Rodgers, J.; Shepard, S.; Li, M.; Galya, L.; Metcalf, B.; Yue, T. Y.; Liu, P.; Zhou, J. Enantioselective synthesis of Janus kinase inhibitor INCB018424 via an organocatalytic aza-Michael reaction. *Org. Lett.* **2009**, *11*, 1999–2002.

59. Ehrhardt, C.; Irie, O.; Lorthiois, E. L. J.; Maibaum, J. K.; Ostermann, N.; Sellner, H. Preparation of 3,4-substituted pyrrolidines for treatment of hypertension. patent WO2006100036, 2006.

60. Brown, H. C.; Narasimhan, S.; Choi, Y. M. Improved Procedure for Borane-Dimethyl Sulfide Reduction of Tertiary and Secondary Amides in the Presence of Boron Trifluoride Etherate. *Synthesis* **1981**, *12*, 996–997.

61. Cranwell, P. B.; Harwood, L. M.; Moody, C. J. *Experimental Organic Chemistry*, 3rd ed.; John Wiley & Sons, Hoboken, USA, 2017; pp 108–109, 374–376.

62. Daun, J.; Fields, S.; Kobayashi, S. Novel deazapurnes and uses thereof. patent US20040186127A1, 2004.

63. Frank, K. E.; Burchat, A.; Cox, P.; Ihle, D. C.; Mullen, K. D.; Somal, G.; Vasudevan, A.; Wang, L.; Wilson, N. S. Novel tricyclic compounds. patent WO2012149280, 2012.

64. Kaspersen, S. J.; Han, J.; Nørsett, K. G.; Rydså, L.; Kjøbli, E.; Bugge, S.; Bjørkøy, G.; Sundby, E.; Hoff, B. H. Identification of new 4-N-substituted 6-aryl-7H-pyrrolo[2,3-d]pyrimidine-4-amined as highly potent EGFR-TK inhibitors with Src-family activity. *Eur. J. Pharm. Sci.* **2014**, *59*, 69–82.

65. Miller, W. D.; Fray, A. H.; Quatroche, J. T.; Sturgill, C. D. Suppression of a Palladium-Mediated Homocoupling in a Suzuki Cross-Coupling Reaction. Development of an Impurity Control Strategy Supporting Synthesis of LY451395. *Org. Process Res. Dev.* **2007**, *11*, 359–364.

66. Seo, H.; Katcher, M. H.; Jamison, T. F. Photoredox activation of carbon dioxide for amino acid synthesis in continuous flow. *Nat. Chem.; London* **2017**, *9*, 453–456.

67. Jones, P.; Ontoria, J. M. O.; Scarpelli, R.; Ingenito, R.; Schultz-Fademrecht, C. Heterocycle substituted ketone derivatives as histone deacetylase (hdac) inhibitors. patent WO2007072080A2, 2006.

68. Silverstein, R. M.; Webster, F. X.; Kiemle, D. J.; Bryce, D. L. *Spectrometric Identification of Organic Compounds*; John Wiley & Sons, 2014; pp 75, 80–108.

69. Norman, M. H.; Chen, N.; Han, N.; Liu, L.; Hurt, C. R.; Fotsch, C. H.; Jenkins, T. J.; Moreno, O. A. Bicyclic pyridine and pyrimidine derivatives as neuropeptide y receptor antagonists. patent WO1999040091A1, 1999.

70. Li, Y.-L.; Wang, Z.; Barbosa, J.; Burns, D. M.; Feng, H.; Glenn, J.; He, C.; Huang, T.; Mei, S.; Zhuo, J. Pyrrolotriazine compounds as TAM inhibitors. patent WO2017172596Al, 2017.

71. Chandra, T.; Zebrowski, J. P. Hazards associated with laboratory scale hydrogenations. *J. Chem. Health. Saf.* **2016**, *23*, 16–25.

72. Dyson, P. J.; Jessop, P. G. Solvent effects in catalysis: rational improvements of catalysts via manipulation of solvent interactions. *Catal. Sci. Technol.* **2016**, *6*, 3302–3316.

73. Rajadhyaksha, R. A.; Karwa, S. L. Solvent effects in catalytic hydrogenation. *Chem. Eng. Sci.* **1986**, *41*, 1765–1770.

74. Norman, M. H.; Chen, N.; Chen, Z.; Fotsch, C.; Hale, C.; Han, N.; Hurt, R.; Jenkins, T.; Kincaid, J.; Liu, L.; Lu, Y.; Moreno, O.; Santora, V. J.; Sonnenberg, J. D.; Karbon, W. Structure-Activity Relationships of a Series of Pyrrolo[3,2-d]pyrimidine Derivatives and Related Compounds as Neuropeptide Y5 Receptor Antagonists. *J. Med. Chem.* **2000**, *43*, 4288–4312.

75. Hughes, J. P.; Rees, S.; Kalindjian, S. B.; Philpott, K. L. Principles of early drug discovery. *Br. J. Pharmacol.* **2011**, *162*, 1239–1249.

76. Reiersølmoen, A. C.; Aarhus, T. I.; Eckelt, S.; Nørsett, K. G.; Sundby, E.; Hoff, B. H. Potent and selective EGFR inhibitors based on 5-aryl-7H-pyrrolopyrimidin-4-amines. *Bioorg. Chem.* **2019**, *88*, 102918.

77. Pollok, B. A.; Hamman, B. D.; Rodems, S. M.; Makings, L. R. Optical probes and assays. patent WO2000066766A1, 2000.

78. Rule, G. S.; Hitchens, T. K. *Fundamentals of Protein NMR Spectroscopy*; Springer, 2006; pp 48–49.

79. Jeannerat, D. Computer optimized spectral aliasing in the indirect dimension of ^{1}H–^{13}C heteronuclear 2D NMR experiments. A new algorithm and examples of applications to small molecules. *J. Magn. Reson.* **2007**, *186*, 112–122.

80. Njock, G. B. B.; Pegnyemb, D. E.; Bartholomeusz, T. A.; Christen, P.; Vitorge, B.; Nuzillard, J.-M.; Shivapurkar, R.; Foroozandeh, M.; Jeannerat, D. Spectral aliasing: a super zoom for 2D-NMR spectra. Principles and applications. *CHIMIA Int. J. Chem.* **2010**, *64*, 235–240.

81. Friebolin, H. *Basic One- and Two-Dimensional NMR spectroscopy*, 5th ed.; Wiley-VCH, 2011; pp 44–46, 49, 64–65, 74, 313–314.

82. Fulmer, G. R.; Miller, A. J. M.; Sherden, N. H.; Gottlieb, H. E.; Nudel-

man, A.; Stoltz, B. M.; Bercaw, J. E.; Goldberg, K. I. NMR Chemical Shifts of Trace Impurities: Common Laboratory Solvents, Organics, and Gases in Deuterated Solvents Relevant to the Organometallic Chemist. *Organometallics* **2010**, *29*, 2177.

83. Kuhn, B.; Mohr, P.; Stahl, M. Intramolecular Hydrogen Bonding in Medicinal Chemistry. *J. Med. Chem.* **2010**, *53*, 2601–2611.

84. Pitner, T. P.; Sternglanz, H.; Bugg, C. E.; Glickson, J. D. Proton Nuclear Magnetic Resonance Study of Hindered Internal Rotation of the Dimethylamino Group of N6, N6-Dimethyladenine Hydrochloride in Aqueous Solution. *J. Am. Chem. Soc.* **1975**, *97*, 885–888.

85. Hanada, S.; Ishida, T.; Motoyama, Y.; Nagashima, H. The Ruthenium-Catalyzed Reduction and Reductive N-Alkylation of Secondary Amides with Hydrosilanes: Practical Synthesis of Secondary and Tertiary Amines by Judicious Choice of Hydrosilanes. *J. Org. Chem.* **2007**, *72*, 7551–7559.

86. Zhong, Z.; Wang, Z.-Y.; Ni, S.-F.; Dang, L.; Lee, H. K.; Peng, X.-S.; Wong, H. N. C. Ligand-Free Iron-Catalyzed Carbon (sp2)-Carbon (sp2) Oxidative Homo-Coupling of Alkenyllithiums. *Org. Lett.* **2019**, *21*, 700–704.

A   Spectroscopic data for compound 1
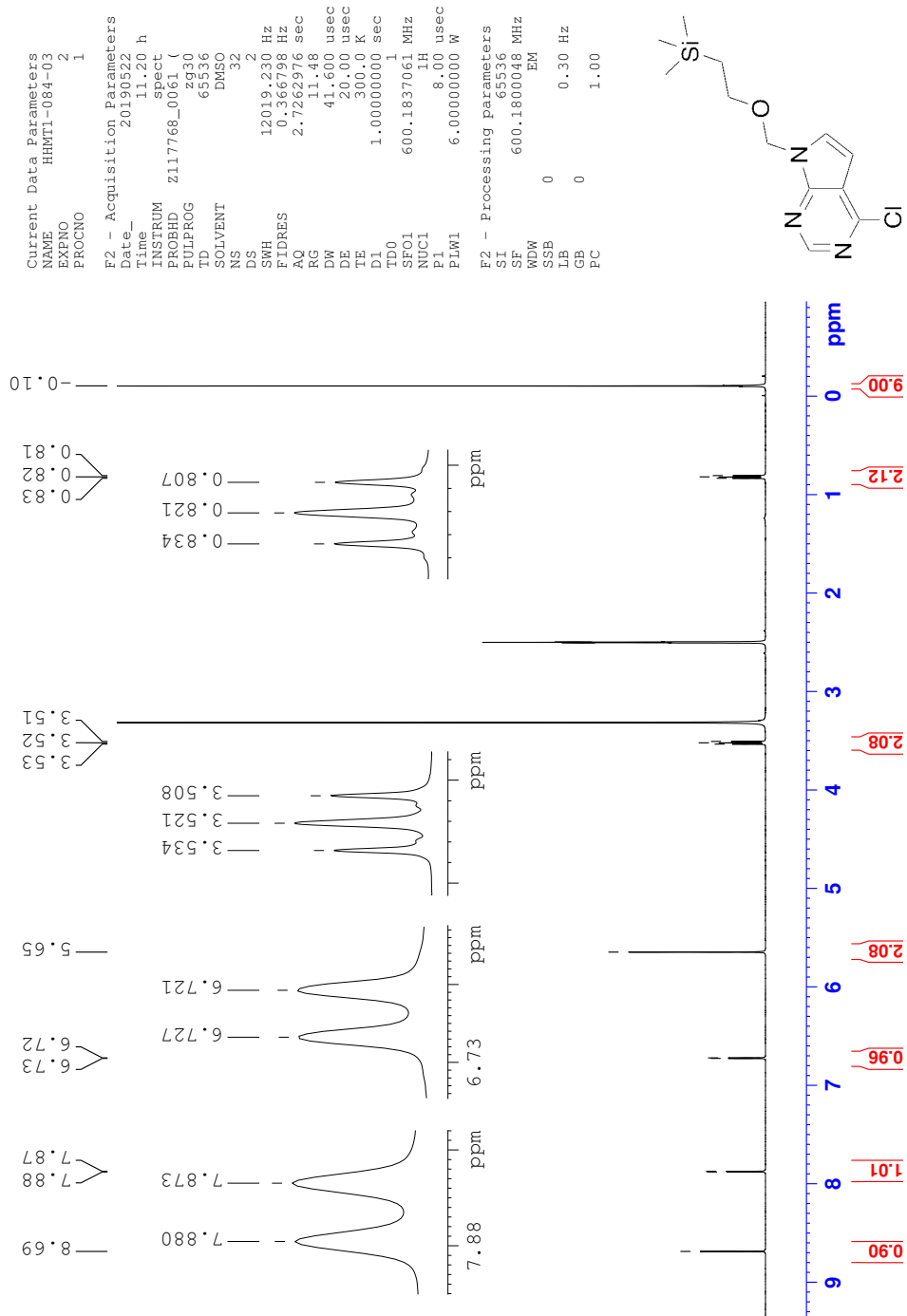
Figure 4.1: ^{1}H-NMR spectrum (600 MHz, DMSO-d_6) of compound **1**.

I
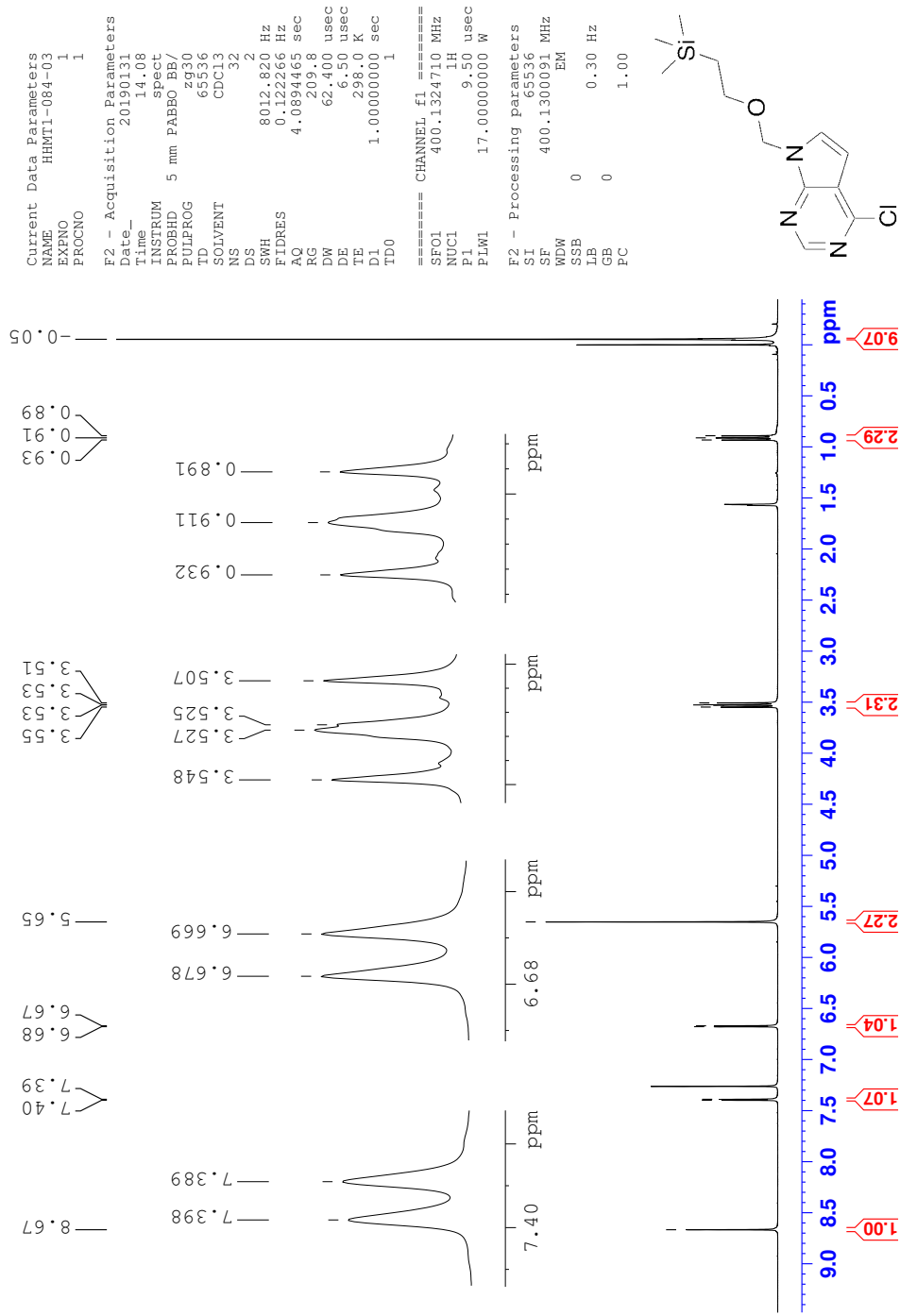
Figure 4.2: ^{1}H-NMR spectrum (400 MHz, CDCl$_3$) of compound **1**.

B   Spectroscopic data for byproduct 2
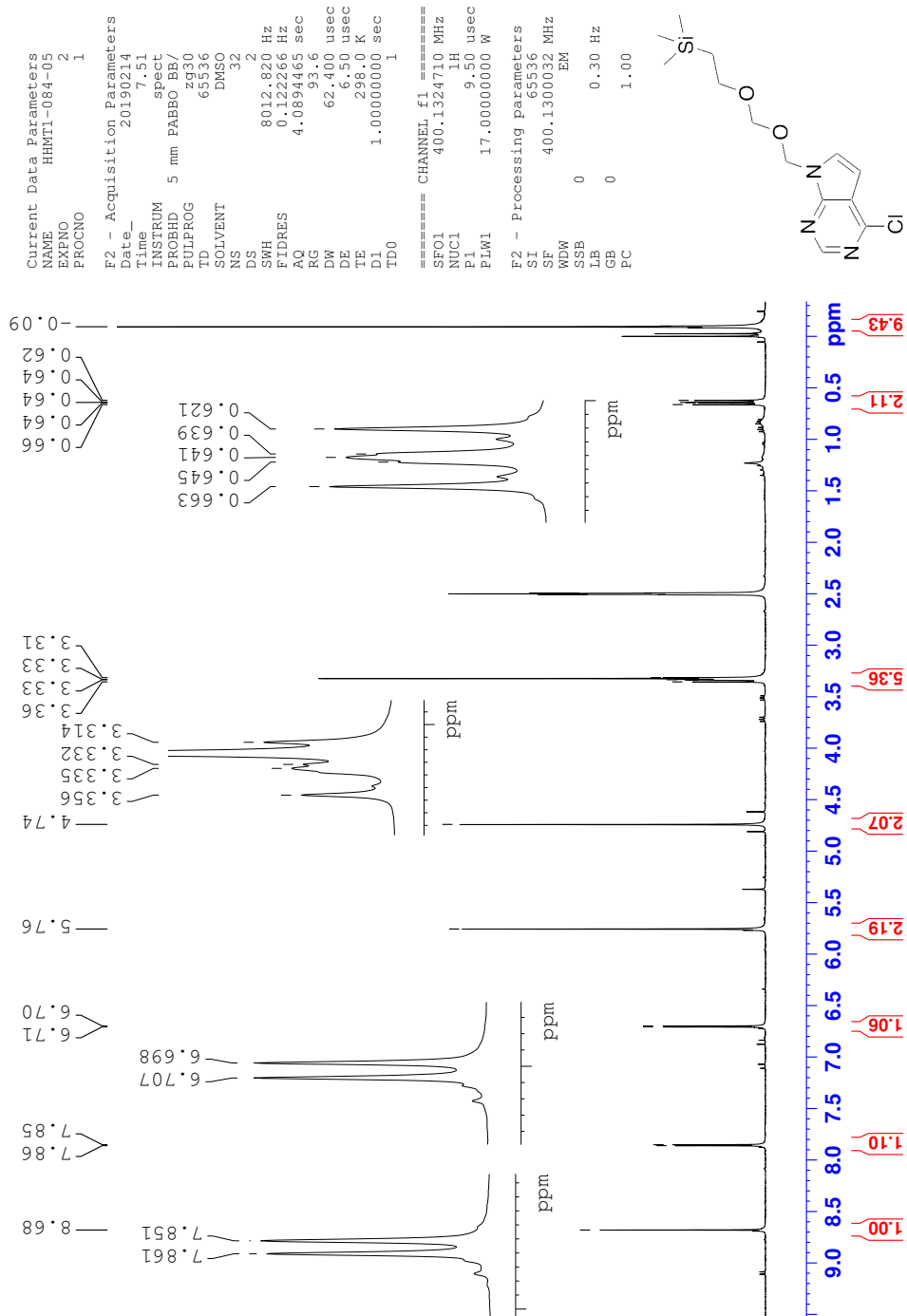
Figure 4.3: ^{1}H-NMR spectrum (400 MHz, DMSO-d_6) of byproduct **2**.

C   Spectroscopic data for compound 3 and byproduct 4
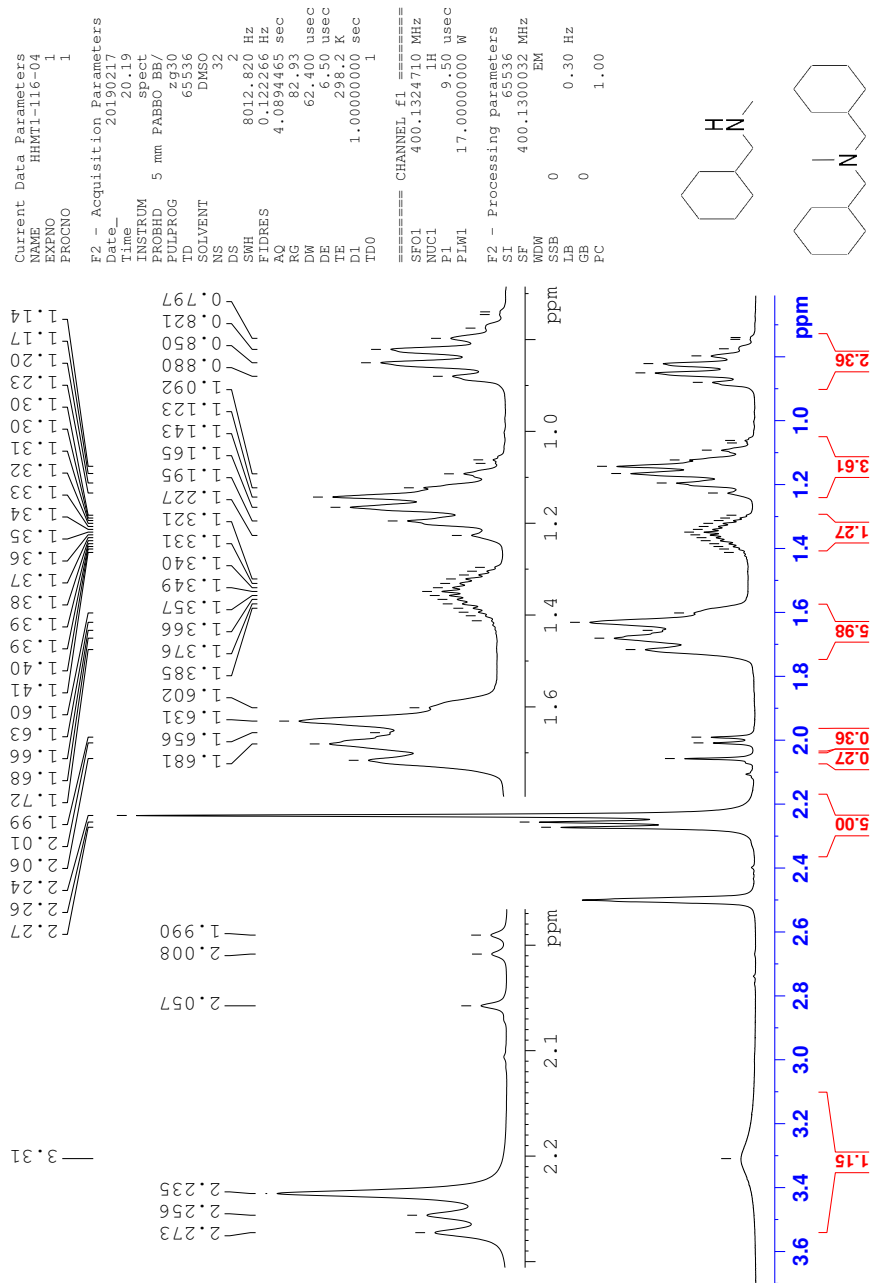
Figure 4.4: ^{1}H-NMR spectrum (400 MHz, DMSO-d_6) of compound **3** and byproduct **4**.

D Spectroscopic data for compound 3 standard
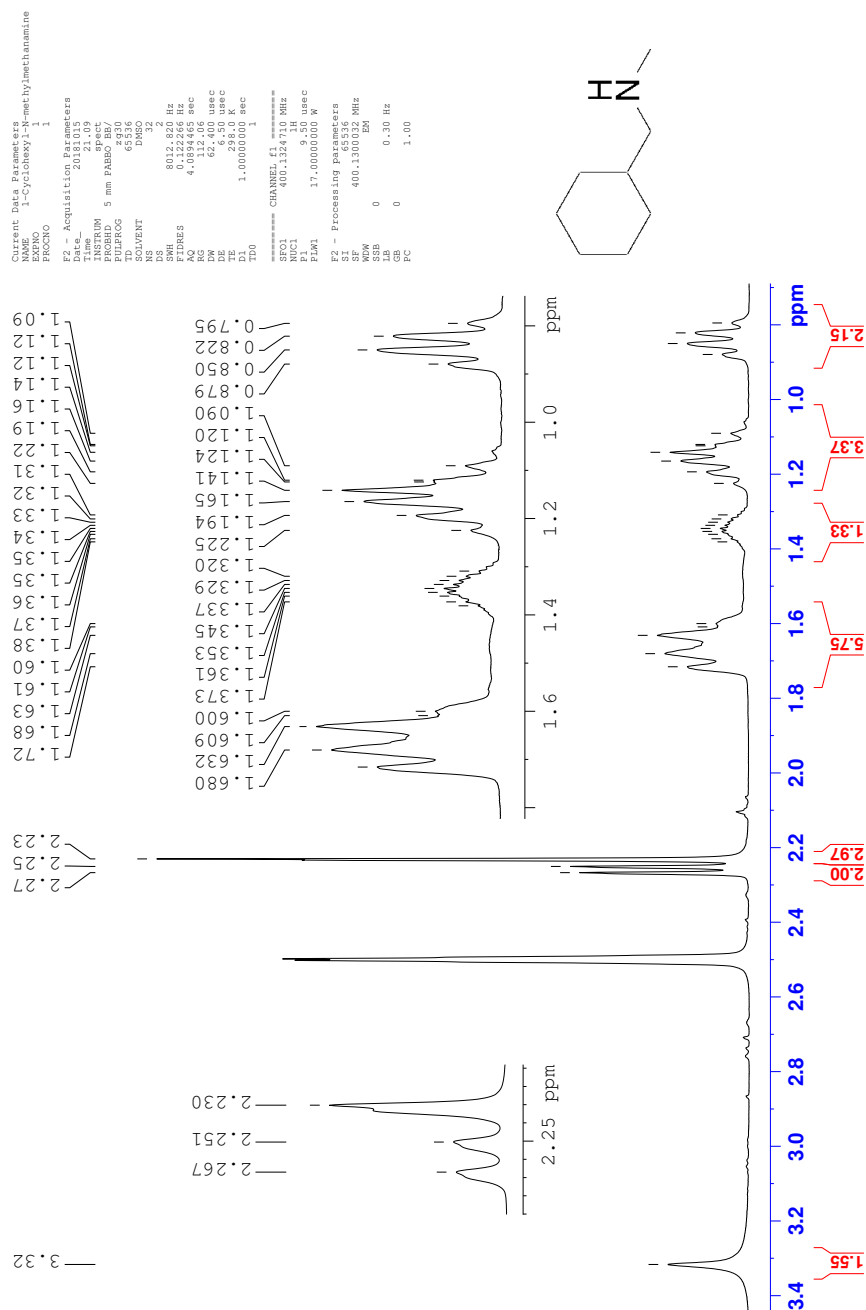
Figure 4.5: ^{1}H-NMR spectrum (400 MHz, DMSO-d_6 of 1-cyclohexyl-N-methylmethanamine (**3**) from Sigma-Aldrich.

E   Spectroscopic data for compound 5
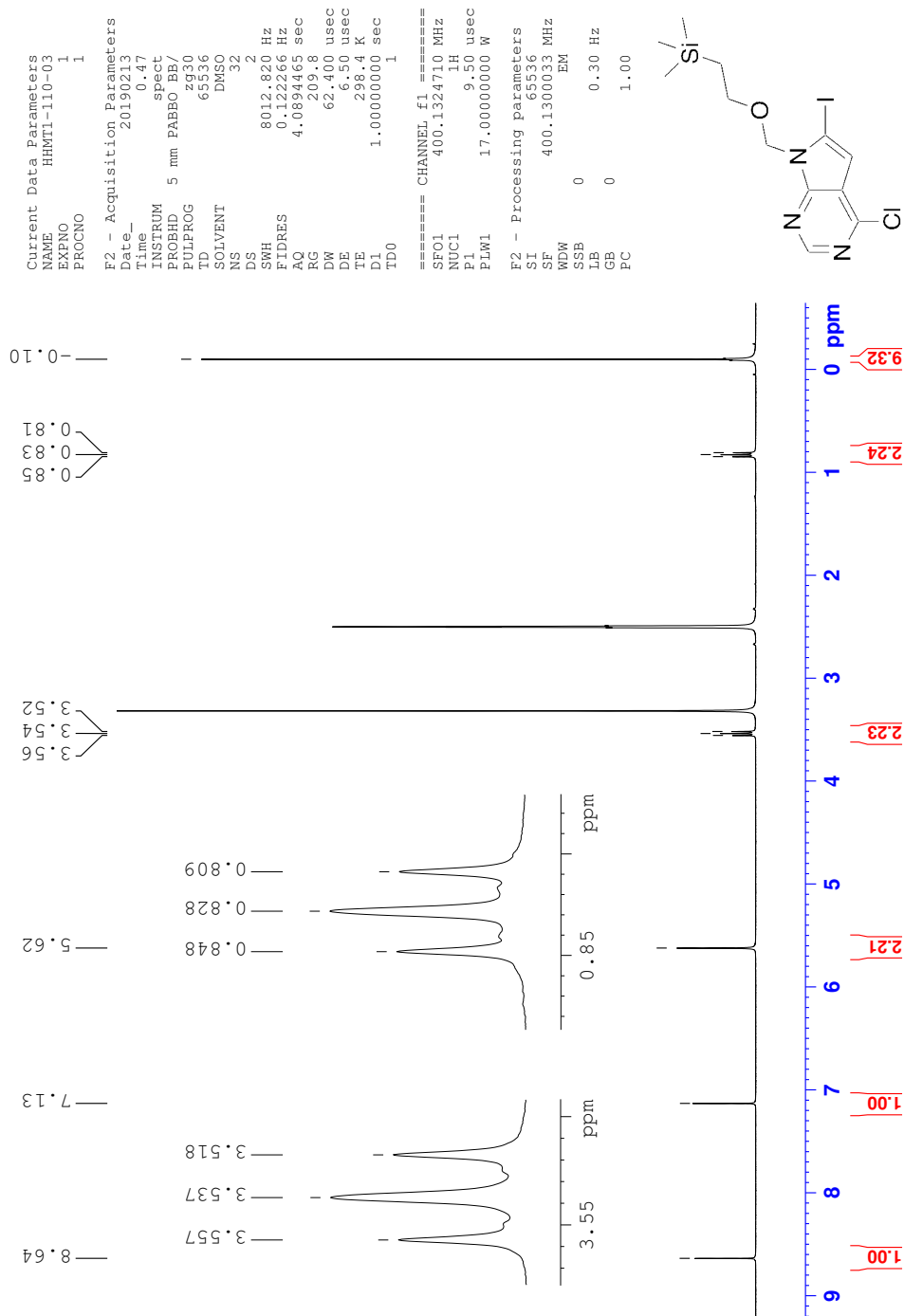
Figure 4.6: ^{1}H-NMR spectrum (400 MHz, DMSO-d_6) of compound **5**.
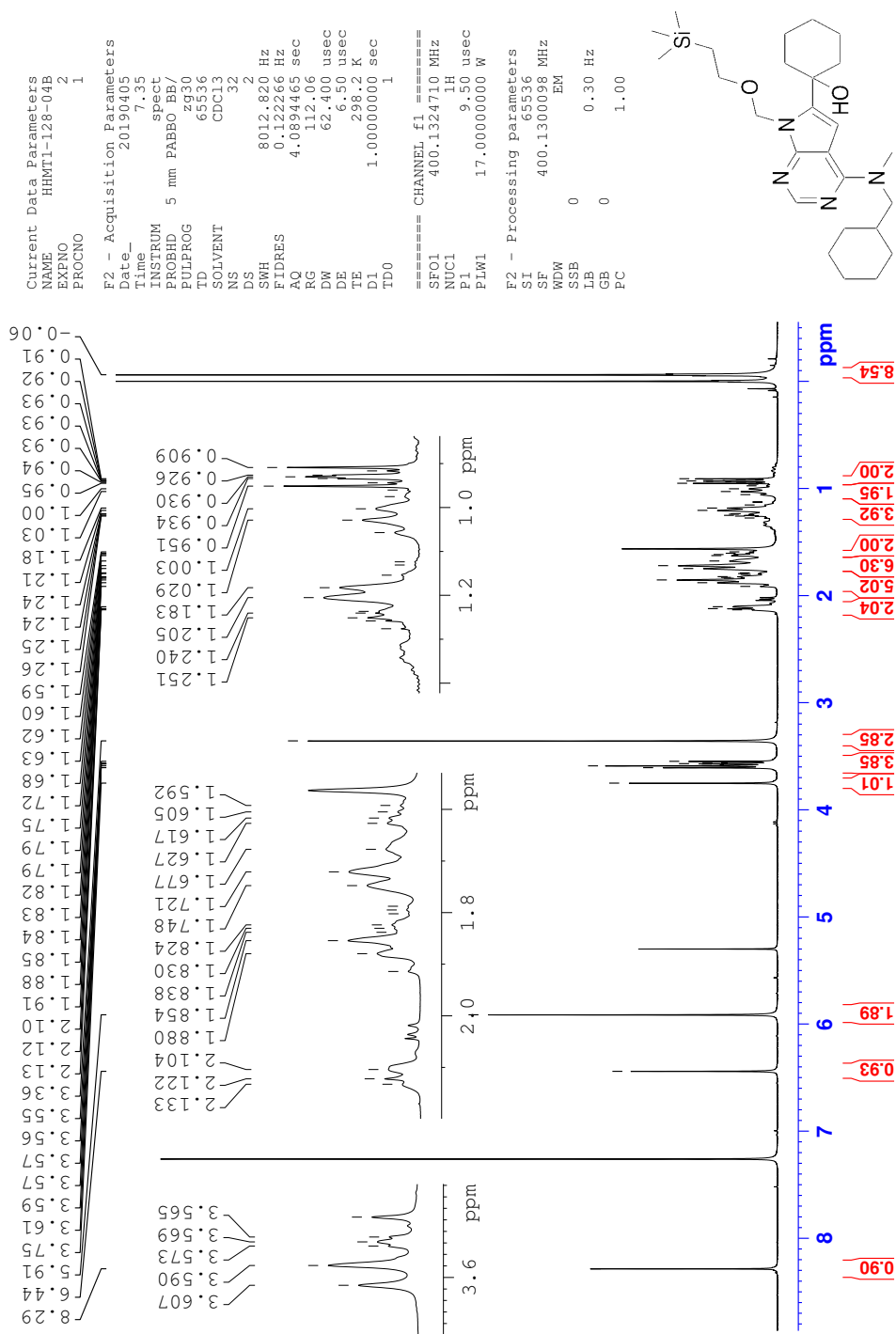
F Spectroscopic data for compound 6

Figure 4.7: ^{1}H-NMR spectrum (400 MHz, DMSO-d_6) of compound **6**.
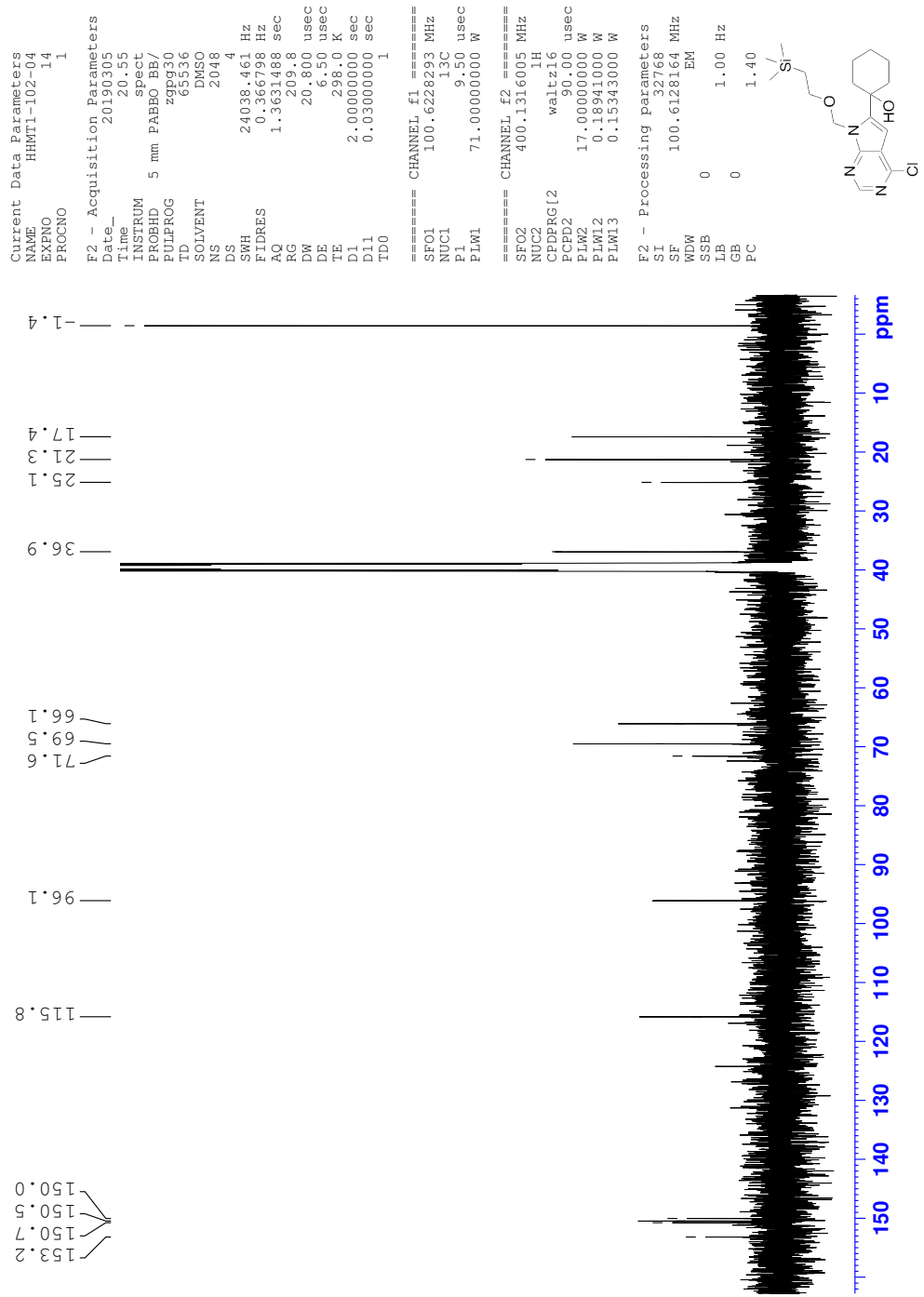
Figure 4.8: ^{13}C-NMR spectrum (100 MHz, DMSO-d_6) of compound **6**.

Figure 4.9: COSY spectrum of compound **6** in DMSO-d_6.

Figure 4.10: HSQC spectrum of compound **6** in DMSO-d_6.

Figure 4.11: HMBC spectrum of compound **6** in DMSO-d_6.
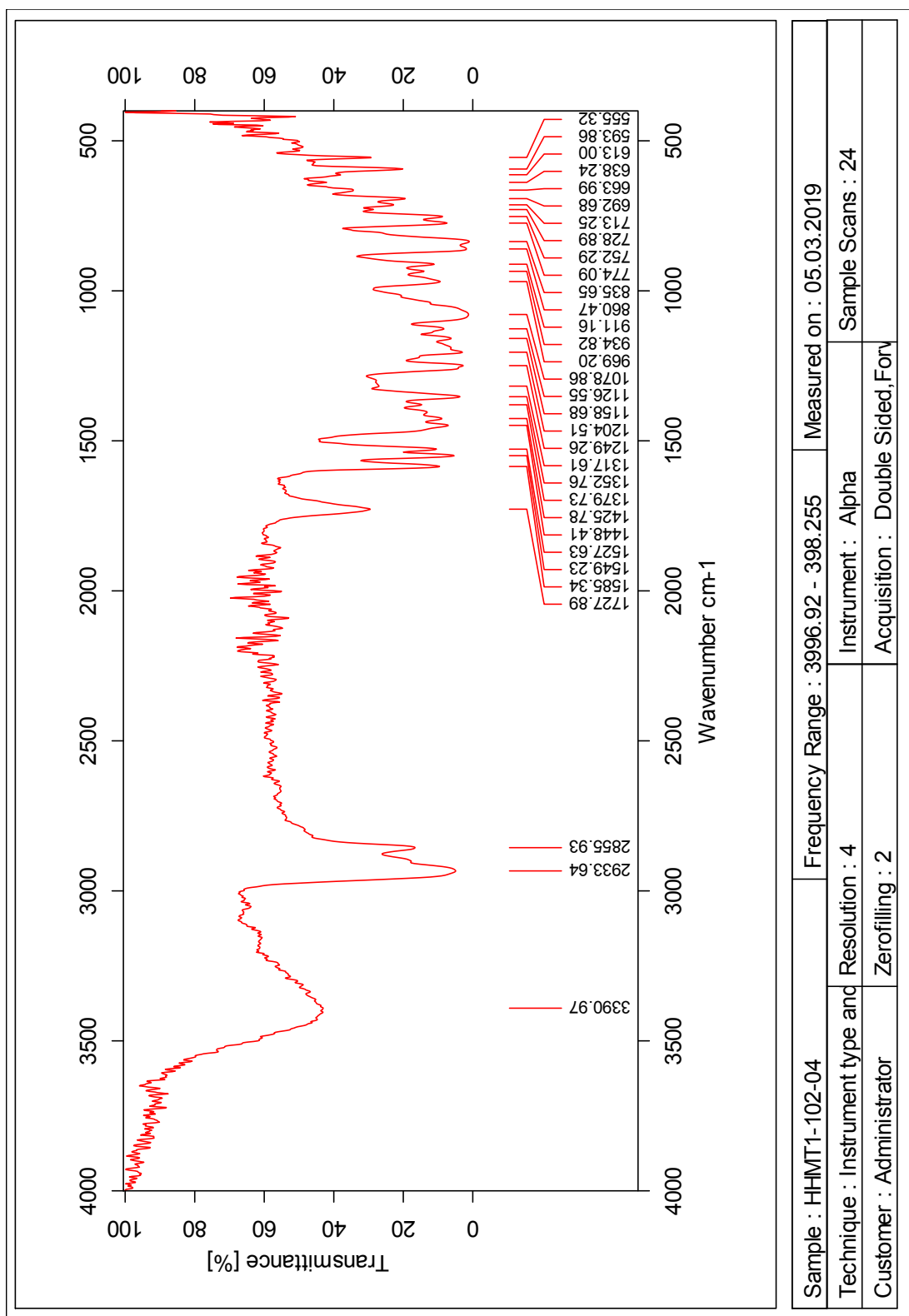
Figure 4.12: IR spectrum of compound **6**.

Single Mass Analysis
Tolerance = 2.0 PPM   /   DBE: min = -2.0, max = 50.0
Element prediction: Off
Number of isotope peaks used for i-FIT = 3

Monoisotopic Mass, Even Electron Ions
2222 formula(e) evaluated with 3 results within limits (all results (up to 1000) for each mass)
Elements Used:
C: 0-100   H: 0-150   N: 0-5   O: 0-10   Si: 0-2   Cl: 0-2
2019-153 46 (0.913) AM2 (Ar,35000.0,0.00,0.00); Cm (45:51)
1: TOF MS ASAP+
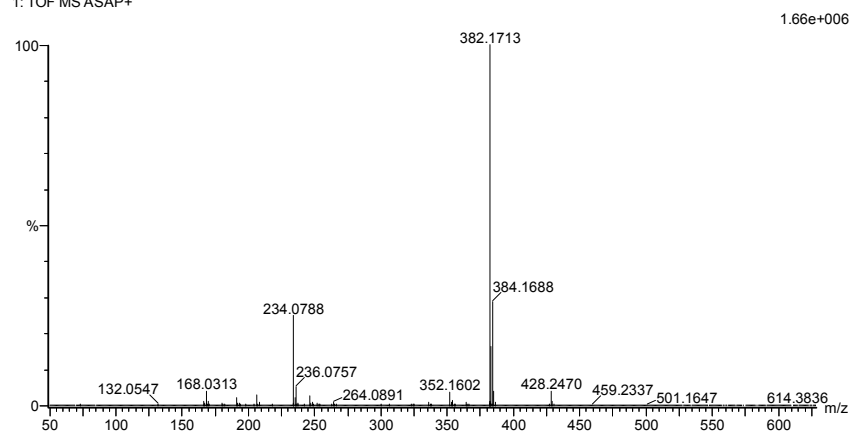

```
Minimum:                          -2.0
Maximum:                  5.0   2.0   50.0

Mass        Calc. Mass  mDa   PPM   DBE   i-FIT   Norm   Conf(%)  Formula

382.1713    382.1713    0.0   0.0   2.5   1198.3  12.315 0.00     C15 H28 N O10
            382.1717   -0.4  -1.0   1.5   1193.4  7.381  0.06     C14 H32 N O7
                                                                  Si2
            382.1718   -0.5  -1.3   6.5   1186.0  0.001  99.94    C18 H29 N3 O2 Si
                                                                  Cl
```

Figure 4.13: MS spectrum of compound **6**.

G   Spectroscopic data for compound 7
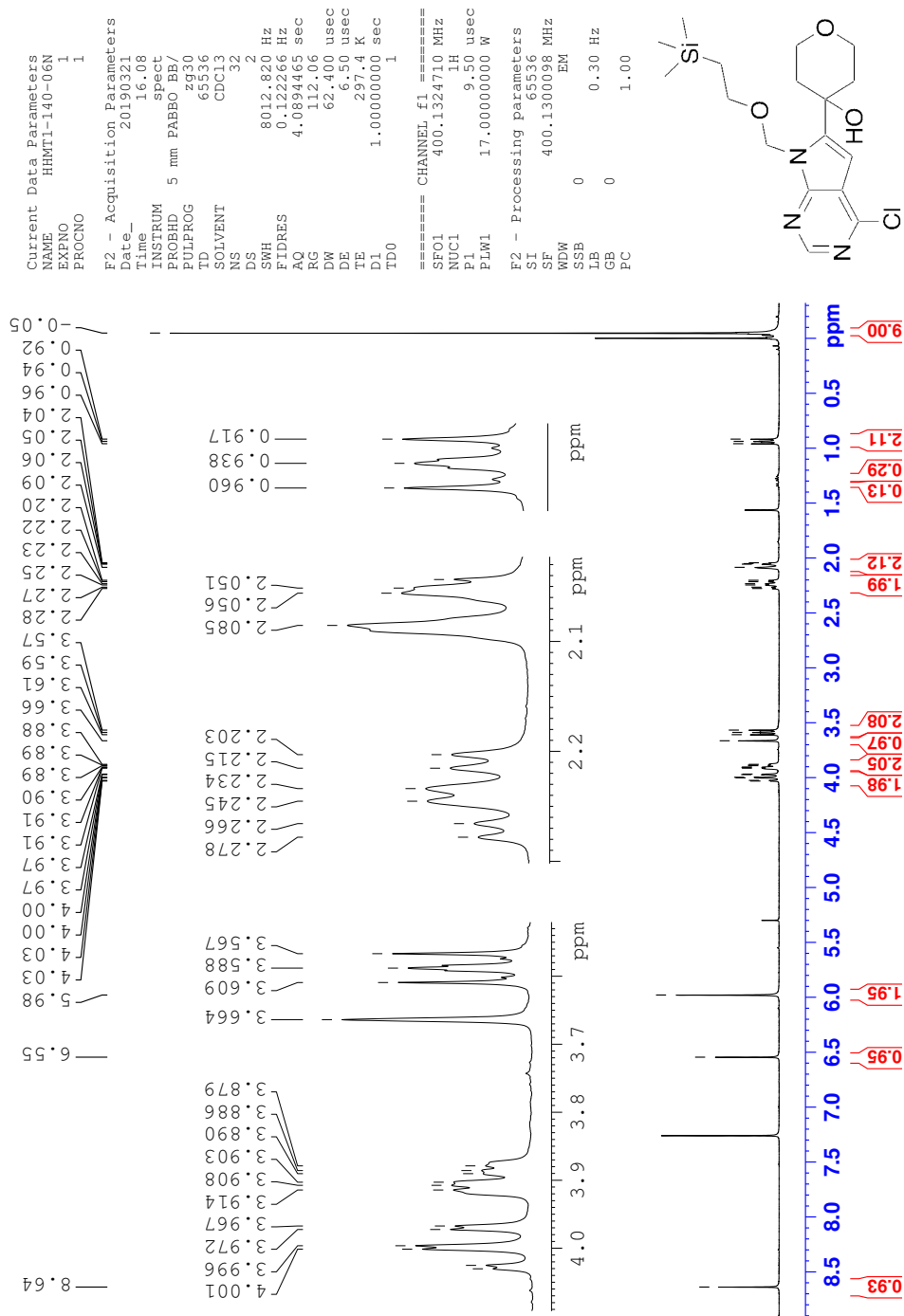
Figure 4.14: ^{1}H-NMR spectrum (400 MHz, CDCl$_3$) of compound **7**.
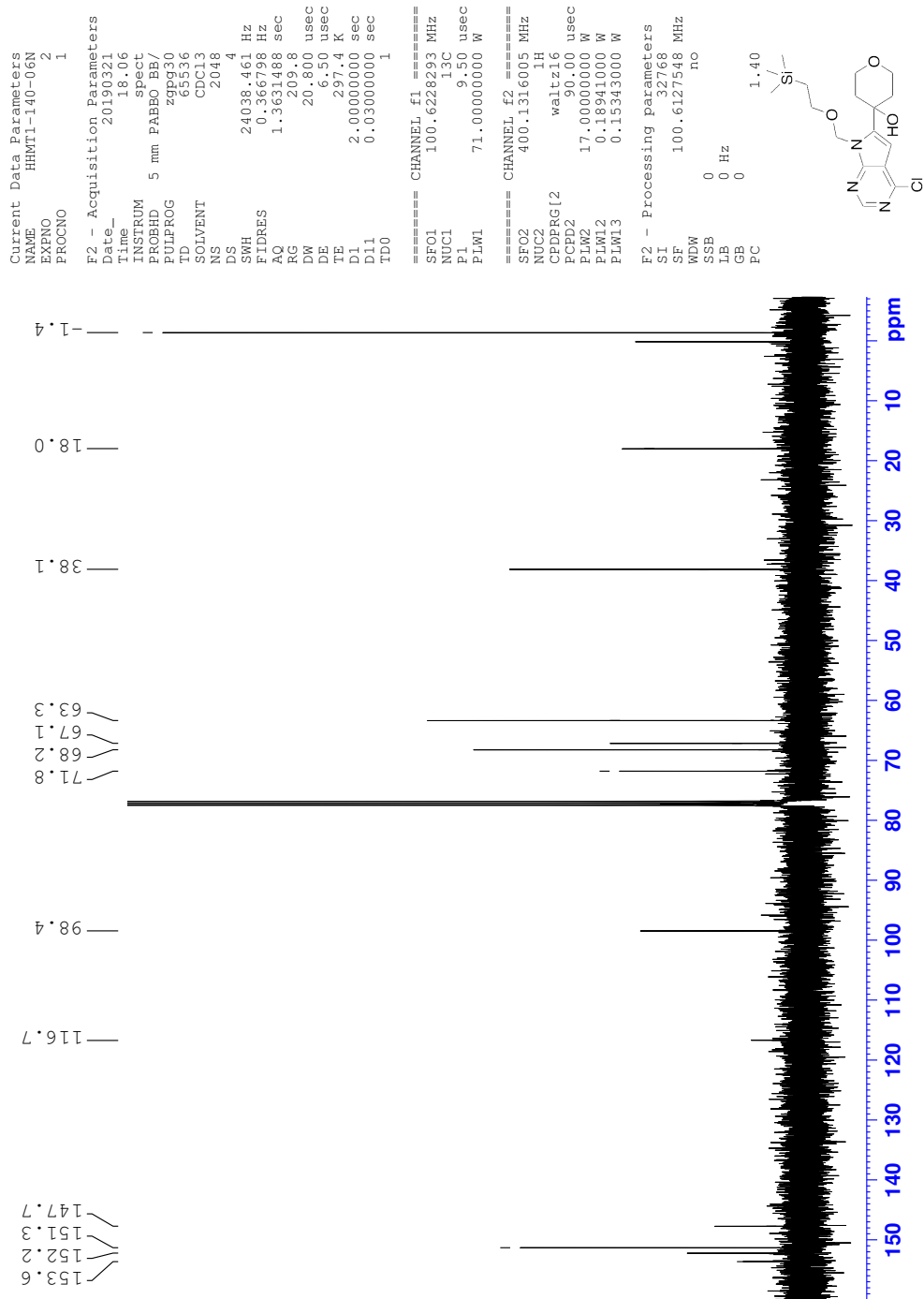
**Figure 4.15:** ^{13}C-NMR spectrum (100 MHz, CDCl$_3$) of compound **7**.

Figure 4.16: COSY spectrum of compound **7** in CDCl₃.

Figure 4.17: HSQC spectrum of compound **7** in CDCl$_3$.

XVII
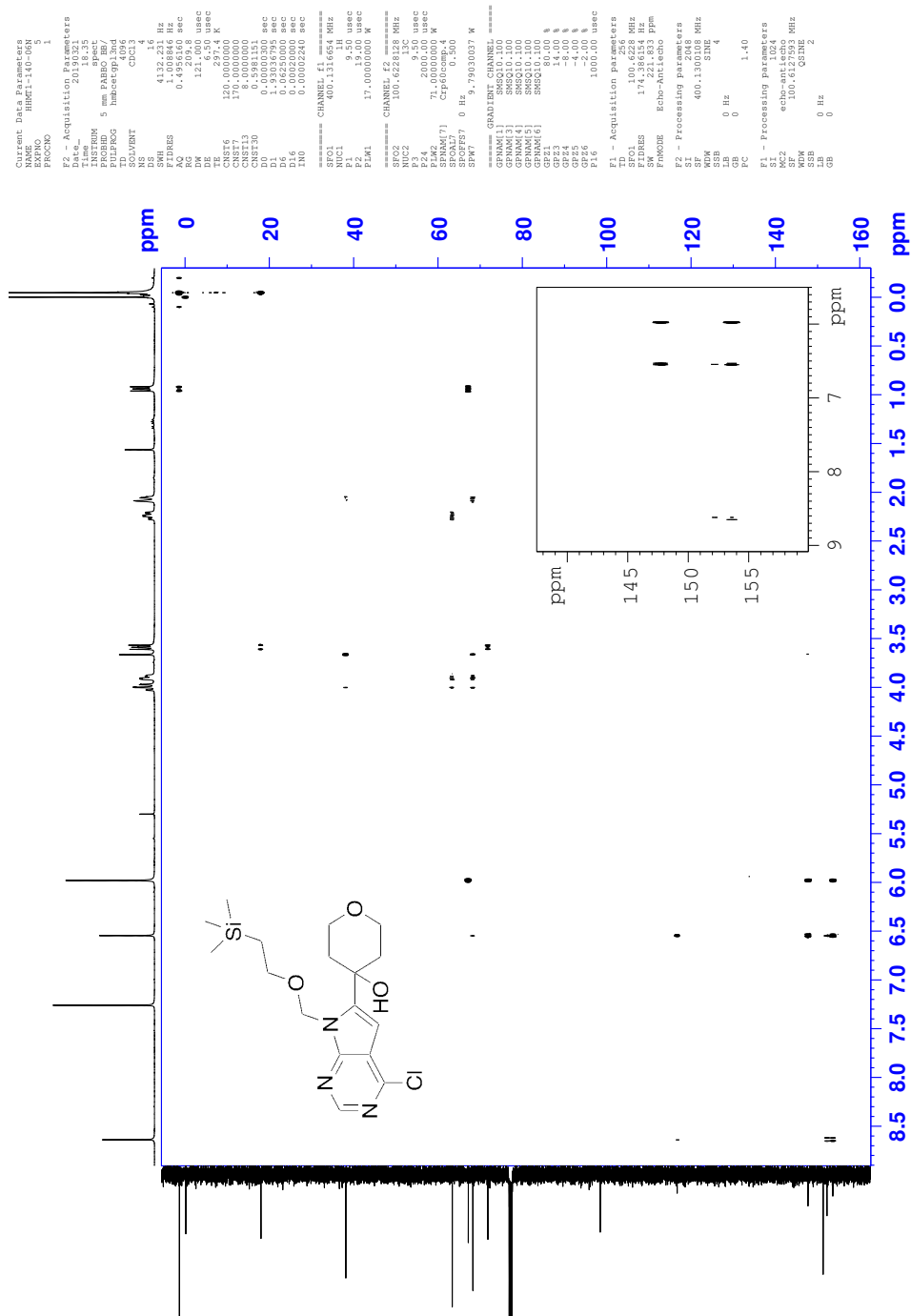
Figure 4.18: HMBC spectrum of compound **7** in CDCl₃.
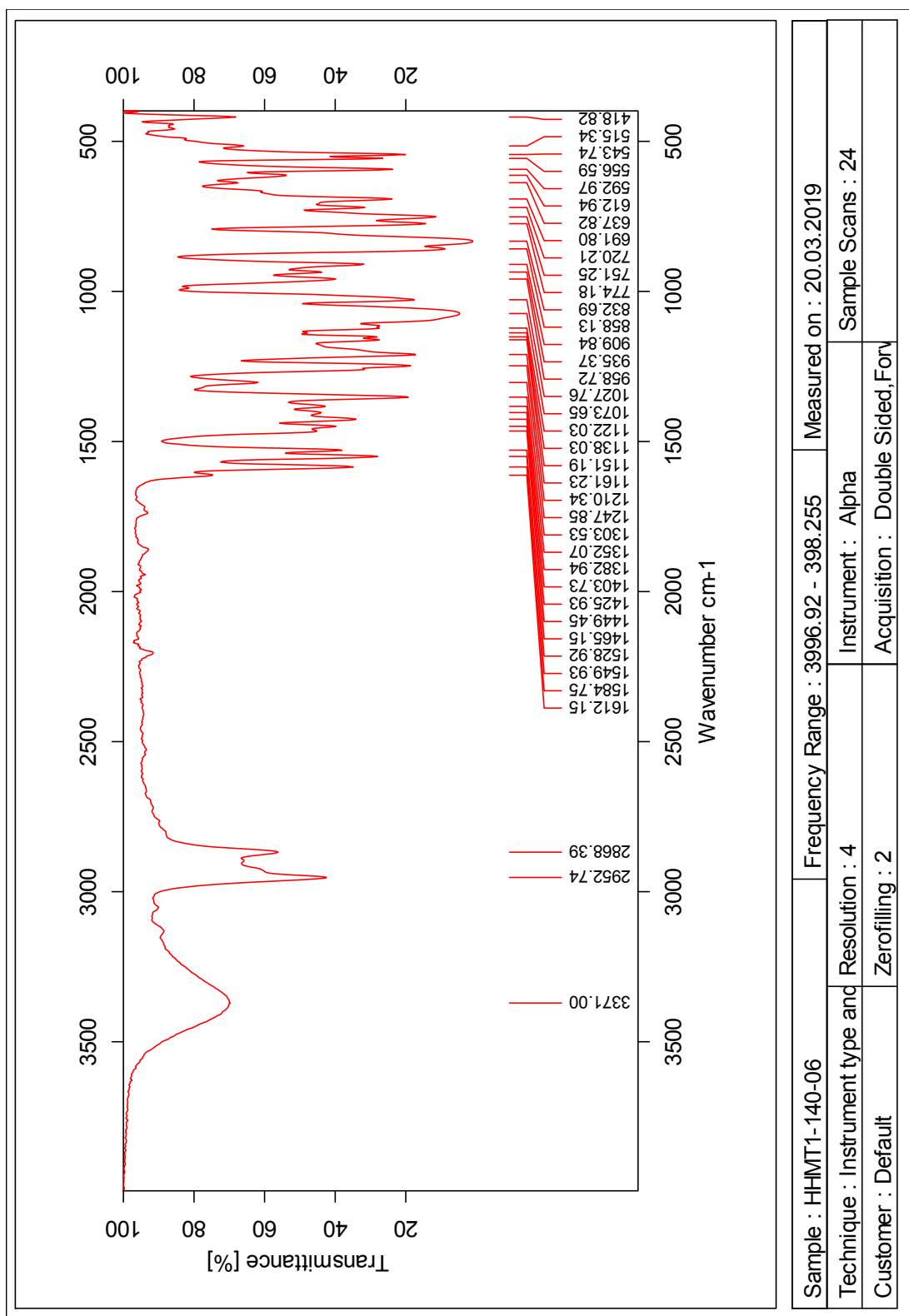
Figure 4.19: IR spectrum of compound **7**.

Single Mass Analysis
Tolerance = 2.0 PPM   /   DBE: min = -50.0, max = 50.0
Element prediction: Off
Number of isotope peaks used for i-FIT = 3

Monoisotopic Mass, Even Electron Ions
8129 formula(e) evaluated with 4 results within limits (all results (up to 1000) for each mass)
Elements Used:
C: 0-100   H: 0-150   N: 0-5   O: 0-10   Cl: 0-2   Si: 0-3

2019-249 63 (1.241) AM2 (Ar,35000.0,0.00,0.00); Cm (57:63)
1: TOF MS ASAP+

7.88e+004
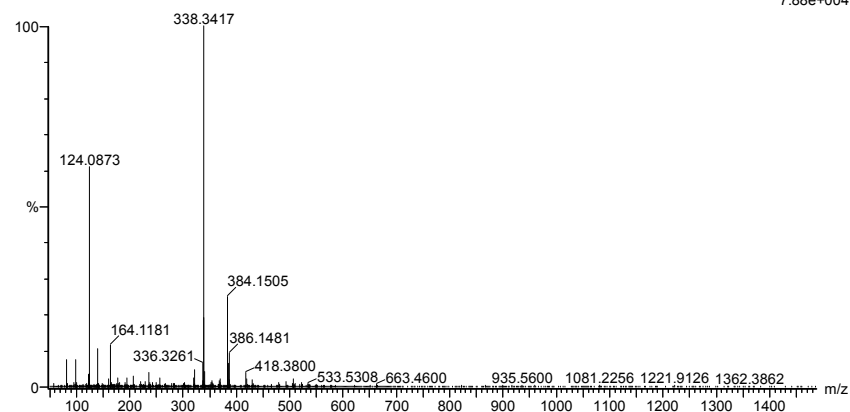

```
Minimum:                        -50.0
Maximum:               5.0   2.0  50.0

Mass        Calc. Mass  mDa   PPM   DBE    i-FIT   Norm   Conf(%) Formula

384.1505    384.1510   -0.5  -1.3   6.5    471.1   0.333  71.69   C17 H27 N3 O3 Cl
                                                                  Si
            384.1501    0.4   1.0  -2.5    472.0   1.262  28.31   C8 H31 N5 O6 Cl
                                                                  Si2
            384.1510   -0.5  -1.3   1.5    482.6  11.820  0.00    C13 H30 N O8
                                                                  Si2
            384.1501    0.4   1.0  20.5    488.7  17.894  0.00    C27 H18 N3
```

Figure 4.20: MS spectrum of compound **7**.

H Spectroscopic data for byproduct 8
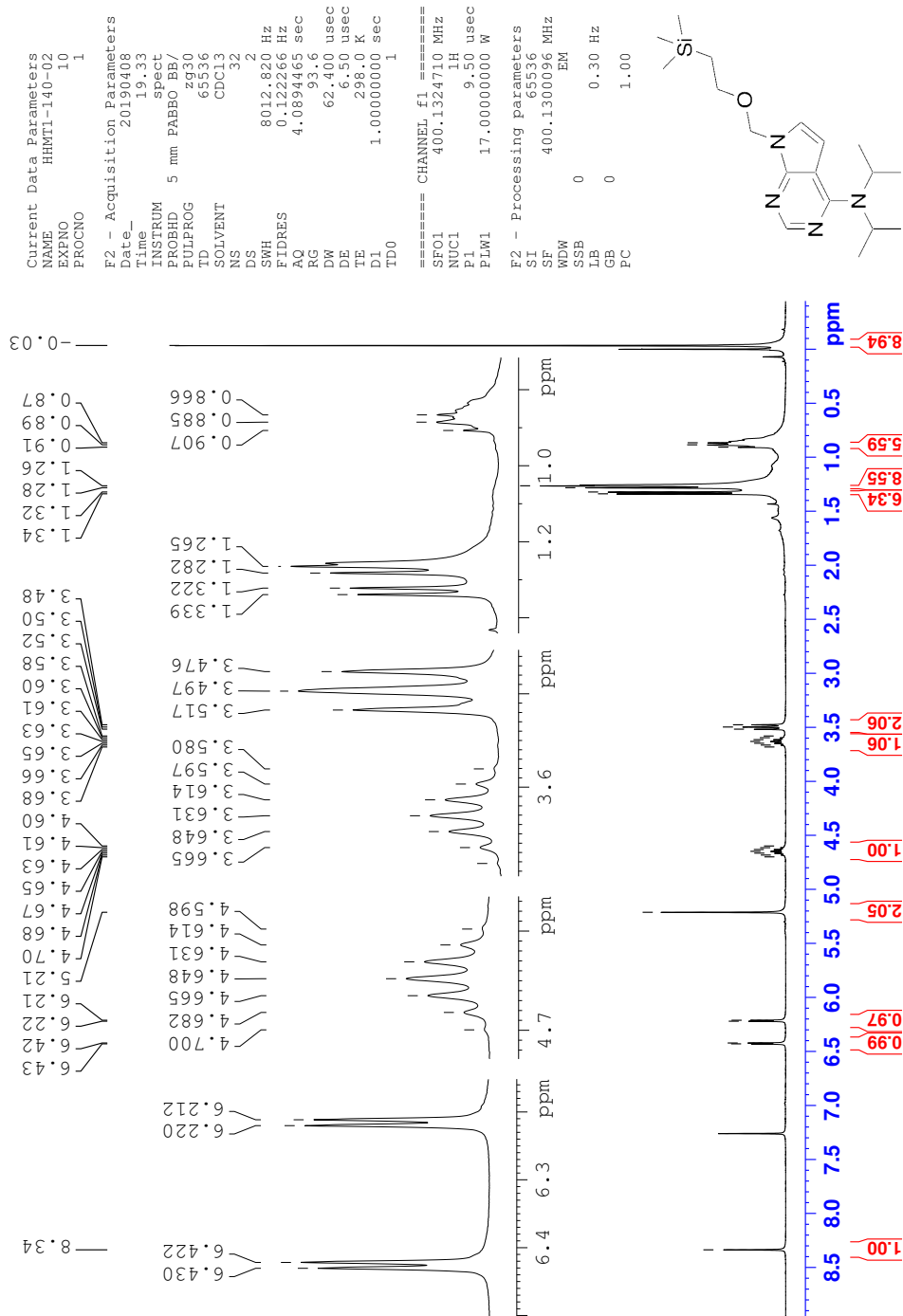
Figure 4.21: ^{1}H-NMR spectrum (400 MHz, CDCl$_3$) of byproduct **8**.

Current Data Parameters
NAME   HHMT1-140-02
EXPNO   11
PROCNO   1

F2 - Acquisition Parameters
Date_   20190408
Time   21.42
INSTRUM   spect
PROBHD   5 mm PABBO BB/
PULPROG   zgpg30
TD   65536
SOLVENT   CDCl3
NS   2048
DS   4
SWH   24038.461 Hz
FIDRES   0.366798 Hz
AQ   1.3631488 sec
RG   209.8
DW   20.800 usec
DE   6.50 usec
TE   300.0 K
D1   2.00000000 sec
D11   0.03000000 sec
TD0   1

======== CHANNEL f1 ========
SFO1   100.6228293 MHz
NUC1   13C
P1   9.50 usec
PLW1   71.00000000 W

======== CHANNEL f2 ========
SFO2   400.1316005 MHz
NUC2   1H
CPDPRG[2   waltz16
PCPD2   90.00 usec
PLW2   17.00000000 W
PLW12   0.18941000 W
PLW13   0.15343000 W

F2 - Processing parameters
SI   32768
SF   100.6127684 MHz
WDW   EM
SSB   0
LB   1.00 Hz
GB   0
PC   1.40

- −1.4
- 17.8
- 23.9
- 29.7
- 46.0
- 47.1
- 66.0
- 73.4
- 74.5
- 109.8
- 116.3
- 119.8
- 150.7
- 152.1

Figure 4.22: ^{13}C-NMR spectrum (100 MHz, CDCl$_3$) of byproduct **8**.
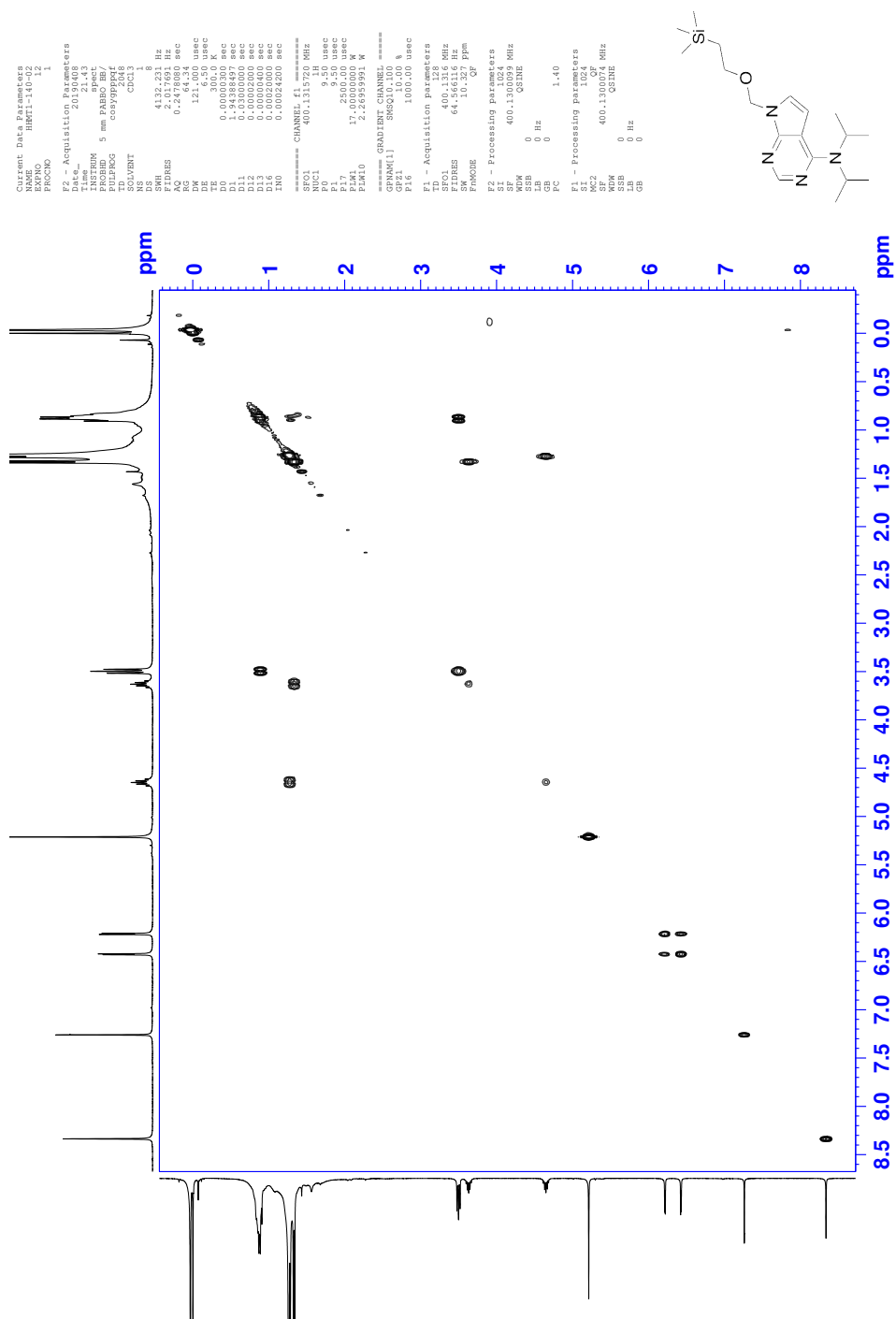
Figure 4.23: COSY spectrum of byproduct **8** in CDCl$_3$.

Figure 4.24: HSQC spectrum of byproduct **8** in CDCl$_3$.
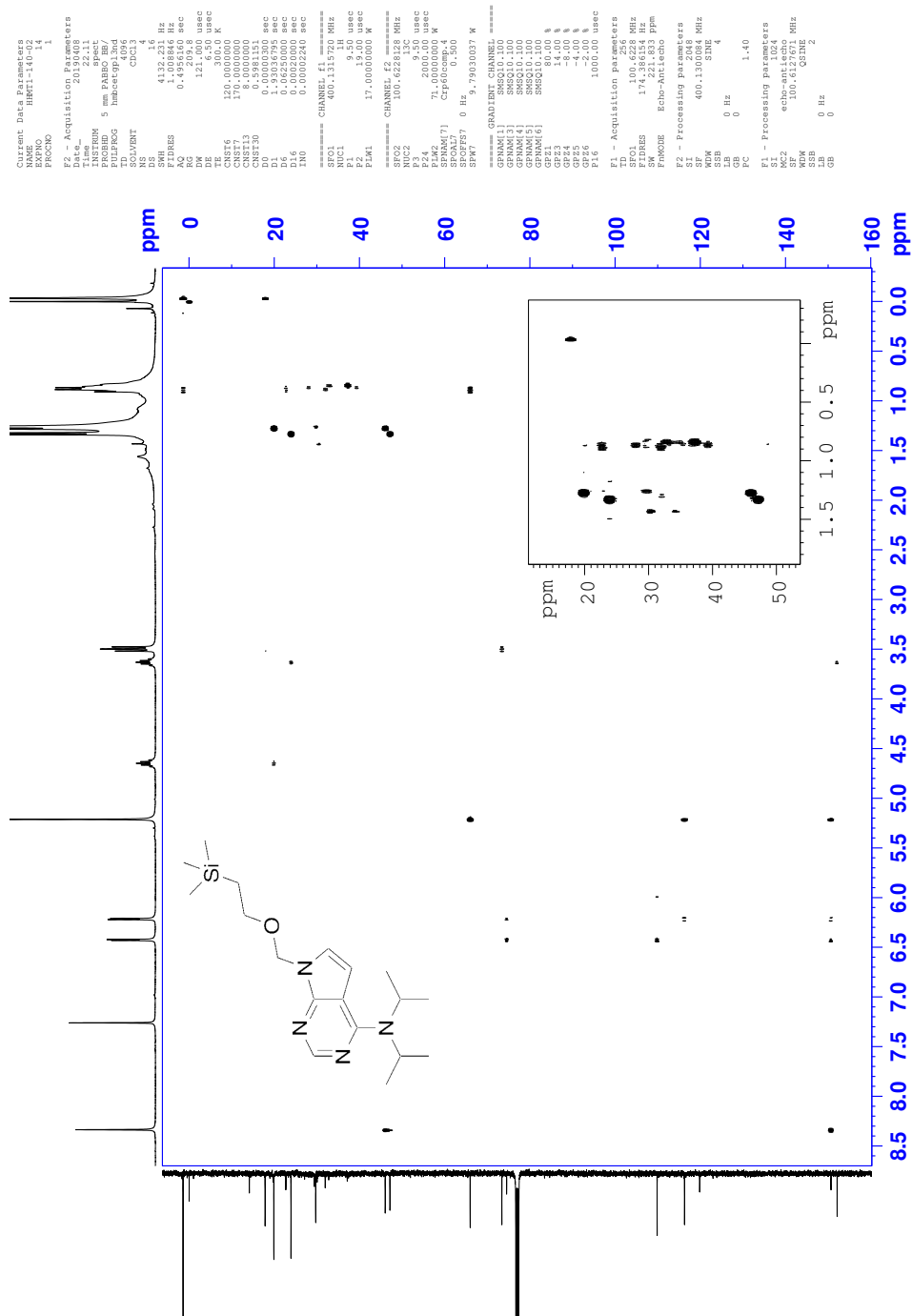
Figure 4.25: HMBC spectrum of byproduct **8** in CDCl$_3$.
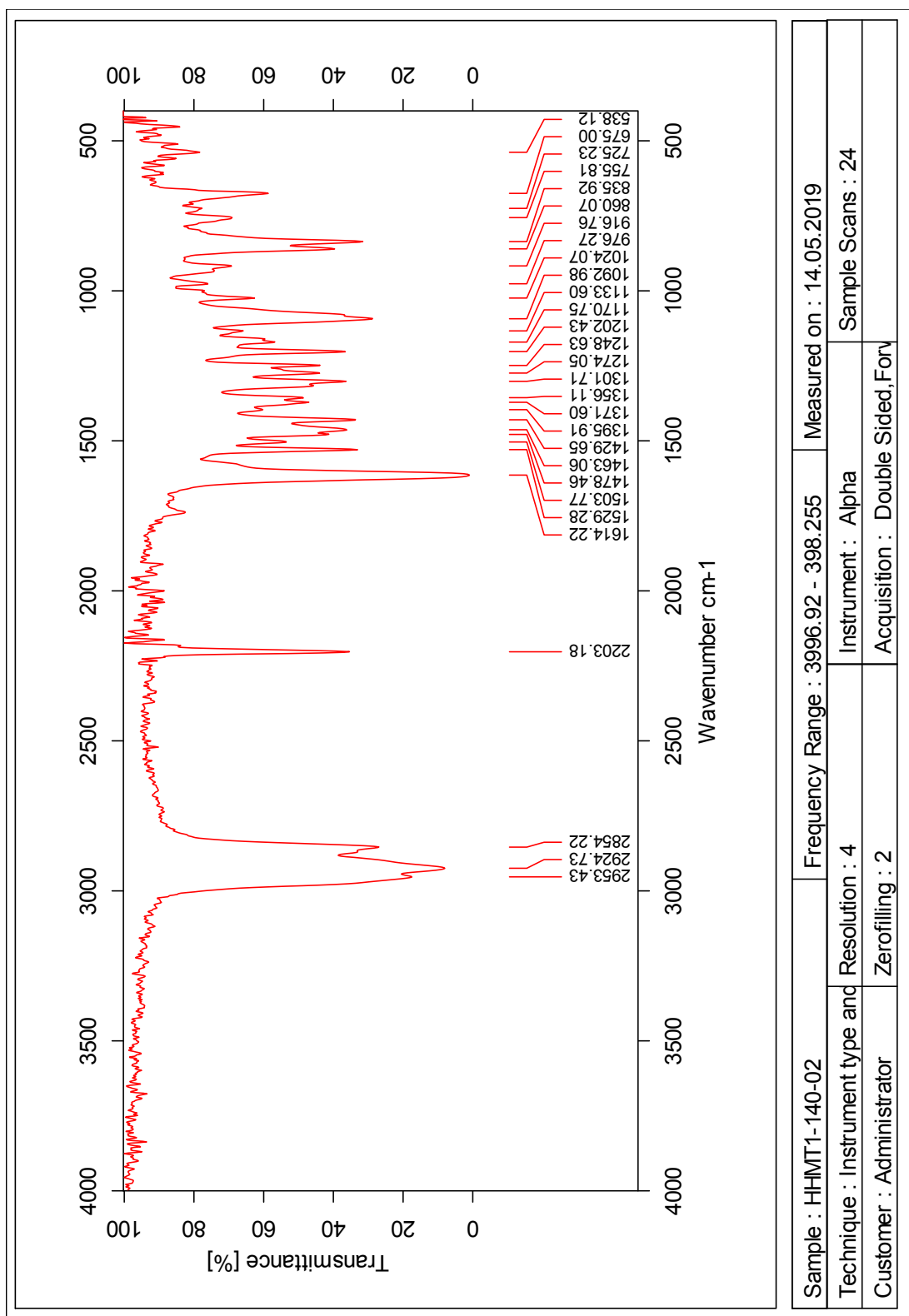
Figure 4.26: IR spectrum of byproduct **8**.

Single Mass Analysis
Tolerance = 2.0 PPM   /   DBE: min = -50.0, max = 50.0
Element prediction: Off
Number of isotope peaks used for i-FIT = 3

Monoisotopic Mass, Even Electron Ions
2765 formula(e) evaluated with 2 results within limits (all results (up to 1000) for each mass)
Elements Used:
C: 0-100   H: 0-150   N: 0-6   O: 0-5   Na: 0-1   Si: 0-2

2019-424 21 (0.431) AM2 (Ar,35000.0,0.00,0.00); Cm (20:24)
1: TOF MS ASAP+
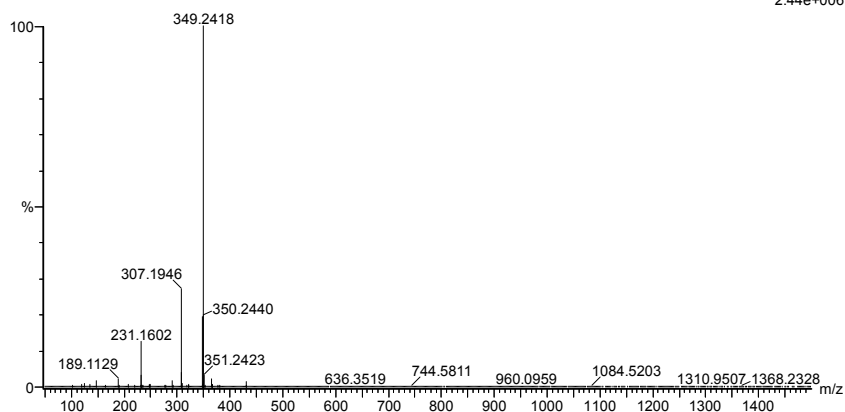

```
Minimum:                              -50.0
Maximum:                   5.0    2.0   50.0

Mass      Calc. Mass   mDa    PPM    DBE    i-FIT   Norm   Conf(%)  Formula

349.2418  349.2415     0.3    0.9   -3.5    1330.1  5.227  0.54     C9 H37 N6 O4
                                                                    Si2
          349.2424    -0.6   -1.7    5.5    1324.9  0.005  99.46    C18 H33 N4 O Si
```

Figure 4.27: MS spectrum of byproduct **8**.

I Spectroscopic data for compound 9
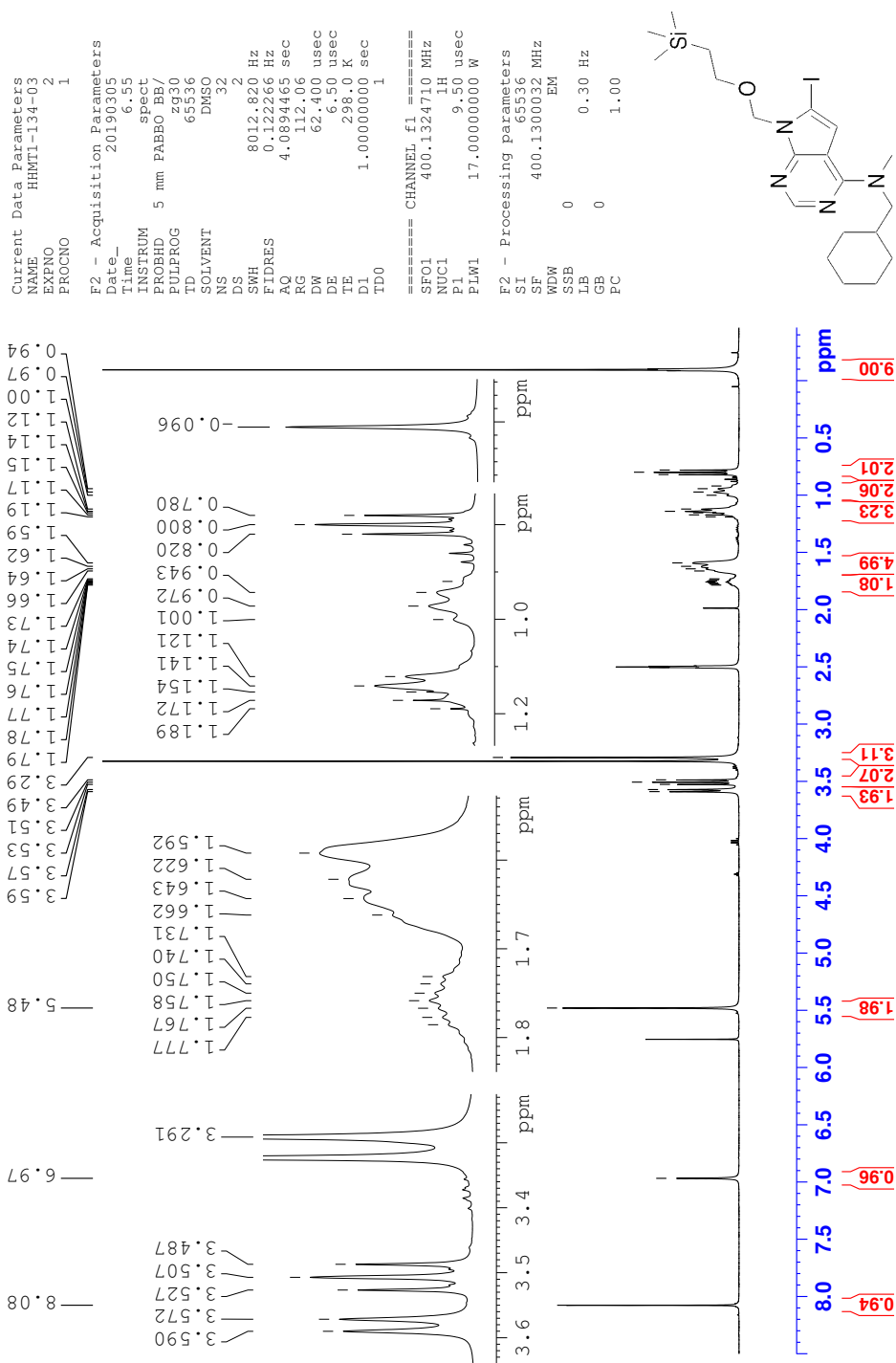
Figure 4.28: ^{1}H-NMR spectrum (400 MHz, DMSO-d_6) of compound **9**.

J   Spectroscopic data for compound 10

Figure 4.29: ^{1}H-NMR spectrum (400 MHz, CDCl$_3$) of compound **10**.

- −1.4

- 18.0
- 22.1
- 25.8
- 26.1
- 29.6
- 31.0
- 37.4
- 38.2
- 39.4

- 57.3

- 66.4
- 70.2
- 71.3

- 100.8
- 101.7

- 141.7

- 151.6
- 153.5
- 157.2
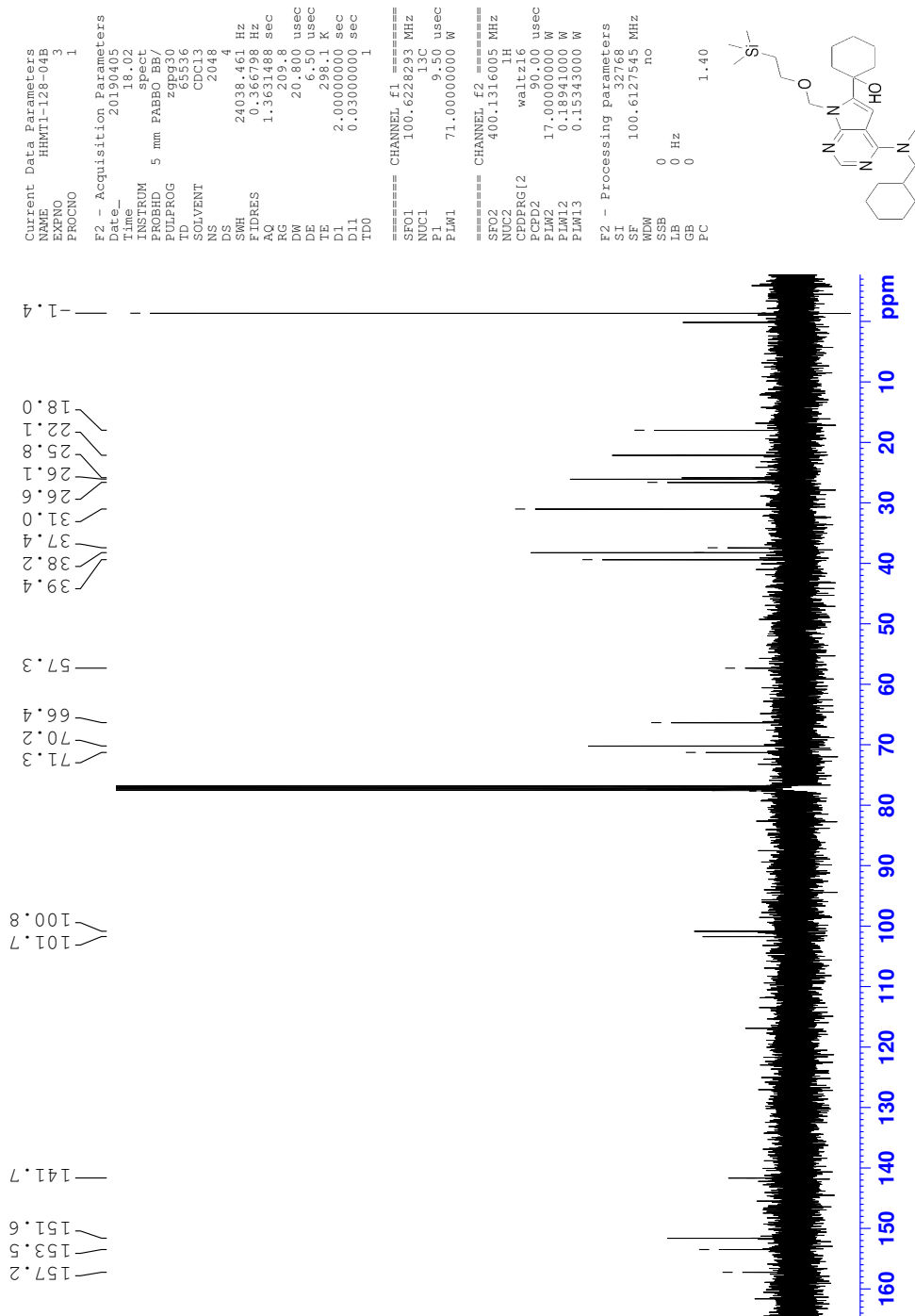
Figure 4.30: ^{13}C-NMR spectrum (100 MHz, CDCl$_3$) of compound **10**.

XXX

Figure 4.31: COSY spectrum of compound **10** in CDCl$_3$.

Figure 4.32: HSQC spectrum of compound **10** in CDCl$_3$.
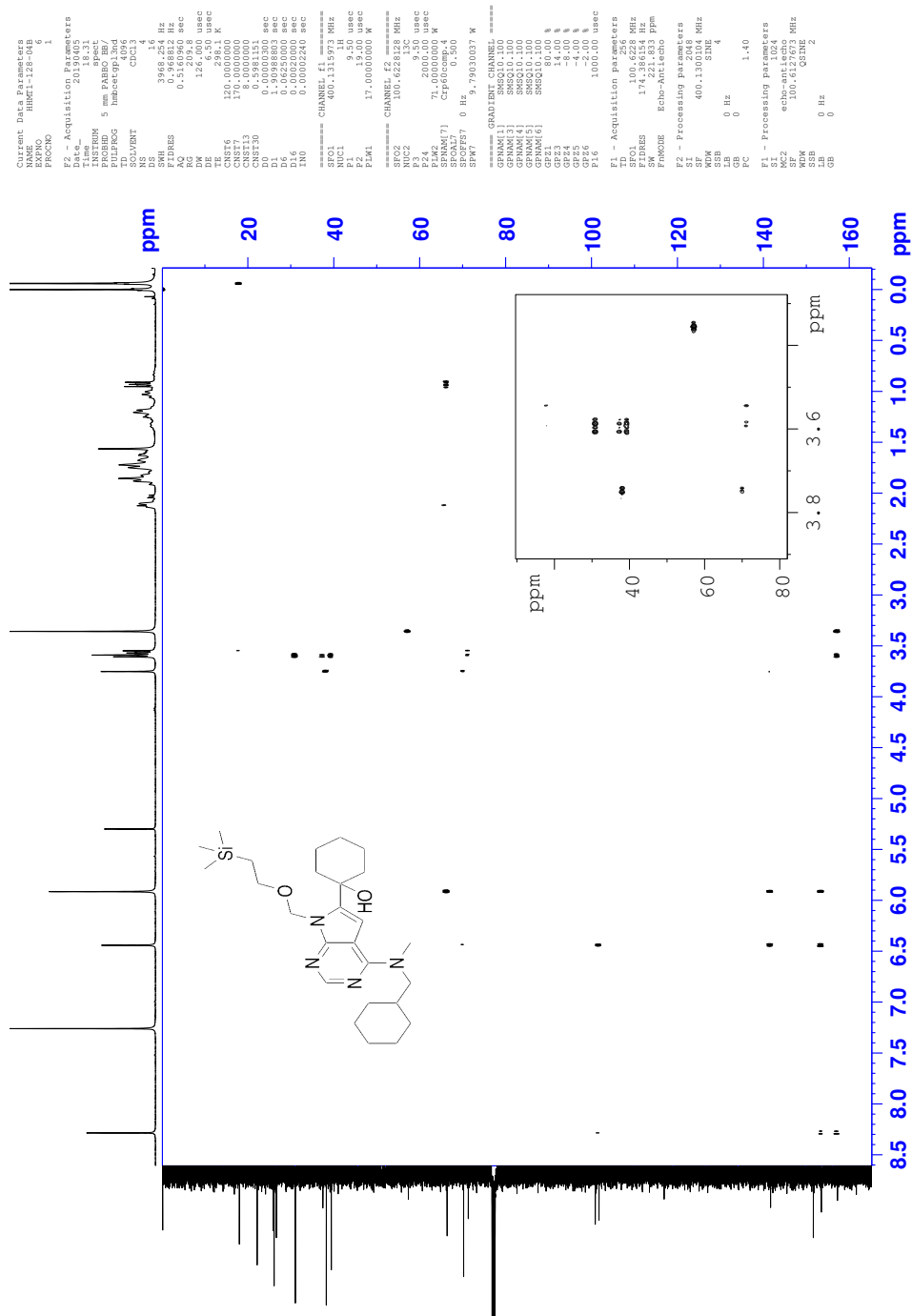
Figure 4.33: HMBC spectrum of compound **10** in CDCl$_3$.
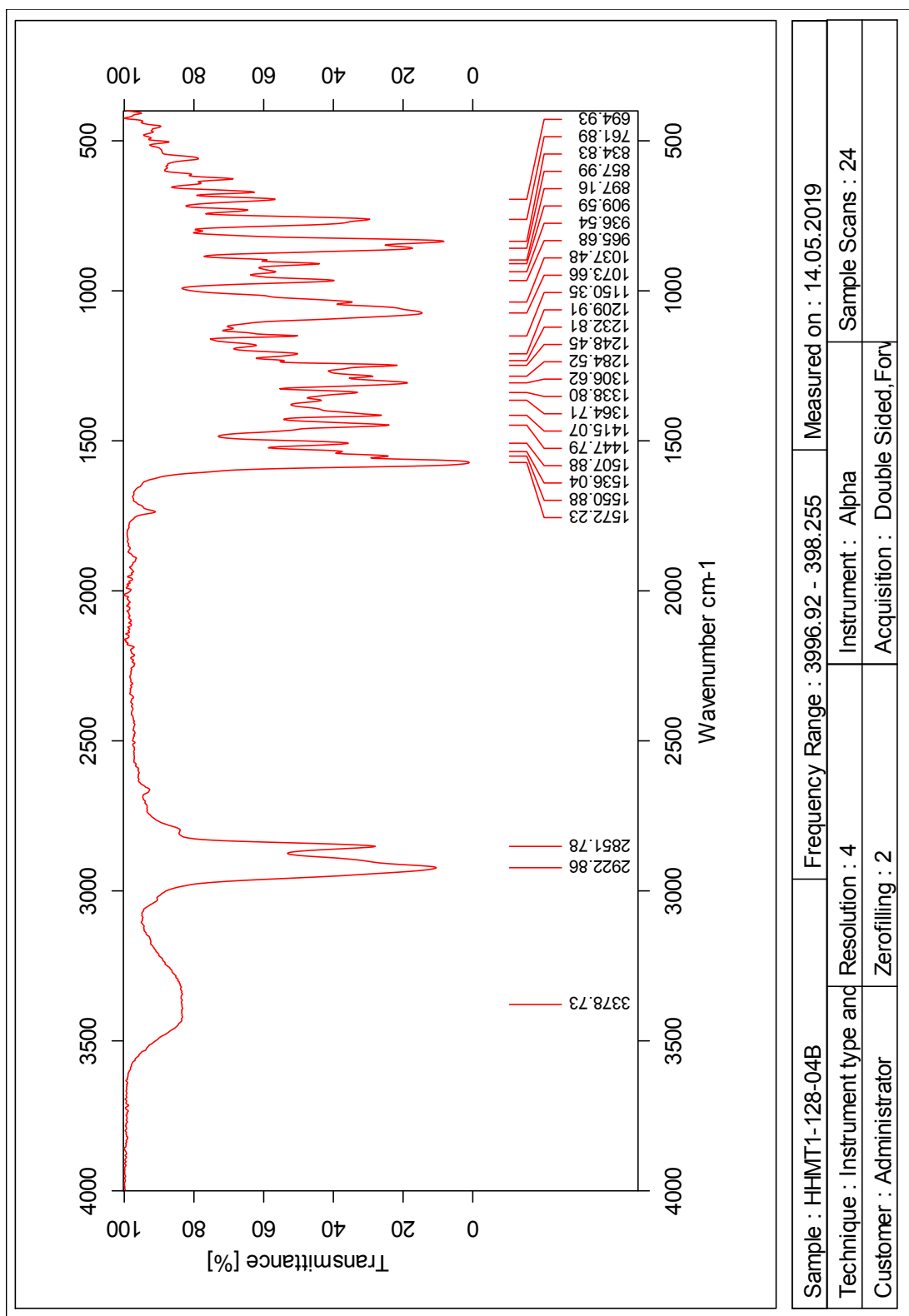
Figure 4.34: IR spectrum of compound **10**.

Single Mass Analysis
Tolerance = 2.0 PPM   /   DBE: min = -50.0, max = 50.0
Element prediction: Off
Number of isotope peaks used for i-FIT = 3

Monoisotopic Mass, Even Electron Ions
3617 formula(e) evaluated with 3 results within limits (all results (up to 1000) for each mass)
Elements Used:
C: 0-100   H: 0-150   N: 0-6   O: 0-6   Na: 0-1   Si: 0-2

2019-421 63 (1.240) AM2 (Ar,35000.0,0.00,0.00); Cm (61:64)
1: TOF MS ASAP+

3.70e+005
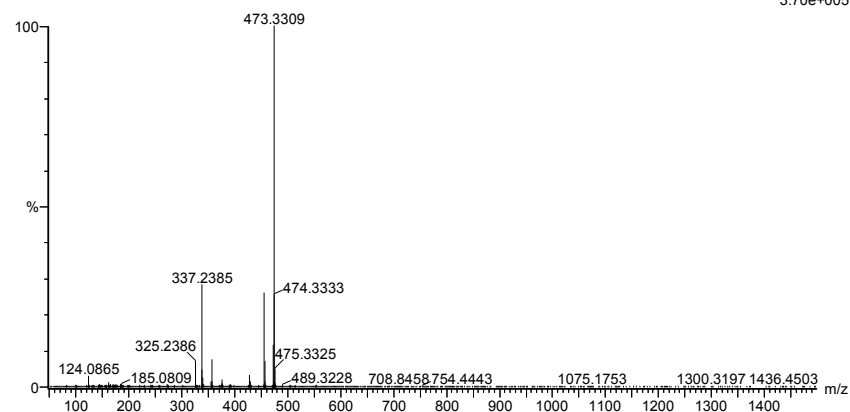
```
Minimum:                      -50.0
Maximum:            5.0   2.0   50.0

Mass       Calc. Mass   mDa    PPM    DBE    i-FIT    Norm    Conf(%)  Formula

473.3309   473.3312     -0.3   -0.6   7.5    832.6    2.530   7.96     C26 H45 N4 O2
                                                                       Si
           473.3315     -0.6   -1.3   0.5    830.2    0.085   91.87    C21 H46 N4 O6
                                                                       Na
           473.3303      0.6    1.3  -1.5    836.5    6.379   0.17     C17 H49 N6 O5
                                                                       Si2
```

Figure 4.35: MS spectrum of compound **10**.

K   Spectroscopic data for byproduct 11

Figure 4.36: ^{1}H-NMR spectrum (400 MHz, DMSO-d_6) of byproduct **11**.
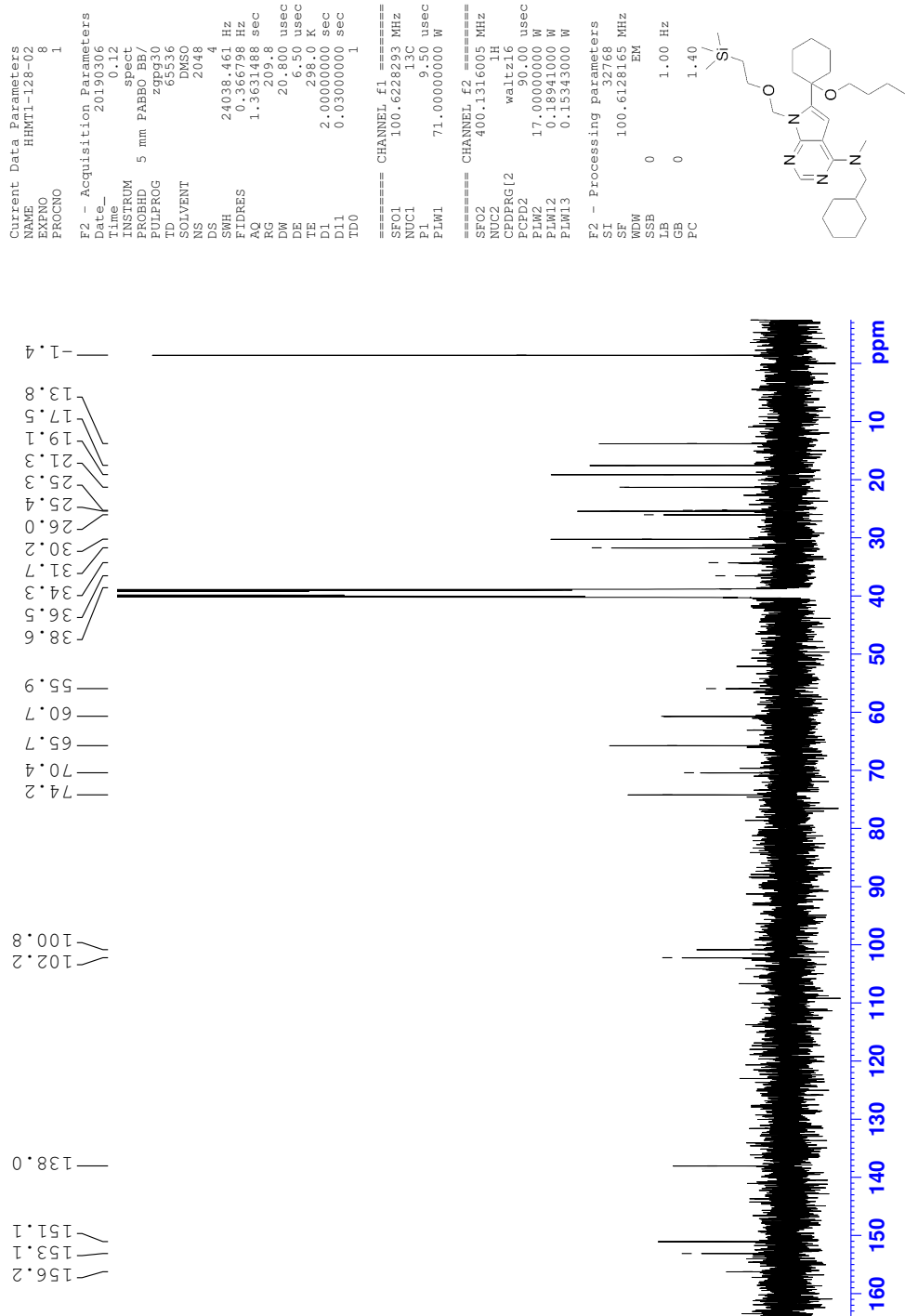
Figure 4.37: ^{13}C-NMR spectrum (100 MHz, DMSO-d_6) of byproduct **11**.

Figure 4.38: COSY spectrum of byproduct **11** in DMSO-d_6.

Figure 4.39: HSQC spectrum of byproduct **11** in DMSO-d_6.
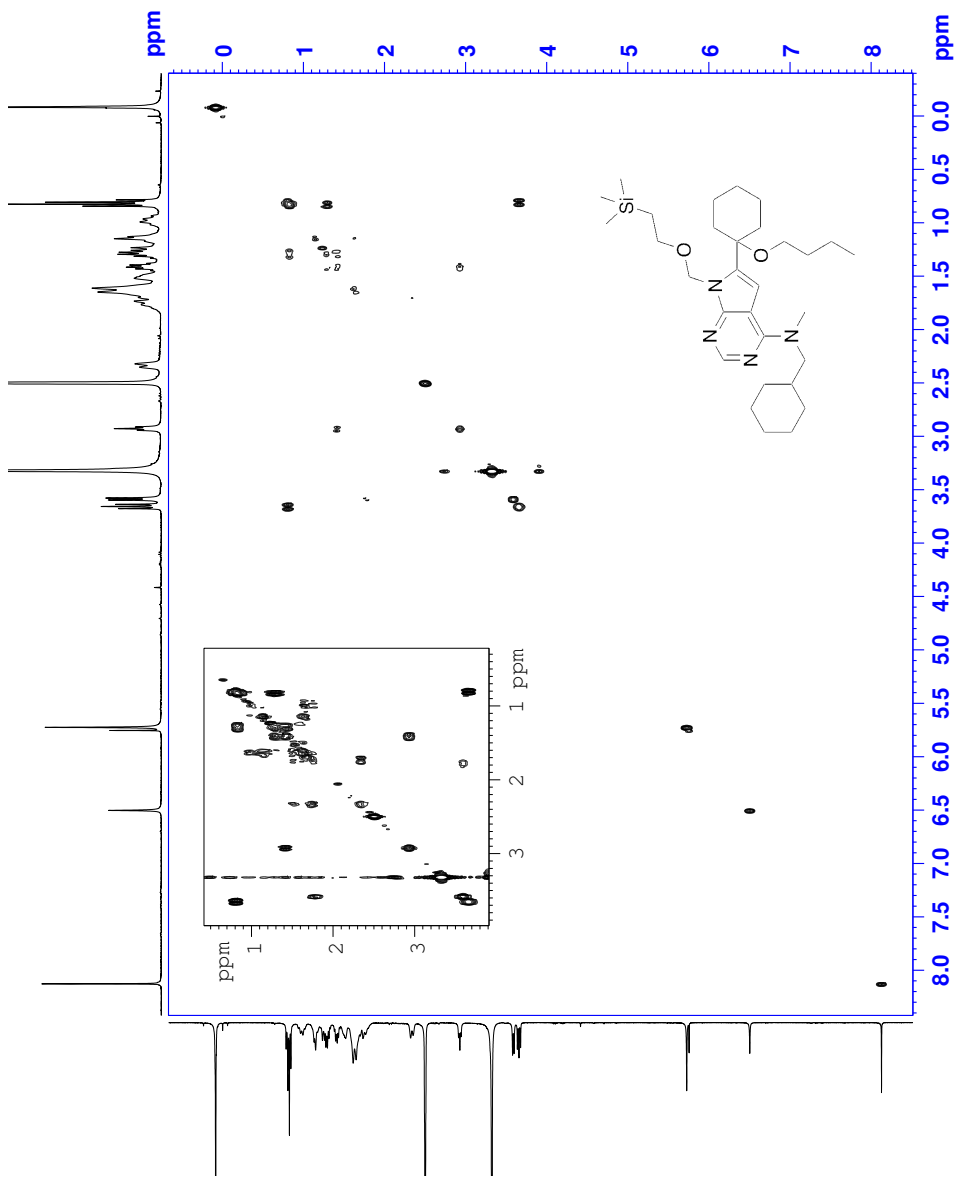
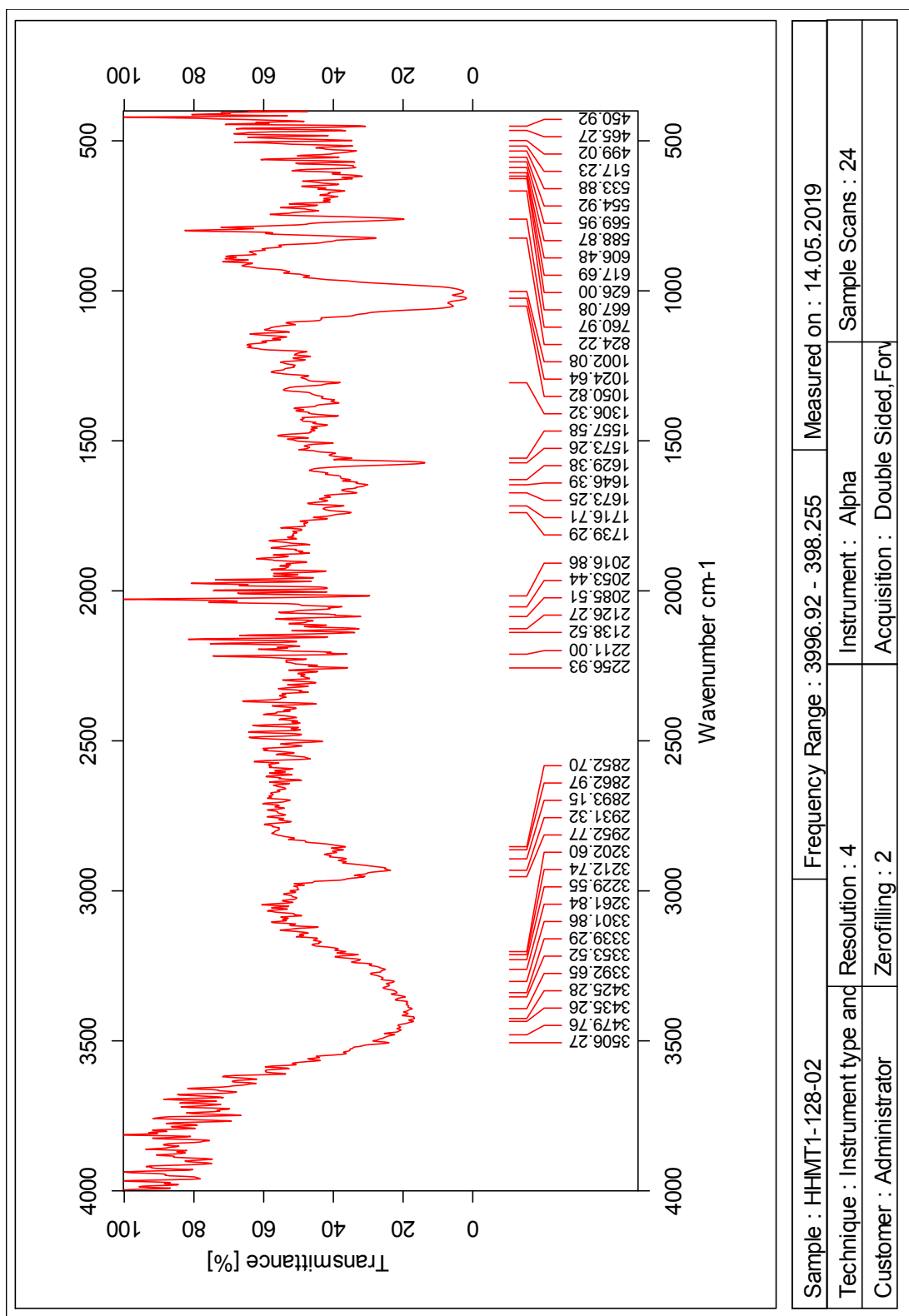**Figure 4.40:** HMBC spectrum of byproduct **11** in DMSO-d_6.

Figure 4.41: IR spectrum of byproduct **11**.

Single Mass Analysis
Tolerance = 2.0 PPM   /   DBE: min = -50.0, max = 50.0
Element prediction: Off
Number of isotope peaks used for i-FIT = 3

Monoisotopic Mass, Even Electron Ions
1881 formula(e) evaluated with 2 results within limits (all results (up to 1000) for each mass)
Elements Used:
C: 0-100   H: 0-150   N: 0-6   O: 0-6   Si: 0-2
2019-215 129 (2.535) AM2 (Ar,35000.0,0.00,0.00); Cm (127:132)
1: TOF MS ASAP+

1.36e+007
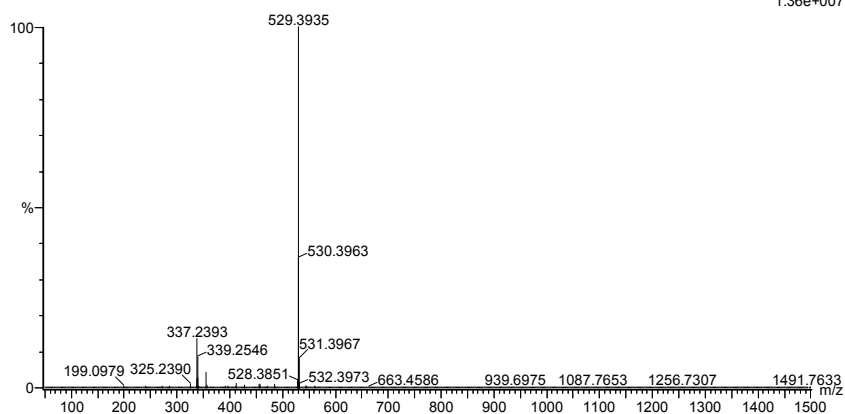
Mass	Calc. Mass	mDa	PPM	DBE	i-FIT	Norm	Conf(%)	Formula
Minimum:				-50.0				
Maximum:		5.0	2.0	50.0				
529.3935	529.3938	-0.3	-0.6	7.5	1084.3	0.001	99.94	C30 H53 N4 O2 Si
	529.3929	0.6	1.1	-1.5	1091.7	7.365	0.06	C21 H57 N6 O5 Si2

Figure 4.42: MS spectrum of byproduct **11**.

L   Spectroscopic data for byproduct 12
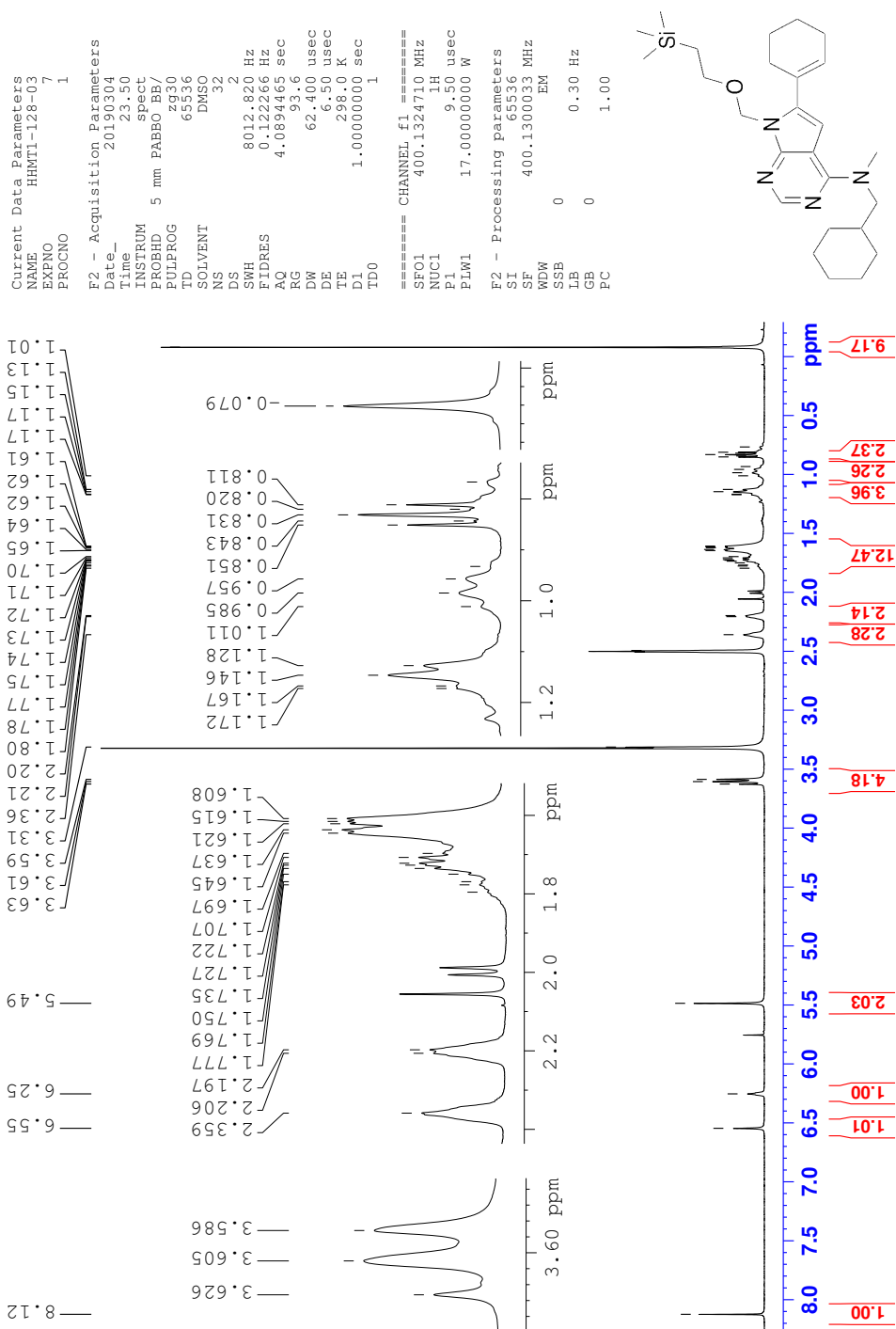
Figure 4.43: ^{1}H-NMR spectrum (400 MHz, DMSO-d_6) of byproduct **12**.

M   Spectroscopic data for compound 13

Figure 4.44: ^{1}H-NMR spectrum (400 MHz, CDCl$_3$) of compound **13**.

Current Data Parameters
NAME   HHMTi-158-03
EXPNO   3
PROCNO   1

F2 - Acquisition Parameters
Date_   20190406
Time   18.25
INSTRUM   spect
PROBHD   5 mm PABBO BB/
PULPROG   zgpg30
TD   65536
SOLVENT   CDC13
NS   2048
DS   4
SWH   24038.461 Hz
FIDRES   0.366798 Hz
AQ   1.3631488 sec
RG   209.8
DW   20.800 usec
DE   6.50 usec
TE   298.1 K
D1   2.00000000 sec
D11   0.03000000 sec
TD0   1

======== CHANNEL f1 ========
SFO1   100.6228293 MHz
NUC1   13C
P1   9.50 usec
PLW1   71.00000000 W

======== CHANNEL f2 ========
SFO2   400.1316005 MHz
NUC2   1H
CPDPRG[2   waltz16
PCPD2   90.00 usec
PLW2   17.00000000 W
PLW12   0.18941000 W
PLW13   0.15343000 W

F2 - Processing parameters
SI   32768
SF   100.6127685 MHz
WDW   EM
SSB   0
LB   1.00 Hz
GB   0
PC   1.40

Figure 4.45: ^{13}C-NMR spectrum (100 MHz, CDCl$_3$) of compound **13**.
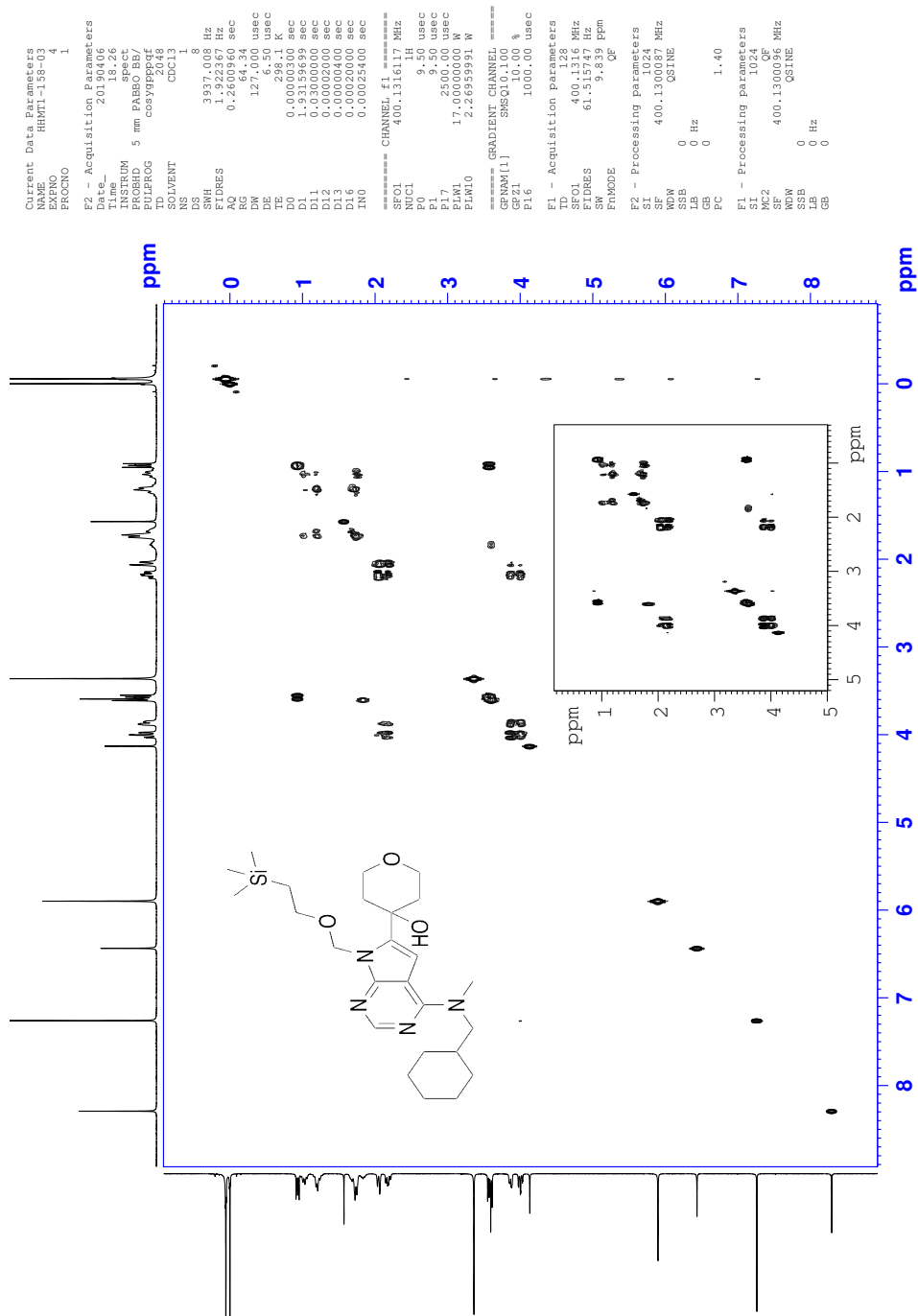
Figure 4.46: COSY spectrum of compound **13** in CDCl₃.

Figure 4.47: HSQC spectrum of compound **13** in CDCl$_3$.

Figure 4.48: HMBC spectrum of compound **13** in CDCl₃.

Figure 4.49: IR spectrum of compound **13**.

Single Mass Analysis
Tolerance = 2.0 PPM   /   DBE: min = -50.0, max = 50.0
Element prediction: Off
Number of isotope peaks used for i-FIT = 3

Monoisotopic Mass, Even Electron Ions
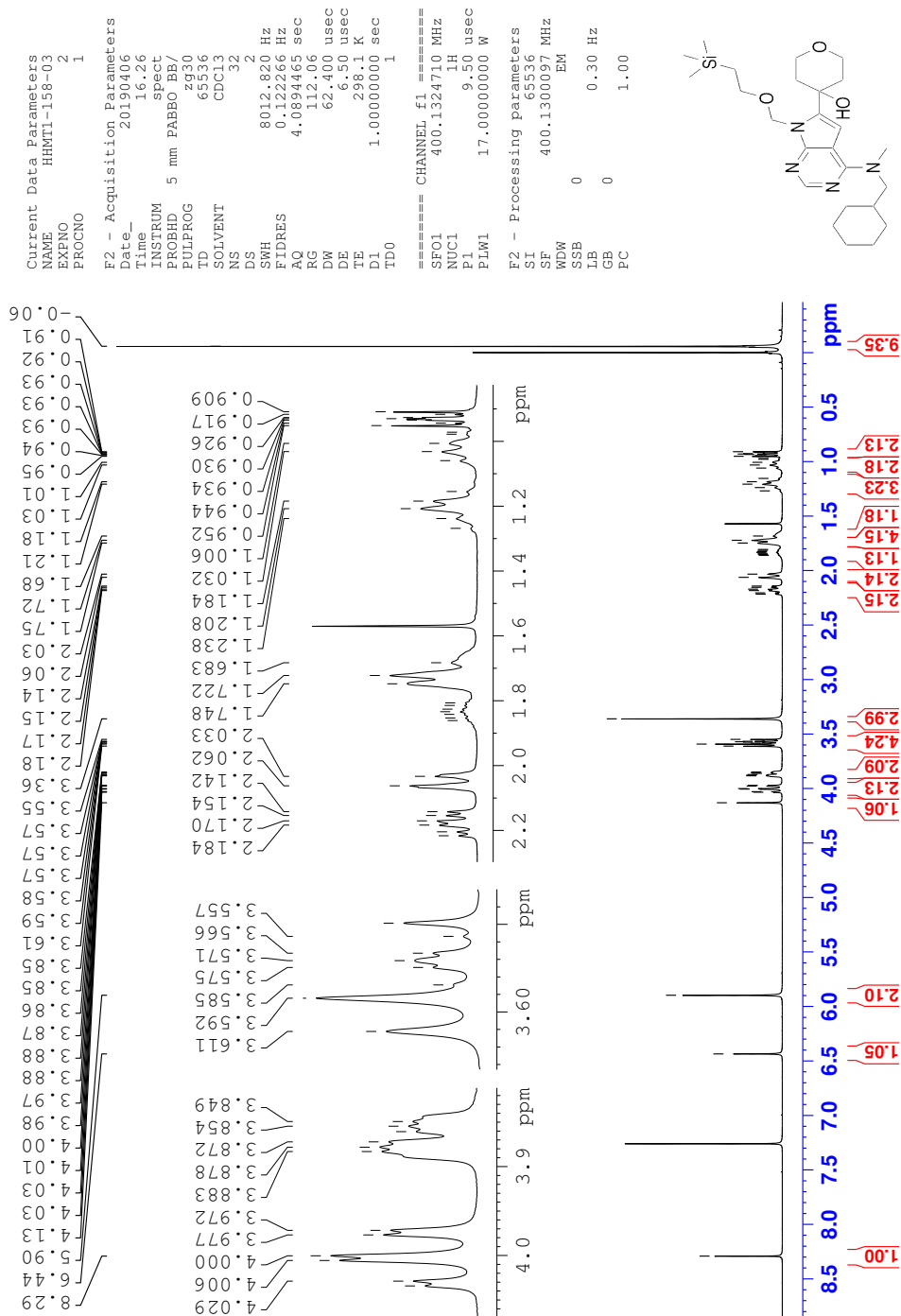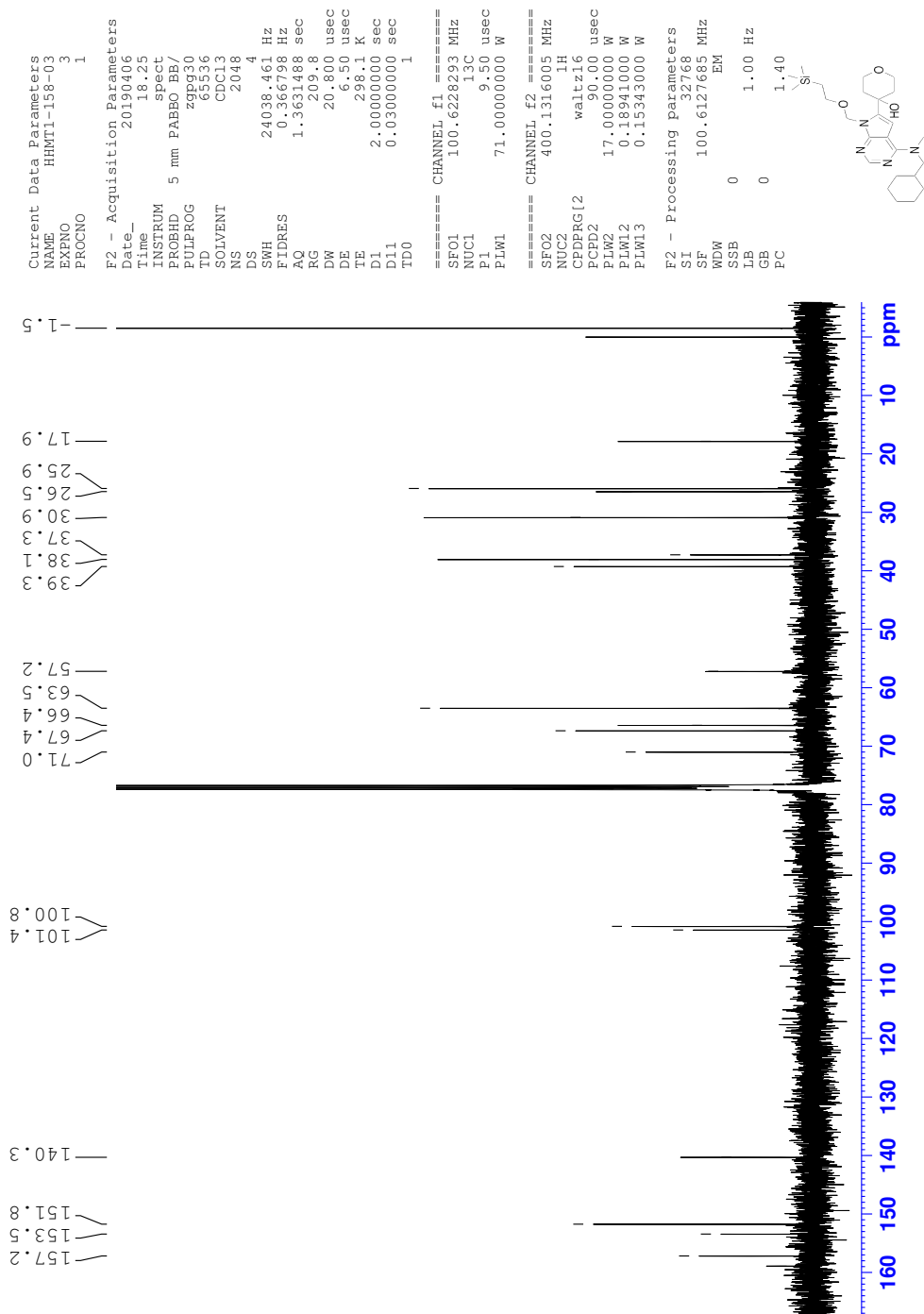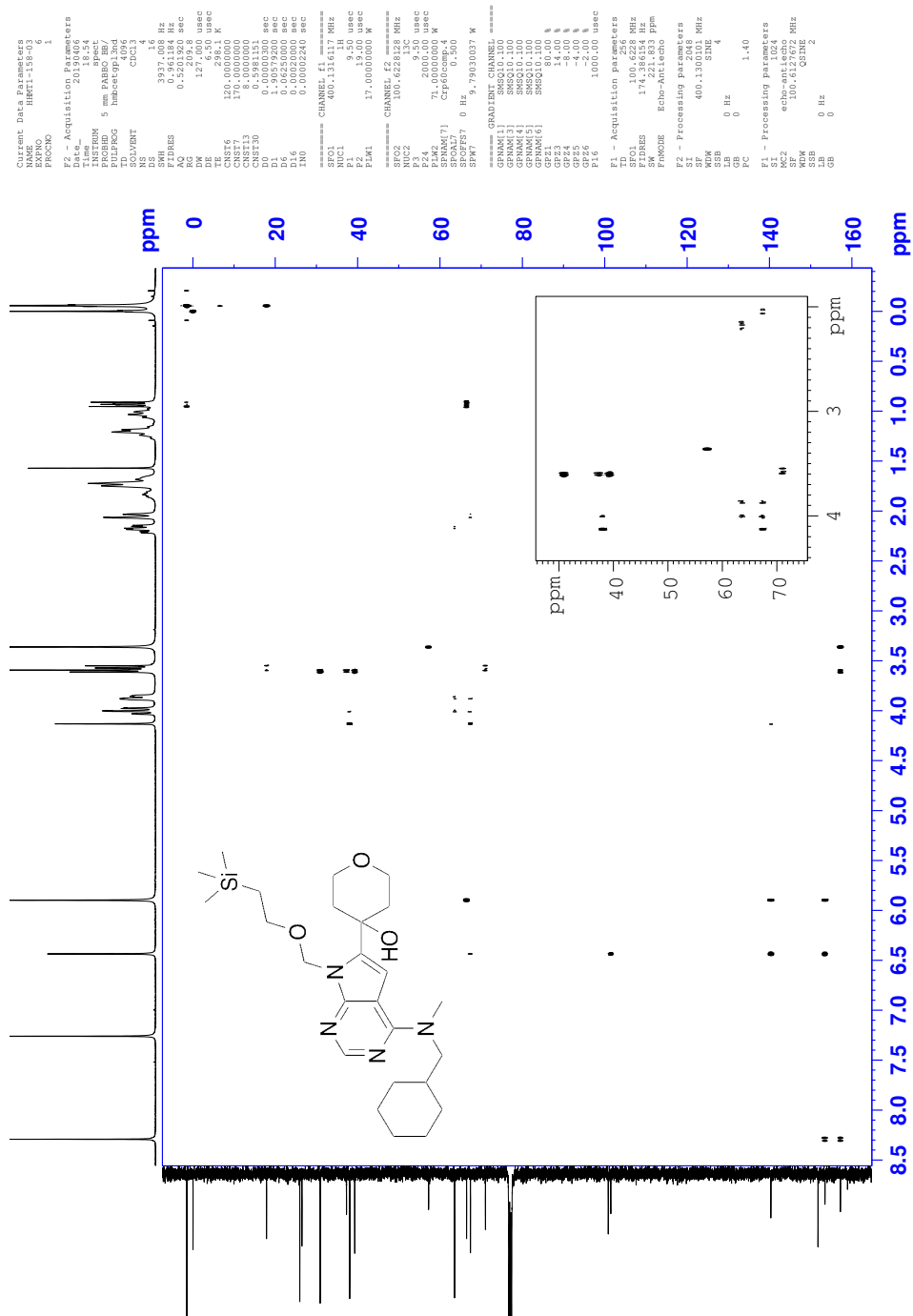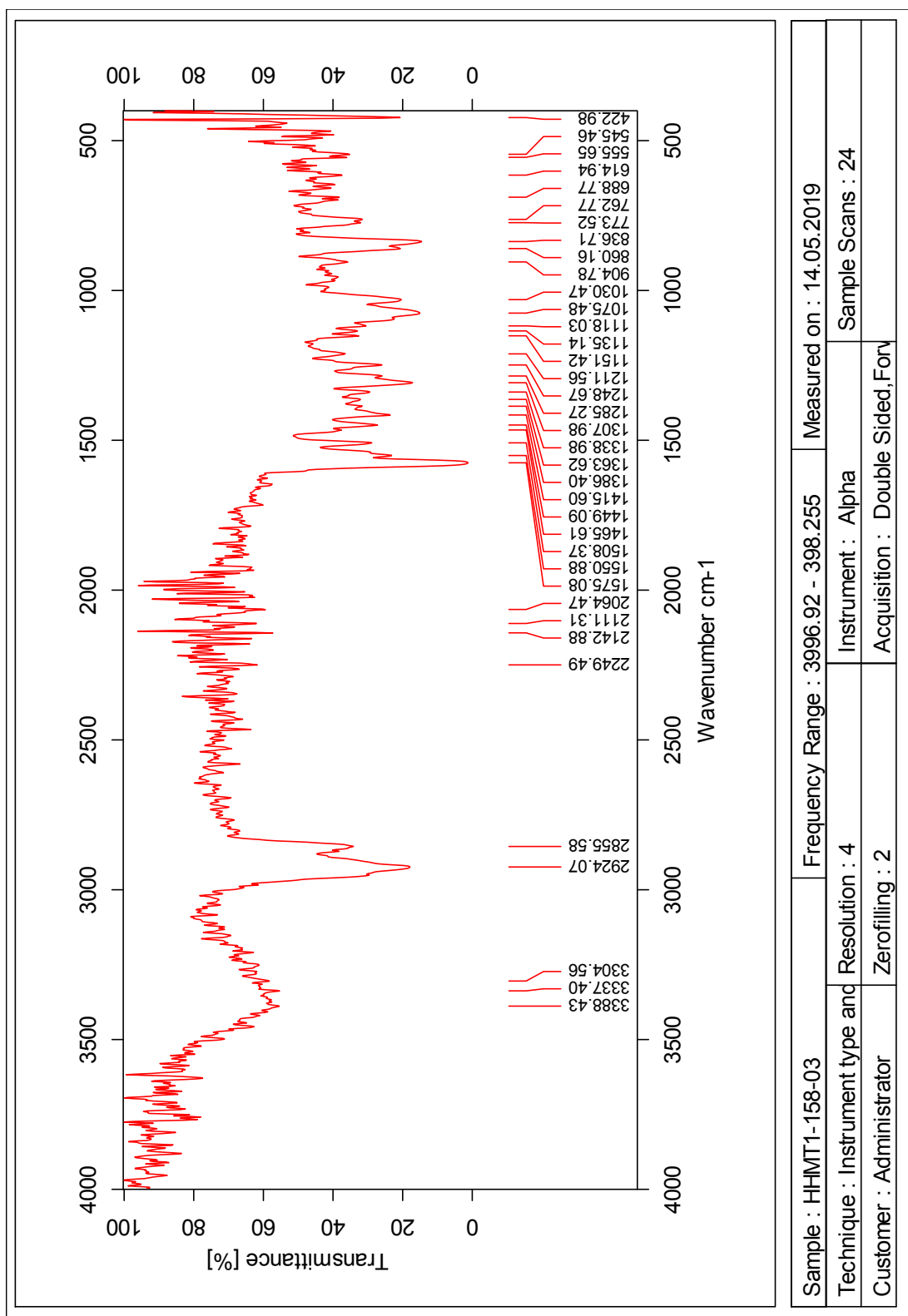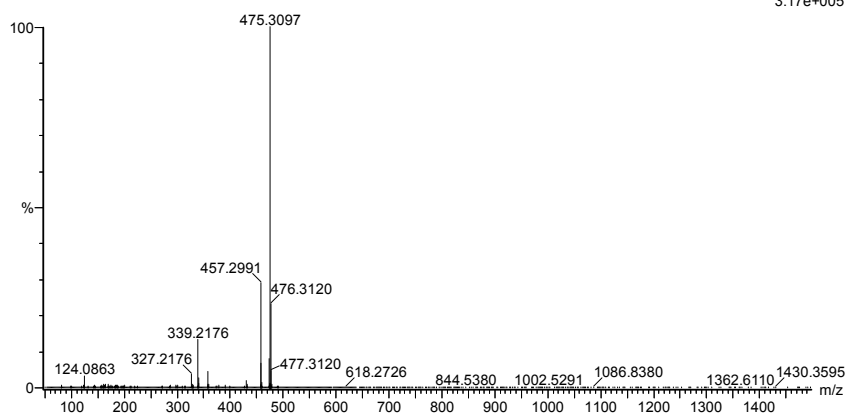3626 formula(e) evaluated with 3 results within limits (all results (up to 1000) for each mass)
Elements Used:
C: 0-100   H: 0-150   N: 0-6   O: 0-6   Na: 0-1   Si: 0-2
2019-422 72 (1.412) AM2 (Ar,35000.0,0.00,0.00); Cm (69:72)
1: TOF MS ASAP+

3.17e+005

Minimum:				-50.0			
Maximum:		5.0	2.0	50.0			
Mass	Calc. Mass	mDa	PPM	DBE	i-FIT	Conf(%)	Formula
475.3097	475.3096	0.1	0.2	-1.5	760.5	4.522	1.09	C16 H47 N6 O6 Si2
	475.3104	-0.7	-1.5	7.5	756.0	0.018	98.18	C25 H43 N4 O3 Si
	475.3089	0.8	1.7	13.5	760.9	4.913	0.74	C32 H40 N2 Na

Figure 4.50: MS spectrum of compound **13**.

L

N   Spectroscopic data for compound 14
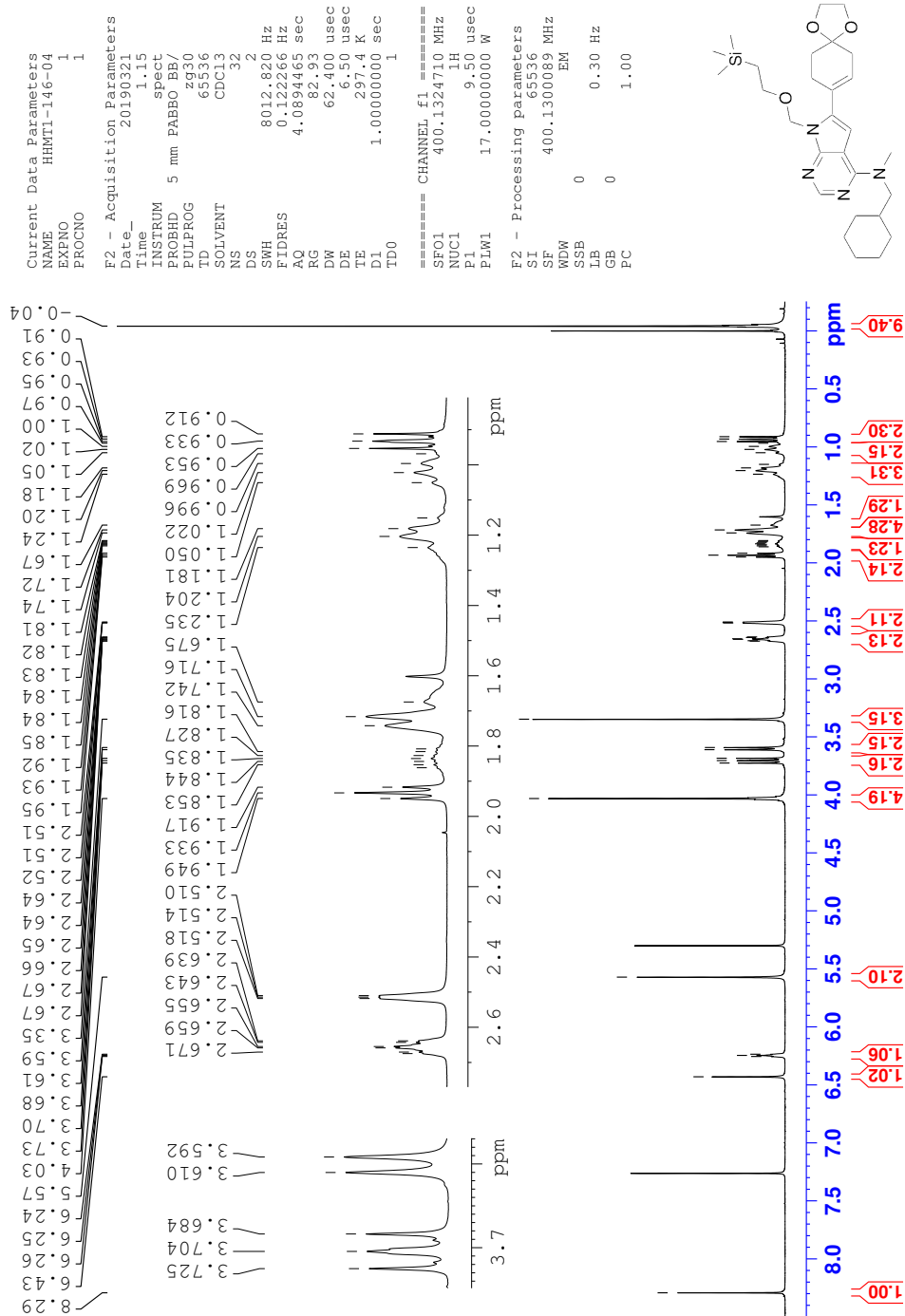
Figure 4.51: ^{1}H-NMR spectrum (400 MHz, CDCl$_3$) of compound **14**.

-1.4
18.0
25.9
26.5
28.3
30.8
31.4
36.2
37.2
39.1
57.1
64.5
66.1
70.8
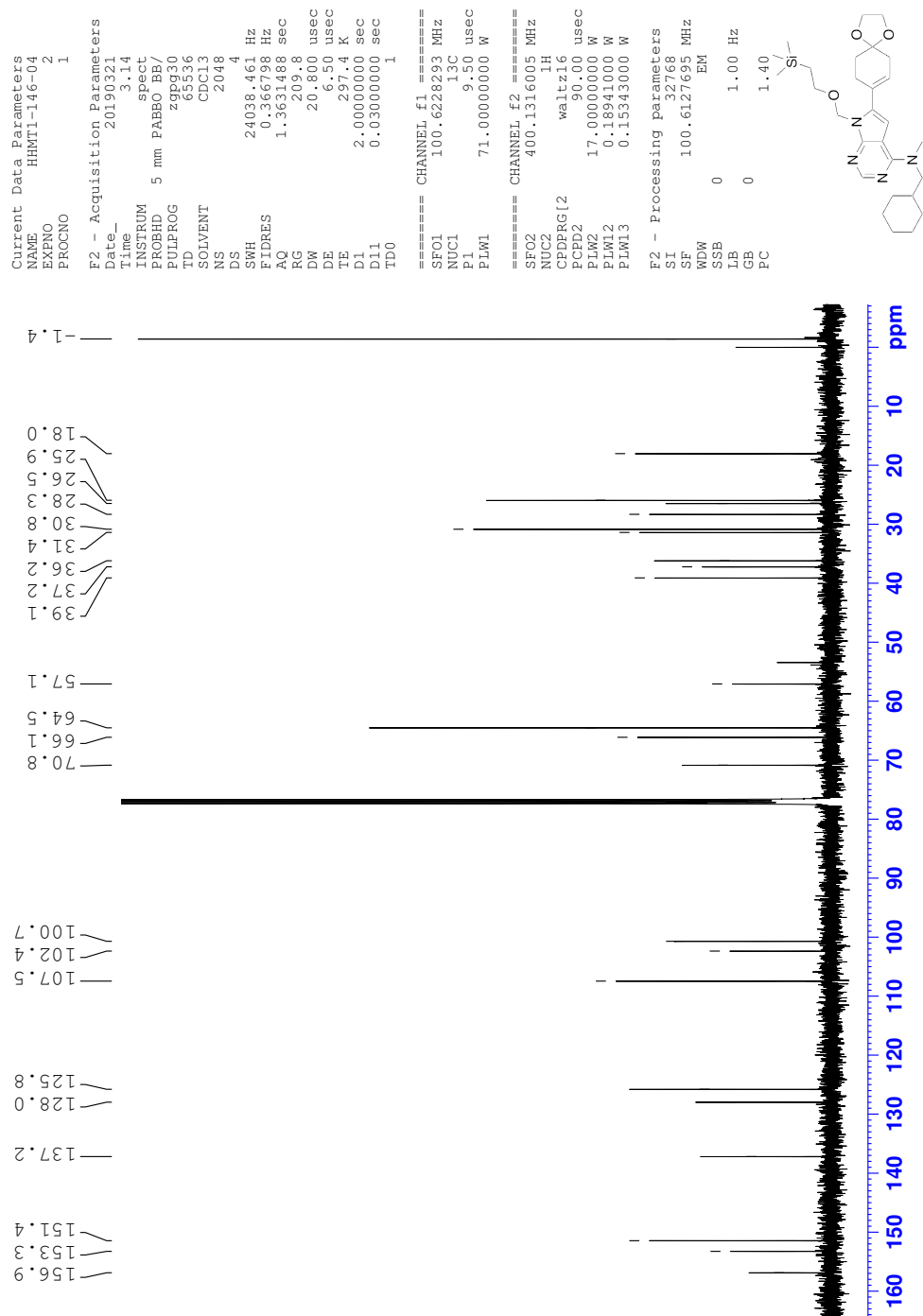100.7
102.4
107.5
125.8
128.0
137.2
151.4
153.3
156.9

Figure 4.52: ^{13}C-NMR spectrum (100 MHz, CDCl$_3$) of compound **14**.

Figure 4.53: COSY spectrum of compound **14** in CDCl₃.

Figure 4.54: HSQC spectrum of compound **14** in CDCl$_3$.
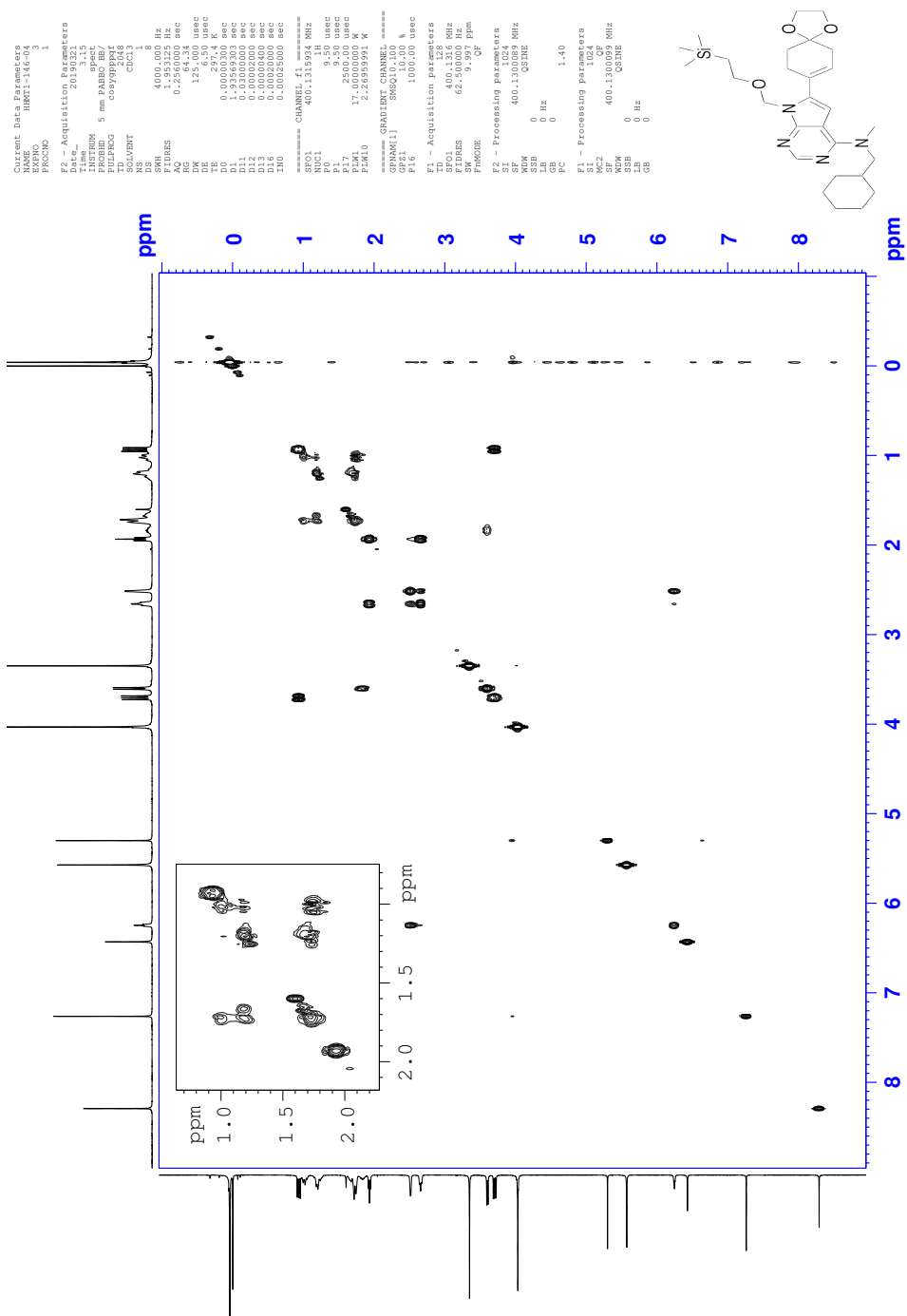
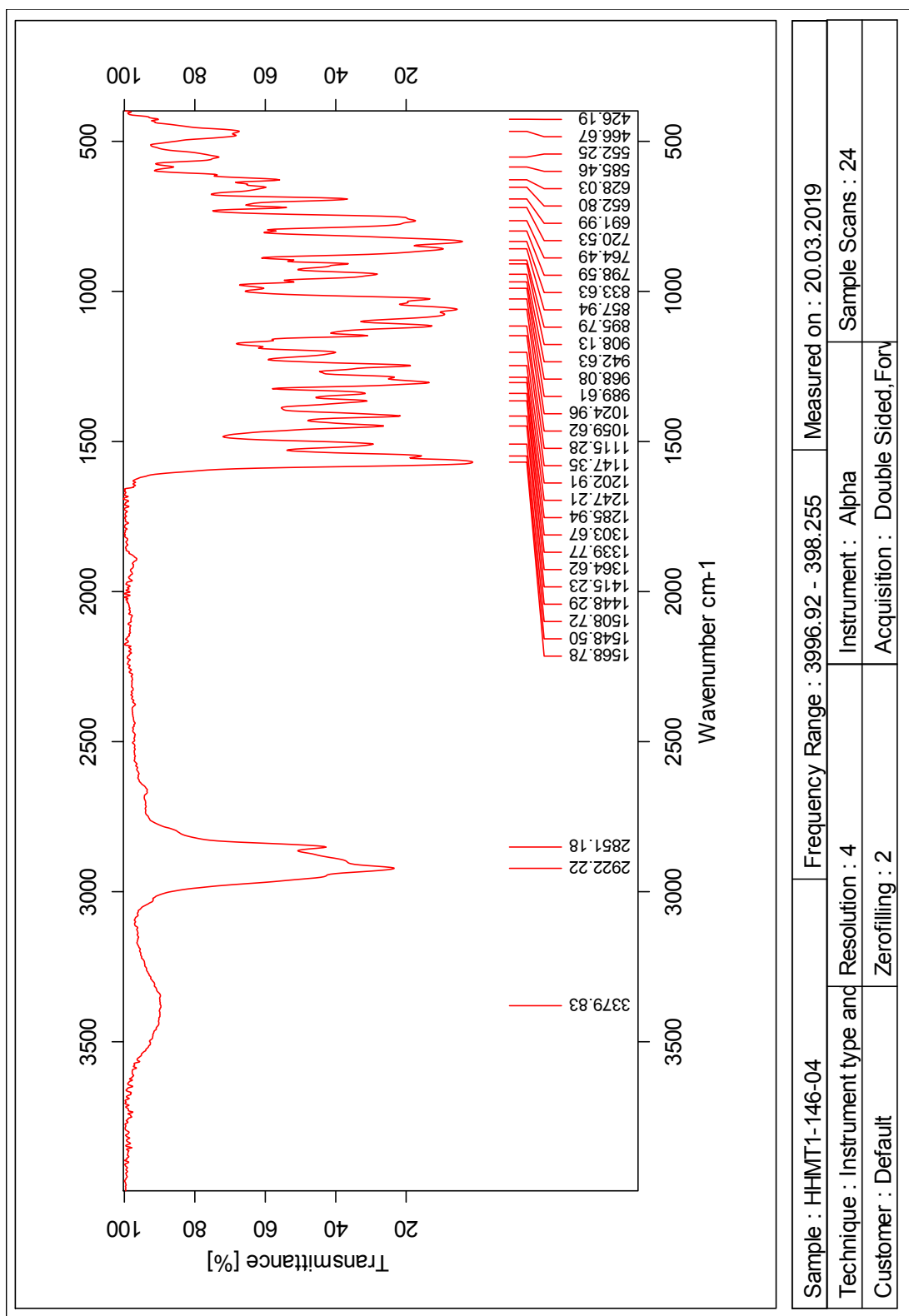**Figure 4.55:** HMBC spectrum of compound **14** in CDCl$_3$.

Figure 4.56: IR spectrum of compound **14**.

Single Mass Analysis
Tolerance = 2.0 PPM   /   DBE: min = -50.0, max = 50.0
Element prediction: Off
Number of isotope peaks used for i-FIT = 3

Monoisotopic Mass, Even Electron Ions
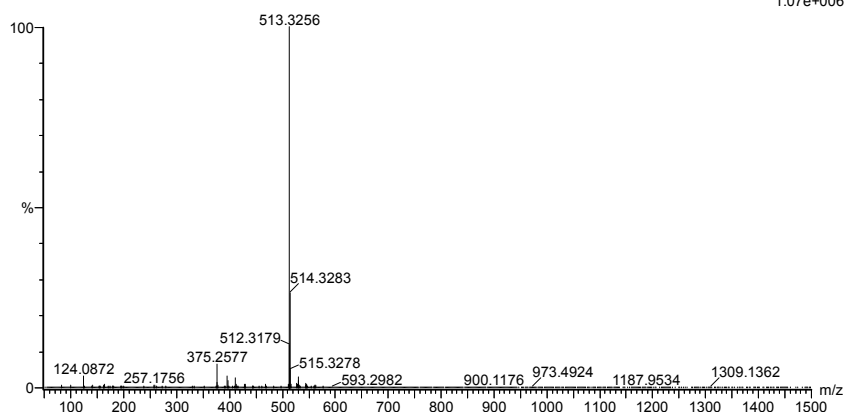3282 formula(e) evaluated with 4 results within limits (all results (up to 1000) for each mass)
Elements Used:
C: 0-100   H: 0-150   N: 0-5   O: 0-10   Si: 0-3
2019-250 78 (1.534) AM2 (Ar,35000.0,0.00,0.00); Cm (78:84)
1: TOF MS ASAP+

1.07e+006


```
Minimum:                          -50.0
Maximum:              5.0    2.0   50.0

Mass      Calc. Mass  mDa   PPM   DBE   i-FIT   Norm   Conf(%)  Formula

513.3256  513.3252    0.4   0.8   3.5   865.8   6.347  0.18     C26 H53 O4 Si3
          513.3261   -0.5  -1.0   9.5   860.2   0.764  46.58    C28 H45 N4 O3
                                                                Si
          513.3248    0.8   1.6   4.5   860.1   0.638  52.82    C27 H49 O7 Si
          513.3265   -0.9  -1.8   8.5   864.9   5.466  0.42     C27 H49 N4 Si3
```

Figure 4.57: MS spectrum of compound **14**.
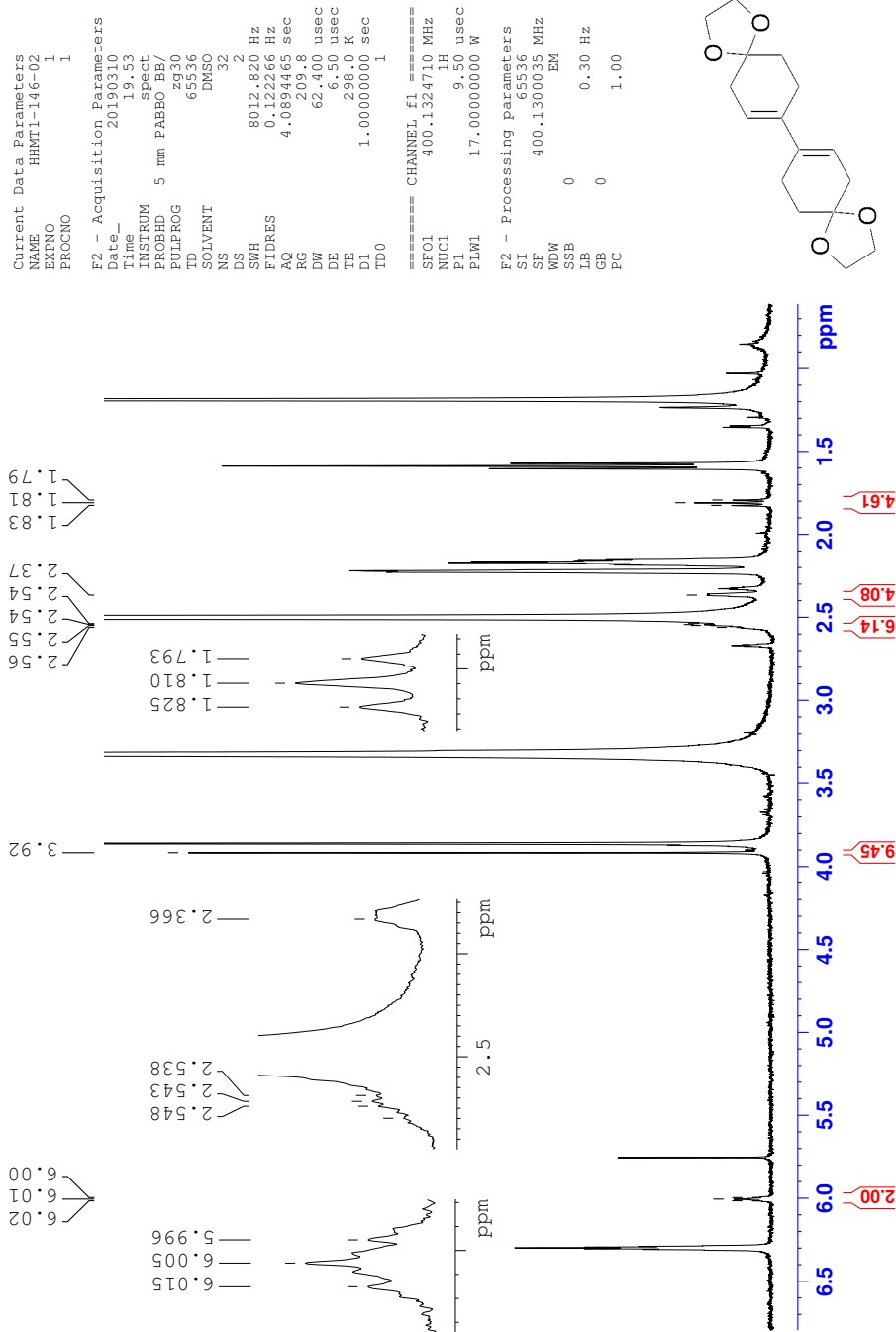
O Spectroscopic data for suspected byproduct 15

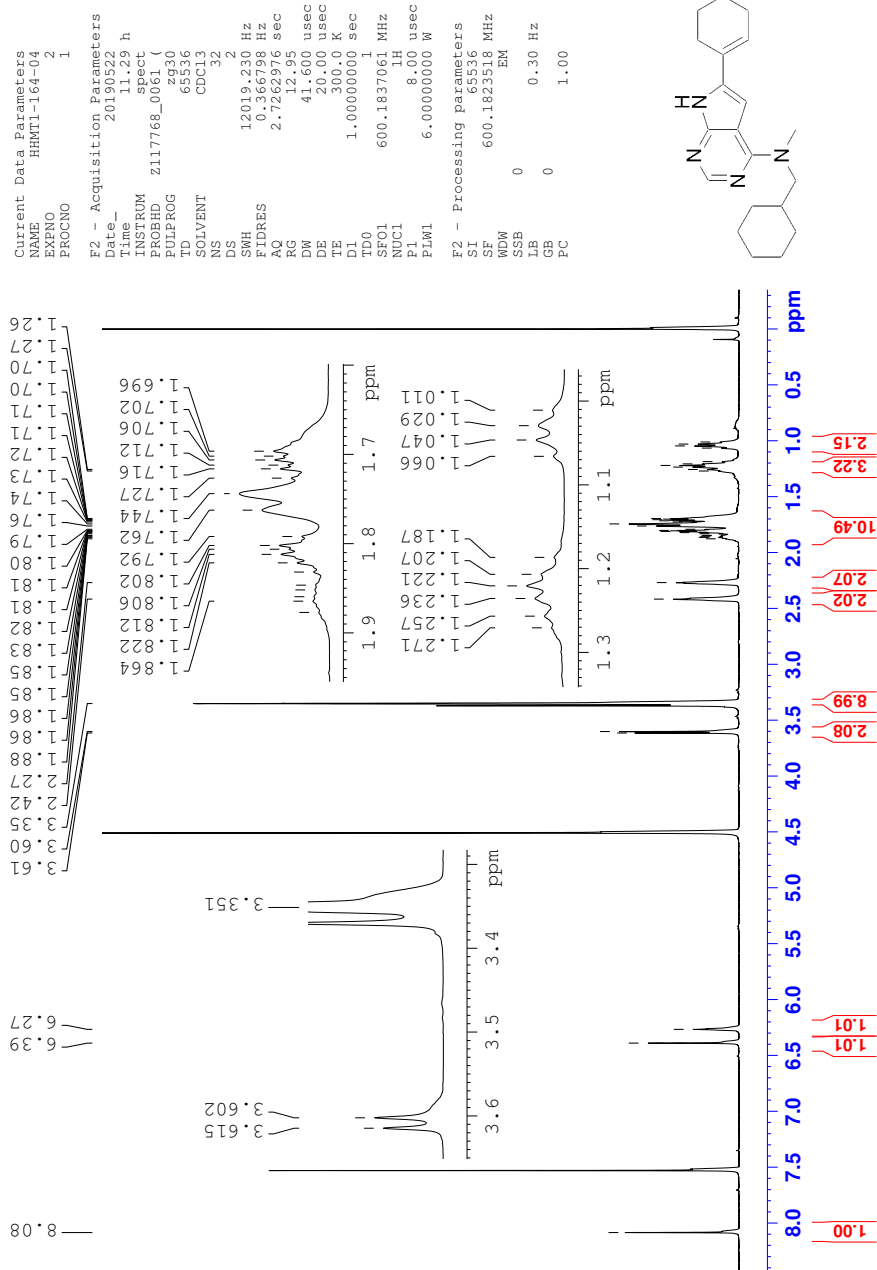**Figure 4.58:** ^{1}H-NMR spectrum (400 MHz, DMSO-d_6) of suspected byproduct **15**.

P Spectroscopic data for compound HHMT-070

Figure 4.59: ^{1}H-NMR spectrum (600 MHz, CD$_3$OD:CDCl$_3$, 1:1) of compound **HHMT-070**.
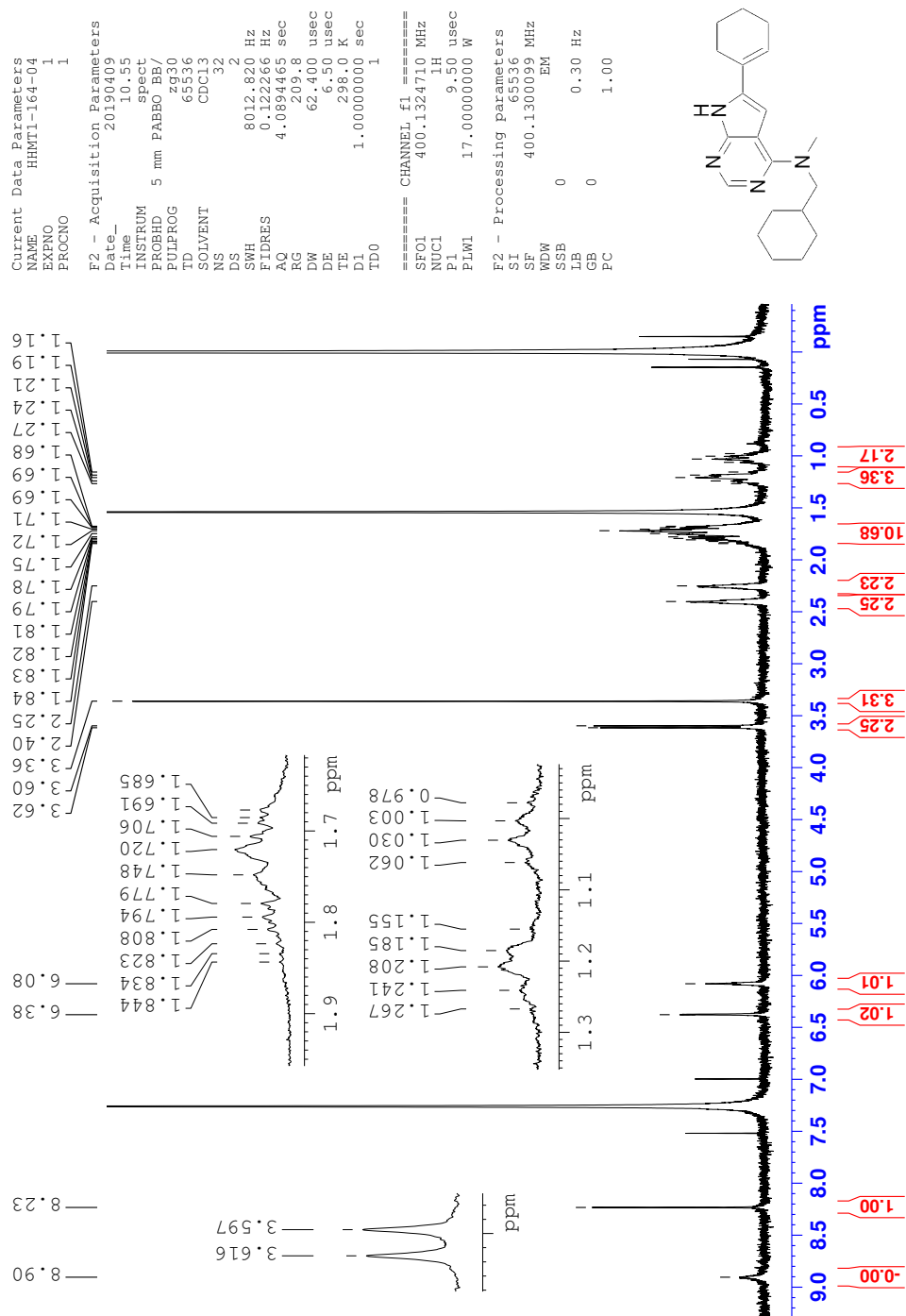
Figure 4.60: ^{1}H-NMR spectrum (400 MHz, CDCl$_3$) of compound **HHMT-070**.

Q   Spectroscopic data for compound HHMT-170
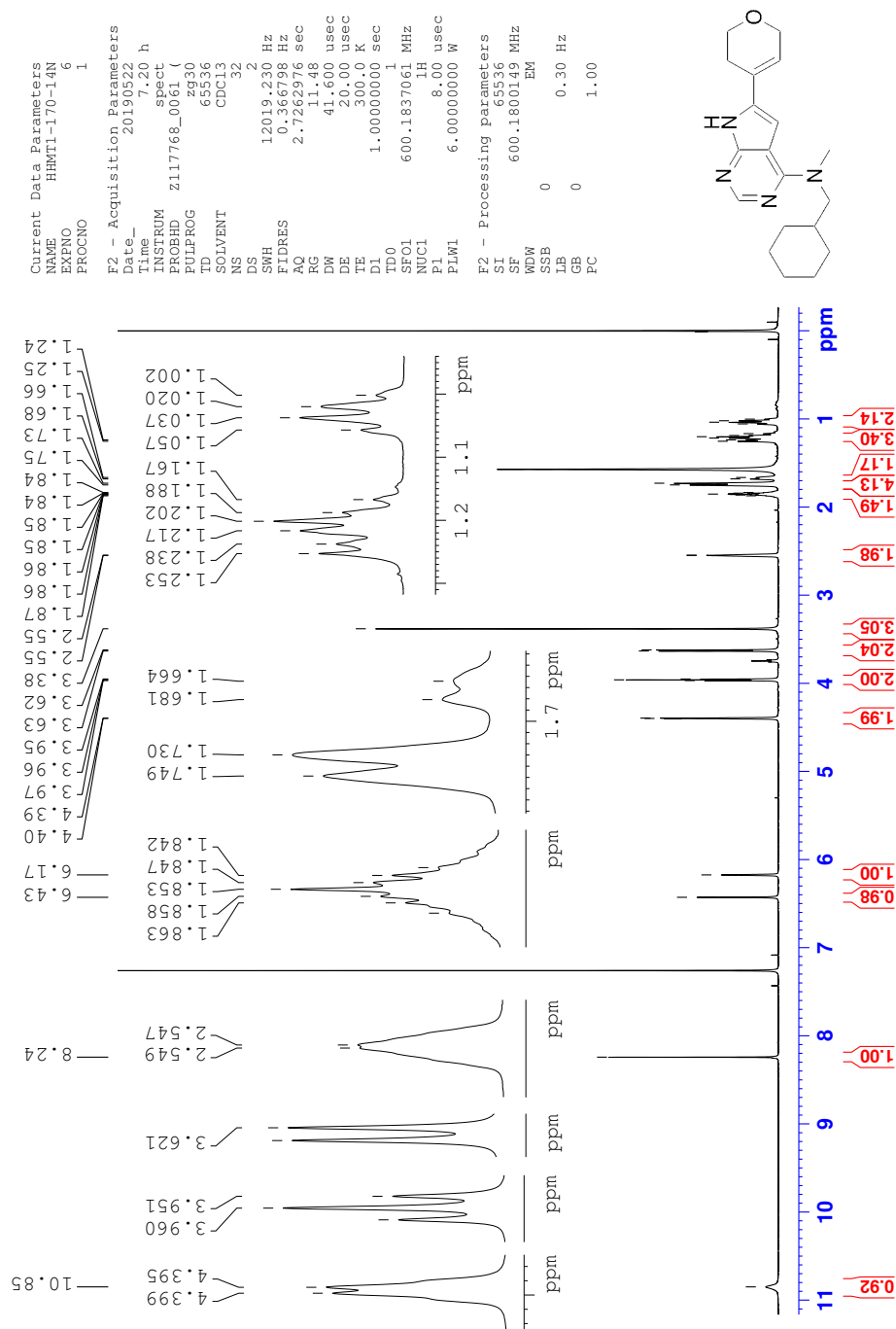
Figure 4.61: ^{1}H-NMR spectrum (600 MHz, CDCl$_3$) of compound **HHMT-170**.

Figure 4.62: ^{13}C-NMR spectrum (150 MHz, CDCl$_3$) of compound **HHMT-170**.
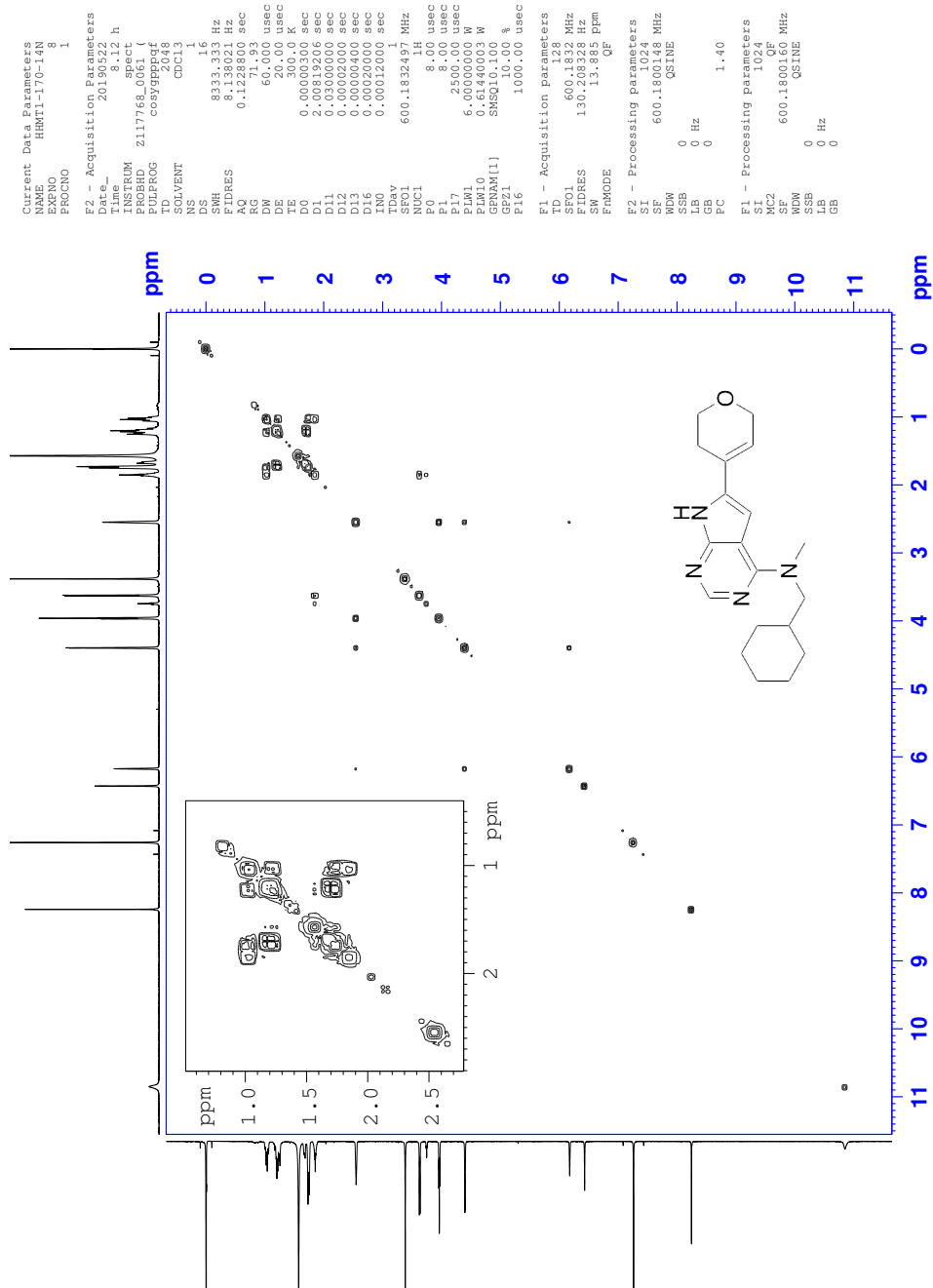
Figure 4.63: COSY spectrum of compound **HHMT-170** in CDCl₃.

Figure 4.64: HSQC spectrum of compound **HHMT-170** in CDCl$_3$.

Figure 4.65: HMBC spectrum of compound **HHMT-170** in CDCl$_3$.
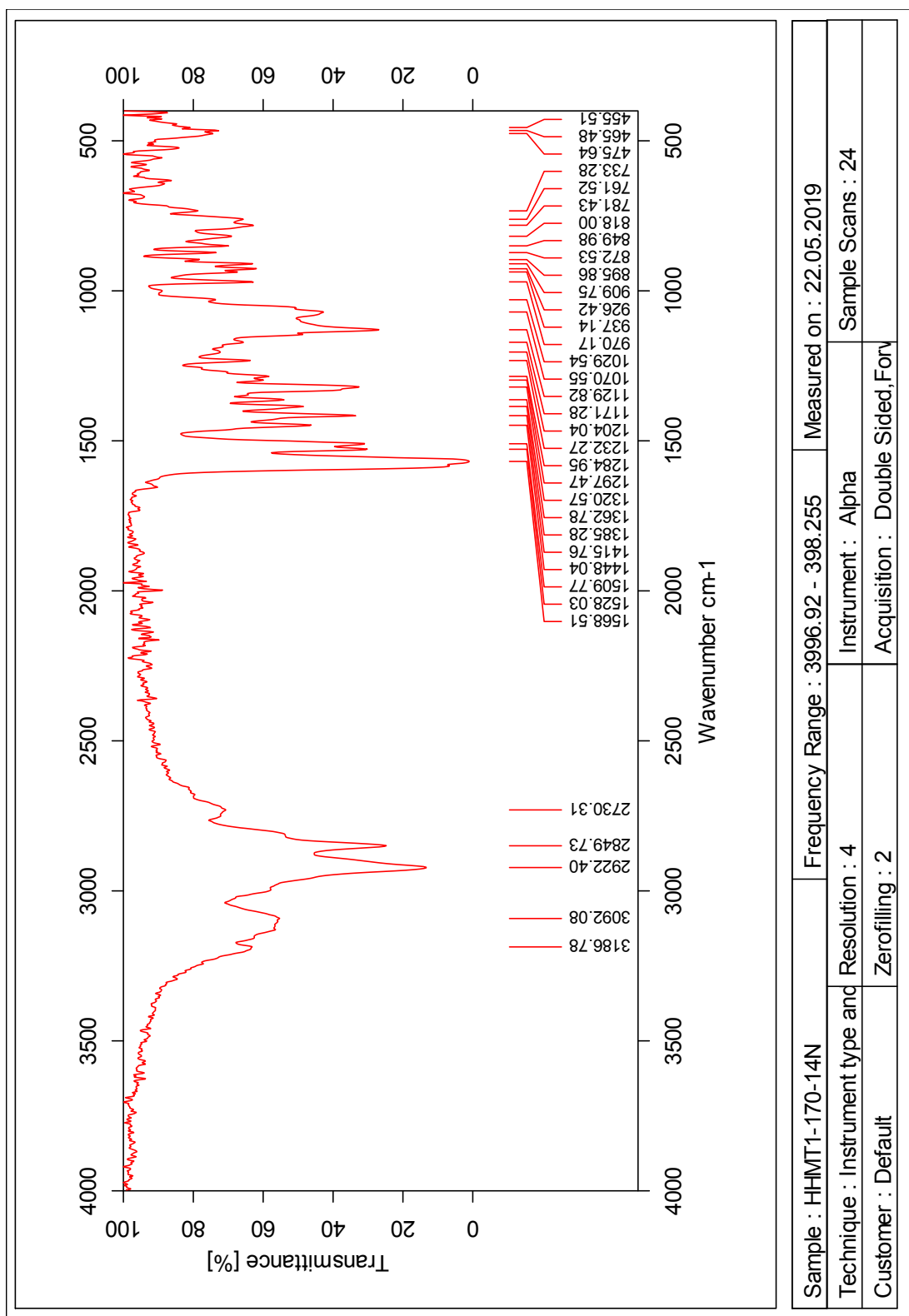
Figure 4.66: IR spectrum of compound **HHMT-170**.

Single Mass Analysis
Tolerance = 2.0 PPM   /   DBE: min = -50.0, max = 50.0
Element prediction: Off
Number of isotope peaks used for i-FIT = 3

Monoisotopic Mass, Even Electron Ions
1212 formula(e) evaluated with 1 results within limits (all results (up to 1000) for each mass)
Elements Used:
C: 0-100   H: 0-150   N: 0-10   O: 0-10
2019-525 94 (1.844) AM2 (Ar,35000.0,0.00,0.00); Cm (81:94)
1: TOF MS ASAP+
                                                                                          1.09e+006
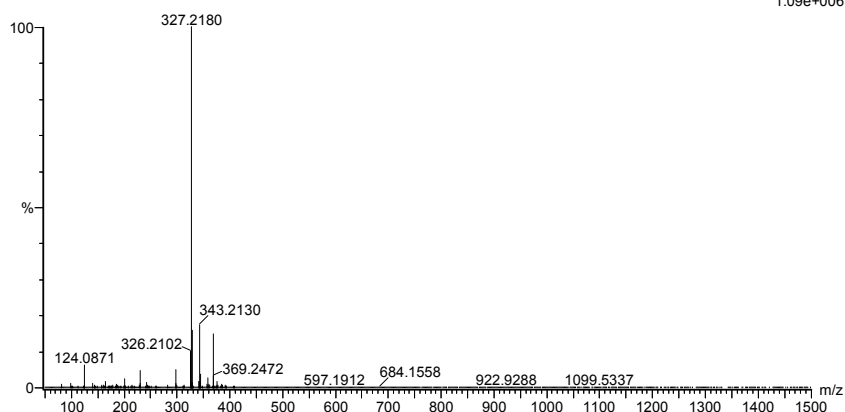
Minimum:			-50.0				
Maximum:		5.0	2.0	50.0			
Mass	Calc. Mass	mDa	PPM	DBE	i-FIT	Norm	Conf(%)	Formula
327.2180	327.2185	-0.5	-1.5	8.5	1212.7	n/a	n/a	C19 H27 N4 O

Figure 4.67: MS spectrum of compound **HHMT-170**.

R Spectroscopic data for compound HHMT-178

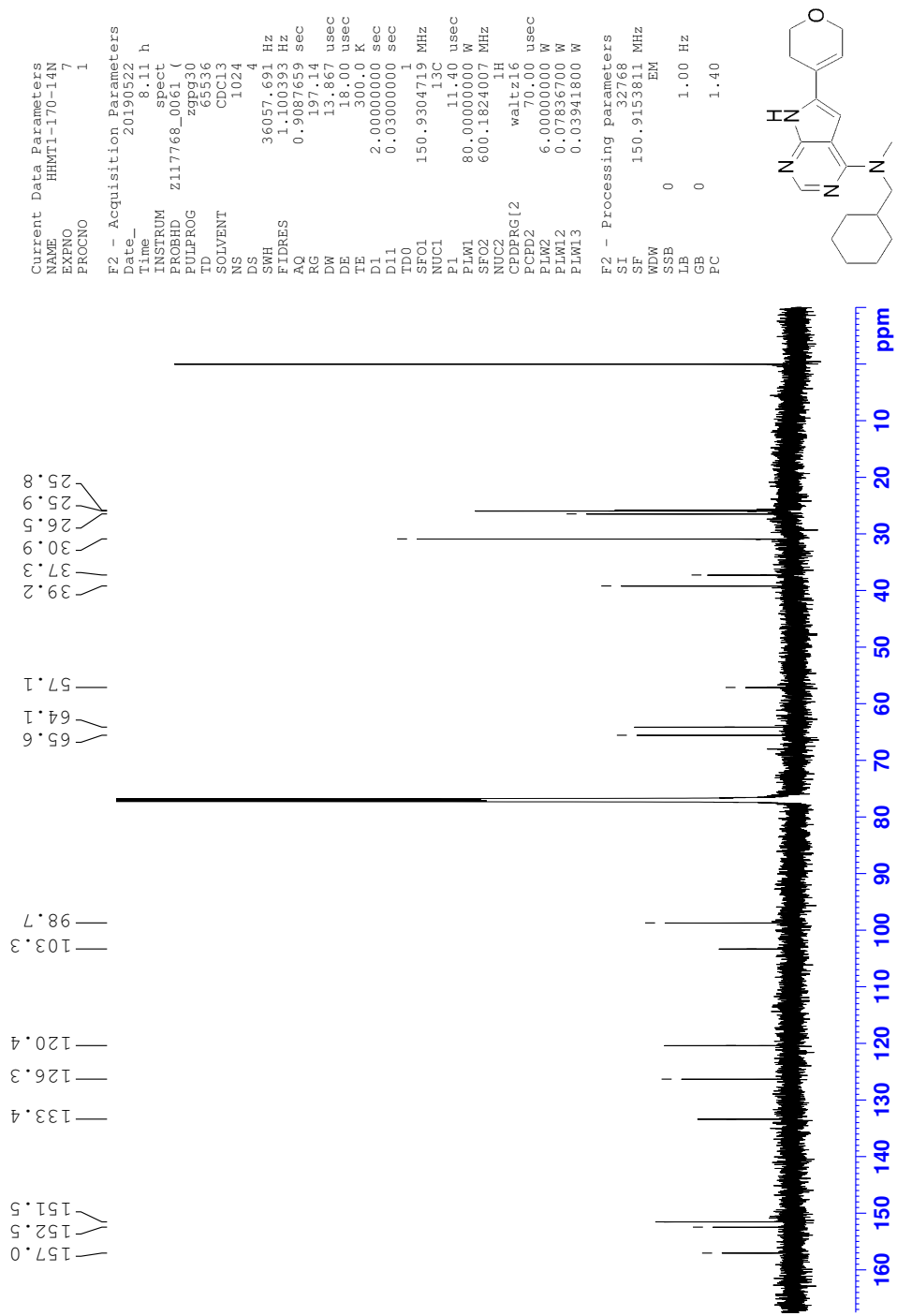**Figure 4.68:** ^{1}H-NMR spectrum (400 MHz, CDCl$_3$) of compound **HHMT-178**.

Current Data Parameters
NAME   HHMT1-178-10
EXPNO   2
PROCNO   1

F2 - Acquisition Parameters
Date_   20190517
Time   18.02
INSTRUM   spect
PROBHD   5 mm PABBO BB/
PULPROG   zgpg30
TD   65536
SOLVENT   CDCl3
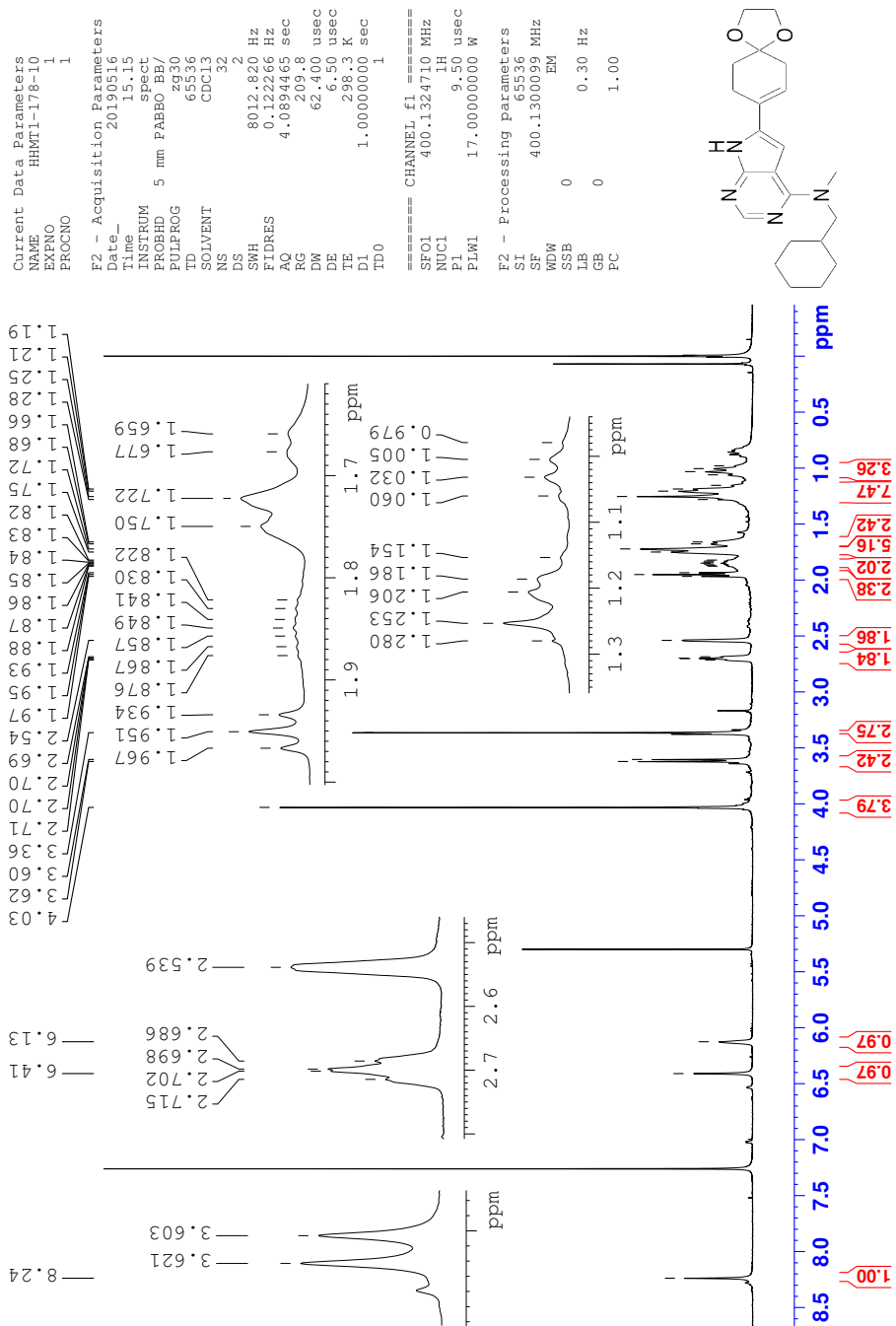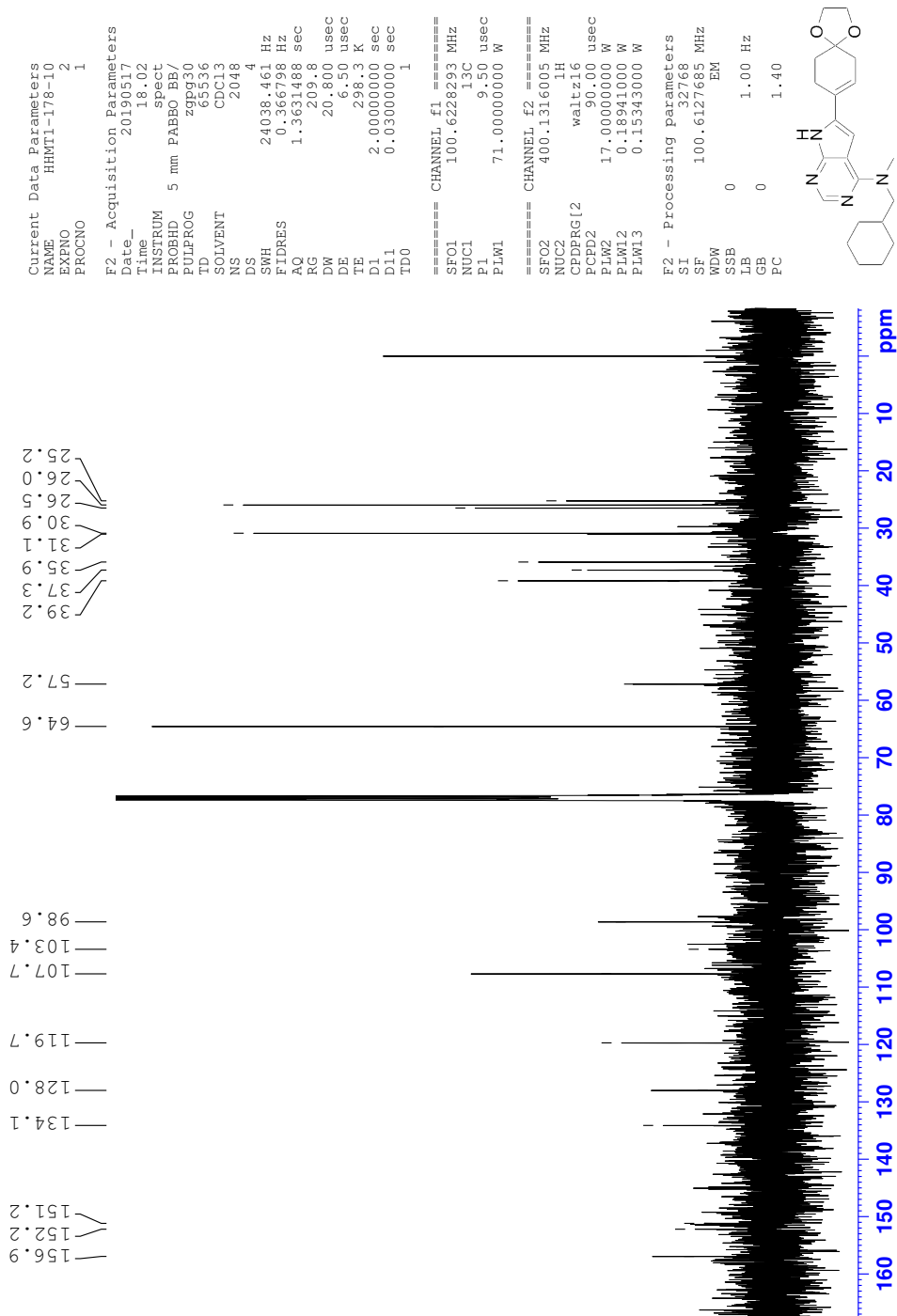NS   2048
DS   4
SWH   24038.461 Hz
FIDRES   0.366798 Hz
AQ   1.3631488 sec
RG   209.8
DW   20.800 usec
DE   6.50 usec
TE   298.3 K
D1   2.00000000 sec
D11   0.03000000 sec
TD0   1

======== CHANNEL f1 ========
SFO1   100.6228293 MHz
NUC1   13C
P1   9.50 usec
PLW1   71.00000000 W

======== CHANNEL f2 ========
SFO2   400.1316005 MHz
NUC2   1H
CPDPRG[2   waltz16
PCPD2   90.00 usec
PLW2   17.00000000 W
PLW12   0.18941000 W
PLW13   0.15343000 W

F2 - Processing parameters
SI   32768
SF   100.6127685 MHz
WDW   EM
SSB   0
LB   1.00 Hz
GB   0
PC   1.40

Figure 4.69: ^{13}C-NMR spectrum (100 MHz, CDCl$_3$) of compound **HHMT-178**.
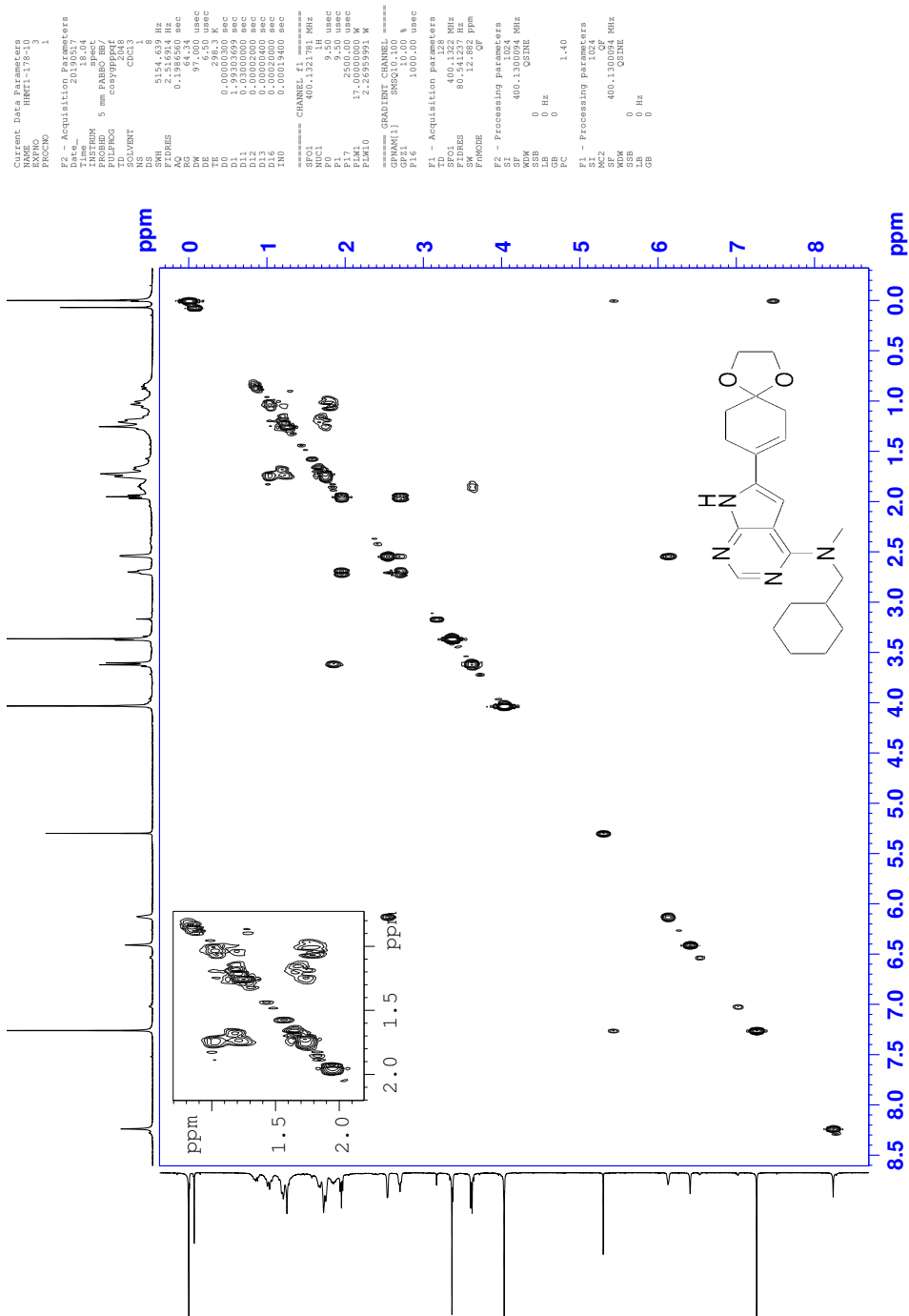
Figure 4.70: COSY spectrum of compound **HHMT-178** in CDCl₃.

Figure 4.71: HSQC spectrum of compound **HHMT-178** in CDCl$_3$.

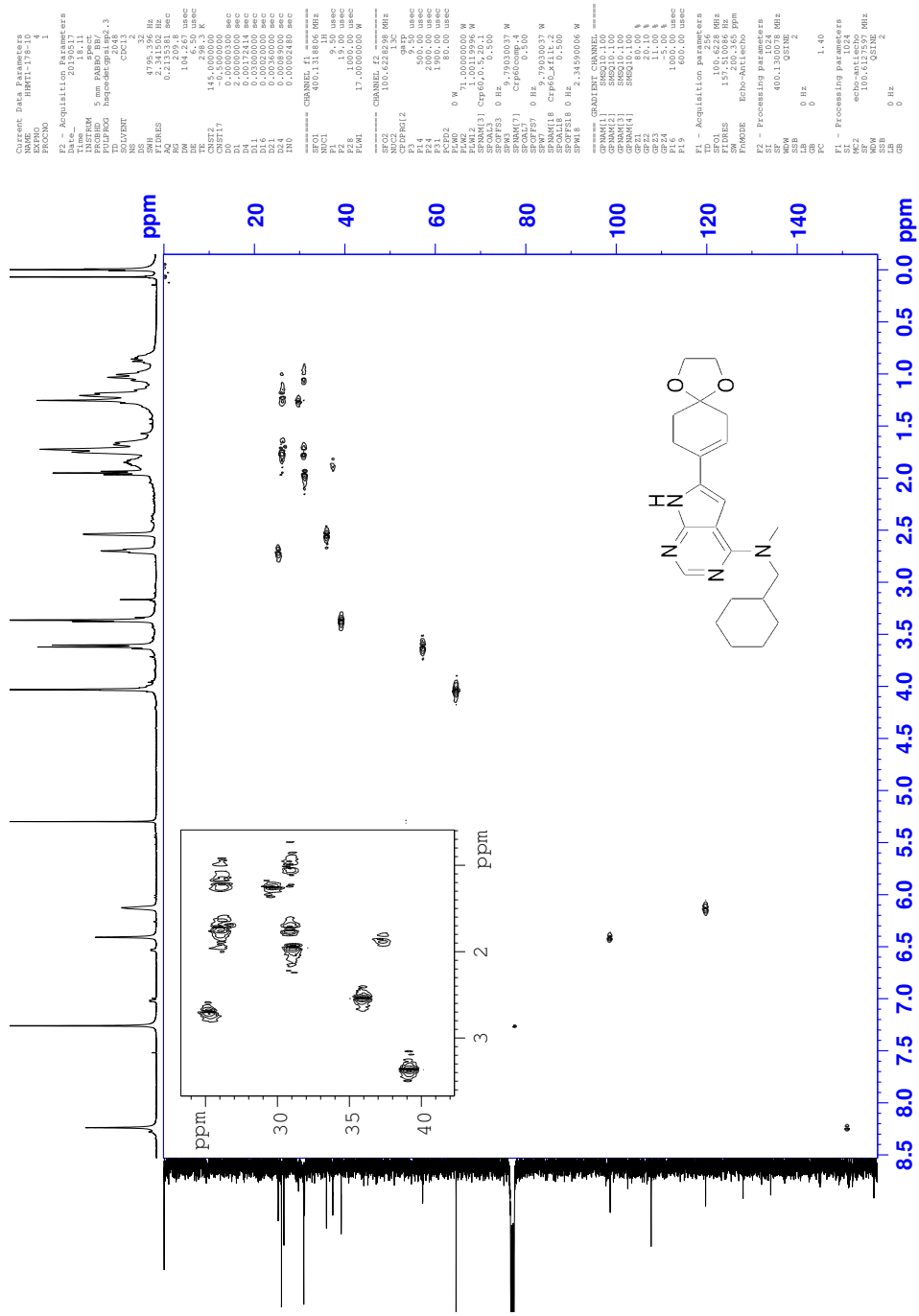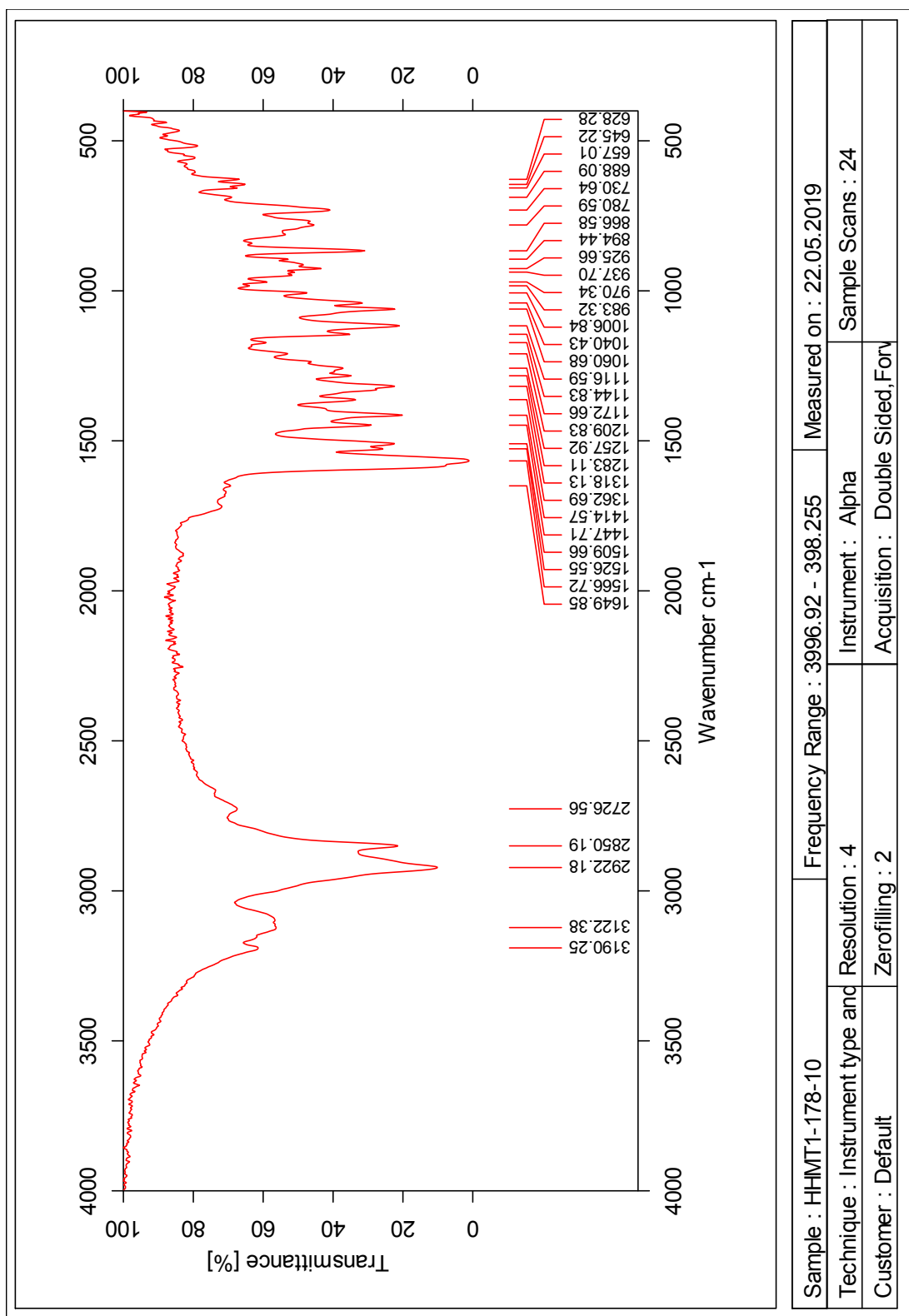**Figure 4.72:** HMBC spectrum of compound **HHMT-178** in CDCl₃.

Figure 4.73: IR spectrum of compound **HHMT-178**.

Single Mass Analysis
Tolerance = 2.0 PPM / DBE: min = -50.0, max = 50.0
Element prediction: Off
Number of isotope peaks used for i-FIT = 3

Monoisotopic Mass, Even Electron Ions
1343 formula(e) evaluated with 1 results within limits (all results (up to 1000) for each mass)
Elements Used:
C: 0-100 H: 0-150 N: 0-10 O: 0-10
2019-526 27 (0.271) AM2 (Ar,35000.0,0.00,0.00); Cm (27:39)
1: TOF MS ES+
1.38e+007


```
Minimum:                        -50.0
Maximum:              5.0    2.0  50.0

Mass       Calc. Mass  mDa   PPM  DBE   i-FIT    Norm   Conf(%) Formula

383.2448   383.2447   0.1    0.3  9.5   1456.9   n/a    n/a     C22 H31 N4 O2
```

Figure 4.74: MS spectrum of compound **HHMT-178**.

Single Mass Analysis
Tolerance = 2.0 PPM   /   DBE: min = -50.0, max = 50.0
Element prediction: Off
Number of isotope peaks used for i-FIT = 3

Monoisotopic Mass, Even Electron Ions
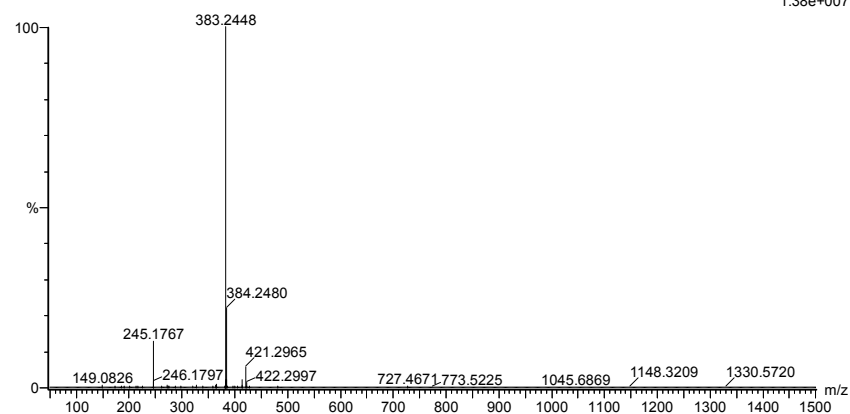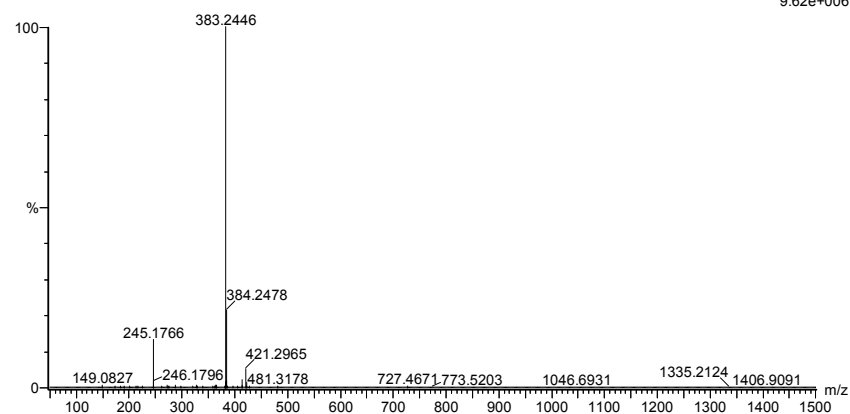857 formula(e) evaluated with 1 results within limits (all results (up to 1000) for each mass)
Elements Used:
C: 0-100   H: 0-150   N: 0-10   O: 0-10
2019-526 96 (0.908) AM2 (Ar,35000.0,0.00,0.00); Cm (95:109)
1: TOF MS ES+

9.62e+006


```
Minimum:                            -50.0
Maximum:                  5.0    2.0    50.0

Mass      Calc. Mass   mDa    PPM    DBE    i-FIT    Norm   Conf(%)  Formula

245.1766  245.1766     0.0    0.0    6.5    1482.5   n/a    n/a      C14 H21 N4
```

Figure 4.75: MS spectrum of suspected impurity isolated with compound **HHMT-178**.
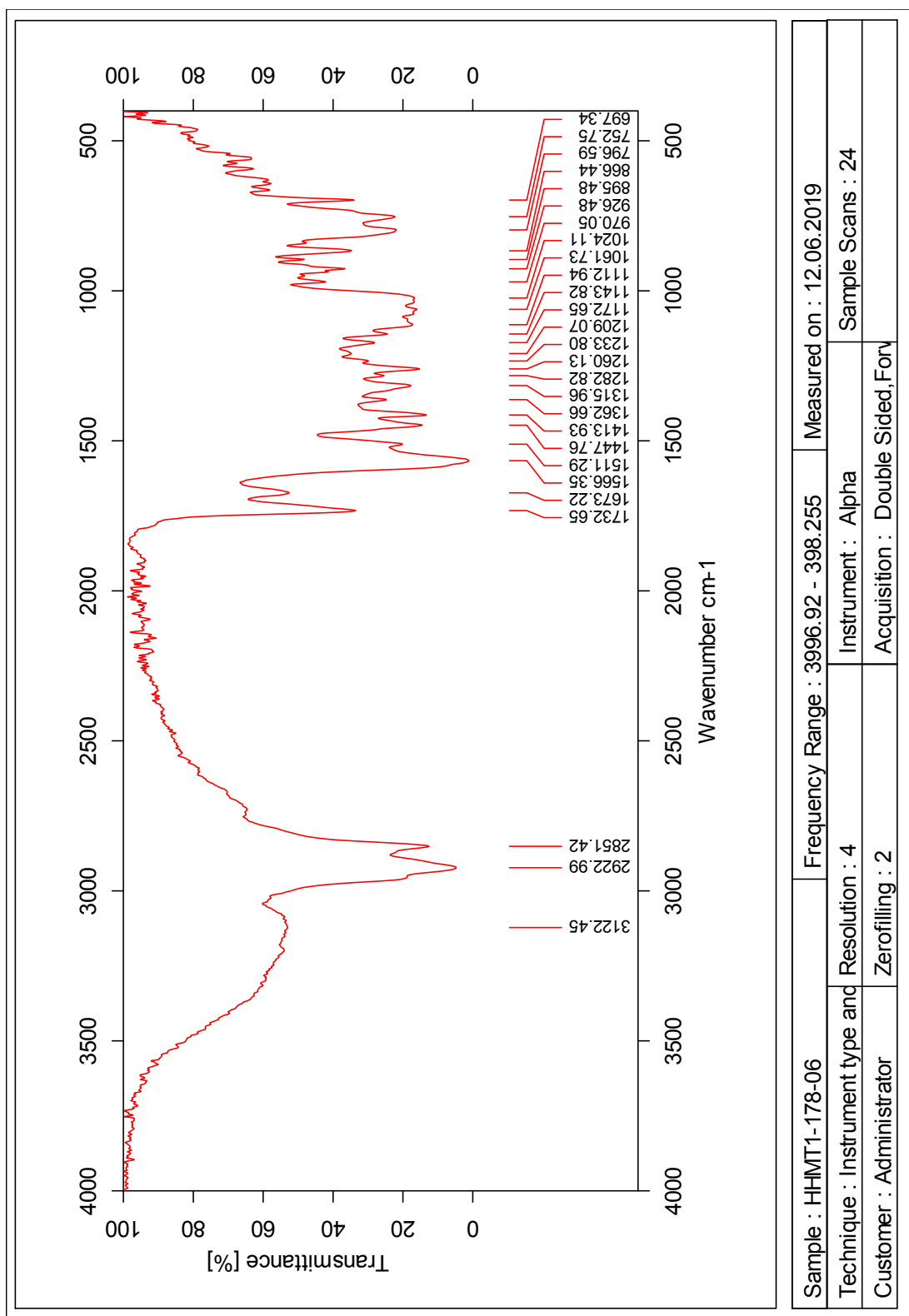
Figure 4.76: IR spectrum of crude product before isolation of compound **HHMT-178**.

S CSF-1R IC$_{50}$ measurements of HHMT-170 and PLX3397

Data for percent inhibition of CSF-1R at different concentrations of **HHMT-170** and PLX3397 given in two sets of data for each compound, see Table 4.1.

Table 4.1: Percent inhibition of CSF-1R at different concentrations of **HHMT-170** (IC$_{50}$: 0.367 nM) and PLX3397 (IC$_{50}$: 10.2 nM) in two sets of data points.

Conc. [nM]	**HHMT-170** Set 1	Set 2	PLX3397 Set 1	Set 2
0.0495	8	7	11	6
0.152	29	29	-2	-3
0.457	63	61	1	-4
1.37	77	78	12	10
4.12	90	99	35	30
12.3	91	94	59	57
37	94	97	57	90
111	105	97	105	114
333	115	104	102	111
1000	108	104	106	109

Hay Man Hilde Tsui

NTNU

Norwegian University of
Science and Technology